Life cycle sustainability of novel monopropellant systems

Pepijn Deroo

TU Delft

Life cycle sustainability of novel monopropellant systems

A comparative LCSA of a LEO minisatellite case study

by

Pepijn Deroo

to obtain the degree of Master of Science

at the Delft University of Technology,

to be defended publicly on Tuesday January 23, 2024 at 10:30 AM.

Student number:	4778332	
Project duration:	April 2023 - January 2024	
Thesis committee:	Dr. A. Cervone,	TU Delft, Chair
	Ms. I. Uriol Balbín,	TU Delft, Examiner
	Dr. B.V.S. Jyoti,	TU Delft, Supervisor
	Dr. A.R. Wilson,	Glasgow Caledonian University, Supervisor

Cover: Preparations for hydrazine fuelling of the Meteosat Third Generation Imager (above) [1] and a miner in a South African platinum mine (below) [2].

TU Delft

Acknowledgements

Throughout my thesis, I have been aided by the advice and support of several people, who should know that this report could not have been written without their help. Firstly, I would like to thank my supervisors, Dr. B.V.S. Jyoti and Dr. Andrew Wilson, for their guidance and enthusiasm throughout the project. I have worked together with Jyoti on several projects since 2019, and her approach to research, combining idealism and pragmatism, has taught me a great deal and made me a better researcher. Andrew's knowledge and experience in the exciting new world of space sustainability nourished my motivation to contribute to this research field. Without his eagerness to supervise and guide me in this endeavour, I would not have been able to realise as much of my original plan for this thesis as I have.

I am also indebted to all the people who provided me with information throughout my project. It is thanks to the replies and approximations that they sent to me, based on their professional experience, that I can be confident in my results. As the evolution towards a more sustainable space industry will only be achieved through collaboration, it was encouraging to notice how many people were glad to help me without expecting anything in return.

I am grateful for my friends, in Delft and elsewhere, for the distractions, laughter and conversations in the past months. Their passions and interests have inspired me and our discussions about politics, sports, music and films keep my mind bright and sharp.

I would also like to thank my family for their care and support during my time in Delft. The warmth of their presence, felt at home or from afar, provides the stable foundation from which I am able to pursue all my ambitions and interests. A final word of gratitude to Lena for her limitless and loving spirit, which encourages and enables me to put my abilities to the best use.

Pepijn Deroo
Delft, January 2024

Summary

For over 50 years, hydrazine has been the industry standard for monopropellant propulsion systems used in space. Due to the propellant's toxicity however, the related handling and fuelling costs are high. This financial and logistical burden is most problematic for small satellites, which is an unfavourable outcome given the aim of improving space sustainability and reducing the amount of space debris orbiting the Earth. Furthermore, hydrazine has been included in the European Chemical Agency's candidate list of Substances of Very High Concern, such that its regulatory future is uncertain. In order to solve these issues, a key topic within space propulsion research for the past three decades has been to find suitable replacements for hydrazine.

While the reduced toxicity and improved performance of novel monopropellants have been the subject of numerous studies, there have been few efforts so far to more thoroughly investigate their overall sustainability as compared to hydrazine. This is a significant research gap, not only due to the misleading use of the term "green monopropellants", but also in light of the increasing application of Life Cycle Assessments (LCAs) in the European space industry. As the European Space Agency (ESA) aims to adapt its activities for a more sustainable future, it has played a key role in harmonising and promoting the use of LCA studies for space technology development. While environmental issues have been the main focus for space LCAs, Andrew Wilson's development of the Strathclyde Space Systems Database (SSSD) has adapted the Life Cycle Sustainability Assessment (LCSA) framework for use in the space sector, thereby also facilitating the evaluation of social and economic sustainability. In an effort to bring this more advanced concept of three-pillar sustainability to the field of novel monopropellants, this thesis research had the goal of investigating the impact of propellant choice on the environmental, economic and social sustainability of a representative monopropellant system.

To answer this research question, four propulsion systems were designed for the same use case, being the main propulsion system of an Earth Observation minisatellite of around 150 kg, orbiting in Low Earth Orbit, using either hydrazine, the American novel monopropellant ASCENT, the Swedish novel monopropellant LMP-103S, or 98% concentrated High Test Peroxide (H_2O_2, HTP). For each of these systems, a full LCSA was carried out, considering the Life Cycle Inventory (LCI) from raw material extraction to the point at which the propulsion system is fuelled before launch. In the LCI definition, new datasets were added to the SSSD, using data from literature and other public sources. The overall impact of these systems was assessed for 23 midpoint impact categories, included in the SSSD Sustainability Life Cycle Impact Assessment (LCIA) method, 21 of which concern environmental impacts, with the economic and social impact being quantified in single scores.

The results from this comparative LCSA indicate that the LMP-103S system leads to the highest environmental impact, closely followed by the ASCENT propulsion system, due to their use of iridium and rhenium in the thrusters' combustion chambers. These rare metals are required to withstand the high combustion temperature of these propellants, but their extraction processes are energy- and resource-intensive and therefore polluting. The impact category that is most relevant in the life cycle environmental damage caused by the propulsion systems is freshwater ecotoxicity. The propulsion system using 98% HTP showed the lowest environmental impact, as it does not feature the environmental hotspots of requiring significant amounts of iridium or rhenium in its thruster design, or of hydrazine production and fuelling.

In terms of economic sustainability, the cost of propellant fuelling dominates the results, while it is important to note that this assessment used a rough cost estimate for this activity, which may be overly conservative. Nonetheless, the economic impact assessment indicates that the hydrazine propulsion system would be the most expensive, with an estimated life cycle cost of 2.4 million € in 2023. The cost estimates of the novel monopropellant systems lie close together, at around 1.7 million € in 2023. The main factor differentiating these systems is the cost of the thrusters used, with the ASCENT and

LMP-103S systems being more expensive than the 98% HTP system.

The social sustainability score of the four propulsion systems shows less variation, being mostly dependent on the propulsion system assembly process, ranging from 106% of the hydrazine system's impact for the LMP-103S system to 83% for the 98% HTP system. Within this assessment, which is based on the number of labour hours related to specific processes, the contribution of expensive thruster components, such as the flow control valve and combustion chamber, also plays a significant role. For future research it is recommended to include the social impact of upstream processes, as material extraction of rare elements such as iridium and rhenium potentially cause significant harm.

This research has shown that an in-depth sustainability assessment of monopropellant propulsion systems can provide useful insights for future design trade-offs or other comparisons. For the promising novel monopropellants ASCENT and LMP-103S, which are increasingly being used in small satellite applications, the usage of iridium and rhenium in the thrusters has been identified as an environmental hotspot. The economic and social impact of clean room fuelling has been quantified, and the relative importance of fuelling for both sustainability dimensions has been investigated. In future research, it is recommended to improve the accuracy of the datasets used in this study and to quantify the uncertainty contained within the LCIA results. It is also recommended to perform similar comparative LCSAs for other monopropellant use cases, including different propellants than the ones considered here. This would allow for a further characterisation of sustainable space propulsion technologies and provide potential research avenues for space propulsion engineers.

Contents

List of Figures

List of Tables

Nomenclature

Abbreviations

Abbreviation	Definition
ACS	Attitude Control System
ADN	Ammonium Dinitramide
AOCS	Attitude and Orbit Control System
APOS	At Point Of Substitution
AOL	Active Oxygen Loss
C	Completeness (data quality criterion)
CB	Catalyst Bed
CC	Combustion Chamber
CNC	Computer Numerical Control
COTS	Commercial-Off-The-Shelf
DB	Database
DLR	German Aerospace Center
DQR	Data Quality Rating
ECHA	European Chemical Agency
EF	Environmental Footprint
ei	ecoinvent
EIL	Energetic Ionic Liquid
EO	Earth Observation
EOL	End-Of-Life
EPDM	Ethylene Propylene Diene Monomer
ESA	European Space Agency
E-LCA	Environmental Life Cycle Assessment
FCV	Flow Control Valve
FEP	Fluorinated Ethylene Polymer
FOI	Swedish Defence Research Agency
FU	Functional Unit
GEM	Green Electric Monopropellant
GPIM	Green Propellant Infusion Mission
GPRCS	Green Propellant Reaction Control System
GPS	Global Positioning System
GR	Geographical Representativeness (data quality criterion)
GSD	Ground Sample Distance
GWP	Global Warming Potential
HAN	Hydroxylammonium Nitrate
HEHN	Hydroxylethylhydrazinium Nitrate
HPGP	High-Performing Green Propellant
HTP	High Test Peroxide
IPA	Iso-Propanol Alcohol
ISA	International Standard Atmosphere
JAXA	Japan Aerospace Exploration Agency
LCA	Life Cycle Assessment
LCC	Life Cycle Costing
LCI	Life Cycle Inventory

Abbreviation	Definition
LCIA	Life Cycle Impact Assessment
LCSA	Life Cycle Sustainability Assessment
LEO	Low Earth Orbit
LUMIO	Lunar Meteoroid Impact Observer
LV	Launch Vehicle
M	Methodological appropriateness and consistency (data quality criterion)
MEO	Medium Earth Orbit
MMF	Monomethylformamide
NASA	National Aeronautics and Space Administration
NO	Nitrous Oxide
NOFB	Nitrous Oxide Fuel Blend
O/F	Oxidiser to Fuel
P	Precision/uncertainty (data quality criterion)
PGM	Platinum Group Metal
PMD	Propellant Management Device
PS	Propulsion System
RACS	Roll and Attitude Control System
RER	Europe
RGHP	Rocket Grade Hydrogen Peroxide
SCAPE	Self-Contained Atmospheric Protection Ensemble
SD	Standard Deviation
SDG	Sustainable Development Goal
SMAD	Space Mission Analysis and Design
SSO	Sun-Synchronous Orbit
SSSD	Strathclyde Space Systems Database
S-LCA	Social Life Cycle Assessment
TBD	To Be Determined
TeR	Technological Representativeness (data quality criterion)
TiR	Temporal Representativeness (data quality criterion)
TIG	Tungsten Inert Gas
TRL	Technology Readiness Level
UN	United Nations
USD	United States Dollar

Symbols

Symbol	Definition	Unit
a	Orbit semi-major axis	[m]
c	Concentration	[-]
m	Mass	[kg]
$\dot{m}$	Mass flow	[kg/s]
i	Orbit inclination	[$^\circ$]
p	Pressure	[Pa]
r	Radius	[m]
t	Thickness	[m]
A_c	Combustion chamber cross-sectional area	[m^2]
A_s	Catalyst specific area	[m^2/g]
BDR	Blow-down ratio	[-]
D	Days per orbit repeat cycle	[-]

Symbol	Definition	Unit
F_t	Thrust	[N]
G	Catalyst bed loading	[$kg/m^2/s$] or [$lbm/in^2/s$]
I_{sp}	Specific impulse	[s]
K_{shell}	Tank shell mass correction factor	[-]
L_B	Catalyst bed length	[m] or [in]
M_{press}	Pressurant molar mass	$[kg/mol]$
P	Orbital period	[s]
P_c	Chamber pressure	[Pa] or [psi]
R	Revolutions per orbit repeat cycle	[-]
S	Surface area	[m^2]
SF_y	Yield stress safety factor	[-]
V	Velocity	[m/s]
V	Volume	[m^3] or [L]
ϵ	Nozzle expansion ratio	[-]
η_{exp}	Expulsion efficiency	[-]
$\eta_{I_{sp}}$	Specific impulse quality factor	[-]
ρ	Density	[kg/m^3]
σ	Tensile stress	Pa
Δl	Adjacent ground track distance	[m]
ΔV	Velocity increment	[m/s]
$\dot{\Omega}$	Orbital nodal precession rate	[rad/s]

1 Introduction

In the past decade, space sustainability has matured to become a serious and complex topic in the European space industry. This rise may be motivated by reasons that are also relevant for other industries, for example the increasing public awareness of global issues such as climate change, but the concept of space sustainability is more intricate than sustainability in other sectors for at least two reasons. Firstly, the space industry inherently affects environments other than that of the Earth. As a result, issues such as the increase in space debris left by decommissioned satellites are key to space sustainability [3]. The uniqueness of these issues has the dangerous side effect of obscuring the impact of space activities on the Earthly environment, however. This has been addressed by the European Space Agency's (ESA's) Clean Space Initiative, with the promotion of the Life Cycle Assessment (LCA) methodology to quantify the environmental impact of space missions over their entire life cycle [4].

A second factor complicating the notion of space sustainability follows the insight that new space technologies are key enablers for a more sustainable future. This is especially true for the recent growth in small satellite megaconstellations, providing frequently updated Earth Observation data, accommodating internet access in remote areas, or facilitating improved global navigation and communication. While these systems certainly provide great benefits on Earth and may contribute to the transition to a sustainable future, the environmental impact of developing, producing and operating these systems should also be addressed [5], [6]. In that regard, the development of propulsion systems suitable for use in small satellites, featuring high performance and a low environmental footprint, should be considered as one area of priority to enable truly sustainable space technology in the future [7]–[9]. Improving the technological capabilities in this field would not only mitigate the issues of space debris by allowing small satellites to avoid collisions and de-orbit after their operational life, but also reduce the environmental harm caused on Earth during the life cycle of these satellites.

Within the field of chemical space propulsion, the usage of hydrazine (N_2H_4) has been presented for the past three decades as the cause of serious sustainability issues for small satellite propulsion systems. Hydrazine is the industry standard for monopropellant and bipropellant systems for in-space propulsion, due to its high performance, good storage characteristics and extensive heritage. However, the substance is highly toxic, which has led to very stringent handling precautions and its inclusion in the European Chemical Agency's (ECHA's) candidate list of Substances of Very High Concern, potentially leading to restricted use or a complete ban in the future [10], [11]. The high cost related to hydrazine handling procedures and the regulatory uncertainty of its use have motivated an effort to find less toxic alternatives to hydrazine. These developments have been most successful in the realm of monopropellants, which is also the most relevant for the use case of small satellites [8], [12]. The promise of these "novel monopropellants" is often that they can provide improved performance compared to hydrazine, whilst greatly reducing the handling costs and not requiring excessive adaptations to existing hydrazine propulsion system architecture. These advantages would also increase the feasibility of including dedicated propulsion systems in most small satellites in the future.

While the inclusion of novel monopropellant systems may therefore be sure to aid in-space sustainability, it is not yet clear what their environmental impact is on Earth. Despite their description of being ”green monopropellants” in various sources, the main reasons for their adoption until now have been the cost reductions and regulatory certainty that they facilitate, and not necessarily their potentially reduced environmental harm or even their reduced toxicity [8], [13]. This thesis will therefore aim to further characterise the overall sustainability of novel monopropellant systems in comparison to conventional hydrazine monopropellant technology. This research goal is made attainable by the recent advancement of LCA methodologies and databases in the space industry, allowing for in-depth sustainability assessments of space systems [14], [15].

The rest of this report is structured as follows. Firstly, the state of the art in monopropellant research and sustainability assessments in the space industry is presented in Chapter 2. Following the identified research gaps, Chapter 3 will discuss the specific research questions that the thesis aims to answer, using the methodology formulated in Chapter 4. Chapters 5 and 6 set up the case study for which the comparative sustainability assessment will be performed. Then, in Chapter 7, the sustainability assessment is carried out following the fixed methodology of a life cycle sustainability assessment (LCSA). The results of this comparative LCSA are validated and evaluated in Chapter 8, after which Chapter 9 concludes the report with recommendations for future research.

2

Literature Review

2.1. Introduction

Before the research questions and methodology for this study were formulated, an in-depth literature review was performed, which is discussed in full in a separate report [16]. The main goals of the literature review were to gain a better understanding of the current state of art in liquid propulsion technology, the role of sustainability within this research field, the different interpretations of ”greenness” and ”sustainability” in the context of space technology, and the application of sustainability assessments within the space industry. This chapter will provide a shortened version of the literature review, mostly focused on the information that is used in the rest of the thesis.

An important note to preface this chapter is that the choice to focus on monopropellant systems in this research is a deliberate one. This narrow scope is not only a necessity due to the limited research time, but the result of a qualitative comparison between monopropellants and cryogenic and storable bipropellants, considering the typical use cases, the availability of conventional and novel propellant options and the key factors influencing the environmental, social and economic sustainability of the systems. The comparison found that economic sustainability is usually the prime motivation behind the replacement of conventional propellant options. In the case of monopropellants for example, it is the toxicity of hydrazine and the resulting high handling costs that have led to the development of new propellants. This will be discussed further in Section 2.2.

Furthermore, the overview identified that the introduction of potentially less environmentally harmful propellants has been most prominent for the case of monopropellants, with various demonstrations to date. Lastly, it was also deemed that the projected increase of small satellites in Low Earth Orbit (LEO) may cause serious harm to the Earth and LEO environment [5]. To protect the LEO environment, the amount of space debris introduced by each satellite must be limited, which can be achieved by including an on-board propulsion system. Including a propulsion system in a satellite may also lead to an increased impact on the Earth’s environment however, due to the production and pre-launch preparations for this system. As most small satellites use either electric or monopropellant propulsion, this presented another reason to investigate the life cycle sustainability of monopropellant systems in this thesis.

Section 2.2 will provide a summary of the state of the art in monopropellant systems, with a special focus on the wide range of monopropellants being proposed to replace hydrazine, being referred to as ”novel”, ”green” or ”non-toxic” monopropellants. To maintain a terminological clarity regarding sustainability, this report will henceforth refer to this group of propellants as *novel monopropellants*. After this, an overview will be given in Section 2.3 of the current understanding of sustainability within the space industry and the efforts underway to assess and improve the sustainability of space systems. This overview is mostly centred around the European industry and the application of the Life Cycle Assessment (LCA) therein. Finally, Section 2.4 will close the chapter with concluding remarks.

2.2. State of the art of monopropellant systems

This section gives an overview of the state of the art of monopropellant systems. Various authors indicate that there are generally five monopropellant types with acceptable performance, namely: hydrazine, hydrogen peroxide-based propellants, nitrous oxide-based propellants, Energetic Ionic Liquids (EILs), broadly made up of those based on ammonium dinitramide (ADN) and hydroxylammonium nitrate (HAN), and water electrolysis propulsion [7], [12], [13]. These options will be discussed in Subsection 2.2.1. Afterwards, Subsection 2.2.2 will provide an overview of typical monopropellant system architectures.

2.2.1. Conventional and novel monopropellants

Hydrazine

By far, the most commonly used monopropellant is hydrazine, which is defined by the chemical formula N_2H_4. After being identified and further developed by NASA as a highly performant and versatile substance, it was first used as a monopropellant in space in 1966 [17]. Since then, hydrazine technology has matured to become the standard for in-space propulsion, with numerous heritage orbital and interplanetary missions proving its reliability and performance. Some prominent examples among these are the propulsion systems for the GPS satellite constellation, the Cassini probe and the Voyager 1 and 2 spacecraft [17]–[19].

Hydrazine is valued as a propellant for several reasons: it has a relatively high density and high energy content, it can be reliably and simply decomposed with various catalysts that do not require pre-heating, and its end products have no carbon content, such that no soot is deposited on the combustion chamber and nozzle walls [20]. Because most high performing aerospace materials, such as inconel, titanium and various aluminium alloys, are compatible with hydrazine and able to withstand its moderate decomposition temperature, designing hydrazine systems is also rather straightforward [13]. Table 2.1 gives an overview of the most important physical properties of hydrazine.

Table 2.1: Physical properties of hydrazine, data from [21], [22]. Specific impulse (I_{sp}) for a nozzle expansion ratio (ϵ) of 50.

Parameter	Value	Unit
Chemical formula	N_2H_4	-
Molecular weight	32.05	g/mol
Density at 20 $^\circ C$	1010	kg/m^3
Vapour pressure at 20 $^\circ C$	1.4	kPa
Freezing point at 1 atm	1.5	$^\circ C$
Boiling point at 1 atm	95.5	$^\circ C$
Theoretical vacuum I_{sp}	225-250	s
Theoretical vacuum $\rho \cdot I_{sp}$	225-250	$g/cm^3 s$
Adiabatic decomposition temperature	850-1150	$^\circ C$

When stored in the absence of catalytic materials, hydrazine is relatively stable and does not decompose at a high rate, even when exposed to elevated temperatures. However, as one of its major strengths, it is very reactive when it comes in contact with specific catalysts. The first catalyst that was able to rapidly promote hydrazine decomposition at room temperature is Shell 405, which is made of iridium (Ir) deposited on a granulated alumina (Al_2O_3) support [23]. The catalyst is now produced as S-405 in the USA (and as H-KC12GA in Europe) and still used in the majority of commercial monopropellant hydrazine thrusters, even though iridium is a rare and expensive metal [23]–[25].

While using hydrazine allows for very simple, reliable and highly performing monopropellant systems, the substance itself is more problematic. First and foremost, pure hydrazine is highly toxic and must be handled with extreme caution. It is fatal if inhaled, toxic if swallowed and in contact with skin, causes severe skin burns and is a suspected carcinogen [11]. In addition to these hazards, hydrazine has also

been included in the European Chemical Agency's (ECHA) candidate list of Substances of Very High Concern (SVHC), as a part of the Registration, Evaluation, Authorisation and Restriction of Chemicals (REACH) Regulation, meaning that its use within the European Union may be restricted or only partially authorised in the future.

Handling hydrazine in a safe manner necessitates complex and strict procedures, which substantially increase the risk, cost and duration of spacecraft fuelling. The most well-known component of hydrazine loading procedures is probably the SCAPE suit, but this specialised piece of equipment is only one part of the added cost and effort related to hydrazine handling. Using SCAPE suits results in limited crew working periods, additional personnel that needs to stand by in case of emergencies and the high toxicity of hydrazine vapours requires very costly sensors to monitor the air for vapour concentrations [10]. The loading crew members also need to undergo regular medical checks. Hydrazine fuelling and the subsequent decontamination of loading equipment is lengthy and resource-intensive, resulting in hundreds of litres of contaminated water and iso-propanol alcohol (IPA) [26]. In summary, hydrazine's toxicity results in a multitude of issues that affect different parts of the life cycle.

Hydrogen peroxide-based propellants

Hydrogen peroxide (H_2O_2) is a chemical with numerous applications when used at a low concentration of 30-50%. At higher concentrations, >85%, it is often named High-Test Peroxide (HTP) and at even higher concentrations, >95%, the terms Rocket Grade Hydrogen Peroxide (RGHP) or Rocket Grade HTP are also used [12], [27]. It is one of the first rocket propellants that was researched and successfully used and saw different uses in the post-war period as well [27]. As a monopropellant, the USA used HTP for attitude control of several early launch vehicles and satellites and in turbopump gas generators, the latter application also being used in the Soviet Union and still in the current Russian launch vehicles [27], [28].

However, as soon as hydrazine monopropellant systems gained maturity in the USA, most research efforts for HTP monopropellant systems were halted [29]. The most commonly mentioned motivations for not using hydrogen peroxide are its stability and material compatibility issues (many of which are disputed and claimed to be outdated), the absence of a catalyst that is as reliable and durable as Shell 405 is with hydrazine, and HTP's lower inherent performance [13], [29], [30]. Indeed, when used in a typically achievable concentration of 98%, HTP's theoretical vacuum I_{sp} only equals 192 s, a 15% decrease from hydrazine's worst-case performance [31]. Hydrogen peroxide's other physical properties are shown in Table 2.2. Two notable advantages of HTP over hydrazine are its higher density and density I_{sp}, which can be valuable for volume limited applications.

Table 2.2: Physical properties of 98% hydrogen peroxide, data from [22], [31]. I_{sp} for $\epsilon = 50$.

Parameter	Value	Unit
Chemical formula	H_2O_2	-
Molecular weight	33.7	g/mol
Density at 20 $^\circ C$	1440	kg/m^3
Vapour pressure at 20 $^\circ C$	0.21	kPa
Freezing point at 1 atm	-2	$^\circ C$
Boiling point at 1 atm	148	$^\circ C$
Theoretical vacuum I_{sp}	190	s
Theoretical vacuum $\rho \cdot I_{sp}$	274	$g/cm^3 s$
Adiabatic decomposition temperature	940	$^\circ C$

HTP can be used on its own as a monopropellant, by thermally or catalytically promoting its exothermic decomposition reaction into oxygen and water. The simplicity and non-hazardous nature of this reaction is one of the reasons why HTP is still considered as one of the best candidates to replace hydrazine. Since the increased awareness of hydrazine's toxicity, starting in the 1990s, there have been numerous research efforts aiming to improve the performance of HTP monopropellant systems. Researchers at the Łukasiewicz Institute of Aviation in Warsaw have researched the performance of

various catalysts for HTP decomposition, and have recently started developing a full HTP monopropellant propulsion system suitable for minisatellites (< 500 kg) [32]–[34]. At the Korean Advanced Institute of Science and Technology (KAIST), various researchers have tested the performance of HTP blended with ethanol, including various full-scale thruster tests [35]–[38].The GRASP research project, funded by the European Commission, also led to various advances in HTP monopropellant technology, focusing on the development of new catalysts and a 20 N thruster [21], [39].

One additional advantage of HTP is that it can be stably blended with fuels, which combust with the superheated oxygen generated when HTP catalytically decomposes. With this additional reaction, the combustion chamber temperature and I_{sp} of HTP-based propellants can be increased. Several hydrocarbons can serve as suitable blending fuels, as long as they are hydrophilic and do not make the resulting blend too volatile or unstable. Baek et al. indicate that light alcohols are preferred as blending fuels, given that their short carbon chain can reach complete combustion [38]. With a blend of 70% HTP and ethanol at a stoichiometric oxidiser to fuel (O/F) ratio, Baek et al. calculate a theoretical maximum I_{sp} of 282s,thus higher than hydrazine, achieved at a combustion chamber temperature of around 1850 $^{\circ}C$ [38]. When more highly concentrated HTP is used, both performance metrics increase further [36].

The increased combustion chamber temperature presents a difficult trade-off for blended HTP propellants: the higher the O/F ratio, the higher the I_{sp}, but this comes at the price of having to use structural and catalytic materials that are able to withstand the very high combustion temperature. Historically, silver mesh catalysts were used to decompose HTP, but as the HTP concentration and adiabatic decomposition temperature increase, this material is no longer suitable, due to its melting point at 962 $^{\circ}C$ [33]. Instead, metals such as platinum and iridium, or various manganese oxides, deposited on a ceramic base such as alumina or different hexaaluminate compounds have proven to be active catalysts for HTP decomposition, where little catalyst preheating is required [36], [40], [41]. However, Lee and Kwon point out that the γ phase alumina support, which is used in S-405 catalyst, is unsuitable as it undergoes a phase shift at elevated temperatures, which greatly reduces its effective surface area, thereby decreasing its catalytic activity [36]. Another issue is that the Ir catalyst can become deactivated over several restarts, due to the oxidation of Ir and the inclusion of stabilisers in the HTP solution [40].

Stabilisers are added to HTP solutions to prevent the slow decomposition of HTP when stored during long periods of time. The rate at which HTP decomposes depends on various factors, from the HTP production process to the material and shape of the storage container. In the past, this slow decomposition and the limits it poses on the materials used in HTP propulsion systems have been used to argue that HTP has serious storability issues [17]. However, more modern data indicates that HTP solutions can be stored safely for a long time if the right material is used, such as various aluminium and zirconium alloys [42].

Although hydrogen peroxide is much more environmentally benign than hydrazine, it does contain some hazards for human health, as it is harmful if swallowed or inhaled and can also cause severe skin burns [43]. The ECHA also indicates that hydrogen peroxide is a strong oxidising liquid, stating that it may cause fire or explosion [43]. Even though HTP has non-negligible hazards, it is still likely to result in much safer, cheaper, shorter and more flexible handling procedures compared to hydrazine.

Nitrous oxide-based propellants

Nitrous oxide (N_2O) is another propellant that has been researched since the early days of rocketry [44]. After a period of limited interest in its use as a monopropellant, the past decade has seen an increase in research projects from commercial and institutional organisations. The research is mainly centred around the formulation of various Nitrous Oxide Fuel Blends (NOFBs), where liquefied nitrous oxide is blended with different hydrocarbons, acting as the fuel combusting with nitrous oxide as the oxidiser [12]. For example, the German Aerospace Center (DLR) has ongoing research on blends of nitrous oxide with ethene (C_2H_4) or ethane (C_2H_6), under the name ”Hydrocarbons mixed with Nitrous Oxide” (HyNOx) [45]. In a European Space Agency (ESA) funded research project, an NOFB using ethanol was selected through a trade-off and tested for handling safety and thruster performance [46]. Finally, another blend of nitrous oxide with a hydrocarbon was developed in the USA, by a company called

Firestar Engineering, with the name NOFBX [12], [47]. Although very high performance is claimed in the few papers that are written on this novel monopropellant, very little is known in general about NOFBX and Firestar Engineering seems to have been taken over or shut down.

NOFBs are able to provide I_{sp} in the range of bipropellant systems, as the blended monopropellants contain both fuel an oxidiser. Another benefit of NOFBs directly results from the physical properties of nitrous oxide; due to its high vapour pressure, nitrous oxide can be used in so-called self-pressurised systems, where the liquid propellant is contained in a tank pressurised by its own vapour, thus removing the need for a separate pressurant gas, such as nitrogen or helium. This could result in a substantial decrease in the propulsion system mass and complexity and also may enable in-space refuelling in the future [48]. The physical properties for nitrous oxide are presented in Table 2.3. Note that the density shown is for liquid nitrous oxide, which will only be present in the propellant tank if the internal pressure equals or exceeds the saturated vapour pressure of 52 bar. Due to the low density, the density specific impulse is also quite low compared to other monopropellants, making nitrous oxide or NOFBs less suitable for volume-limited applications.

Table 2.3: Physical properties of nitrous oxide, data from [12], [22]. I_{sp} for $\epsilon = 200$.

Parameter	Value	Unit
Chemical formula	N_2O	-
Molecular weight	44.01	g/mol
Liquid phase density at 20 $^\circ C$	745	kg/m^3
Vapour pressure at 20 $^\circ C$	5000	kPa
Freezing point at 1 atm	-91	$^\circ C$
Boiling point at 1 atm	-88	$^\circ C$
Theoretical vacuum I_{sp}	206	s
Theoretical vacuum $\rho \cdot I_{sp}$	154	$g/cm^3 s$
Adiabatic decomposition temperature	1640	$^\circ C$

The performance of the different NOFBs is presented in Table 2.4. Although the various thruster tests or simulations determining I_{sp} performance were conducted for different combustion chamber pressures, the table is meant to give an indication of the attainable performance of NOFBs. Each of the fuel blends presents superior I_{sp} than any of the other novel monopropellants in the HTP and EIL categories, which make NOFBs such an interesting option. However, due to the lower density, the density specific impulse is not as impressive. The high combustion temperature of the NOFBs also requires very specific design adjustments to the thrust chamber. Werling et al. report that the current DLR test thruster uses heat sink cooling with a copper alloy chamber structure, while Mayer et al. indicate that active cooling will be required when operating a full-scale NOFB thruster and Taylor describes that regenerative cooling was already implemented in NOFBX thruster tests [45]–[47].

Table 2.4: Performance parameters for various Nitrous Oxide Fuel Blends, data from [12]

Parameter	N_2O	HyNOx (ethene)	N_2O/Ethanol	NOFBX	Unit
Density at 20 $^\circ C$	745	879	892	700	kg/m^3
Theoretical vacuum I_{sp}	206	303	331	350	s
Theoretical vacuum $\rho \cdot I_{sp}$	154	266	295	245	$g/cm^3 s$
Maximum flame temperature	1640	2991	2820	2927	$^\circ C$

Although N_2O decomposition can be activated by Ir/Al_2O_3 catalysts such as S-405, the high decomposition temperature makes it so that the catalyst is deactivated after several restarts, creating issues similar to those found for HTP blended monopropellants [44]. This could be solved by using mixed metal oxide catalysts, as researched by Wallbank et al., but in general, especially for the NOFBs, external igniters are used in the various research efforts. For the HyNOx systems, spark plug and torch ignition using gaseous H_2 and O_2 have been tested and the NOFBX thrusters used spark plug ignition

[45], [47]. Another difficulty posed by the combustion of NOFBs is the possibility of flame flashback, due to the high vapour pressure and explosive nature of N_2O. To prevent this from happening, flashback arresters may be used, which introduce a certain flow resistance and thus quench the flame by reducing the pressure of the flame front travelling upstream [45].

Nitrous oxide is practically completely non-toxic. However, due to its very high vapour pressure it is a powerful asphyxiant, such that long periods of exposure may lead to a person feeling dizzy, losing consciousness and suffocating in the worst case [49]. Furthermore, the ECHA classification notes that nitrous oxide's strongly oxidising nature may cause or intensify fires. As it is usually stored in high pressure containers, the exposure to increased temperature may also lead to explosions. The historical use of nitrous oxide for propulsion applications also shows that the propellant holds significant dangers. During a testing activity of the Scaled Composites SpaceShipTwo in 2007, a large nitrous oxide tank exploded, killing three people [50]. Werling et al. also note that a further development project based on NOFBX, which was supported by the US Defense Advanced Research Projects Agency (DARPA), was cancelled due to explosions during ground tests [45].

EILs: Ammonium dinitramide-based propellants

Ammonium dinitramide (ADN, $[NH_4]^+[N(NO_2)_2]^-$) is a salt that was initially formulated in the 1960s in the USSR as a smokeless solid propellant oxidiser, for use in ballistic missiles and later re-invented in the USA in the late 1980s [21]. Its potential as a solid oxidiser was also identified by the Swedish Defence Research Agency (FOI). In 1995, the Swedish National Space Board started funding the development of novel monopropellants to replace hydrazine. In the project, the Swedish company ECAPS invented the LMP-103S monopropellant and the related "High-Performing Green Propellant" (HPGP) thruster technology, now developing models with thrust levels between 100 mN and 200 N. This novel monopropellant was flight-proven with a 1 N thruster on the ESA PRISMA mission and has since then been used on a number of commercial Earth observation satellites in the SkySat constellation [51]. The modern method to produce ADN is patented by the Swedish government and the Swedish company EURENCO Bofors is currently the only licensed ADN supplier in the world [21].

LMP-103S is an aqueous solution (13.95% H_2O) of the oxidiser ADN (63.00%), methanol (18.40%) used as a fuel and ammonia (4.65%) as a stabiliser. The inclusion of methanol in this propellant increases the volatility of the substance, which is undesirable for storage and safety concerns. As such, FOI continued the development of ADN-based monopropellants and formulated a less volatile propellant named FLP-106, composed of water, ADN and monomethylformamide (MMF) [52]. The main physical properties for both propellants are given in Table 2.5. Note that instead of a freezing temperature, the precipitation temperature is given, which indicates the point when the dissolved salt particles form a solid precipitate. It is clear that the I_{sp} of both novel monopropellants exceeds that of hydrazine. Due to their higher density, the $\rho \cdot I_{sp}$ is also much greater than that of hydrazine.

Table 2.5: Physical properties of ADN-based propellants LMP-103S and FLP-106, data from [21], [52], [53]. I_{sp} for $\epsilon = 40$.

Parameter	LMP-103S	FLP-106	Unit
Chemical composition	13.95 water, 63.00 ADN, 18.40 methanol, 4.65 ammonia	23.90 water, 64.60 ADN, 11.50 MMF	wt%
Molecular weight	87.36	91.24	g/mol
Density at 25 $^\circ C$	1238	1357	kg/m^3
Vapour pressure at 25$^\circ C$	13.6	<2.1	kPa
Precipitation temperature at 1 atm	-7	0	$^\circ C$
Boiling point at 1 atm	120	?	$^\circ C$
Theoretical vacuum I_{sp}	254	258	s
Theoretical vacuum $\rho \cdot I_{sp}$	314	350	$g/cm^3 s$
Maximum flame temperature	1645	1904	$^\circ C$

The HPGP thrusters developed by ECAPS operate by decomposing LMP-103S on a patented high temperature resistant catalyst bed, which uses a hexaaluminate support, since gamma-phase alumina and iridium (as used in S-405) are not suitable for the high combustion temperatures of ADN-based propellants [26]. This catalyst bed needs to be preheated to 340-360 $^{\circ}C$ to operate nominally, which is seen as a disadvantage when compared to hydrazine's catalytic decomposition with S-405, which can take place without preheating. The high combustion temperature of the ADN-based monopropellants not only affects the catalysts that can be used, but also the thruster's structural material. To withstand the high temperature, the ECAPS thrust chamber assembly uses a wall composed of rhenium (Re) and iridium (Ir), two rare metals with very high melting temperatures [51]. These thrust chamber assemblies are manufactured through an electroforming process named "EL-Form", patented by the American company Plasma Processes [54]. To eliminate the need of using these refractory metals, which complicate manufacturing processes, ECAPS has also developed a variant of LMP-103S with a lower combustion temperature and I_{sp}, while still outperforming hydrazine in terms of $\rho \cdot I_{sp}$. This "Green Propulsion" (GP) technology has not yet been flight proven, however [55]. Regarding general material compatibility, Freudenmann and Ciezki indicate that the ADN-based monopropellants are incompatible with copper and copper alloys, but generally compatible with other materials typically used with hydrazine, such as inconel and the Ti-6Al-4V titanium alloy [56].

The hazards related to LMP-103S are disclosed in a safety data sheet published by EURENCO Bofors and indicate that the propellant is harmful when swallowed, inhaled or in contact with skin [57]. The data sheet also indicates that LMP-103S contains fire and projection hazards. It is also relevant to consider the health hazards related to the separate components of the ADN-based propellants: although these substances will not easily exit the mixture, to be inhaled or ingested in a pure form, the separate health hazards are relevant for the production phase of the monopropellant. The most harmful substances in the ADN-based EILs are probably methanol and MMF. For methanol, the ECHA classification indicates that it is toxic via oral, dermal and inhaled contact and may damage the optic nerve and central nervous system [58]. MMF, on the other hand, is harmful in contact with skin, causes serious eye irritation and may damage fertility or the unborn child [59]. ADN by itself is less toxic: it is a flammable and explosive solid, is harmful if swallowed and may damage the stomach if orally ingested [60].

Through the PRISMA and SkySat launch campaigns and a dedicated loading demonstration at the NASA Wallops Flight Facility, LMP-103S has been qualified for range safety and loading operations at most major launch sites across the world, from Kourou to Vandenberg, Chennai and Baikonour [51], [61]. These campaigns have shown that standard personal protective gear, such as chemically resistant gloves, splash resistant clean room suits and safety glasses, is sufficient when loading the propellant [62]. These simplified loading requirements led to a cost reduction between 66 and 73% compared to hydrazine loading and an order of magnitude reduction in the amount of contaminated wastewater [26], [61]. Additionally, LMP-103S has received a United Nations (UN) certification 1.4S, so that it can be transported as air cargo in a specified container, leading to more affordable and flexible transportation procedure [62].

EILs: Hydroxylammonium nitrate-based propellants

Hydroxylammonium nitrate (HAN, $[NH_3OH]^+[NO_3]^-$) is another salt that has seen an increased research and development interest in the field of monopropellants in the past three decades. In the USA, research by the Army on propellants for artillery guns led to the formulation of several HAN-based monopropellants in the 1990s, each of which dissolved HAN in an aqueous solution with different hydrocarbon nitrates [63]. The potential of these propellants for small satellite applications was identified by NASA and in an effort to replace hydrazine for this mission type, further development of HAN-based monopropellants was funded. In 1998, the US Air Force Research Lab (AFRL) formulated AF-M315E, which is a blend of HAN, water and a fuel which is only described as "highly hygroscopic" in publications by Aerojet and NASA employees [64]. However, a recent publication by Chai et al. states that this fuel is hydroxylethylhydrazinum nitrate (HEHN) [65]. This is also confirmed by a patent filed to develop catalysts for use with HAN-based propellants [66].

To increase the maturity of the AF-M315E monopropellant technology, Aerojet developed new 1 and 22 N thrusters, named GR-1 and GR-22, the former of which was demonstrated in space during the NASA Green Propellant Infusion Mission (GPIM) [67]. Since then, AF-M315E has been renamed as

"ASCENT" and has become commercially available, such that other companies now also produce ASCENT thrusters for miniaturised propulsion (in the order of 100 mN) [65]. A NASA CubeSat mission, named Lunar Flashlight, was meant to investigate the presence of water on the Moon and be the first demonstration of novel monopropellant technology on an interplanetary CubeSat [68]. However, since its launch in December 2022, three out of the four 100 mN thrusters are underperforming, due to a suspected blockage in the propellant lines [69].

The Japanese space agency JAXA has supported the development of another HAN-based monopropellant since 2000. This propellant is called SHP163 and is made up of HAN, methanol, water and ammonium nitrate (AN) [70]. The performance of SHP163 has been flight-proven with a 1 N thruster in the Green Propellant Reaction Control System (GPRCS) on the JAXA RAPIS-1 satellite and tests with 20 N thrusters have also been performed on ground [70], [71]. There are other ionic liquid monopropellants using HAN, such as the High-performance Non-detonating Propellant (HNP) family, which substantially reduces the combustion temperature, or the Green Electric Monopropellant (GEM), developed by the American company Digital Solid-State Propulsion, which has an even higher I_{sp} than ASCENT or SHP163 [12]. However, these monopropellants are at a less advanced state than ASCENT and SHP163 and have not yet been flight qualified. As such, the further discussion will only consider ASCENT and SHP163 as HAN-based monopropellants.

Table 2.6 shows the main physical properties of the two HAN-based monopropellants. The I_{sp} of both options provides a substantial improvement with respect to hydrazine, but this comes at the expense of a very high combustion temperature. Furthermore, because it is a fully ionic liquid, Spores et al. indicate that ASCENT has no real freezing point: it rather becomes much more viscous after a glass transition point [67]. No data could be found regarding the boiling point of the propellants.

Table 2.6: Physical properties of HAN-based propellants ASCENT (AF-M315E) and SHP163, data from [12], [66]. I_{sp} for $\epsilon = 100$.

Parameter	ASCENT	SHP163	Unit
Chemical composition	11 water, 44.5 HAN, 44.5 HEHN	6.2 water, 73.6 HAN, 16.3 methanol, 3.9 AN	wt%
Molecular weight	106.62	80.15	g/mol
Density at 20$^\circ C$	1470	1400	kg/m^3
Vapour pressure at 25 $^\circ C$	1.4	?	kPa
Freezing temperature at 1 atm	<-80	<-30	$^\circ C$
Boiling point at 1 atm	?	?	$^\circ C$
Theoretical vacuum I_{sp}	260-270	276	s
Theoretical vacuum $\rho \cdot I_{sp}$	$\sim$390	386	$g/cm^3 s$
Maximum flame temperature	1893	2128	$^\circ C$

The decomposition of the HAN-based monopropellants is activated by preheated catalyst beds, similar to the ADN monopropellant technology. Iridium coated alumina, available commercially as S-405, has shown to be an active catalyst for HAN, but once again it has been reported that this catalyst rapidly loses its activity over extended operation periods [65]. Little is known about the LCH-240 catalyst used in the GPIM thrusters, as this technology is patented [67].

Regarding material compatibility, HAN starts to decompose when in contact with iron or copper particles [56]. Therefore, any alloy containing these metals is unsuitable as a tank material, whereas the popular Ti-6Al-4V alloy is suitable. At the other end of the propulsion system, the HAN-monopropellant thrusters are designed to deal with the high combustion temperature. The Aerojet GR thrusters use a similar combustion chamber as the ECAPS thrusters, made up of electroformed rhenium and iridium, separated from the flow control valve section via a thermal stand-off structure [67]. Another way of

dealing with the high combustion temperature is to use a thicker combustion chamber wall structure, which seems to have been implemented in the Japanese GPRCS thruster [70].

One of the main advantages of the HAN-based monopropellants is their reduced toxicity. Because ASCENT uses ionic liquids exclusively, its vapour pressure is negligible, which allows for open container handling without respiratory masks [64]. Furthermore, its viscosity is much higher than that of hydrazine, meaning that a leak or crack in the propulsion system will not result in a very large spillage of propellant. Nonetheless, ASCENT does pose severe hazards to human health if handled improperly, as it is toxic when inhaled, swallowed or in contact with skin, and may cause genetic defects if swallowed [72]. Additionally, ASCENT is classified as an explosive liquid (UN classification 1.4C). According to the safety data of SHP163 presented by Hori et al., this propellant is less toxic than ASCENT, as the oral and dermal toxicity are qualified as "Harmful" and not "Toxic" [70]. Considering the toxicity of the separate components in the HAN-based monopropellants, HAN is harmful if swallowed and toxic when in contact with skin, and it is a suspected carcinogen [73]. In addition, the ECHA notifies that HAN is an explosive with a mass explosion hazard.

A quantification of the loading costs saved by using HAN-based monopropellants as opposed to hydrazine has not yet been performed. However, Masse et al. indicate that per NASA safety regulations, the leakage of ASCENT is not considered to be a catastrophic failure, meaning that a single fault tolerance is allowed for handling procedures [64]. This leads to a great reduction in the complexity and cost of loading equipment and procedures: according to Masse et al., this could save tens of millions of US dollars for large interplanetary missions [64].

Water electrolysis

The final novel monopropellant technology uses liquid water as the carrier of both oxidiser (O_2) and fuel (H_2). The working principle is as follows, as explained by Gotzig [7]. Water is stored in liquid phase in a low pressure vessel, before it is fed to a electrolyser, splitting it into gaseous hydrogen and oxygen, which are then stored in separate high pressure tanks. The thruster then effectuates a bipropellant combustion of gaseous H_2 with gaseous O_2, such that theoretical I_{sp} values of up to 330 s may be achieved [74].

To date, only one water electrolysis propulsion system has been demonstrated in flight, namely on the NASA Pathfinder Technology Demonstrator CubeSat mission. For this application, the American company Tethers Unlimited developed the HYDROS-C propulsion system, demonstrating a maximum thrust of 2 N and an I_{sp} of 241 s in orbit, with an initial gaseous tank pressure of around 6.90 bar [75]. Researchers at the University of Stuttgart and ArianeGroup are developing a similar propulsion system [74]. Through funding of the DLR and ESA, ArianeGroup has developed and tested an integrated electrolyser/thruster model on ground, and plans to launch a technology demonstrator in 2026.

The physical and performance parameters of water are shown in Table 2.7. Note that the performance is shown for an O/F ratio of 8, as this is the stoichiometric ratio by which O_2 and H_2 are generated through the electrolysis of water [76]. A consequence of such an oxygen-rich propellant mix is the very high combustion temperature. This necessitates the use of film cooling, which is incorporated in the ArianeGroup thruster design [76]. There are various options to ignite gaseous oxygen/hydrogen combustion: next to catalytic ignition, spark and glow plugs are also common options for conventional LOX/LH_2 bipropellant systems. Hwang et al. produced platinum coated monolithic catalysts made with a porous ceramic support and achieved acceptable ignition delay times, but also noted that the reactivity decreased due to catalyst deactivation [77].

Using water as a propellant has a great amount of advantages. Firstly, as it is completely non-toxic and environmentally benign, there are practically no safety issues during ground handling, which removes many costly precautions and allows for new handling and transport concepts and improved flexibility. Secondly, water is suspected to be present on various celestial bodies in the Solar system, which makes in-situ resource utilisation an interesting concept to extend the lifetime of spacecraft using water electrolysis propulsion [75]. Thirdly, the generation of gaseous H_2 and O_2 could be used synergistically with other subsystems: the former in hydrogen fuel cells and the latter in life support systems for crewed spaceflight [77]. Lastly, the performance that water electrolysis propulsion achieves at a low power

Table 2.7: Physical properties of water, data from [76], [78]. I_{sp} for $\epsilon = 2.3$ and O/F = 8.

Parameter	Value	Unit
Chemical formula	H_2O	-
Molecular weight	18.02	g/mol
Density at 20 $^\circ C$	998.21	kg/m^3
Vapour pressure at 20 $^\circ C$	2.33	kPa
Freezing point at 1 atm	0	$^\circ C$
Boiling point at 1 atm	100	$^\circ C$
Theoretical vacuum I_{sp} (gH_2/gO_2 comb.)	325	s
Theoretical vacuum $\rho \cdot I_{sp}$ (gH_2/gO_2 comb.)	324.42	$g/cm^3 s$
Adiabatic combustion temperature (gH_2/gO_2 comb.)	2977	$^\circ C$

makes it more efficient than other electric propulsion technologies, while still exceeding the I_{sp} of most other monopropellant options, without including an explosive or toxic substances.

The main issues that currently limit the application of water electrolysis propulsion are the fact that its feasibility on a larger scale has not yet been tested. Scaling up the technology would probably lead to more challenging thermal management issues, necessitating a more complex active cooling system. Furthermore, if the chamber pressure should increase, the electrolysis and storage of the gases may also become more challenging. Another limitation of water electrolysis propulsion is that its performance depends strongly on the amount of gas that has been generated and stored, as chamber pressure drops off while the tank is emptied.

2.2.2. Typical monopropellant system architectures

Next to the propellant, the choice of the top-level system architecture is probably the design decision that has the largest impact on the propulsion system's performance and sustainability. One can categorise different monopropellant system architectures based on the manner by which the propellant is driven out of the storage tank. Two broad categories exist: pressure-fed systems and pump-fed systems.

Pressure-fed systems

Most commonly, a pressurised gas (the pressurant) is used to drive the propellant out of the tank to the thrusters, once the appropriate valves are opened. If the thruster performance is allowed to decrease over time, a so-called blow-down system can be used, in which the total amount of pressurant is stored in the propellant tank, where it expands and loses its initial pressure over the operational life. These systems are simple and robust, but have the disadvantage of a decreasing thrust level over the system lifetime.

Figure 2.1 shows the blow-down monopropellant system architecture used in the PRISMA mission, which was the first in-space use of the novel monopropellant LMP-103S [62]. Starting at the top, the system features a pressurant service valve to initially fill the pressurant side during the propellant loading procedure. This specific system uses gaseous Helium (GHe) as a pressurant. To ensure that the propellant is always located at the outlet of the tank, use is made of either a diaphragm, propellant management devices (PMDs) or a combination of both. Diaphragms can be made out of elastomers or metallic materials, the latter option resulting in a rolling diaphragm tank with superior sealing [79]. When an elastomeric diaphragm is used, special attention is required to ensure that the propellant is compatible with the diaphragm. In the case of the PRISMA system shown in Figure 2.1, a diaphragm using a new synthetic rubber, named SIFA-35, was qualified, as the standard diaphragm material used with hydrazine, AF-E-332, was not compatible with LMP-103S due to its silica content [80]. As an alternative to using a diaphragm spanning across the tank, a bladder tank uses an elastomeric bag fully encapsulating the propellant within the metallic tank shell, which is then emptied due to the pressure difference with the pressurant outside the bladder. Propellant management devices, on the other hand,

make use of the physical phenomena of adhesion and surface tension to contain the propellant within a desired volume in the tank when operating in a zero-gravity environment. Metallic vanes, sponges and other structures are used in this case to attract and ”trap” liquid propellant and direct it towards the outlet port.

Continuing along the propellant path in Figure 2.1, an orifice just downstream of the propellant tank is added to set the pressure and mass flow for the rest of the system. Next, the propellant service valve allows for the propellant side of the tank to be filled and emptied. A pressure transducer is present to monitor the propellant pressure in the lines, as well as a filter, to prevent any solid particles from entering the thruster assembly. The latch valve included just downstream of the filter acts as an isolation valve, to ensure that no propellant inadvertently reaches the thruster assembly. Finally, the thruster assembly may contain one or more thrusters, depending on the application, which each feature their own set of valves for redundant safety and thrust control. In the architecture shown in Figure 2.1, each thruster has a double seat flow control valve (FCV), which is a normally closed, series redundant solenoid valve to modify the mass flow and thrust delivered by the system [62]. In total, the system is thus double fault tolerant, meaning that if two valve seats open by accident, a third valve still needs to be activated to allow propellant flow to the thruster. This is especially crucial for hydrazine, as exposure to unprotected ground crew is catastrophic, with the additional danger that the propellant decomposes on a cold catalyst. For less toxic and reactive propellants, single fault tolerant systems may be safe enough, which would lead to substantial cost and schedule savings [9]. However, this system simplification also needs to be qualified with respect to the relevant regulations.

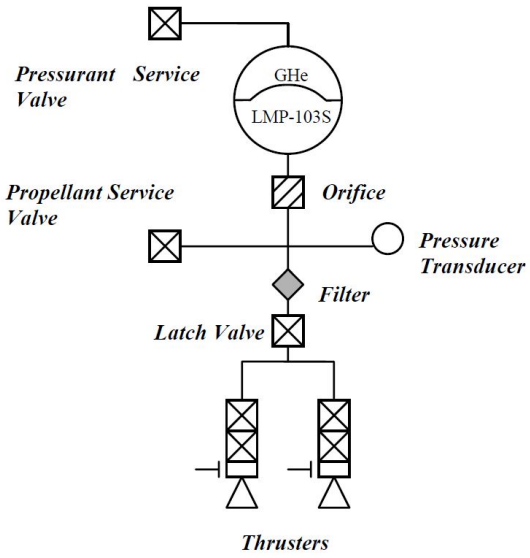

Figure 2.1: Schematic of a blow-down monopropellant system, from [62]

An alternative to the blow-down architecture is a self-pressurised system, where propellants with a high vapour pressure may be employed to maintain a phase equilibrium within the tank, such that the portion of propellant in the gaseous phase acts as a pressurant. As mentioned above, this is one of the advantages of the nitrous oxide-based propellants. While self-pressurisation reduces the total mass and complexity of the propulsion system and the complexity of the loading procedures, it also has some drawbacks and hazards that should be accounted for, such as temperature dependent tank pressure peaks and the non-linearly decreasing tank pressure over time [48].

If a constant tank pressure, and thus constant maximum delivered thrust, is desired throughout the system lifetime, a constant pressurant pressure is required. This is achieved in a pressure regulated system, where the pressurant is stored in a separate tank and fed to the propellant tank at a constant pressure using a pressure regulating device. This typically results in a larger, heavier and more complex system. Figure 2.2 shows a schematic of this architecture type. In this case, four propellant tanks are used due to system integration considerations. Furthermore, as the system uses the novel

monopropellant FLP-106, single fault tolerance is implemented, such that only two valves are placed between the tanks and the thruster. In the architecture of Figure 2.2, gaseous nitrogen (GN2) is stored in a tank for which the pressure is monitored with a pressure transducer (the icon with a P inside a circle) and then reduced with the pressure regulator before entering the propellant tanks. As in the blow-down architecture of Figure 2.1, various filters and valves throughout the system ensure that uncontaminated propellant or pressurant only leaves the respective tanks if the appropriate control signal is provided.

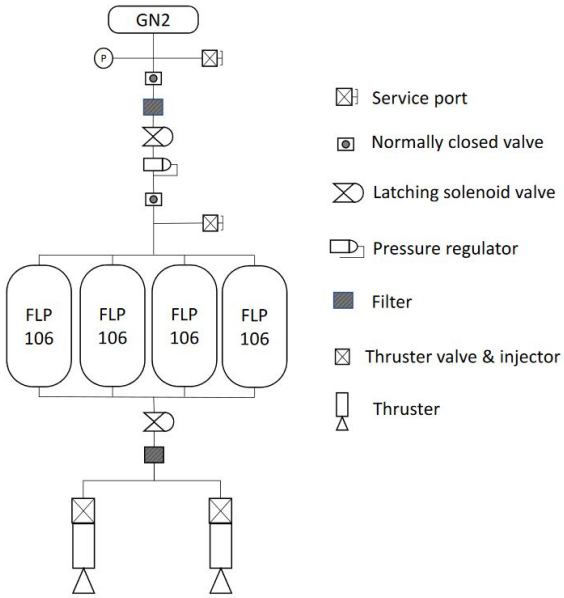

Figure 2.2: Schematic of a pressure regulated monopropellant system, from [81]

Pump-fed systems

Instead of using a pressurant gas to ”push” the propellant out of a pressurised tank, a pump can instead be used to ”pull” the propellant towards the thruster. One of the advantages of a pump-fed system is that the propellant does not need to be stored at high pressure, as the pump will increase the pressure of the fluid before entering the thruster assembly. This means that the propellant tank does not need to be designed as a pressure vessel, which reduces structural weight and provides more design freedom. This may be useful for certain nano-satellites, specifically the popular CubeSat standard, where a cuboid tank is more space-efficient than a cylindrical tank. In the Georgia Tech/NASA Lunar Flashlight Mission, a 6U CubeSat uses a cuboid tank in conjunction with a micropump which directs and pressurises the propellant into the thrusters [68]. The schematised architecture is shown in Figure 2.3. Note that the diagram shows a circular shape for the propellant tank, while it is actually a cuboid volume.

To maintain a sufficient tank pressure for the proper operation of the micropump, a small ullage volume of gaseous nitrogen is included in the AF-M315E propellant tank [83]. Furthermore, as the diagram indicates, vanes at the bottom of the tank serve as a propellant management device, ensuring that the liquid propellant is collected at the tank opening. Once again, single fault redundancy is implemented in the system. In this case, a solenoid propellant isolation valve must be opened before the propellant can flow through the orifice and micro-pump and then through each of the four single seat flow control valves to the thrusters.

For large liquid propulsion systems, pumps are usually complex and highly performing components, as the large propellant mass flow must be brought to chamber pressures of 100 bar and higher [84, p.365]. The pump shaft power is then typically provided by a gas turbine, which is driven by a portion of the fuel mass flow, or by the end products of a separate gas generator. However, in the case of miniaturised propulsion systems such as the one used in the Lunar Flashlight satellite, electric power is sufficient to drive the pump [83]. This reduces the complexity, risk and size of the pump, allowing its use for simple monopropellant systems, but it does place an additional burden on the total power budget.

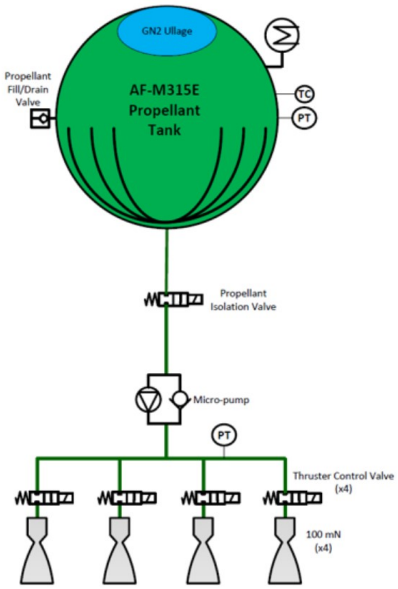

Figure 2.3: Schematic of a pump-fed monopropellant system, from [82]

2.3. Sustainability and space engineering

In this section, a brief overview will be presented of the current discourse regarding sustainability and green technology within space propulsion research and the space industry as a whole. This topic has gained importance in the past years, especially due to the activities of the European Space Agency (ESA) in its Clean Space initiative, which was founded in 2012 [85]. Subsection 2.3.1 will first delve into the history and definition of sustainability and greenness, to provide context for the way in which these terms are used in relation to novel monopropellants. This discussion is especially relevant as it does not yet appear as though there is a consensus on this terminology within novel monopropellant literature. After this, the state of the art in sustainability assessments in the space industry is discussed in Subsection 2.3.2, mainly focusing on the adoption of the LCA methodology. An important goal of this section is to highlight the different meanings of sustainability in novel monopropellant research and in the emerging field of ecodesign and LCA within the space sector.

2.3.1. Defining sustainability and greenness

While the term ”sustainability” has become more popular in the past years, it is rooted in a long history which arguably started centuries ago, before being categorised as related to ”sustainable development” in the late 1960s and early 1970s. In a comprehensive review article on the discourse of sustainability and sustainable development, Purvis et al. point to the famous publication of ”The Limits to Growth”, a report commissioned by the Club of Rome in 1972, as the first time that the terminology of sustainability was used in the modern understanding of the concept [86]. ”The Limits to Growth” was a very influential report, as it was the first to present the inherent issues related to (unsustainable) economic growth, which does not take into account environmental aspects such as resource depletion, global warming, and other damage to ecosystems [87]. After its publication, a large movement adopted its main idea, questioning the centrality of economic growth in the forms of capitalism which were emerging in the post-war ”development” of the world that was supported by European and American powers. This movement was made up of various political and academic actors, under the broad call for sustainability or sustainable development.

However, the fact that various groups with different motives jointly shaped what ”sustainability” means, has turned sustainability into a somewhat vague term. One definition that is accepted in a multitude of academic and professional fields, is that proposed by the UN Brundtland Commission, which published their report ”Our Common Future” in 1987. Sustainable development was defined by the commission

as *"meeting the needs and aspirations of the present generation without compromising the ability of future generations to meet their needs"* [88]. This definition also contains the triple pillar character of sustainability, namely that a solution can only be truly sustainable if it is able to combine economic, environmental and social concerns, as represented by the diagram in Figure 2.4. Developing a sustainable technology thus necessitates an understanding of its impact on the economic, environmental and social frame in which it operates. The idea of triple pillar sustainability is also contained within the 17 UN Sustainable Development Goals (SDGs), where concrete goals are set out for companies or countries to strive towards, in an effort to tackle current social, economic and environmental issues [89].

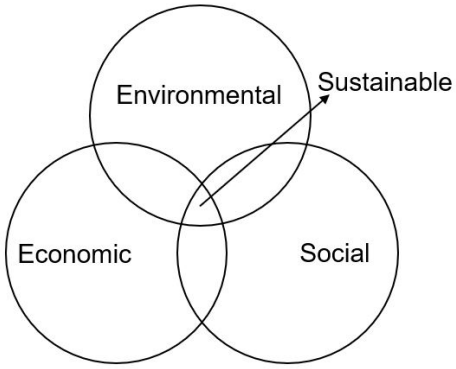

Figure 2.4: Triple circle representation of sustainability

Interestingly, in the context of novel monopropellants, the adjective ”green” is used much more often than ”sustainable”. However, the definition of ”greenness” in this context is not entirely clear either. Colloquially, green technologies refer to developments with a reduced environmental impact, but Carlotti and Maggi find that the meaning of ”green” in the context of ”green propulsion” is probably best encapsulated by the broad field of Green Chemistry [22]. This scientific approach towards chemical processing was devised by Paul Anastas in the early 1990s and defined as: *"the design of chemical products and processes that reduce or eliminate the use and generation of hazardous substances"*, clearly being relevant for the case of conventional monopropellants [90]. Notably, Anastas and Lankey mention that Green Chemistry is ”economically driven rather than economically draining”, indicating that Green Chemistry is seen as a synergy between environmental and economic sustainability [91]. Reducing the toxicity and danger of chemicals being used in industry can also have important social benefits, however, related to worker well-being and the reduced risk of polluting shared natural resources such as potable water.

While the terms ”green” and ”non-toxic” are most often used when discussing potential replacements for hydrazine, Marshall and Deans consider this to be misleading, as novel monopropellants are neither inherently environmentally benign nor completely non-toxic [8]. Furthermore, most researchers consider the greatest advantages of novel monopropellants not to be their reduced toxicity per se, but rather the potential reduction in propellant handling and fuelling costs, and the increase in performance [10], [13]. This is also the reason why the EIL novel monopropellants are seen as the most promising replacements for hydrazine; a reduced loading cost has been demonstrated and their I_{sp} exceeds that of hydrazine, enabling increased mission performance. This consideration may indicate that most novel monopropellant research has not been in search of a more environmentally or socially sustainable type of space propulsion, but a more economically sustainable one, as the life cycle cost of hydrazine has become overly inhibitory towards newer, smaller and commercial satellites.

2.3.2. Sustainability assessments in space engineering

More or less separately from the increased interest in novel monopropellants, there has been a growing notion within the space industry, primarily in Europe, that sustainability should have a more central role within the future of spaceflight. The quote *"If you love space, you love clean space"*, by former

Director General of ESA Jean-Jacques Dordain at the 2023 ESA Clean Space Industry Days, very nicely expresses the sentiment that there will be no future of spaceflight unless it is a ”clean” one, adding another term to the ambiguous dictionary of sustainability. Still, this sentiment brings up a valid point, for a variety of reasons. Firstly, the increasing issue of space debris makes it more risky and expensive, and potentially impossible in the future, to launch new satellites into useful orbits, primarily in LEO. Secondly, there are also economic incentives to improve the sustainable use of resources within the space sector, for example related to reusable launch vehicles or in-orbit servicing [92]. Lastly, as for any industry, the space industry will have to reduce its environmental impact in the coming decades in order to play its part in averting an impending climate catastrophe due to global warming. As proposed future space projects would greatly increase the frequency of launches, it is especially relevant now to assess and minimise the environmental damage that these activities would induce, before it is too late [5].

With these issues in mind, ESA formally created its Clean Space initiative in 2012, after an initial project, named Ecosat, performed an LCA for a conceptual satellite in 2009 [85]. The Clean Space office has three focal areas: Management of end of life, In-orbit servicing and Ecodesign. Whereas the first two mostly relate to in-space sustainability, minimising space debris, facilitating in-orbit recycling and safe re-entry, the Ecodesign branch is concerned more with reducing the life cycle impact of space activities on the Earth’s environment. ESA has been on the forefront of the emergent field of space sustainability, supporting missions such as ClearSpace-1, which aims to become the first satellite to actively remove space debris, and new companies such as MaiaSpace, striving to develop more sustainable launch vehicles [93], [94]. The annual Clean Space Industry days are another initiative through which the Clean Space office has continually promoted and coordinated the inclusion of sustainability within the European space sector.

Application of life cycle assessment in the space industry

When it comes to the assessment of sustainability, one of the Clean Space office’s main goals has also been to promote and over time require the application of environmental LCAs (E-LCAs) within European space activities. The choice to specifically choose the LCA method as a way to quantitatively estimate the environmental impact of specific activities is not at all arbitrary, as it has been developed since the 1990s and been adopted in various other industries [95]. Standardised in ISO 14040:2006, the LCA method has several key benefits due to its comprehensive and well-structured nature [96], [97]. While the method will be described in more detail in Chapter 4, a brief overview is given here of the most important characteristics of an LCA.

Firstly, the LCA method emphasises a clear definition of the system boundaries, ensuring that the LCA practitioner and anyone interpreting the results clearly understands what falls inside the scope of the study. Within these boundaries, the included life cycle phases must also be specified, desirably being as complete as possible, but certainly indicating whether the assessment considers the activity or product from the point of raw material extraction to the start of its use (cradle-to-gate), to its disposal (cradle-to-grave) or potential recycling (cradle-to-cradle). For the product being studied in the LCA, it is thus required to have a clear overview of the various processes involved in its life cycle, with the material inputs and outputs being listed in the life cycle inventory (LCI). This insight into a product’s life cycle can also provide benefits outside of quantifying its environmental impact, as it may identify potential development improvements or sensitive areas within the supply chain [98]. In the end, an E-LCA assesses the product’s environmental impact based on a multitude of impact categories covering various environmental issues, such as acidification, climate change, eutrophication or resource depletion. The inclusion of a product’s entire life cycle and of a variety of environmental impact categories are two key advantages of the LCA method when compared to other environmental impact assessment methodologies, primarily because it solves the issue of burden shifting [97]. Burden shifting occurs when a specific environmental issue in a product’s life cycle is seemingly solved by a design or process change, while it actually leads to an increased impact in another life cycle phase or environmental impact category. This cannot occur unnoticed in a proper LCA, however.

Since the first application of the LCA method for a space system with the Ecosat project, ESA Clean Space has taken up the task of adjusting and harmonising the application of environmental LCA for space technologies. Because the space industry differs from other industries with regards to typical

system life cycles, the length of system development, the geographic spread of various actors within the life cycle, and the eventual disposal of the system, an ESA handbook has been published providing guidelines for space LCA practitioners to deal with these differences [99]. Additionally, space systems often use very specific materials or processes, making the use of standard LCA databases less reliable [98]. As primary data collection (i.e. directly from the sources that the LCA is studying) is quite challenging in the space industry, ESA has therefore also created an LCA database that can be requested freely by anyone with a valid license to the LCA database ecoinvent, which is a popular database containing a great number of high-quality datasets for processes in a variety of industries, such as the electricity, transport and metal industries [100], [101]. The requirement for a valid ecoinvent license comes from the fact that the ESA LCA database uses ecoinvent datasets to model various upstream processes.

The open call from ESA towards academia and industry to perform E-LCAs to validate and add new data in the ESA LCA database has indeed resulted in a growth in the space LCA literature [4]. Many of these studies have been performed in collaboration with ESA, but some studies have also been performed in the USA, primarily investigating the environmental impact of launch vehicles [102], [103]. Among the LCA studies performed in Europe, a large part is not publicly available, but both review papers and the ESA LCA database itself indicate that most research has gone into LCAs of materials and propellants [4]. Larger scale LCA studies have also been performed for the Ariane 5 launch vehicle, with LCA findings being actively used during the development of Ariane 6 as well [104], [105]. In his master's thesis, Schabedoth has provided a comparative LCA of launch vehicles using different propellant options [106]. In-depth LCAs have also been performed for the Proba V and Sentinel 3B ESA missions, resulting in ecodesign options that may be applied to reduce the environmental impact of future satellites [107]. In many of the studies referenced here, the main difficulties are similar, relating to achieving an accurate representation of system life cycles within the complex space sector and obtaining primary data from industrial actors [108].

Life cycle sustainability assessment: the next step in space sustainability?

The efforts to assess and include sustainability in the space industry discussed so far have only focused on the environmental impact of space activities and technologies. However, as indicated by the triple-pillar understanding of sustainability, schematised in Figure 2.4, sustainability entails more than just the protecting the natural environment. If the economic and social dimensions of sustainability are not included when analysing space systems, one runs the risk of burden shifting in the sense that the mitigation of an environmental impact may result in an unbearable social or economic cost. Within the field of LCA studies, this realisation has led to the development of the Life Cycle Sustainability Assessment (LCSA) methodology wherein the results of an environmental LCA are combined with those from a social LCA (S-LCA) and an economic Life Cycle Costing (LCC) [109]. An LCSA practitioner is presented with a choice as to how to combine or compare the results related to the three sustainability dimensions, but what is certain is that LCSA results may present a more complete and useful overview of a system's sustainability. The fact that the economic advantages of novel monopropellant handling have been a key driver in replacing hydrazine also makes the LCSA methodology apt in this specific case, as these advantages should also be reflected in the end results.

In his doctoral thesis, Wilson developed a comprehensive LCSA method specifically for the assessment of space systems, with the prime motivation of aligning the field of space sustainability with more recent developments in sustainability studies [110]. This LCSA method is made up of an E-LCA in line with the ESA guidelines, an S-LCA based on the assessment of risks with respect to various stakeholder groups, and an LCC compiling the costs and revenues throughout the life cycle. Because of the inclusion of triple-pillar sustainability and the fact that the method was developed specifically for space systems, it was decided to use this methodology in this research. As such, more details on the method will be provided in Chapter 4.

Next to developing an LCSA methodology fit for use in the space sector, Wilson has also created an LCA database of space-specific processes, including all necessary data to perform environmental, social and economic LCAs, as well as the combined LCSA. This database is called the Strathclyde Space Systems Database (SSSD) and is freely available to anyone with a valid ecoinvent license, as ecoinvent is used for secondary data, similar to how the ESA LCA database is constructed [111]. While the SSSD includes more information per process than the ESA LCA database, as it includes social

and costing data next to the material inputs and outputs required to perform an E-LCA, the ESA LCA database includes more datasets for specific processes. A portion of the SSSD datasets have also been validated with the ESA LCA database. Overall, the goal of the SSSD is not to replace the ESA LCA database, but to provide a simpler, easy to use database and methodology to include LCSA results in early design stages.

The SSSD is increasingly being applied for a variety of research scopes, from informing specific ecodesign choices to comparing the exploitation of reusable launch vehicles or assessing the global impact of proposed space activities [5], [14], [92]. Regarding an assessment of monopropellants specifically, one publication presents two LCSAs, first comparing the overall sustainability of the production of 1 kg of hydrazine versus that of 1 kg of LMP-103S, and then comparing the overall sustainability of using hydrazine or LMP-103S in the propulsion system of a conceptual mission [112]. In this article, it is found that the production of LMP-103S and the LMP-103S system both result in a reduced environmental and social impact, while it does cost more compared to hydrazine production and the hydrazine propulsion system, respectively. Interestingly, a more recent publication reverses the conclusion related to the production of LMP-103S, indicating that this has a larger environmental impact than hydrazine production [14]. Still, the LCSA of mission using LMP-103S does lead to a smaller environmental impact compared to the option using hydrazine, due to the mass savings related to LMP-103S's superior propulsive performance. These results point out how important it is within LCSA studies to consider the most recent data and to understand what the system-level implications of design changes will be, even if they fall outside the LCSA system boundaries. Other case studies have also indicated that the use of germanium in solar arrays often leads to an environmental hotspot, and that the replacement of argon by ASCENT as a propellant for the Attitude and Orbit Control System (AOCS) does not result in substantial environmental savings [110].

2.4. Conclusion

This chapter has discussed an increasing focus on sustainability concerns within the space industry from two perspectives. First, an overview was given of the growing field of novel monopropellant research, which has the main purpose of identifying and developing propellants (and compatible propulsion systems), that are less toxic than hydrazine, which has been a standard choice within monopropellant systems since the 1960s. With the reduction in propellant toxicity, it is expected that spacecraft fuelling would become much cheaper, thereby increasing the feasibility of using chemical monopropellant systems in smaller and cheaper satellites. It was found that there are generally four types of novel monopropellants around which the bulk of research and development is centred. Of these four groups, the EIL monopropellants, based on ADN or HAN, have most recently and clearly demonstrated their ability to replace hydrazine in a variety of use cases, exceeding the conventional monopropellant's performance whilst being much easier to handle.

While the novel monopropellants each have their advantages with respect to hydrazine, they certainly also have features making it less easy or desirable to replace hydrazine with them. Most of these issues are related to the different materials that must be used in the propulsion system when replacing hydrazine. For example, the increased combustion temperature of nitrous oxide fuel blends, EILs or water electrolysis propulsion necessitate the use of active cooling, resulting in complex nozzle structures, or of refractory metals in the chamber and nozzle walls, which are able to withstand the extreme temperatures. Furthermore, the robust chemical reaction by which hydrazine decomposes catalytically over Ir/Al_2O_3 catalysts is not easily reproducible with novel monopropellants, as these may poison the catalytic component over time, or weaken the structural support because of a high combustion temperature.

The main conclusion following the review of novel monopropellant technologies could be that there are various promising avenues being followed by different countries and institutions, each requiring additional development before proving to be an adequate replacement for hydrazine. If one would have to indicate a single propellant that is the most capable drop-in replacement of hydrazine, it would probably be LMP-103S, an ADN-based EIL, which has been used in space successfully in more than 20 LEO satellites to date [51]. However, it is also important not to fixate on the idea of finding a propellant that

works in exactly the same type of architecture as used in hydrazine systems. As the NOFB and water electrolysis options indicate, unique propellant characteristics may also allow for additional system benefits that hydrazine is unable to facilitate, for example related to self-pressurisation or the dual use of propellants in other spacecraft subsystems.

A second way in which sustainability has recently become a more salient topic in the space industry is through the advancement of the LCA methodology specifically tailored to space systems. Primarily due to the efforts of the ESA Clean Space initiative and its goal of integrating ecodesign within standard space design activities, various environmental LCAs have been performed for past and conceptual space missions, all of which improve the quality of future LCAs within the sector. By releasing a handbook and database to perform E-LCAs, ESA also aims to harmonise the LCA methodology throughout Europe.

However, as a brief historical review of the concept has indicated, a comprehensive view of sustainability should also deal with social and economic concerns, with the overall goal of meeting today's needs without compromising the ability of future generations to do so as well [88]. In the specific case of novel monopropellants, it is additionally valuable to include the social and economic perspectives because it is often from these perspectives that the hegemony of hydrazine is seen as unsustainable. To assess the impact of a system on all three pillars of sustainability, the LCA methodology has been adapted in the past, leading to the concept of a Life Cycle Sustainability Assessment, which combines environmental, social and economic LCA results. Wilson has developed an LCSA framework and database to specifically facilitate the application of LCSA for space systems [110]. This framework is aligned with the ESA LCA methodology and is continually being improved and updated, such that it creates a useful tool for LCSA practitioners in the space sector.

Comparing the state of the art of novel monopropellants and of sustainability studies in the space industry, a few insights and differences are especially prominent. Firstly, it is remarkable that the use of the term "green" and "sustainable" in novel monopropellant research is used in a vague manner, leading to unclear motivations for why certain novel monopropellants are preferred over others. Secondly, there is a rather large focus on the issue of propellant toxicity and handling cost in novel monopropellant research, while other environmental, social and economic issues are not investigated with the same amount of detail. Thirdly, while the application of LCAs and LCSAs in the space industry has matured over the past years, there have been few studies systematically comparing propulsion options, or novel monopropellant options specifically. This finding is also uncertain however, as many results from space LCA studies are not publicly available. With these conclusions in mind, Chapter 3 will identify the research gap that this thesis will aim to fill and formulate suitable research questions to structure the rest of the study.

3

Research Questions

3.1. Introduction

In this chapter, the findings of the literature review will be used to identify the gap in the existing literature that this thesis could fill. To that end, Section 3.2 will summarise the main areas within the literature where additional research would be beneficial and prioritise a specific area for this thesis. Thereafter, Section 3.3 will present the main research question of this thesis and the subquestions that it can be broken up into. Lastly, Section 3.4 will conclude the chapter.

3.2. Research gaps

One of the main findings in Chapter 2 was that there is a discrepancy between the increasingly nuanced understanding of how to assess and incorporate sustainability in space systems from the perspective of LCA and LCSA studies, which include a multitude of impact categories and consider the entire life cycle of systems, and the more basic comparison of conventional and novel monopropellants, where there is a single focus on the toxicity and cost of handling of the various propellants. This finding leads to various possible avenues for future research. One possibility could be to identify other metrics, separate from toxicity, which influence the overall sustainability of using a specific propellant. Developing a methodology to combine this variety of metrics would then facilitate a more robust comparison.

Secondly, there is a lack of research on the environmental hotspots within a propellant's life cycle. While E-LCAs have been performed for a few monopropellants, no comprehensive assessment has presented the actual impact of propellant handling on the environment, or the severity of this impact compared to other environmental damage resulting from propellant production, transport or usage. As the toxicity of the propellant might actually be more problematic at the level of individual workers and the economic cost of ensuring safety, it could also be useful to develop a methodology which qualitatively compares or integrates these impacts with more traditional E-LCA impact categories.

Another area where additional research would be beneficial is in the application of LCAs to guide or augment the development of new space technologies. At the moment, many publications regarding the LCA of space systems are not peer-reviewed and serve to further improve the ESA LCA framework and database [4]. With the intricate details that LCA results are able to uncover, not only on the environmental impacts of a system but also on the characteristics of a system's life cycle, an LCA could be used to quantitatively verify or assert specific claims when performing a design trade-off, for example. As the comparison of expendable and reusable launch vehicles using various propellants is currently an important topic of discussion within the space industry, various research papers and presentations have performed LCAs of high quality to objectively provide an insight into the environmental facet of this comparison [92], [103], [106], [113]. Similar LCA studies outlining the environmental impacts of other contemporary and future plans in the space industry, for example regarding the development of

several commercial space stations in LEO, or of settlements on the Moon or Mars, have only been performed in a limited manner [5].

In the field of novel monopropellant research, the insight provided by LCA or LCSA studies is sorely missing, leading to unsubstantiated claims of ”green” propellants, something which is also acknowledged within the novel monopropellant research community itself [21]. One of the key research gaps that the literature review has also identified is that the impacts of system-level design changes required to accommodate novel monopropellants, whether environmental, social or economic, have not yet been investigated in detail. This deficiency is deemed to be rather important, as it is undesirable that the options replacing hydrazine propulsion systems would lead to unforeseen or aggravated issues from an environmental, social or economic perspective. This research gap leads to the research objective of this thesis, as expressed in the following section.

3.3. Main research questions

Considering the research gaps identified through literature, the main research objective of this thesis will be:

To gain a better understanding of the three-pillar, system-level sustainability of novel and conventional monopropellant systems, using the analytical tools afforded by life cycle assessment methodologies.

Aiming to lend a practical insight into the comparative sustainability of the various monopropellant options, the main research question is the following:

How does the choice of propellant impact the environmental, social and economic life cycle sustainability of a representative monopropellant system?

While this main question frames the research in a way that is agnostic to which propellants might be used in a ”representative monopropellant system”, the research will take hydrazine as a baseline option and then compare this to several novel monopropellant options. Furthermore, the choice is made to include all three sustainability dimensions, firstly because this is feasible when applying the LCSA methodology and secondly because the insight into all three aspects would be most useful for researchers or engineers trading off hydrazine and other propulsion options in practice. Lastly, the research question narrows its scope to a specific usage of monopropellants, namely a ”representative monopropellant system”, such that it is feasible to perform a complete LCSA of this system and to clearly indicate what the final results of the research will be valid for.

As the main research question is quite broad, it is divided into several subquestions which will provide a guideline for the overall research methodology presented in Chapter 4. The subquestions are categorised in three sets: the first aims to define what a ”representative monopropellant system” is, the second considers the overall findings of the sustainability assessment, and the third wishes to link the answers from the second set to the propulsion system design, to be able to formulate design recommendations.

The subquestions of the first set are listed below and will be answered mostly in Chapter 5 and Chapter 6. The answers to these questions serve not only to structure the rest of the research, but also to provide an indication of what a design process including conventional and novel monopropellants might look like.

- SQ-1.1: For which use case of monopropellant systems is a better understanding of life cycle sustainability most valuable?
- SQ-1.2: What are the propulsion system requirements for the use case found in SQ-1.1?
- SQ-1.3: Which novel monopropellants are best suited for the use case found in SQ-1.1?
- SQ-1.4: Which sustainability issues are currently considered to be the most problematic for the use case found in SQ-1.1?
- SQ-1.5: What is the design of a propulsion subsystem fulfilling each of the system requirements found in SQ-1.2, for each of the monopropellants selected in SQ-1.3?

The second set of questions, moving to the sustainability assessment itself, will be answered in Chapter 7 and Chapter 8. In Chapter 4, the methodological choice to perform LCSAs for the various monopropellant system designs will be discussed. At this point however, the formulation of the subquestions already assumes this and reflects the fact that the results will elucidate impacts in multiple impact categories in all three pillars. The subquestions related to the LCSA results themselves are:

- SQ-2.1: Which monopropellant system scores the best in each of the sustainability dimensions (environmental, social, economic)?
- SQ-2.2: Which monopropellant system is the most sustainable overall?
- SQ-2.3: Which impact categories feature the largest and smallest differences between the different monopropellant systems?
- SQ-2.4: Which life cycle phases feature the largest and smallest differences between the different monopropellant systems?

The final set of subquestions aims to analyse which design and process features drive the major impacts identified in the second set of subquestions. In the future, the most problematic components or life cycle steps may then be targeted for further development as to minimize their environmental, social and economic burdens. Additionally, this might lead to a better insight into the sustainability of other monopropellant technologies that may not be included in this research but use similar components or materials. The subquestions of the third set, which will be answered in Chapter 7 and Chapter 8, are:

- SQ-3.1: Which components in the monopropellant systems have the largest impact in each of the sustainability dimensions?
- SQ-3.2: Which components in the monopropellant systems drive the differences between the sustainability scores of each of the options?
- SQ-3.3: Which activities and processes in the life cycle of the monopropellant systems have the largest impact in each of the sustainability dimensions?
- SQ-3.4: Which activities and processes in the life cycle of the monopropellant systems drive the differences between the sustainability scores of each of the options?

3.4. Conclusion

In this chapter, the findings of the literature study have been used to identify relevant gaps in the literature that might be filled by future research. It was found that the assessment of sustainability within the field of novel monopropellant systems is still rather simplistic, and that this could be aided by the implementation of LCA or LCSA methodologies. Some research gaps are therefore related to the development of new sustainability assessment methods, combining the current focus on human toxicity and handling cost within novel monopropellant research with a broader view on sustainability as presented in the LCA methodology. In this thesis however, the goal will be to better understand how a change in monopropellant impacts the propulsion system design, and how that in turn affects the entire system's sustainability, in terms of the environmental, social and economic impact.

The main research question proposed is therefore: *"How does the choice of propellant impact the environmental, social and economic life cycle sustainability of a representative monopropellant system?"* This main research question has been divided into three sets of subquestions, 13 in total, each centred around a different part of the research. The first set of questions is concerned with defining for which use case of monopropellants a sustainability assessment would be most relevant and useful. The second set delves into the the results of the sustainability assessment itself, already positing that this will be performed with an LCSA, and aims to identify the main conclusions therein. The final set considers the propulsion system at the level of its components and the processes that make up its life cycle, investigating which of these have the largest impact on the LCSA results and which drive the differences between the propellant options included in the study.

4

Research Method and Materials

4.1. Introduction

With an overview of prior research being established in Chapter 2 and the research questions defined in Chapter 3, this chapter presents the methodology that will be applied in this research. The development of a suitable research method to answer the main research question may be subjective at certain points, which is why Section 4.2 will indicate key methodological choices and provide the rationale for each of them. Providing a general structure of the research also serves to delineate what the end results actually mean and in which capacity they answer the research questions. The research is broadly divided in two parts, the first selecting a case study for the use of monopropellants and designing propulsion systems for various propellant options, and the second performing an LCSA for each of these propulsion system designs. The overall methodology used for each part will be specified in Section 4.3 and Section 4.4 respectively. This chapter aims to give a general overview of the research method and the most important methodological choices, while more specific details within the methodology are only included in later chapters, such that their impact on the results can be appreciated more clearly. This is mostly the case in Chapter 6, where the calculations made in the design of the propulsion systems are presented. As the research will make use of different computer programmes and many data sources, especially during the LCSA portion of the project, a brief discussion on this aspect is presented in Section 4.5. As always, the chapter is ended by a concluding section.

4.2. General research structure

As indicated by the division of subquestions in Chapter 3, an adequate answer to the main research question is deemed to be composed of three steps. First, a specific use case of monopropellants should be defined, for which an insight into the system sustainability is most feasible and useful, and propulsion systems should be designed for a number of monopropellants. Secondly, LCSAs are performed for the system of each considered propellant option. Lastly, the results from these LCSAs are compared and interpreted, to investigate how the sustainability of the propulsion system is affected by the difference in propellant. This general structure is reflected in the work flow diagrams presented in Figure 4.1 and Figure 4.2, which will now be discussed in more detail, providing a rationale for the methodological choices made in each of the research steps.

The first step in the research will be to select and properly define a use case for which the monopropellant propulsion systems will be designed and analysed in the LCSAs, split up in tasks T-1.1 to T-1.3 in Figure 4.1. While the research could have also considered two or more use cases, to evaluate how the impact of propellant choice differs depending on the use case, priority was given to the total number of monopropellants included in the comparison, thereby limiting the scope to a single use case. The selection of a suitable case study will be done qualitatively, assessing both the feasibility of performing a

full LCSA, mostly regarding data availability, and the relevance of the final results, considering aspects such as the likelihood of novel monopropellants being used in each use case and the potential absolute improvements that could be achieved by using more sustainable propulsion systems. The preliminary selection of use cases is mostly the result of the literature study performed before [16].

Once a use case is selected, a rough conceptual design of the mission will be performed, specifying stakeholders and mission requirements which inform the relevant propulsion system requirements. The method followed here is based on the Space Mission Analysis and Design (SMAD) textbook by Wertz et al. [114]. Next, the propulsion system requirements will inform the definition and weighting of a set of trade-off criteria, which are used to select a suitable monopropellants for the chosen use case in T-1.7. In a graphical trade-off, hydrazine will be included as a baseline and a number of novel monopropellants will be selected, again keeping in mind the feasibility and relevance of performing an LCSA for each. After the propellant selection is completed, a top level propulsion system design will be completed, fulfilling the case study's propulsion system requirements, for each of the propellant options. By designing a propulsion system from the ground up, for each of the considered monopropellants, it is ensured that all considerations with respect to component and material compatibility are taken into account. For the components that need to be sized according to the total propellant load, a simple Python script will be written in T-1.8, carrying out the required calculations. The end result of the first part of the research will be a component selection and comprehensive set of specifications for three to five propulsion systems, each using a different monopropellant, which will provide the necessary information to set up a complete life cycle inventory in each of the LCSAs.

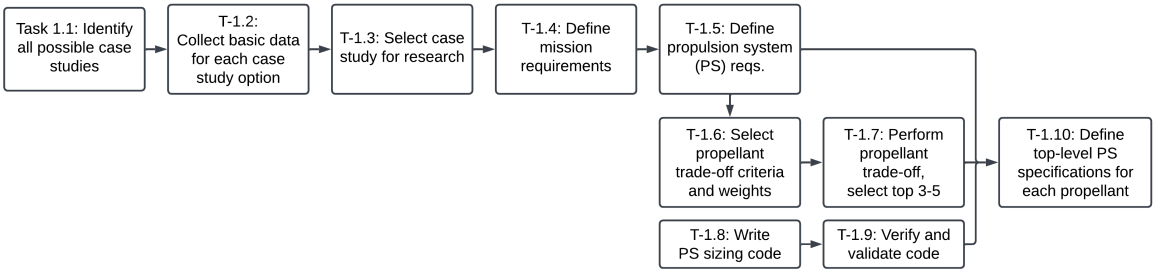

Figure 4.1: Work flow diagram of part 1 of the thesis research

The tasks shown in Figure 4.2 are concerned with assessing the overall sustainability of each designed monopropellant system and analysing the results from this assessment to find answers to the second and third set of subquestions. In this part of the research method, there are three key choices which have a large impact on the overall results: firstly that the LCSA framework is used, secondly that LCSAs are performed for each propulsion system separately, and thirdly that this is done using the SSSD and its corresponding methodology.

The motivation for performing an LCSA for each designed propulsion system is that a better understanding is sought of the life cycle impact of these systems for all three sustainability dimensions. There are also other ways in which this goal could be reached. For example, separate analyses could be performed to assess the impact in each of the dimensions, presenting results from an E-LCA, S-LCA and LCC as uncoupled assessments of the same system. That approach would allow for more methodological flexibility for the S-LCA and LCC, as these would no longer have to completely fit within the frame of an E-LCA, an aspect of the LCSA method that will become apparent in Section 4.4 and Chapter 7. The potential advantage would then be that the results of these assessments could be more closely connected to the specific system being analysed, especially for the S-LCA where developing quantified impact scores tends to move the level of assessment away from the product to that of organisations or countries [97]. For the economic dimension, there may also be more advanced assessment methods that are not entirely compatible with the E-LCA framework [95].

Still, performing LCSAs with the framework that Wilson has previously developed in conjunction with

the SSSD, in [110], has a number of very useful advantages, making it the best way of comprehensively answering the research question of this thesis. The first is the certitude that this LCSA methodology is capable of reflecting specificities of space systems, for example in the way that costs can be attributed to specific mission segments or in the characterisation of emissions that are unique to the space industry. A second major advantage is the fact that this LCSA framework has been developed in accordance with the LCA guidelines set up by ESA in 2016 [99]. This not only improves the consistency of LCA studies within European space LCA research, but also ensures that other practitioners in the field of space system LCAs will be able to correctly interpret the results. A third, more obvious advantage of using the SSSD, is the fact that it indeed facilitates an integrated LCSA, whereas the data and assessment methods of the ESA LCA database are only fit for E-LCAs. The SSSD and its LCSA framework also include a normalisation and weighting calculation, based on the European Environmental Footprint (EF) and UN SDGs [14], [115], by which the final environmental, social and economic impacts can be combined in a single score. Furthermore, the integration of all three sustainability dimensions within the overarching LCSA framework ensures that the assessment of each dimension uses the same system boundaries and includes the same components within its life cycle inventory. Another advantage of using the SSSD is that it already contains datasets of specific space systems or materials, which may be used when modelling the life cycle of the components of the compared propulsion systems. Additionally, the SSSD uses ecoinvent as a secondary data source for most of the upstream processes, also affording this possibility to the creation of new datasets. Finally, the SSSD is set up to be used in the free LCA software openLCA, increasing its ease of use. More discussion regarding this aspect is saved for Section 4.5, however.

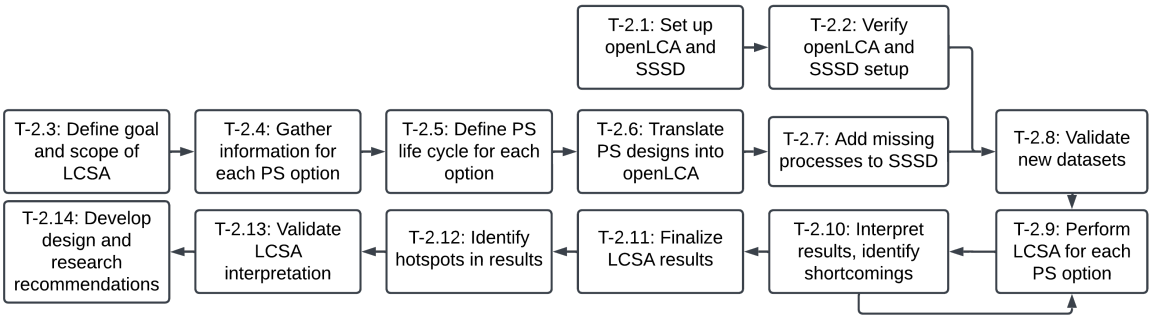

Figure 4.2: Work flow diagram of part 2 of the thesis research

The second large methodological choice that was mentioned above, of performing LCSAs for each of the propulsion systems from the ground up, is made to ensure the inclusion of all specific design and process considerations of each monopropellant, from material compatibility to the origin of the components used in the system. After the setup of the SSSD in openLCA has been completed in T-2.1 and T-2.2, the research will therefore move on to compile the life cycle inventory of each of the propulsion systems separately, in accordance with the system boundaries and scope of the LCSA. It is expected that many datasets will have to be added to the SSSD, as no LCSAs have been performed in the past for monopropellant propulsion systems. Therefore, T-2.7 will most likely be the most time-consuming step of the LCSA, as the accuracy of the added data must also be evaluated and maintained to a certain standard. To that end, the life cycle inventories of new processes will be validated as best as possible, using the ESA LCA database or other sources. After the LCSA is completed with the impact assessment of each of the propulsion systems, the final steps in the research will be to identify the driving processes within these impacts and once again validate these findings and the resulting implications. With the final results of this second part of the research, a detailed answer will be provided to the main research question, additionally resulting in recommendations for future design and research.

4.3. Case study design methodology

As indicated in the chapter introduction, the discussion presented here of the case study design methodology will remain at a high level, as the calculations used for the sizing of the system for each of the propellant options will be discussed in Subsection 6.2.5. This is done for the overall legibility of this report, considering that these calculations are rather specific and dependent on the case study that will be selected in Chapter 5. In this section, the focus will be on the overall design philosophy and requirements to complete the goal of serving as useful input data for the LCSA.

The general idea for the design of the different systems in the case study comparison is that it should reach the level of detail where the main differences between the propellant options become apparent and where a minimal amount of extra design choices or assumptions have to be made during the definition of the life cycle inventory. Regarding design choices, this might indicate that it has to be clear which material is used in the combustion chamber of the thrusters for each propellant, as this is a key system difference between the various options, as indicated in Section 2.2.

Before the various systems are designed however, the use case itself must be specified to an appropriate level of detail as well. The use case is an application of a monopropellant propulsion system within a satellite or other space system, meaning that the propulsion system requirements depend on the requirements of that larger system. This is why it is deemed necessary to perform a conceptual mission design in this research project, included in T-1.4 in Figure 4.1, to ensure that the resulting propulsion system requirements are realistic and complete. The requirement generation process will be based on the SMAD handbook by Wertz et al. and the V model used in many systems engineering practices [114], [116]. This entails that a mission need statement will be defined, after which key stakeholders, key stakeholder requirements and mission requirements will be outlined, based mostly on heritage missions and other literature. The final output of this research step will be a set of propulsion system requirements, serving both as a source of inspiration for propellant trade-off criteria and as a list of requirements for the subsequent propulsion system design.

While hydrazine will be included regardless of its performance in the propellant trade-off, other monopropellants will be selected as though the trade-off was being performed in an actual design process, judging the various options based on overall merit for the specific use case. A graphical trade-off will be performed, as opposed to a numerical trade-off or a more complicated method such as an analytical hierarchy process (AHP), as a qualitative assessment is deemed most appropriate for this conceptual stage of system design. Furthermore, the trade-off will also qualitatively take into account the feasibility and value of including certain propellant options in the LCSA comparison. In that regard, the availability of data for each propellant and the overall variety of the selected propellants are deemed to be important. These two factors will also inform how many propellants are actually selected: Figure 4.1 indicates that this may be between three to five, but this will ultimately depend on the number of propellants for which an LCSA is deemed feasible. A sensitivity analysis of the trade-off will also be performed, by adapting criteria weights and certain scores, evaluating the robustness of the final selection of propellants.

With the mission requirements set in the definition of the case study, the main input parameters for the propulsion system sizing are the total velocity change provided by the propulsion system (the ΔV budget) and the choice of propellant. The latter not only determines the system's specific impulse (I_{sp}), but also the required propellant tank volume and selected materials, thus strongly influencing the system's wet and dry mass. The assumptions and parameters used in the propulsion system sizing are based on various sources, primarily Zandbergen's Thermal Rocket Propulsion course reader and Sutton and Biblarz's Rocket Propulsion Elements [84], [117], and will be further discussed in Subsection 6.2.5. In addition to sizing the propellant tank, the propulsion system design will also include a component selection suitable for each of the selected propellants. Once again, the main objective of this task is to provide enough information to perform a proper LCSA.

4.4. Life cycle sustainability assessment methodology

This section will present the methodology of the life cycle sustainability assessment performed later in this report. To have a proper understanding of the general method, Subsection 4.4.1 will first outline the typical structure of LCA and LCSA studies, before Subsection 4.4.2 will detail the approach used in the SSSD framework and this research. As for the methodology of the case study design, it is acknowledged that certain methodological details and choices related to the LCSA may only be specified in Chapter 7, but this is again done for the overall clarity of the report.

4.4.1. Standard LCSA structure

Because the concept of a life cycle sustainability assessment was primarily conceived as an improved version of the environmental life cycle assessment, a great deal of its structure and methodology follows that of the ”normal” environmental life cycle assessment, which has been developed since the 1990s and standardised in ISO 14040:2006 [96]. As such, the structure presented here is based on the LCA ISO standard and the LCSA method proposed by Klöpffer and Finkbeiner et al. [97], [109].

The standardised LCA framework in Figure 4.3 shows that any LCA and LCSA is made up of four main steps. First, in the Goal and scope definition, the motivation for performing the LCSA should be specified, as well as the scope of activities that will be included in the LCSA. This is generally done by defining the Functional Unit (FU) of the LCSA, for example: *”The production and delivery of 1 kg of liquid oxygen propellant to the Kourou spaceport in French Guyana.”* A proper FU statement should unambiguously indicate what the final LCSA results hold for, in terms of the exact system being assessed and ideally also in terms of the included life cycle phases. In addition to the FU, LCSA practitioners often present a schematic showing the system boundaries considered, showing the life cycle phases and activities included in the LCSA and specifying which of these are considered as ”upstream” and ”core” processes. Core processes are generally fairly obvious to the FU, for example related to the manufacture or usage of the product, whereas upstream processes may relate to raw material extraction and transport.

The selected system boundaries also decide the type of allocation method is used for processes with multiple outputs or the potential of recycling [118]. For example, if certain processes in the LCSA produce a waste product (from the perspective of the LCSA FU) that can be reused in another life cycle, an option would be to consider the impacts that are avoided due to this reuse of material, and subtract this from the total impacts found for the FU at hand. This would constitute a consequential allocation approach. Another option would be to start with the total impact within the FU’s life cycle and only allocate a specific portion of that impact to the FU itself, with the rest of the impact allocated to the other useful products created during the considered life cycle. This is called attributional allocation. Another option is the cut-off approach, which does not consider the co-products along the life cycle at all, cutting off any processes related to their further development or integration into useful end products.

The next step in the LCSA framework is Inventory analysis. This step is often the lengthiest of the entire LCA or LCSA, as it consists of cataloguing and analysing each activity within the FU’s life cycle. In openLCA, the LCA software that will be used in this research project, the following terminology is used: a *Product System* is the system for which the LCSA is performed, meaning that it should model the FU as best as possible. A Product System is created based on a *process*, which models a specific activity. For example, a process may be set up to model the production of 1 kg of Al5254 aluminium alloy. Any process is then defined by the input and output *flows* that it is composed of, indicating which components or materials are taken from or emitted to the technological or natural environment. Any process is expressed as either a *Unit process*, being made up of flows which are provided by other processes, or as a *System process*, where all input and output flows are *elementary flows*, directly extracting from or emitting to the natural environment. For each process, one reference flow is selected in the output, such that it can act as a *provider* in case the flow is used in another Unit process. The Inventory analysis thus consists of defining and modelling which processes make up the considered phases of the life cycle of the FU, and quantifying which flows are the inputs and outputs of these processes. For upstream processes, the quantification of these flows can become quite complex, as one may to know the exact amount of aluminium particles released to the air, using the example above.

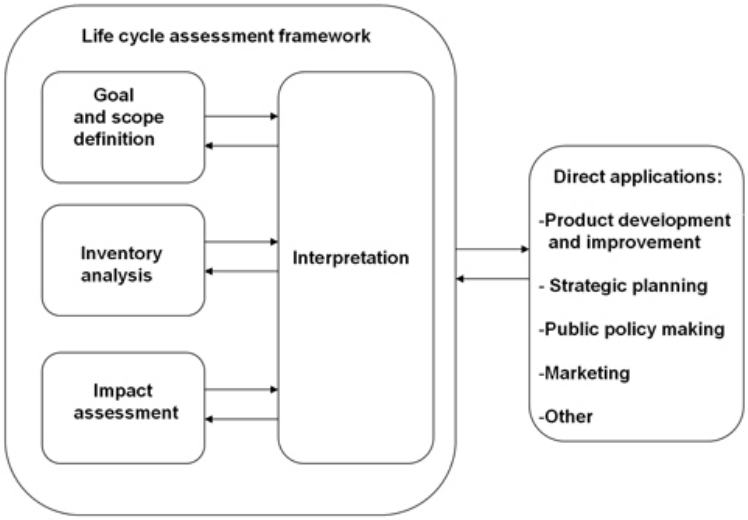

Figure 4.3: Life Cycle Assessment framework, from [96]

Because of this, secondary data sources are often used to model upstream processes, whereas the definition of core processes should ideally be based on primary data sources that are relevant for the FU at hand. When there is not enough data available to accurately model a specific process, a *proxy* with a more accurate LCI may be used, as long as the proxy is similar enough to the process being modelled. When building up an inventory for a particular system, certain cut-off criteria can also be used, to limit the scope of the LCI and the number of processes or flows considered in its composition.

For the specific case of an LCSA, the inventory analysis of the different processes will entail not only the material inputs and outputs, but also the factors affecting the social and economic realm. This may be done in different ways, depending on how the social and economic impact are determined, but generally this involves cataloguing the cost of the process and how it affects various stakeholders connected to the activity. As the application of the E-LCA method is more advanced than that of the S-LCA or LCC methods, especially in the context of space systems, there is generally less data available for the economic and social inventories of processes. Additionally, it may be more difficult to use reliable proxies for the specific socio-economic conditions of processes. Lastly, it is also typical for social LCI data to be characterised only at the level of a country or country-specific sector, making it less specific to the defined FU [97].

The third step in the LCSA methodology is the Impact assessment of all processes included in the scope of the LCSA. This operation depends on the selected impact assessment method, which defines the impact categories included in the LCSA and the characterisation factors for each of these categories. Depending on the goal and scope of the LCSA, a number of impact categories may be selected, with a key advantage of the E-LCA method being that a multitude of environmental issues can be investigated with the same detail. In the definition of impact categories, there is generally a distinction between midpoint and endpoint impact categories. Midpoint indicators express the impact of flows for a range of environmental issues, while endpoint indicators go further and quantify these impacts in terms of the damage they cause for certain areas of protection, typically Human Health, the Natural Environment and Natural Resources [99]. Some impact categories characterise flows at the input of processes, for example the midpoint indicators related to resource depletion, while others are more relevant for output flows, for example considering climate change. A reference unit is accorded to each impact category, such that impacts of various flows can be made comparable. Reference units are generally decided upon by a broader scientific consensus; when considering climate change for example, results are usually expressed in $kg\ CO_2\ eq$.

The life cycle impact assessment (LCIA) is the most computationally demanding task of an LCA, as it requires each flow within the Product System to be characterised with respect to every impact category included. In case an LCA software is used, this calculation is carried out automatically by the software.

Adapting this step for the LCSA methodology is once again not very complicated, as the inclusion of the social and economic dimensions can be facilitated either by using multiple impact assessment methods or by adding social and economic impact categories to the list of environmental impact categories [109]. In the LCIA method used in this research, the latter approach will be followed. The main challenge when developing an LCSA methodology is then to select suitable characterisation factors for each of these impact categories.

The final step in the LCA framework is the Interpretation of the LCIA results, which includes a critical and iterative review of how these results are influenced by the choices made in the previous steps, as indicated by the double arrows in Figure 4.3. Any conclusion that is drawn from the results must therefore be validated and considered in the context of the assumptions and limitations included in the definition of the LCA's scope and life cycle inventory. As such, by iterating on the previous steps in the LCA and identifying shortcomings or mistakes, the LCA practitioner can improve the accuracy of the final results. This step is extremely important, as the particularities of the LCA methodology can easily lead to false conclusions, for example if specific flows are characterised incorrectly or if the LCI is missing key processes.

4.4.2. LCSA method in this research

In this research, it is chosen to use the LCSA method developed by Wilson in 2019 with the specific purpose of performing LCSAs of space systems and missions [14], [110]. This choice was made as it allows for the comparative LCSA in the study to have a broader scope and include more propellants within the research timeline afforded by the thesis project. Furthermore, the SSSD LCSA framework is more than adequately able to address the areas of interest that the literature review has identified within the comparison of novel monopropellant systems and is therefore a suitable method to answer the research questions. An overview will be given here of the SSSD LCSA methodological guidelines or exact methods to perform each of the four activities within the typical LCSA framework. This is based on the SSSD user guide [119] and methodological description [14].

Goal and scope definition

For the definition of the FU and system boundaries for an LCSA of a space system, the SSSD framework refers to the guidelines of the ESA LCA handbook [99]. This handbook gives recommendations for the scope of LCAs of various processes, from an entire space mission down to the level of the production of a specific material. As this study will compare the LCSA results of different propulsion systems, the guidelines given for equipment are most relevant, which give a generic functional unit of: "One piece/kg of equipment Y at the output gate" [99]. Furthermore, the recommendations for system boundaries advise to leave research and development (R&D) and supporting activities such as office work outside the scope of the LCA. These and other guidelines in the ESA LCA handbook will be followed for the actual definition of the FU, which will be presented in Section 7.2.

Life cycle inventory database

The Strathclyde Space Systems Database is organised in five levels, each representing a different scope for the system or activity being investigated in the LCA or LCSA. An overview of this architecture is shown in Figure 4.4. In total, the first version of the SSSD contained 410 new datasets modelling space-specific activities. The bulk of these new datasets can be found in the Background Inventory, which has grown to contain close to 500 datasets since the publication Figure 4.4, and as this research will be concerned with LCSA at the level of equipment and build new Product Systems to model each of the considered propulsion systems, this level is the most relevant. The new processes that will be defined in this research during the LCI analysis will also be to the Background Inventory of the SSSD.

The SSSD provides LCI data for many unique space processes based on both primary data, collected within the space industry and through literature research, and secondary data. The secondary data used is sourced from ecoinvent versions 2.2, 3.3 and 3.8, and the European Life Cycle Database (ELCD). The fact that these supporting databases are included in the SSSD environment within openLCA

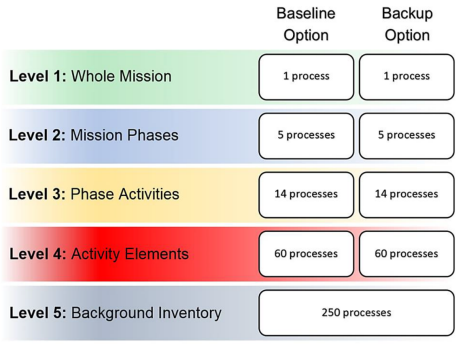

Figure 4.4: Strathclyde Space Systems Database architecture, from [119]

makes it easy to create new processes based on secondary data providers. The SSSD also includes a clear description of the scope and sources used for each process in the database, such that it is easier to maintain methodological consistency when adding new datasets.

Furthermore, 75 out of 250 datasets in the original SSSD background inventory have been validated with the ESA LCA database [110]. This ensures consistency and improves the accuracy of the SSSD, as the ESA LCA database has the advantage of several industrial partners contributing to its growth. Additionally, regular contact and joint projects between the moderators of the SSSD and ESA LCA database have resulted in a further convergence between the databases, where discrepancies are investigated and corrected if necessary. Nonetheless, this report will validate key LCI datasets with the newest version of the ESA LCA database (October 2023 release) in Section 8.2, to check the accuracy of newly added processes where possible.

Data quality assessment

An important part of life cycle inventory analysis is the estimation and quantification of the data quality of the included datasets. Not only does this provide useful information for future LCA practitioners who may not know how a specific LCI dataset was created, it also allows for sensitivity analyses to be performed using Monte Carlo simulations. Due to the limited research time and data availability, a full sensitivity analysis and uncertainty quantification will not be performed in this research. Nonetheless, the data quality of newly added datasets will be quantified.

There are several standardised ways of assessing and communicating data quality. A common approach is to fill in a so-called *pedigree matrix*, which includes a number of data quality indicators which are scored from 1 to 5 based on the most applicable description of the dataset at hand. In this research, the pedigree matrix created by ESA based on European Commission's Environmental Footprint (EF) guidelines will be used to evaluate the new processes added to the SSSD [99]. This matrix is shown in Figure 4.5 and includes six indicators judging Technological representativeness, Geographical representativeness, Temporal representativeness, Completeness, Precision, and Methodological appropriateness and consistency. While the evaluation of each of these indicators is still somewhat subjective or subject to uncertainty itself, this method does provide a basis to estimate the overall value of an LCI dataset.

Sustainability impact assessment method

In this research, the SSSD Sustainability LCIA method with midpoint impact categories will be used, which has been recently updated (September 2023) to be in line with the impact categories included in the European Commission's EF3.0 framework [115]. This LCIA method includes 23 impact categories in total, of which 21 are environmental categories, and uses 16 of these environmental impact categories to calculate an environmental single score. All but three of all LCSA impact categories are based on existing LCIA methods, meaning that the characterisation of flows is already in place and validated. An overview is provided in Table 4.1. A source is provided for each of the impact categories,

	Level 1	Level 2	Level 3	Level 4	Level 5
Technological representativeness (TeR)	Technology aspects have been modelled using data from enterprises, processes and materials under study.	Technology aspects have been modelled using data from processes and materials under study, but from different enterprises.	Technology aspects have been modelled using data from processes and materials under study, but from different technology.	Technology aspects have been modelled using data related to processes or materials, using the same technology.	Technology aspects have been modelled on related processes or materials but different technology or unknown.
Geographical representativeness (GR)	Involves data from the specific area under study.	Involves average data from a larger area in which the area under study is included.	Involves data from an area with similar production conditions.	Involves data from an area with slightly similar production conditions.	Involves data from unknown area or area with very different production conditions or unknown.
Temporal representativeness (TiR)	All the data sources refer to the defined time and are ≤3 years of difference to the year of study.	Most of the data sources refer to the defined time and are 3 to 6 years difference.	At least half of the data sources refer to the defined time and are 5 to 10 years difference.	Less than half of the data sources refer to the defined time and are 10 to 15 years difference.	None of the data sources refer to the defined time or age of the data is unknown.
Completeness (C)	>80% of process completeness determined flows have been evaluated and given a value, and ≥15 considered impact categories.	60-79% of determined flows have been evaluated and given a value, and 12-14 considered impact categories.	40-59% of determined flows have been evaluated and given a value, and 8-11 considered impact categories.	<40% of determined flows have been evaluated and given a value, and 5-7 considered impact categories.	Process completeness not scored or unknown, and ≤5 considered impact categories.
Precision/uncertainty (P)	Very low uncertainty and/or very high precision.	Low uncertainty and/or high precision.	Fair uncertainty and/or fair precision.	High uncertainty and/or low precision.	Very high uncertainty and/or very low precision or unknown.
Methodological appropriateness and	Inclusion of all LCA stages (with the EoL stage). Consideration of allocation procedures. Completion to a very high degree.	Inclusion of most LCA stages. Consideration of allocation procedures. Completion to a high degree.	Inclusion of a sufficient amount of LCA stages. Consideration of allocation procedures. Completion to a sufficient degree.	Inclusion of a low amount of LCA stages. Consideration of allocation procedures. Completion to a low degree.	Inclusion of LCA stages insufficient. No consideration of allocation procedures (multifunctionality has not been solved according to the situational context).

Figure 4.5: ESA LCA data quality pedigree matrix, from [15]

but these are not included in the report's bibliography. The reader is instead directed to [110] and [14] for more information on these impact assessment methods.

The table also presents the normalisation and weighting factors for most of the impact categories. For the environmental categories, these factors are used to calculate a single environmental score, by first dividing the impact assessment result by the normalisation factor, then multiplying it by the weighting factor, and finally summing up all impact category contributions. With the environmental single score and the normalised economic and social scores, a single sustainability score can also be calculated with the formula shown in Equation 4.1, where LCSA, E-LCA, LCC and S-LCA indicate the single score results respectively for the life cycle sustainability assessment and environmental, economic and social impact categories. The weighting factors in Equation 4.1 have been defined by considering the number of UN SDGs related to each of the sustainability dimensions [110]. This approach is admittedly quite basic and will therefore only be used as a rough indication of which propulsion system is most sustainable "overall".

$$\text{LCSA} = 0.18 \cdot \text{E-LCA} + 0.29 \cdot \text{LCC} + 0.53 \cdot \text{S-LCA} \tag{4.1}$$

In the three subsections below, a short description will be given of the impact assessment for the environmental, economic and social impacts separately.

Environmental impact assessment method

Each of the environmental impact categories included in the methodology, except for that related to *Critical raw materials*, is taken from a pre-existing LCIA method, as indicated in the second column of Table 4.1. For each of them, the SSSD contains a list of characterised flows, i.e. elementary flows which affect this impact category. The characterisation of this impact is performed in consistent units, such that a proportional impact may be accorded to each amount of characterised flow. For example, 1 kg of methane emitted to the air results in 36.8 $kg\ CO_2eq$ in the *Climate change* impact category [111]. For some impact categories, flows are also characterised differently depending on where they are emitted or extracted, making it crucial to be as accurate as possible when creating the LCI of processes.

The normalisation and weighting factors reported in Table 4.1 for the impact categories included in the environmental single score are based on guidelines provided in the EF framework [14]. Therein, every impact category result is first normalised by dividing the absolute value by the annual footprint of an average world citizen. Next, the impact categories are also weighted to reflect the estimated severity of each environmental concern reflected in the categories. This is again based on the EF framework.

Economic impact assessment method

The economic impact assessment method within the SSSD is quite straightforward, as it follows a standard LCC approach. Its general methodology is that the LCI data within the SSSD contains information regarding costs, revenues or net balances for each process, expressed in a specific currency and year. In the economic LCIA, the costs are subtracted from the revenues, added to the reported net balances and adjusted for inflation to be expressed in Euro for the year 2000. To gain a better insight into the composition of the total net balance, the different cost elements are categorised into the related mission segments and then related to specific cost divisions, as indicated in Table 4.2.

Table 4.2: Categorisation of cost elements included in SSSD economic LCIA method, from [119]

Cost Segments	Cost Divisions
Ground segment - Costs	End of life
Ground segment - Income	Energy & fuel
Ground segment - Net balance	Facilities management
Infrastructures - Costs	Income & profits
Infrastructures - Income	Initial investment
Infrastructures - Net balance	Integration & testing
Launch segment - Costs	Labour
Launch segment - Income	Launch
Launch segment - Net balance	Operations & maintenance
Space segment - Costs	Overheads & miscellaneous
Space segment - Income	Production & manufacturing
Space segment - Net balance	Transportation & travel

The normalisation of the economic single score follows a similar approach as the normalisation of the environmental impact categories, comparing the absolute result to a larger scale metric to estimate how the relevance of the LCC outcome. In this case, the average amount of money spent per EU citizen on space activities is taken as the normalisation factor [111]. Additionally, the normalisation factor shown in Table 4.1 has a negative sign to adjust for the fact that the economic LCIA outputs the net balance, whereas the environmental and social impact categories relate poor performance to a high, positive score.

Social impact assessment method

The LCIA for the social score follows a somewhat less direct approach to calculate the impact of the system's life cycle for various social stakeholders. Firstly, the only flow that is characterised is the number of labour hours related to a process. This information is included in SSSD datasets, together

with the country where that labour takes place. Then, based on these two parameters, a social score is quantified by evaluating the social conditions within that country based on a multitude of potential social burdens, called stakeholder subcategories, connected to six stakeholder categories, being: Children, Consumers, Local community, Society, Value chain actors and Workers. This approach was based on the S-LCA guidelines of the UN Environment Programme (UNEP) and Society of Environmental Toxicology and Chemistry (SETAC) [14]. At the moment, the social impact is only assessed at a national level. While the LCIA does allow for information at an organisational level to be used, the required data in this regard is very limited, with companies not being eager to provide information on the risk of specific social harm occurring due to their activities. Furthermore, the LCIA method is limited to the Value chain actors and Worker stakeholder categories, as it was deemed that only these categories can be represented accurately enough at a national level. An overview of the considered social burdens is given in Table 4.3.

Table 4.3: Overview of stakeholder subcategories included in SSSD social LCIA method, from [119]

Stakeholder Category	Stakeholder Subcategory
Value Chain Actor	Fair competition Promoting Social Responsibility Respect of Intellectual Property Rights Supplier Relationships Wealth Distribution
Worker	Child Labour Employment Relationship Equal Opportunities/ Discrimination Fair Salary Forced Labour Freedom of Association and Collective Bargaining Health and Safety Sexual Harassment Social Benefits/ Social Safety Wellbeing of Staff Working Hours

Each of the stakeholder subcategories in Table 4.3 is assessed based on a number of social indicators with equal weights. For every social indicator, an evaluation scheme is defined in the SSSD, which uses one or more parameters or statistics for which data can be found for the relevant country providing the labour hours. For example, the ”Child Labour” stakeholder subcategory within the Worker category, is made up of three social indicators, namely: Amount of child labour, Number of children exposed to hazardous work and Total children in employment. Then, the indicator ”Amount of child labour”, is assessed by considering the percentage of the total workforce made up of children, based on statistics from the International Labour Organisation (ILO). The evaluation scheme specifies that ”No Risk” of child labour is related to 0%, whereas a ”Very High Risk” is present when more than 10.60% of the total workforce are children. This exact upper bound is based on the global average as estimated by the ILO.

In each evaluation scheme, a (typically uniform) distribution is set up from ”No risk” to ”Very High Risk”, relating each risk category to a range of the social indicator metric. Each of these risk categories is then related to a score from 0 to 100, based on the approach shown in Table 4.4. Regarding the weights of each part of the social LCIA architecture in the SSSD, every stakeholder category contributes equally to the social score, resulting in a weight of 16.666...%, which is then equally divided over each of the stakeholder subcategories within the stakeholder category. These stakeholder subcategory weights are in turn equally split up among the included social indicators per subcategory. Thus, taking all the quantified scores for the social indicators and performing a weighted sum of all of them results in the total social score.

Table 4.4: Risk evaluation scheme used in SSSD social LCIA, from [110]

Band	No Risk	Very Low Risk	Low Risk	Medium Risk	High Risk	Very High Risk	Not Applicable	No Data
Score	0	20	40	60	80	100	0	50

In practice, the current version of the SSSD only quantifies the social score for two out of six stakeholder categories, such that the result for the social score must be multiplied by three before it can be normalised and used in the sustainability single score calculation. The normalisation factor for the social score is based on the average social score performance for European companies, which is multiplied by the number of labour hours in a year and divided by the total number of EU citizens to develop a metric for the annual social score per EU citizen [14]. Wilson admits that this approach is very approximate, leading to a high uncertainty for the normalised social score result, but attributes this to the general lack of S-LCA normalisation methods in literature. Once again, it is also important to note that the sustainability single score will only be a minor part of the overall results in this research.

4.5. Software and data sources

Throughout the research, various software tools will be used to perform calculations or support other steps within the overall methodology. Firstly, Microsoft Excel is used to compile and compare information in general, aiding in the case study design definition in Chapter 5 and the propellant trade-off and propulsion system design in Chapter 6, setting up the life cycle inventories and performing basic calculations to complete the datasets for new processes in Chapter 7, and finally presenting the LCSA results and facilitating deeper insight in Chapter 8.

Next, the programming language Python is used in Chapter 6 in the sizing of the various propulsion systems. A script will be written which uses the selected propellant, initial tank pressure and total δV budget to calculate the required tank size and mass, and sums the mass of all other required propulsion system components to provide the dry and wet mass of the system. This code will also be verified and validated in Subsection 6.4.1.

Finally, the open source LCA software openLCA will be used in Chapter 7 and Chapter 8 to generate and evaluate the LCSA results. This programme was first released in 2006 by the German company GreenDelta and can be downloaded on a dedicated website, which also provides a set of free or commercial LCA databases in the openLCA Nexus [120]. The version that will be used in this research is openLCA 2.0.3. The choice to use openLCA as the software to perform the LCSA was informed by the fact that the SSSD was constructed in this programme, making it easier to navigate and add new processes to the database. Furthermore, the presentation of LCA results within openLCA facilitates an intuitive evaluation process to identify potential hotspots. Another reason to use openLCA over other LCA software is that this programme is completely free to use, lowering the boundary for future research to reproduce or build onto the results of this thesis.

Next to the software used in different parts of the research, it is also important to acknowledge the data sources that will inform the definition of the LCIs for newly added processes in the SSSD. Generally, new processes are constructed as Unit processes, using flows from the SSSD and ecoinvent 3.3 or 3.8 [101], [111]. The usage of datasets from ecoinvent 2.2 is deemed to be undesirable as this version of the ecoinvent LCA database was released in 2010, meaning that many datasets have been updated or corrected since then. Some flows from ecoinvent 2.2 are still used in the processes already existent in the SSSD and this was not fully corrected due to the limited thesis timeline. Nonetheless, wherever flows are used related to electricity production or transport, ecoinvent 2.2 data is replaced by ecoinvent 3.8 data, as the data for these flows has changed greatly in the past years. With the goal of updating SSSD processes that are key to the case study modelled in the LCSA, a comparison will be made with the ESA LCA database to check whether the older SSSD data is still valid.

In addition to defining which flows are used in new processes, a quantification must also be made of how much of these flows are required in each specific process. Gathering sufficient information to do

this accurately is expected to be a very time-consuming step of the research, the results of which will be shown in Section 7.4. The required information will generally be sourced from open literature online or relevant proxy information already included in the SSSD or ESA LCA database. Whenever possible, an effort will be made to collect primary data by contacting company employees or other professionals who can provide more accurate data related to the overall structure and quantity of flows included in new processes. For any information in the LCI, Section 7.4 will clearly indicate the source. The origin of these sources will also be the most decisive factors when filling in the data quality matrix for each new process.

4.6. Conclusion

This chapter has outlined how the research questions in this thesis are planned to be answered. Overall, the methodology is split up in two parts. The first is concerned with identifying and further detailing the monopropellant use case for which a comparison of the overall sustainability would be most valuable and feasible, selecting the propellants that are most suitable for this use case, and creating conceptual propulsion system designs for each of these propellants. The second part will then perform an LCSA for each of these propulsion systems and compare these results to understand how the design differences between the systems lead to differences in their environmental, social and economic sustainability.

The general LCA methodology has been presented, which follows four main steps, being the Goal and scope definition, Inventory analysis, Impact assessment and Interpretation. For each of these steps, the specificities of the space industry require the LCA practitioner to make changes or correctly apply existing LCA methods in the LCA of space systems. Both the ESA LCA and SSSD handbooks provide guidelines to this end and a coherent approach for each of the LCSA steps in this research has been defined based on these documents [99], [119]. The most important conclusions from this LCSA methodology are that new datasets will be added to the SSSD to adequately represent the LCI of the considered propulsion systems, and that the selected impact assessment method is the SSSD Sustainability LCI with Midpoint impact categories. This LCIA method will provide results for 21 environmental impact categories and single scores for the social and economic impacts.

Lastly, it is relevant to point out that LCI data for new processes will mostly be based on publicly available data, out of necessity. This will most likely reduce the reliability of the final results, as limited public data availability has been indicated before as a major hurdle for LCA in the space industry [4]. This and other methodological limitations and drawbacks will be further evaluated in Section 8.4, when the effect of these limitations on the final results will be clearer.

Table 4.1: Overview of impact categories included in SSSD Sustainability Midpoint LCIA method, from [111]. * indicates that the impact category is included in the EF3.0 framework and in the environmental impact single score calculation [115].

Impact category	Source	Reference unit	Normalisation factor	Weighting factor
Acidification*	EF: Accumulated Exceedance	mol H+ eq	55.5	0.062
Air acidification	CML 2001	kg SO2 eq	-	-
Climate change*	EF: IPCC (2013)	kg CO2 eq	8400	0.2106
Critical raw materials	SSSD 2019	kg mass	-	-
Economic impact, single score	SSSD 2019	EUR 2000	-7.17	1
Ecotoxicity, freshwater*	EF: USEtox	CTUe	11800	0.0192
Ecotoxicity, marine	CML 2001	kg 1,4-dichlorobenzene eq	-	-
Eutrophication, freshwater*	EF: ReCiPe Midpoint (H)	kg P eq	0.734	0.028
Eutrophication, marine*	EF: ReCiPe Midpoint (H)	kg N eq	28.3	0.0296
Eutrophication, terrestrial*	EF: Accumulated Exceedance	mol N eq	117	0.0371
Human toxicity, cancer*	EF: USEtox	CTUh	3.85E-05	0.0213
Human toxicity, non-cancer*	EF: USEtox	CTUh	0.000475	0.0184
Ionising radiation*	EF: Human Health Effect Model (1995)	kBq U-235 eq	4220	0.0501
Land use*	EF: LANCA (2016)	Pt	1400000	0.0794
Ozone depletion*	EF: WMO (1999)	kg CFC11 eq	0.0234	0.0631
Particulate matter*	EF: UNEP (2016)	disease inc.	7.18E-04	0.0896
Photochemical ozone formation*	EF: ReCiPe Midpoint (H)	kg NMVOC eq	40.6	0.0478
Resource use, fossils*	EF: CML 2001	MJ	65300	0.0832
Resource use, minerals and metals, reserve base	CML 2001	kg Sb eq	-	-
Resource use, minerals and metals, ultimate reserve*	EF: CML 2001	kg Sb eq	0.0636	0.0755
Social impact, single score	SSSD 2019	Social Score	32916.5866	1
Total cumulative energy demand	Cumulative Energy Demand	MJ	-	-
Water use*	EF: AWARE (2016)	m^3 depriv.	11500	0.0851

5

Case Study Definition

5.1. Introduction

To make a quantified comparative assessment life cycle sustainability impact of various monopropellants, LCSAs will be performed for a specific case study. Narrowing down this research to a single use case is necessary and useful for various reasons. Firstly, there is a limit to what can be achieved within this thesis research, which requires a limited yet justified scope for the research. Secondly, due to the nature of the LCSA methodology, it is desirable to have a very clear definition of the investigated system at hand, so that data can be properly collected and the use of information in databases can be properly justified. Furthermore, the precise definition of the system investigated in the LCSA is important for the interpretation and potential extrapolation of results. Thirdly, the selection of a specific use case will influence which monopropellants are most suitable for this application.

This chapter will thus discuss the selection and definition of the use case of monopropellant propulsion for which several possible propellants will be selected in Chapter 6 and for which Chapter 7 will perform a comparative LCSA. While the LCSA will only be performed for the propulsion system, the definition of the entire use case is important as it provides the context and requirements for which the propulsion system will be designed. Some possible use cases, informed by the findings of the literature study, are discussed in Section 5.2 and a qualitative selection is made. Then, Section 5.3 will set up the conceptual mission design for this case study, by considering key mission requirements. Finally, Section 5.4 will consider relevant heritage missions for the selected use case and compute important mission parameters based on the requirements defined in Section 5.3.

5.2. Case study options and selection

As illustrated in Chapter 2, there is a great variety of applications for which monopropellant propulsion systems are used. Generally, monopropellant systems are preferred whenever a moderate amount of total impulse is to be delivered, with multiple restarts of the system, for a moderate cost. Because of these reasons, monopropellant systems are often used as the primary propulsion system for the attitude and orbit control of small (<500 kg) satellites, or as a secondary propulsion system for attitude control in larger spacecraft [84, p.264]. In some cases, monopropellant and bipropellant systems can be elegantly combined by using a propellant that is used in both systems; this is possible for hydrazine, which both acts as a monopropellant and a hypergolic fuel with nitrogen tetroxide or another oxidizer.

When selecting a case study for the application of the LCSA, there are certain rough criteria informing what a ”good” choice would be. As stated in Chapter 3, the goal of this research is to determine how propellant choice impacts the three-pillar sustainability of a representative monopropellant system. This firstly implies that the focus is solely on the monopropellant system. To be able to clearly separate the monopropellant system from the rest of the spacecraft, it is therefore desirable to select a case study

where the monopropellant system is the only propulsion system on board. Secondly, it also determines that the scope of the LCSA is limited to the propulsion system, which is an important assumption for Chapter 6 and Chapter 7.

Other important factors in selecting a case study are the relevance of the LCSA results and the feasibility of obtaining these results with an acceptable degree of accuracy. In the specific case of novel monopropellant systems, these two factors are closely related. If a novel monopropellant is more likely to be introduced in one use case than in another, this will mean that it is both more achievable to find reliable data and more useful to share the LCSA results with the research community. Case studies where novel monopropellants have flight heritage are therefore preferred.

Next to the relevance of the results for a wider research community, one should also consider what the absolute impact would be if the investigated case study would be developed more sustainably in the future. In this regard, it is relevant to consider the total number of such spacecraft to be developed and launched each year, the absolute environmental, social and economic impact of each of these spacecraft and the projected market growth of this type of mission. However, making such an assessment at this stage is quite difficult as this is part of the knowledge gap that this thesis project is aiming to fill.

A selection of five possible case studies will now be presented, after which a comparison will be made based on some of the criteria mentioned above. Finally, one case study will be selected and the rest of this chapter will further define that case study.

5.2.1. 6U CubeSat for LEO constellation

A first use case of monopropellant propulsion, which has seen a great growth over the past decade, is that of a microsatellite in the form factor of a CubeSat operating in a Low Earth Orbit (LEO) satellite constellation. While 3U CubeSats usually do not have the means to facilitate a conventional monopropellant system, recent technology advances have made monopropellant propulsion a feasible option for CubeSats larger than roughly 6U [121, p.64]. These CubeSat constellations are mostly used for Earth Observation (EO) or for communication services. As such there are various commercial actors who are planning to or already in the process of constructing a constellation of CubeSats, among others Kepler Communications (18x 6U, communications) [122], Spire Global's Lemur-2 constellation (8x 6U, multifunctional) [123] and the PlanetLabs Doves constellation ($\pm$200x 3U, EO) [124].

In this use case, monopropellant propulsion would make up the main propulsion system of the spacecraft, typically using one thruster of 1 N or four 0.1 N class thrusters [125]. In many cases electric propulsion actually seems to win this design trade study, as evidenced by the Kepler and Spire CubeSats using electric propulsion instead of chemical [122], [123]. However, Aerojet Rocketdyne is developing several CubeSat monopropellant propulsion modules, both for hydrazine and the novel monopropellant ASCENT [125]. Other heritage of novel monopropellants in this use case is the HYDROS water electrolysis system that was demonstrated in space on board the NASA PTD-1 mission [75].

5.2.2. 12U CubeSat for deep space mission

A second use case that could be investigated is that of a larger (6U-12U) CubeSat, used in a deep space science mission. With the return of space exploration to the Moon, there have already been several missions using this concept for Lunar observations and others are planned to launch in the coming years. Notable examples are the ten 6U CubeSats that were deployed as secondary payloads in the Artemis I mission, the 12U NASA CAPSTONE mission, which used a dedicated launch vehicle to test the feasibility of the planned Lunar Gateway orbit, and the 12U ESA Lunar Meteoroid Impact Observer concept (LUMIO) [126]–[128].

With deep space CubeSats inherently providing opportunities for testing experimental technologies, the adoption of novel monopropellants is also likely for this use case. The NASA Lunar Flashlight mission, launched in 2022, was meant to demonstrate a pump-fed ASCENT propulsion system onboard a 6U CubeSat searching for water-ice on the Lunar South Pole [68]. While the propulsion system failed in orbit, the technology development provided a further step in the direction of maturing novel

monopropellant systems [69]. In the LUMIO design study, an LMP-103S system is being considered as the main propulsion system [128]. In the case of conventional hydrazine monopropellant, NASA's CAPSTONE mission included a hydrazine monopropellant system and successfully demonstrated its use for orbital manoeuvring and reaction wheel desaturation [129].

5.2.3. Minisatellite for LEO constellation

The third potential case study is, similarly to the first, a mission type that has seen a tremendous increase in commercial activity over the past years. With a launch mass between 180 and 100 kg [121], minisatellites present a valuable form factor as they are able to house larger payloads than CubeSats, while still allowing for a degree of industrial upscaling in development and production. The most prominent mission types in the category of minisatellites are LEO constellations for EO and communication services, SpaceX's Starlink being the most prominent example [130]. According to BryceTech, 95% of all spacecraft launched in 2022 were small satellites (defined in the report as <600 kg). Of that fraction, 75% were Starlink or OneWeb satellites, the latter of which is a European competitor to Starlink, amounting to 1736 satellites [131]. In the field of Earth Observation constellations, Planet is the most successful company by far, with their RapidEye and SkySat constellations made up of respectively five and 21 minisatellites in LEO [124].

In minisatellites, monopropellant systems are used for orbital control and rough attitude control. Standardised hydrazine monopropellant propulsion modules for minisatellites, for example the Myriade or ROCSAT systems, have been developed and successfully demonstrated in constellations in the past [9], [132]. These systems typically feature a single blow-down diaphragm propellant tank and four thrusters, to allow for manoeuvres in three axes. There is also a considerable history of novel monopropellant technology demonstration in LEO minisatellites. The three technology demonstration missions, PRISMA, GPIM and RAPIS-1, using LMP-103s, ASCENT and SHP163 respectively, were all minisatellites with a wet mass between 150 and 200 kg [62], [67], [70]. Furthermore, 19 operational SkySat satellites employ a HPGP propulsion system developed by ECAPS [133]. As a final ongoing development for novel monopropellant usage specifically for minisatellites, it is worth noting the POLON HTP monopropellant system, being designed at the Łukasiewicz—Institute of Aviation [34].

5.2.4. Medium-sized satellite for MEO constellation

Satellite constellations are not limited to LEO. The most well-known constellations in the space of Medium Earth Orbits (MEO, between 2000 km and geostationary altitude) are the European and American navigational satellite constellations, respectively Galileo and GPS. These satellites are built in large series based on a standardised bus, and feature larger payloads, thereby resulting in a wet mass of 733 kg in the case of Galileo and around 4000 kg in the case of the newest GPS generation [134], [135]. Due to the nature of the mission requirements, the size of these constellations is smaller than those for EO or communications services: for both the GPS and Galileo systems, there are 24 active satellites in the constellation [134], [136].

For this type of satellite, monopropellant systems with higher thrust levels (1-20 N) and more thrusters (eight in the case of the first generation Galileo platform) are used as the main propulsion system for orbit maintenance and attitude control. In the case of the larger third generation GPS satellites, an additional bipropellant engine is included for the initial orbit insertion manoeuvre [135]. As mentioned before, the navigational satellites are built on standardised buses, thereby fully benefiting from the long heritage of hydrazine technology. This fact and the fact that these satellites have a long development time and a high cost, may explain why there is less interest as of yet to introduce novel monopropellants in this use case. On the part of thruster manufacturers ECAPS and Aerojet Rocketdyne, there is an ongoing process to qualify 20 N thrusters for respectively LMP-103S and ASCENT [67], [137]. As novel monopropellant technology continues to mature, it is likely that it could be introduced in the next generation of the MEO constellation satellites.

5.2.5. Roll and attitude control system for medium-lift launch vehicle

The final use case is quite different from the previous four, given that it represents the only case where monopropellant propulsion is decidedly used as a secondary propulsion system, and that it is the only case where the system operates within the Earth's atmosphere. What is considered is the roll and attitude control system (RACS) of a medium-lift launch vehicle, such as ESA's Vega-C, United Launch Alliance's Atlas V or SpaceX's Falcon 9, able to launch between 2000 and 20000 kg into LEO [131]. In the case of the Falcon 9 launch vehicle, attitude control is performed by a cold-gas propulsion system, but this task can also be performed by a monopropellant system, as evidenced by the inclusion of a hydrazine monopropellant system in Vega-C and Atlas V [138], [139]. With the previously discussed growth in the field of small satellites, the market for small- and medium-lift launch vehicles will also grow, presenting new opportunities for the transition to novel monopropellants.

While the use case may be less obvious than the others, the reason for considering it as an option is that it employs thrusters of a different class than the other use cases. While the previous options generally require thrust values around in the range of 0.1, 1 or 20 N, a launch vehicle roll control system would need values in the range of 200 N. As the entire propulsion system is scaled up, this could result in important differences from the perspective of life cycle sustainability. Another reason for including this option is the ongoing development of a new roll control system using HTP, replacing the original hydrazine system of the Vega-C vehicle [138]. This development is led by Nammo and includes a European consortium, indicating that there is industrial interest for this type of usage of novel monopropellants. The environmental severity of spilled hydrazine due to failed rocket launches or stages returning to Earth in the surroundings of the Russian spaceport of Baikonur provide an additional motivation to exclude hydrazine from use in launch vehicles [140].

5.2.6. Overview and selection

The five potential case studies discussed above present the wide variety of monopropellant usage. Considering the LCSA that will be performed later in this report, the five options would potentially result in different impact hotspotss. While this research can only deal with one of the cases, it would certainly be interesting in future research to compare the results between the five options and highlight the most relevant recommendations for each of them.

Based on the above descriptions, Tables 5.1 and 5.2 give an overview of the use cases with the characteristics of their use of monopropellant technology and of the missions themselves. Most of these characteristics are only meant to provide a rough picture of the general order of magnitude; this is especially applicable for the estimated systems launched per year or the development costs, for which the numbers are not entirely comparable across the different cases. While a source is provided for most characteristics, some are based on an overall judgement of the literature.

Table 5.1: Comparison of potential case studies

Use case	Orbit	S/c wet mass [kg]	Thrust [N]	# of thrusters	Novel monoprop. heritage	Propellant load [kg]
6U CubeSat constellation	LEO	12 [121]	0.1-1	1-4	Yes (NASA PTD-1 [75])	1 (Hydrazine [125])
12U CubeSat	Deep-space	24 [121]	0.001-1 [128]	1-8 [128]	Not successful (Lunar Flashlight [68])	1.79 (LMP-103S, LUMIO [128])
Minisatellite constellation	LEO	120 [133]	1 [141]	1-4 [141]	Yes (multiple)	10.5 (LMP-103S, SkySat [141])
Navigational sat. constellation	MEO	750 [134]	1-20 [18]	1-6 [134]	No	45 (Hydrazine [114])
Medium-lift LV RACS	Earth to LEO	210 000 [142]	200 [138]	6 [138]	In development (Vega-C RACS [138])	65 (HTP, based on Vega-C RACS [138])

Table 5.2: Comparison of potential case studies, continued

Use case	Est. systems launched/year	Est. development cost [Mill. €]	Data availability
6U CubeSat constellation	20 (Kepler and Spire) [122], [123] (+50 3U Planet Doves [143])	1.3 (with launch) [144]	Various commercial options and academic publications, some novel monopropellant research
12U CubeSat	1-2	12 (buget for CAPSTONE [127])	Some academic publications, including some novel monoprop. options
Minisatellite constellation	50 (+1500 Starlink and OneWeb) [131]	17 (SMAD [114]) - 32 (GPIM [67])	Various commercial options and academic publications, some novel monopropellant research
Navigational sat. constellation	<10 [134]	122.5 (budget per Next Gen. GPS [135])	Few existing constellations, limited data availability
Medium-lift LV RACS	110 (All Medium-lift launches [145])	275 Mill. (Vega-C [142])	Few existing options, very limited data availability

Choosing between the different options, there are two factors that are deemed to be most important. As discussed before, novel monopropellant heritage and data availability work hand in hand and are also clear indicators of the feasibility and relevance of the LCSA that will be performed later in this report. With this in mind, the case study of the minisatellite constellation in LEO has a clear advantage with respect to the other options. While the 6U CubeSat option also features ongoing research and an existing base of novel monopropellant heritage, the various demonstrations of novel monopropellant usage in the minisatellite application have been well-documented, especially in the case of SkySat [141].

While the market for minisatellite constellations will most certainly continue to grow in the coming years, it is undeniable that electric propulsion is often preferred over chemical propulsion for this use case. The reason why the Starlink and OneWeb launches have been added in brackets in Table 5.2 is that these spacecraft currently use electric propulsion [130]. However, if regulations related to collision avoidance and de-orbiting become more demanding in the future to ensure a safe LEO environment, it could be that electric propulsion is no longer suitable to fulfil all propulsion system requirements. Furthermore, one of the reasons why chemical propulsion is currently not always preferred is that the use of hydrazine may not be feasible within the tight schedule and budget of commercial minisatellites [9]. With the advancement of novel monopropellants, some of these issues could also be mitigated, thereby improving the position of chemical propulsion vis-à-vis electric propulsion.

Due to the availability of relevant data and the current and future relevance of the use case, the LEO minisatellite constellation is thus selected as the case study for the comparative LCSA. While the LCSA will only be performed for the propulsion system of one of the (identical) satellites in the constellation, it is important to state that the satellite is part of a moderately sized constellation, as this will greatly influence the propulsion system requirements. Due to the available documentation and the important historic value of the mission, the SkySat platform will be used throughout the report as an important reference for mission and system design.

5.3. Case study mission requirements

With a general case study selected, the next step is to further specify this case to the level of detail where it can usefully inform the key propulsion system requirements for the considered spacecraft. The choice is made to design a system used for Earth Observation as this is a use case where novel monopropellant technology has been demonstrated before in the SkySat system, and because chemical propulsion is most probably better suited than electric propulsion for this mission type. From this point on, the mission being designed will be generically named the ”*EO system*”.

Following the guidelines of Wertz and Larson [114], and the systems engineering V model [116], the mission design starts by defining a mission need statement, after which the most relevant stakeholders of the mission can be defined. Then, the key stakeholder requirements are set up, remaining at a non-technical level and being defined in the language of the stakeholders in Subsection 5.3.2. Finally, the key stakeholder requirements inform the key mission requirements in Subsection 5.3.3, which may then flow down to the top level mission design parameters and the propulsion system requirements in Subsection 6.2.1. Throughout the mission design process, systems engineering tools such as the stakeholder needs analysis and the requirements discovery tree are used.

The mission need statement of the *EO system* is defined as follows:

EO-MNS: *”As the global climate and different (man-made) systems are becoming more dynamic and unpredictable, various stakeholders need high-resolution, regularly updated images of specific parts of the Earth, so that their interests can be monitored and decision making can be informed by relevant data.”*

5.3.1. Key stakeholders

Considering the most relevant stakeholders for the *EO system*, there are three main groups. Firstly there are the users of the EO data, each with their own requirements regarding the spatial, spectral and temporal resolution of the EO data, potentially requiring the mission designer of an EO system to prioritise specific users [146]. For the purposes of brevity, stakeholders using data or products derived from the primary EO data will not be considered.

Secondly, there are also the stakeholders that are actively involved in the mission’s success. The most prominent of these are the companies contracted to deliver components for the spacecraft, transportation companies, the launch provider, ground station operators and data processors. There are active stakeholders throughout the system’s entire life cycle, and the requirements that they set need to be

met at the risk of the entire mission not functioning properly.

Finally, there are the stakeholders who are passively in contact with the *EO system*, meaning that they have an influence on its success or are indirectly influenced by it. This group includes various regulatory bodies dealing with the use of communications bandwidths or the pollution of orbital space, to name two examples. The owners of other satellites are also passive stakeholders, as well as some scientific groups being passively affected by the system in orbit: the astronomic community has often voiced concerns that the immense growth of satellite constellations will interfere with their observations [147]. Lastly, the ”general public” is another important passive stakeholder, firstly including the local communities that may be affected by the production of the *EO system* and secondly referring to society as a whole, as the environmental impact of the *EO system* will contribute to global climate change. Furthermore, the data provided by the *EO system* also affects society in the sense that a better understanding of climate dynamics and weather systems can help to predict natural disasters and as such prevent excessive human suffering. An overview of the key stakeholders for the *EO system* is given in Table 5.3.

Table 5.3: Overview of key *EO system* stakeholders

Users		Active		Passive	
SH-US-01	Industrial: agriculture, transportation, resource extraction, construction, navigation	SH-AV-01	Suppliers	SH-PV-01	Regulators
SH-US-02	Scientific: environmental, hydrology, biology, geology, cartography, archaeology	SH-AV-02	Transportation companies	SH-PV-02	Other spacecraft owners
SH-US-03	Political: lawmakers, international institutions, non-profit groups, intelligence services	SH-AV-03	Launch provider	SH-PV-03	Earth-based observers
		SH-AV-04	Ground station operators	SH-PV-04	Local communities
		SH-AV-05	Data processors	SH-PV-05	Society

5.3.2. Key stakeholder requirements

A proper definition of key stakeholder requirements would involve consulting a representative share of the relevant stakeholders, which lies outside of the scope of this research. A non-exhaustive list of key stakeholder requirements is set up instead, based on similar mission heritage and an estimation of the stakeholders' requirements. As the main goal of the use case definition is to inform a proper propulsion system design, only the stakeholder and mission requirements that directly flow down to propulsion system requirements will be completely specified.

Starting with the users, the main requirements are related to the spatial, spectral and temporal resolution of the EO data and the coverage that the *EO system* provides. Whereas industrial and commercial applications of EO data may be mostly based on observations in the band of visual light, scientific users may also require observations in the infrared and ultraviolet spectra. Furthermore, to allow for useful data analysis, the repeatability of observations is another important factor for scientific users. An overview of the main user requirements is given in Table 5.4.

Table 5.4: Overview of key *EO system* user requirements

Label	Description	Rationale
REQ-SH-US-GEN-01	The EO system shall provide images with a resolution of at most [TBD] m.	Users need to be able to discern important details.
REQ-SH-US-GEN-02	The EO system shall provide images which are updated at least every [TBD] days.	Certain users will need regular updates of the images, to monitor changing events or make timely decisions.
REQ-SH-US-GEN-03	The EO system shall be able to image specific areas, in the highest possible detail of the system, within at most [TBD] days.	Certain events may lead to specific areas of focus, which need to be monitored in a timely manner.
REQ-SH-US-GEN-04	The EO system shall cover remote and large stretches of land.	For agriculture or resource extraction, this is especially relevant.
REQ-SH-US-GEN-05	The EO system shall image major inhabited areas.	For the transportation and construction industry and policymakers, this aspect may be more important,.
REQ-SH-US-SCI-01	The EO system shall provide open access to (certain) images.	Providing open access to images increases the potential of scientific research using the data.
REQ-SH-US-SCI-02	The EO system shall provide images in multiple spectral bands.	Different scientific disciplines may require different bandwidth information.
REQ-SH-US-SCI-03	The EO system shall make observations of the same areas over a period of at least [TBD] years.	It is important for scientific research that the area of interest is observed over a long period of time, to be able to generalize or extrapolate results.
REQ-SH-US-SCI-04	The observations made by the EO system shall be repeatable and clearly linked to a specific time.	Repeatability and identical observation conditions are important to conduct reliable scientific research.

Moving to the active stakeholders, there are less requirements on the capabilities of the system and more on its characteristics. From the perspective of the transportation companies and launch provider, the total mass and volume of each of the satellites in the *EO system* will be the most important requirements. For the ground station operators and data processors, the key requirements are focused on the time of contact between the spacecraft and the ground station, and the communication protocols that the spacecraft uses. Once again, it is emphasised that the list of requirements presented in Table 5.5 is certainly not complete, but this is not deemed to be necessary for the purposes of the current investigation.

Table 5.5: Overview of key *EO system* active stakeholder requirements

Label	Description	Rationale
REQ-SH-AV-01	Each spacecraft in the EO system shall have a dry mass of at most [TBD] kg.	The spacecraft should be able to be launched with existing launch vehicles, and be transported to the launch site with exisiting and affordable means.
REQ-SH-AV-02	Each spacecraft in the EO system shall have a volume of at most [TBD] m^3.	The spacecraft should be able to be launched with existing launch vehicles, and be transported to the launch site with exisiting and affordable means.
REQ-SH-AV-03	The spacecraft used in the EO system shall withstand all launch loads provided in the launch vehicle guide.	To ensure that the launch vehicle provider can successfully deliver the payload in orbit, the system should respect the launch vehicle requirements.
REQ-SH-AV-04	The spacecraft used in the EO system shall use communications protocols that are in line with current standards.	To limit costs, the system shall make use of existing ground station infrastructures.
REQ-SH-AV-05	The EO system shall transfer data to Earth in intervals of maximally [TBD] hours.	To limit the data sent per downlink, regular contact with ground stations is preferred.

Finally, the passive stakeholders also set their own requirements for the system. Similar to the active stakeholders identified in this chapter, the passive stakeholders for the *EO system* create requirements for the system over its entire life cycle, thus also affecting the development and end-of-life (EOL) phases. Table 5.6 gives an overview of the key requirements voiced by the passive stakeholders; it is again acknowledged that this list is certainly not exhaustive.

Table 5.6: Overview of key *EO system* passive stakeholder requirements

Label	Description	Rationale
REQ-SH-PV-01	The likelihood of a collision between any spacecraft of the EO system and any other object in space shall never be greater than [TBD]%.	The EO system should not introduce new space debris.
REQ-SH-PV-02	The EO system shall de-orbit at most [TBD] years after its mission ends.	The EO system should not introduce new space debris.
REQ-SH-PV-03	The spacecraft used in the EO system shall use demisable structures and materials for at least [TBD]% of its structural mass.	The EO system should not introduce new space debris.
REQ-SH-PV-04	The EO system shall be visible in at most [TBD]% of the night sky for at most [TBD] minutes, every day.	The EO system should not overly disturb astronomical observations.
REQ-SH-PV-05	The development and production of the EO system shall lead a total greenhouse gas emission of at most [TBD] kg CO2eq.	To avert a worsened climate crisis, industrial activities should reduce the burden they place on the natural environment.
REQ-SH-PV-06	The development of the EO system shall be performed with fair and safe labour conditions, under the definition of the UN SDG 8 [89].	Industrial development should aim to improve the living conditions of those involved in the process, and not perpetuate any existing social injustices.

5.3.3. Key mission requirements

Now that the key stakeholder requirements have been identified, it is possible to formulate the key mission requirements. These requirements relate to the entire *EO system* constellation. The way by which these constellation system requirements flow down to the spacecraft system requirements will be further specified in Section 5.4.

From the stakeholder requirements, there are five functional requirements which seem to hold the most weight, related to the system's spatial, spectral and temporal resolution, its overall coverage and its ability to respond to changing events. Additionally, three non-functional requirements are crucial to keep in mind: the first dealing with the orbit used by the system, the second dealing with the system de-orbiting after its useful lifetime, and the third specifying the mission lifetime itself. An overview of the key mission requirements is given in Table 5.7. Note that no values are filled in yet, as there is no main stakeholder or clear mission goal to inform these values. As such, the existing literature and mission heritage of similar missions will be consulted in Subsection 5.4.1 to determine specific numbers which would make the *EO system* mission requirements feasible and unique.

Table 5.7: Overview of key *EO system* mission requirements

Label	Description	Rationale
REQ-EOS-01	The EO system shall have a nadir pointing ground sample distance (GSD) of [TBD] m.	Linked to REQ-SH-US-GEN-01: GSD is an important parameter to specify the spatial resolution of an image.
REQ-EOS-02	The EO system shall have a revisit time of no longer than [TBD] hours.	Linked to REQ-SH-US-GEN-02: to provide useful monitoring of evolving situations, an adequate temporal resolution is required.
REQ-EOS-03	The EO system shall image in the following spectral bands: [TBD].	Linked to REQ-SH-US-GEN-01, REQ-SH-US-SCI-02: to offer full colour images and other scientific data of interest, the spacecraft payload must be able to image in different spectral ranges.
REQ-EOS-04	The EO system shall cover at least [TBD]% of the globe every day.	Linked to REQ-US-GEN-04, REQ-US-GEN-05: the system should cover a considerable part of the Earth, to enable large-scale monitoring and disaster monitoring.
REQ-EOS-05	The EO system shall be able to adjust its observations to cover an area of [TBD] km^2 at the highest resolution of [TBD] m GSD, within [TBD] days after the provided command.	Linked to REQ-SH-US-GEN-03: ”normal” coverage may be fulfilled with lower resolution off-axis observations, but if required this should be improved, within a short time.
REQ-EOS-06	The EO system shall orbit in Sun-synchronous LEO at an altitude of [TBD] km.	Linked to REQ-SH-US-GEN-01, REQ-SH-US-GEN-02, REQ-SH-US-SCI-03, REQ-US-SCI-04, REQ-SH-AV-05, REQ-SH-PV-01, REQ-SH-PV-02: the SSO orbits in LEO provide similar lighting conditions when observing the same area over time, additionally it allows for a simplified data downlink and de-orbit.
REQ-EOS-07	The EO system shall actively de-orbit within [TBD] years after its service lifetime.	Linked to REQ-SH-PV-01, REQ-SH-PV-02, REQ-SH-PV-03, REQ-SH-PV-04: as a constellation of spacecraft will be used, proper measures should be in place to minimize the risk of collision with other active or inactive spacecraft.
REQ-EOS-08	The EO system shall have a mission lifetime of at least [TBD] years.	Linked to REQ-US-SCI-03, REQ-SH-PV-01: users of the EO data should have the guarantee that the data will be provided over a certain period, and other spacecraft owners should know how long the system will be in orbit.

Although the rationale behind each mission requirement is provided in Table 5.7, an additional note is required for REQ-EOS-06. It may seem as though this requirement is already venturing substantially into the solution domain of the mission design. However, it is deemed that the decision of the orbit type is so high-level and influential for other requirements that it may be something that is decided in conjunction with the overall mission concept. The specific choice for a Sun-synchronous orbit (SSO) is informed by its unique characteristic that the orbit’s node of right ascension, i.e. where the spacecraft crosses the Earth’s ecliptic, precesses at the same rate as the Earth’s rotation around the Sun [148].

This results in the feature that a spacecraft in this orbit can image the Earth under identical lighting conditions throughout the entire year. Furthermore, by selecting the appropriate orbital parameters, one may also specify the orbital repeat period. These features have made the SSO very popular for EO missions, as will be further discussed in the following section.

5.4. Case study mission design

To further specify the mission requirements set up in Subsection 5.3.3, additional information about the *EO system* needs to be obtained. As the mission design for this case study is informed by a very generic mission need statement and does not have external stakeholders to state a clear desired performance, heritage missions similar to the *EO system* concept will be consulted for inspiration. After the most relevant missions have been discussed, Subsection 5.4.2 will perform the basic calculations to further specify and finalise the mission requirements. Furthermore, other key mission parameters will be determined to provide a basis for the propulsion system requirements in Chapter 6.

5.4.1. Mission heritage

As discussed in the motivation for choosing the LEO minisatellite constellation case study, there is a considerable number of well-documented heritage missions to investigate. Uniquely there has already been a successful demonstration of monopropellants in this use case: the SkySat constellation owned by Planet. The constellation consists of two spacecraft that served as a proof of concept, and 19 others that include improved attitude control through reaction wheels and a novel monopropellant system using LMP-103S, developed by ECAPS [133]. The SkySat platform was groundbreaking for several reasons. Firstly, through the use of advanced data processing, the satellite observations achieve a sub-meter resolution for images in full colour [149]. The relatively large size of the constellation also meant that the spacecraft manufacturer, Maxar Technologies, was able to benefit from a learning curve dynamic where the number of labour hours for the production of each subsequent spacecraft decreased, asymptotically approaching a minimum [150]. The application of novel monopropellant technology in this commercial mission is also historically unprecedented and provides a valuable example for future missions.

The main mission parameters for the SkySat constellation are provided in Table 5.8. All 21 spacecraft in the constellation are still active, albeit in three different orbits, as the table indicates. SkySat 1 and 2 orbit in a 600 km altitude SSO, whereas SkySat 3-15 orbit in a 450 km SSO, lowered from the initial 500 km orbit. Lastly, SkySat 16-21 have a non-SSO LEO orbit, which is inclined and at an altitude of 400 km, with the purpose of improving the coverage of the overall constellation. The lower orbits of SkySat 3-21 are possible thanks to the inclusion of the propulsion system that counteracts the atmospheric drag at lower orbit altitudes. The advantage of orbiting at a lower altitude is that this leads to an improved GSD. The GSD presented in Table 5.8 applies to the panchromatic imaging mode of SkySat 16-21, after data processing. Furthermore, one should note that the revisit time given in the table holds for a single spacecraft and indicates the minimum time elapsed before a specific spacecraft in the constellation can image the same target again, possibly with an off-axis observation. This depends on the ground-track repeat period of the spacecraft's orbit but is not exactly the same parameter.

Before the launch of the first SkySat satellite in 2013, another EO constellation had already paved the way in the field of commercial minisatellite constellations. The RapidEye system, developed by the German company RapidEye EG and now also operated by Planet, consists of five identical spacecraft in a SSO at $\pm$ 630 km altitude. The main customers that RapidEye had in mind for the system were the agricultural industry, international institutions and cartographers [153]. The key mission parameters for this mission are given in Table 5.9.

Next to these two commercial constellations, NASA's A-Train is an important example of a scientific EO constellation in LEO. This constellation differs from the SkySat and RapidEye examples in many ways. Firstly, the constellation is made up of six individual spacecraft, each with their own design and mission objectives. Secondly, the observations of each spacecraft serve scientific purposes, mostly related to climate and atmospheric science, as opposed to commercial ones. As such, the advantages of constellation flying lie more in the fact that different scientific observations of the same area can complement

Table 5.8: Key mission parameters for the SkySat constellation, data from [151], [152].

Constellation name:	SkySat
# spacecraft:	21
Best-case GSD [m]:	0.57
Revisit time (spacecraft) [days]:	4-5
Spectral bands [-]:	Blue, Green, Red, Near Infrared, Panchromatic
Constellation orbit(s):	600 km SSO, 450 km SSO, 400 km non-SSO
Planned mission lifetime [years]:	5
Spacecraft wet mass [kg]:	120
Propulsion system type:	SkySat 3-21: 4x1N HPGP monopropellant thrusters

Table 5.9: Key mission parameters for the RapidEye constellation, data from [153], [154].

Constellation name:	RapidEye
# spacecraft:	5
Best-case GSD [m]:	6.5
Revisit time (spacecraft) [days]:	<5
Spectral bands [-]:	Blue, Green, Red, Near Infrared, Red edge
Constellation orbit(s):	630 km SSO
Planned mission lifetime [years]:	7
Spacecraft wet mass [kg]:	150
Propulsion system type:	Xenon cold gas resistojet thruster

and thereby improve each other [155]. Since 2018, there are two spacecraft in the constellation flying in a different orbit, at an altitude 16.5 km lower than the A-Train orbit. This part of the constellation is called the C-Train, named after the CALIPSO and CloudSat missions flying in it [156]. In the overview of constellation parameters presented in Table 5.10, some entries are not specified or only filled in with a range of values, due to the fact that each of the A-Train spacecraft feature very different designs and payloads.

For the case study at hand, the most relevant aspect of the A-Train constellation is the fact that some of the spacecraft are based on a standardised bus. For example, the PARASOL spacecraft, which ended operations in 2013, is built on the Myriade minisatellite platform, with a wet mass of around 120 kg [157]. As another one of the smaller spacecraft in the constellation, the CALIPSO spacecraft uses the CNES/Thales Alenia Space Proteus platform, with a total launch mass of around 590 kg [158], [159]. Both platforms use a monopropellant hydrazine system, providing a valuable design reference for the conceptual design of the propulsion system for the investigated case study.

Moving away from LEO constellations, there are three single satellite missions that are also very relevant for the application of novel monopropellants in LEO minisatellites. The joint Swedish Space Corporation (SSC)/ESA project PRISMA was launched in 2009, serving as a technology demonstrator for the ECAPS 1 N HPGP thruster using LMP-103S, formation flying and micropropulsion [26]. Next, launched

Table 5.10: Key mission parameters for the A-Train constellation, data from [156].

Constellation name:	A-Train and C-Train
# spacecraft:	4 (A-Train) +2 (C-Train)
Best-case GSD [m]:	-
Orbital repeat period [days]:	<16
Spectral bands [-]:	Numerous
Constellation orbit(s):	705 km SSO (A-Train), 688.5 km SSO (C-Train)
Planned mission lifetime [years]:	-
Spacecraft wet mass [kg]:	120-3000
Propulsion system type:	Various, mostly monopropellant hydrazine

in January 2019, JAXA's RAPid Innovative payload demonstration Satellite 1 (RAPIS-1) included a 1 N Green Propellant Reaction Control System (GPRCS) thruster using the Japanese HAN-based EIL, SHP163 [70]. Finally, the NASA Green Propellant Infusion Mission (GPIM), launched in June 2019, demonstrated the performance of ASCENT with Aerojet Rocketdyne's 1 N GR-1 thruster [160]. Each of these novel monopropellant demonstration missions was largely successful, proving the claimed performance improvements that the respective propellant offers with respect to hydrazine. Table 5.11 gives an overview of these technology demonstration missions. While these spacecraft were purposely built to demonstrate the novel monopropellant system and other experimental payloads, the propulsion system design and development process can still be a relevant reference for the investigated use case.

Table 5.11: Overview of novel monopropellant demonstration missions, data from [51], [62], [70], [160], [161].

Mission name	Launch date	Mission duration [years]	Spacecraft wet mass [kg]	Propellant type	Propulsion system architecture
PRISMA	15-06-2010	5	140	LMP-103S, Hydrazine	2x 1N HPGP, 6x 1N hydrazine
RAPIS-1	18-01-2019	1.5	$\pm$ 200	SHP163	1x 1N GPRCS
GPIM	25-06-2019	1.25	$\pm$ 180	ASCENT	5x 1N GR-1

5.4.2. Finalised mission requirements and key design features

Having considered the mission heritage for the *EO system* concept and the mission design process of these spacecraft, there are three design decisions that need to be made before the mission requirements can be specified to a level that usefully informs the propulsion system design. These are: the type of imaging that the system will perform, the exact SSO orbit used by the constellation, and the mission lifetime. Addressing each of these design elements, it is decided that the *EO system* will be considered as a next-generation successor to the RapidEye and SkySat platforms. As the SkySat satellites are approaching their planned mission lifetime, it is deemed realistic that a similar constellation will be designed to maintain the high-resolution imaging services that Planet is able to provide. In fact, the Planet Pelican constellation is meant to do exactly that: planned for a first launch in 2023, this 32 satellite constellation will upgrade the SkySat constellation by providing higher resolution images at a higher revisit rate [162]. While the design is still not entirely known, it is claimed that these spacecraft will use electric propulsion instead of the novel monopropellant propulsion that was successfully demonstrated onboard SkySat [163].

Keeping in mind the design goal of updating SkySat, the *EO system* should have imaging capabilities in the same spectral range. Next, an appropriate Sun-synchronous orbit is selected. Using the methodology provided by Boain, a set of orbit parameters can be selected to achieve a desired revisit time and adjacent ground track distance [148]. In this context, it is firstly important to clarify that adjacent

ground tracks are two tracks separated by the smallest distance on Earth once all the ground tracks of a single orbit repeat cycle have been laid down, i.e. before the orbit ground track starts tracing over itself again. This parameter is important for the coverage provided by the constellation, as the swath width of the imaging payload should ideally cover a large part of the adjacent ground track distance. With Δl being the on-ground adjacent ground track distance and a_e the Earth's radius, R provides the number of orbital revolutions in a single repeat cycle, following Equation 5.1.

$$R = \frac{2\pi a_e}{\Delta l} \tag{5.1}$$

By choosing a desired repeat cycle period, it is then possible to determine the orbital period and thus the orbit's radius, knowing that SSOs are always circular. With D being the desired number of days in a repeat cycle, Equation 5.2 gives the orbital period P, given that a mean solar day is 86400 s. Using the relation between an orbit's semi-major axis and period, Equation 5.3 specifies the orbit's semi-major axis a, with μ being the Earth's gravitational parameter (= 398600 km^3/s^2). To deliver repeatable and intuitive observational products, it is desirable that the repeat cycle occurs after an integer number of days, such that the time of Equatorial crossing of the orbit remains the same after each repeat cycle. Aiming to match SkySat, it is chosen to have a repeat cycle of 7 days for the *EO system*.

$$P = 86400\frac{D}{R} \tag{5.2}$$

$$a = \sqrt[3]{\mu\left(\frac{P}{2\pi}\right)^2} \tag{5.3}$$

To trace exactly the same ground track path in each repeat cycle, the number of revolutions per repeat cycle should be an integer number. For this parameter however, there is no data available from SkySat and RapidEye to base the new system on. Instead, a goal may be to ensure that the orbit's semi-major axis lies in between the SkySat and RapidEye constellations. The reasoning for this is that the mission should ideally have a longer lifetime than SkySat, thereby dictating a slightly higher orbit for reasonable orbit maintenance requirements, while still achieving similar image quality, thus requiring a lower orbit than RapidEye. As an initial goal, an orbit altitude of 550 km is assumed. Then, the adjacent ground track distance is adjusted through trial and error to find a value resulting in an integer number for R while still remaining close to an orbit altitude of 550 km. This process leads to a combination of 105 revolutions per repeat cycle of 7 days, corresponding to an orbit altitude of 566.89 km and an adjacent ground track distance Δl of 381.666... km. In the terminology proposed by Boain, this orbit can be named 7D105R [148].

To verify whether the chosen orbit could facilitate the same degree of temporal resolution and coverage that SkySat provides, one can consider the distance between two consecutive ground track passages, also known as the fundamental interval. This parameter is found by multiplying the adjacent ground track distance by the number of days in the repeat cycle, resulting in a value of 2671.67 km in the *EO system's* case. For SkySat, the fundamental interval equals 2637 km. In a conference paper on SkySat's flight dynamics, Hawkins et al. describe that this spacing between consecutive passes of a single satellite is covered by the successive passes of four other SkySat satellites following the same orbit, in different phasing positions [164]. As such, the effective spacing between ground tracks of the five SkySats together amounts to 527.4 km, which is within the swath width of 585 km of each satellite, assuming an allowable off-nadir angle of 30 $^\circ$. Assuming that the *EO system* would use similar imaging hardware and be made up of at least five spacecraft, the fundamental interval of 2671.67 km is therefore deemed to be acceptable. In reality, the constellation could be made up of many more than five spacecraft, as in SkySat's case, but the choice of constellation size would depend on various other factors which are outside the scope of this conceptual mission design.

The final step in the design of the desired orbit is to calculate which orbital inclination i, results in a Sun-synchronous rate of precession in combination with the orbit's semi-major axis. Once again using the equations provided by Boain, Equation 5.4 provides the angular rate by which the node of right ascension precesses due to the Earth's equatorial bulge, represented by the harmonic coefficient J_2, equal to 0.00108263 [148]. To satisfy the condition of a Sun-synchronous orbit, i should be chosen such that the rate of nodal precession is equal to the orbital rate with which the Earth rotates the Sun, thereby guaranteeing a fixed relative orientation between the orbit and the Sun. With the idealisation that the

Earth's orbit is circular, this rate is equal to: $2\pi/(365.242199 \cdot 24 \cdot 3600) = 1.99097\ rad/s$. Working out Equation 5.4 with the previously calculated value for a, it is found that the orbit should have an inclination of 97.658 °.

$$\dot{\Omega} = -\frac{3}{2} J_2 \left(\frac{a_e}{a}\right)^2 \sqrt{\frac{\mu}{a^3}} \cdot cos(i) \tag{5.4}$$

With the orbit selected, the only mission parameter left to choose is the mission lifetime. Considering the heritage that has been built with SkySat and RapidEye, a first assumption in this decision is that hardware improvements will be possible, increasing the reliability of the spacecraft in the *EO system*. Secondly, it is noted that both the RapidEye and SkySat systems have been able to outlive their planned mission lifetime. Thirdly, it is also assumed that with an increase in the wet mass budget and a higher orbit altitude, the *EO system's* planned lifetime may realistically be chosen to be longer than the SkySat planned mission lifetime of 5 years. Taking the Pléiades Neo EO constellation, built and operated by Airbus, as a reference, a mission lifetime of 10 years is thus envisioned for the *EO system* [165].

With the definition of the desired spectral resolution, the constellation orbit and the mission lifetime, a finalised set of mission requirements for the *EO system* is presented in Table 5.12. REQ-EOS-04 and REQ-EOS-05 are not yet specified, as this would require investigating a feasible size for the *EO system* constellation, which is outside the scope of this research, as mentioned above. While REQ-EOS-05 could place certain requirements on the propulsion system of each spacecraft, it is decided not to account for this functionality in the propulsion system sizing.

Table 5.12: Finalised list of key *EO system* mission requirements

Label	Description	Rationale
REQ-EOS-01	The EO system shall have a nadir pointing ground sample distance (GSD) of at most 1 m.	The EO system shall provide performance similar to SkySat.
REQ-EOS-02	The EO system shall have a revisit time of no longer than 7 days.	The EO system shall provide performance similar to SkySat.
REQ-EOS-03	The EO system shall image in the following spectral bands: Blue, Green, Red, Near Infrared, Panchromatic.	The EO system shall provide performance similar to SkySat.
REQ-EOS-04	The EO system shall cover at least [TBD]% of the globe every day.	The exact number depends on constellation size, which is not yet defined.
REQ-EOS-05	The EO system shall be able to adjust its observations to cover an area of [TBD] km^2 at the highest resolution of 1 m GSD, within [TBD] days after the provided command.	The exact number depends on constellation size, which is not yet defined.
REQ-EOS-06	The EO system shall orbit in Sun-synchronous LEO at an altitude of 566.89 km.	Based on orbital calculations and a target altitude of 550 km.
REQ-EOS-07	The EO system shall actively de-orbit within 5 years after its service lifetime.	Based on a requirement set by the US Federal Communications Commission [121].
REQ-EOS-08	The EO system shall have a mission lifetime of at least 10 years.	Based on a mission target to equal Pléiades Neo performance.

As a starting point for the propulsion system design in Chapter 6, Table 5.13 provides an overview of the key parameters for the *EO system* case study. Each of these parameters is directly defined by one of the mission requirements, except for the selected dry mass of 150 kg. This parameter was instead inspired by the heritage of the RapidEye constellation, where each spacecraft had a wet mass of 150 kg, with a much less performant propulsion system [153]. Considering that the *EO system* is designed to operate for an additional three years and actively de-orbit, it is also likely that the dry mass would be higher. Furthermore, a system dry mass of 150 kg is also approximately in line with the various technology demonstration missions for novel monopropellants shown in Table 5.11, providing a first indication that suitable flight hardware will be available for the design of the propulsion systems in Chapter 6.

Table 5.13: Key mission parameters for the *EO system constellation*

Constellation name:	*EO system*
# spacecraft:	>5
Best-case GSD [m]:	1
Revisit time (spacecraft) [days]:	<7
Spectral bands imaged [-]:	Blue, Green, Red, Near Infrared, Panchromatic
Constellation orbit(s):	566.89 km SSO, 97.66° inclination
Planned mission lifetime [years]:	10
Spacecraft dry mass [kg]:	<150
Propulsion system type:	Monopropellant system

5.5. Conclusion

For the design of the various propulsion systems that will be compared in the LCSA, the definition of a clear use case is beneficial, as this will provide a proper justification for assumptions and also clearly set the requirements that each propulsion system needs to meet. As such, this chapter has investigated various possible case studies and detailed the top-level parameters for the selected use case. The initial qualitative comparison between five possible case studies indicated that the main monopropellant propulsion system for a minisatellite used in an Earth Observation constellation in SSO features existing heritage for novel monopropellants and is of high relevance for the future growth of the space industry. Using systems engineering practices, stakeholder and system requirements for this conceptual mission have been set up, to replicate a realistic mission design process.

The most important mission heritage for this case study was found in the RapidEye and SkySat constellations, both using minisatellites to deliver commercial EO products. Furthermore, various novel monopropellant technology demonstration missions have also been identified to provide useful data for the propulsion system design. By defining the spacecraft's maximum dry mass, its orbital parameters and mission lifetime, the conceptual mission design provides the main input data for the definition of propulsion system requirements in the next chapter.

6

Propulsion System Design

6.1. Introduction

In this chapter, a top-level design is set up for the different propulsion systems that will be investigated in the LCSA. Comparing the system performance and sustainability of various monopropellants can be done in several different ways, each with their own merits and shortcomings. One option is to take a baseline design using hydrazine, then replacing the propellant by another monopropellant, with the same allowable mass or volume, and then considering what improvements or shortcomings this new system has with respect to the baseline design. In the case of a novel monopropellant with improved I_{sp}, this could mean that the feasible mission lifetime may increase. In this way, the functional unit of the LCSA would be a propulsion system with a specified propellant capacity, expressed in terms of mass or volume. Another way of comparing the systems is to start with the system requirements and to design a separate propulsion system, completely fulfilling these requirements, for each of the considered propellants. In this method, the advantages of more energetic propellants are reflected by a lower system mass and thereby a reduction in the amount of materials and energy used during production. Furthermore, this design method ensures that all the selected components in each system are fully compatible with the respective propellants. For the LCSA, the functional unit resulting from this design method would be a propulsion system fulfilling the requirements for a specific use case.

As this research wishes to determine how the choice of propellant influences the system-level sustainability of the propulsion system, it is decided to follow the latter design method, because this approach places the propellant choice at the initial design stage and lets this choice completely influence the sizing and component selection of the propulsion system. It is also deemed that this design approach is more similar to what would take place if the *EO system* was actually developed. The design process is further detailed in Section 6.2, going over the key propulsion system requirements, design constraints and assumptions, as well as the general method used for the propellant trade-off and system sizing. In Section 6.3, a number of propellants will be selected by means of a trade-off. Finally, Section 6.4 discusses the final conceptual design for each of the considered propellants and provides a comparison of their key characteristics.

6.2. Design methodology

In this section, the general design space for the propulsion systems will be outlined. First, a set of propulsion system (PS) requirements will be proposed based on the key mission requirements stated in Table 5.12 and other more general considerations for propulsion systems. Next to the system requirements, Subsection 6.2.2 will set out a general PS concept that each of the propellants' designs should accord to. While certain propellants may allow for design changes at the system-level, increasing the system's efficiency or capability, the main goal of this design exercise is to create a comparable system

design for each of the propellants. To justify the system requirements and constraints, key assumptions are addressed in Subsection 6.2.3. Finally, Subsection 6.2.5 will describe the methodology applied in the propellant trade-off and the relevant calculations for the PS sizing and component selection.

6.2.1. Design requirements

The main mission requirements affecting the propulsion system design are REQ-EOS-06, REQ-EOS-07 and REQ-EOS-08, respectively specifying the spacecraft's orbit, de-orbiting procedure and mission lifetime. These mission features have a great influence on the required manoeuvres and so-called ΔV budget, informing the required propellant mass for the mission. The first step in defining the PS requirements is to determine the ΔV budget and translate this into the main functional requirements for the PS. After defining the ΔV budget of the system, other functional and non-functional requirements will be formulated based on heritage of similar propulsion systems.

There are generally four manoeuvres, either singular or recurring, which make up the ΔV budget of the PS. Firstly, to position the spacecraft into its correct slot in the *EO system's* Sun-synchronous orbit, an initial phasing manoeuvre is performed. Based on a design ΔV budget for the SkySat system, this initial phasing is estimated at 10 m/s [152]. After this manoeuvre, the system enters its operational lifetime wherein it must maintain its orbital altitude and phase position within the constellation. Using an approximation from Wertz et al., the required velocity increment to maintain an orbital altitude of around 550 km and counteract the disturbances due to aerodynamic drag and solar radiation (with the assumption that the Solar activity over the mission is of an average intensity) is around 3 m/s each year [114, p.177]. Multiplying this by the design lifetime of 10 years, this leads to 30 m/s in total. The estimated budget for phase maintenance is again sourced from the SkySat requirements, where a total of 5 m/s is allotted for the mission lifetime of 5 years [152]. As the *EO system's* lifetime is twice as long, a budget of 10 m/s is therefore required for phase maintenance.

The third contribution to the ΔV budget accounts for collision avoidance. Once again, the appropriate velocity increment is taken over from the SkySat propulsion system design. Hawkins et al. describe that for SkySat 3-7, a total of 40 potential collision events were identified over the course of July 2016 to April 2017 for SkySat 3, and mid-September 2016 to April 2017 for SkySat 4-7 [164]. Taking the average per spacecraft per month, this leads to a value of 1.11 potential collision avoidance manoeuvres per month, or 13.33. over the course of a year. With a maximum manoeuvre magnitude of 0.1 m/s, this results in an allocation of 1.33 m/s per year, or 13.33 m/s in total over the mission lifetime.

The last manoeuvre in the *EO system's* ΔV budget is a burn to de-orbit after its mission lifetime. To comply with REQ-EOS-07, the spacecraft should enter an orbit by which it will re-enter in the Earth's atmosphere within 5 years. With the conservative assumptions that the orbital decay acts with minimal Solar activity and for a 100 kg satellite, data from Yost et al. indicates that a 440 km circular orbit would suffice to meet REQ-EOS-07 [121, p.347]. Using standard astrodynamic calculations, one finds that the velocity in the initial 566.89 km orbit is around 7.58 km/s and that an increase of 70.17 m/s is required to reach the circular orbital velocity of 7.64 km/s at the altitude of 440 km. With all the manoeuvres quantified, Table 6.1 gives an overview of the entire ΔV budget. To account for uncertainties and provide a propellant margin, a safety margin of 15% is added to the total velocity increment budget.

Table 6.1: ΔV budget for the *EO system* propulsion system

Manoeuvre	ΔV **[**m/s**]**
Initial phasing	10
Orbit maintenance (drag compensation and phase maintenance)	10 x 4
Collision avoidance	10 x 1.333...
De-orbiting	70.17
Sub-total	133.50
15% margin	20.03
Total	**153.53**

Next to the ΔV budget, there are various other functional requirements specifying how the propulsion system should perform. One can generally consider that a monopropellant propulsion system for a spacecraft has three main tasks. Firstly, it should safely store the propellant for the duration of the mission, considering the mechanical and thermal environment that the spacecraft is exposed to. Secondly, the propulsion system should safely and reliably feed propellant to one or more thrusters. Lastly, the propulsion system should ensure that the desired manoeuvres are performed through the operation of the thruster(s). These three general tasks inform most of the functional requirements.

In the context of non-functional system requirements, it is found that the specification of mission lifetime and reliability are two key specifications. Furthermore, the use of commercial-off-the-shelf (COTS) components is specified to ensure that the design is feasible to produce in the context of a commercial EO constellation. The various space system budgets limiting the mass, volume, power use, data transfer rate and development cost of the PS are also very important non-functional requirements.

Following this identification of requirements for the propulsion system, as well as the findings from a requirements discovery tree, Tables 6.2, 6.3 and 6.4 give an overview of the PS requirements considered in the design process. As in the definition of mission requirements, this list of requirements is not exhaustive, but it is deemed that this enumeration provides a robust basis for the design choices and sizing that will be performed in Section 6.4. The key PS requirements are indicated by a boldfaced label, indicating that they are driving for the PS design.

Table 6.2: Overview of *EO system* propulsion system requirements, part 1. **Bold** indicates key requirements.

Label	Description	Rationale	Verification method
REQ-PS-BUD-01	The propulsion system shall have a total dry mass of less than 11 kg.	Based on SkySat [141].	Inspection
REQ-PS-BUD-02	The propulsion system shall have a total volume of less than 0.04 m^3.	Based on SkySat [152].	Inspection
REQ-PS-BUD-03	The propulsion system shall have a nominal power consumption of up to 32 W.	Based on GPIM and SkySat [67], [141].	Testing
REQ-PS-BUD-04	The propulsion system shall have a peak power consumption of up to 100 W.	Based on GPIM [67].	Testing
REQ-PS-BUD-05	The propulsion system shall have a peak data transmission rate of up to [TBD] bit/s.	Specified at a later design stage.	Testing
REQ-PS-BUD-06	The propulsion system shall have a total development cost of less than [TBD] €.	Specified at a later design stage.	Demonstration
REQ-PS-FEED-01	The propulsion feed system shall deliver propellant to the thrust chamber assembly at a minimum chamber pressure of 25 +- 3 bar at beginning of life.	Common value for similar systems [62], [67], [132].	Testing
REQ-PS-FEED-02	The propulsion feed system shall deliver propellant to the thrust chamber assembly at a minimum chamber pressure of 6.25 +- 1 bar at end of life.	Blow-down of 4:1 is common for similar systems [62], [67], [132].	Testing
REQ-PS-FEED-03	The propulsion system shall be at least double fault tolerant with respect to propellant flowing into the thrust chamber assembly.	Safety precaution for loading and launch procedures.	Inspection
REQ-PS-GEN-01	The propulsion system shall fulfill all its requirements over the mission lifetime of 10 years.	Longer lifetime than SkySat, similar to Pléiades Neo satellites [165].	Analysis
REQ-PS-GEN-02	The propulsion system shall have a total reliability of at least [TBD]%.	Specified at a later design stage.	Analysis
REQ-PS-GEN-03	All components in the propulsion system, with the exception of the propulsion tank and the thruster assembly, shall be readily available as COTS components.	The propulsion system should be produced in series and with reduced cost.	Demonstration

Table 6.3: Overview of *EO system* propulsion system requirements, part 2. **Bold** indicates key requirements.

Label	Description	Rationale	Verification method
REQ-PS-PERF-01	The propulsion system shall provide a velocity increment of 11.5 m/s for initial orbit phasing.	Based on SkySat [152] + 15% margin.	Analysis/ Testing
REQ-PS-PERF-02	The propulsion system shall provide a velocity increment of 4.6 m/s per year for orbit maintenance.	Calculation [114], [152] + 15% margin.	Analysis/ Testing
REQ-PS-PERF-03	The propulsion system shall to provide a velocity increment of 15.33 m/s per year, for collision avoidance.	Based on SkySat [164] + 15% margin.	Analysis/ Testing
REQ-PS-PERF-04	The propulsion system shall provide a velocity increment of 81 m/s for de-orbiting at end of life.	Calculation + 15% margin.	Analysis/ Testing
REQ-PS-PERF-05	The propulsion system shall deliver its nominal thrust with an accuracy of 5% at beginning of life.	Based on HPGP [62].	Testing
REQ-PS-PERF-06	The propulsion system shall achieve a minimum impulse bit of 15 mNs.	Based on GPIM and Aerojet MR-103J [67], [125].	Testing
REQ-PS-PERF-07	The propulsion system shall be capable of 30000 restarts.	Based on POLON [34].	Testing
REQ-PS-PERF-08	The propulsion system shall be capable of a total firing time of 3 hours.	Based on POLON [34].	Testing
REQ-PS-PERF-09	The propulsion system shall be capable of completing a maximum continuous firing time of 75 s.	Based on HPGP [137].	Testing
REQ-PS-PERF-10	The propulsion system shall be capable of completing a minimum firing time of 100 ms.	Based on HPGP [62].	Testing
REQ-PS-PERF-11	The propulsion system shall reach nominal thrust within 70 ms of thruster operation.	Based on HPGP [62].	Testing
REQ-PS-PERF-12	The propulsion system shall deliver [TBD]% of its nominal specific impulse at end of life.	Specified at a later design stage.	Analysis/ Testing
REQ-PS-PERF-13	The propulsion system shall deliver no less than 25% of its nominal thrust level at end of life.	Blow-down of 4:1 is common for similar systems [62], [67], [132].	Analysis/ Testing
REQ-PS-PERF-14	The propulsion system shall have a start-up time of no more than 30 minutes.	Based on SkySat [141]	Testing
REQ-PS-PERF-15	The propulsion system shall be capable of providing impulse changes in 3 degrees of freedom.	To limit the requirements for the ACS, the propulsion system should allow for manoeuvres in different axes.	Demonstration

Table 6.4: Overview of *EO system* propulsion system requirements, part 3. **Bold** indicates key requirements.

Label	Description	Rationale	Verification method
REQ-PS-STOR-01	The propulsion system shall store the propellant during the mission lifetime of 10 years, with an allowable passive decomposition of propellant mass of [TBD]%/year.	Specified at a later design stage.	Testing
REQ-PS-STOR-02	The propulsion system shall store the propellant within a temperature range of 275-387 K.	Baseline for hydrazine [12].	Testing
REQ-PS-STOR-03	The propulsion system shall be at least double fault tolerant with respect to propellant flowing out of the tank.	Safety precaution for loading and launch procedures.	Inspection

6.2.2. Design constraints

Next to the requirements that the design should fulfil, the PS design space is narrowed down at the beginning of the process by setting out a number of design constraints. The first constraint is quite obviously that the system will be a monopropellant system. Using the definition proposed by Nosseir et al., this implies that the system uses ”any propellant that is stored in a single tank and is able to decompose from its storage form by the help of a catalyst or other ignition method, such as thermal or electric ignition [...], as long as it does not require another separately stored propellant for decomposition” [12]. Furthermore, it is fixed that the monopropellant system being designed is the only propulsion system on board the spacecraft. As a result, all the requirements need to be fulfilled solely by this system and all auxiliary components (e.g. heaters, electronics) are designed only to serve the monopropellant system.

Monopropellant systems are developed following different architectures; a prime distinction between the architectures is the way in which the propellant is driven out of the tank, as discussed in Subsection 2.2.2. In the case of monopropellant systems for a use case with a relatively low total impulse, pressure-fed systems are typically preferred due to their simplicity, leading to a lower total mass and cost and a higher reliability than pump-fed systems. Within the category of pressure-fed systems, another distinction is made between pressure regulated and blow-down systems, where the latter option stores the pressurant together with the propellant in a singular tank, leading to a system with lower dry mass, but a decreasing thrust performance over time.

Considering the specifics of the investigated use case, where system simplicity, reliability and development cost are at least as important as the delivered performance, it is decided to use a blow-down system with an elastomeric diaphragm tank for the case study. This choice is motivated not only by the extensive heritage of this type of architecture, being employed in many hydrazine systems and in the technology demonstration missions of the three prominent EIL novel monopropellants [62], [67], [70], [132], but also by the fact that this type of architecture can be proportionally scaled up or down according the required propellant load for each propellant, which is not necessarily the case for blow-down tanks using propellant management devices. For the purposes of the LCSA later in this research, it is desirable that the differences between the designed systems reflect the differences between each of the propellants as much as possible, even if one may have to use fixed component sizes in reality. As implied by the system requirements REQ-PS-FEED-02 and REQ-PS-PERF-13, a blow-down ratio (BDR) of 4:1 will be used, meaning that the volume of the pressurant gas increases fourfold over the mission lifetime. This choice is informed by the design of propulsion systems for similar use cases [62], [67], [132].

Along with the choice of feed system, the rest of the system architecture is also constrained for any choice of propellant. There are three main motivations for imposing this constraint. Firstly, a common system architecture ensures that all designed propulsion systems will comply with the propulsion system requirements set out in Subsection 6.2.1. This is especially relevant for the requirements related to overall system safety and redundancy. Secondly, this design constraint will facilitate a more straightforward approach for data collection in the LCI phase of the LCSA, as similar components will be selected for each propellant option. While this potentially takes away some benefits of specific monopropellants, a third motivation for the constraint does not consider this to be a drawback, as it aims for the different propulsion systems to be as similar as possible. This final motivation is based on the common claim that novel monopropellants can act is simple ”drop-in replacements” for hydrazine, and therefore wishes to allow for a sustainability comparison of such a replacement.

Figure 6.1 provides a schematic for the common system architecture that will be used for each of the monopropellant options. This design is based on heritage architectures found in literature and represents a generic system that is often used in small hydrazine propulsion systems and also been adopted in novel monopropellant demonstration missions [62], [67], [132], [166]. It contains two service valves to fill and drain pressurant and propellant, one spherical propellant tank using an elastomeric diaphragm to separate the helium pressurant from the propellant, an orifice to set the downstream system pressure, one pressure transducer, one filter, one latch valve acting as an isolation valve between tank and thruster, and four 1 N thrusters, each including a doubly redundant flow control valve.

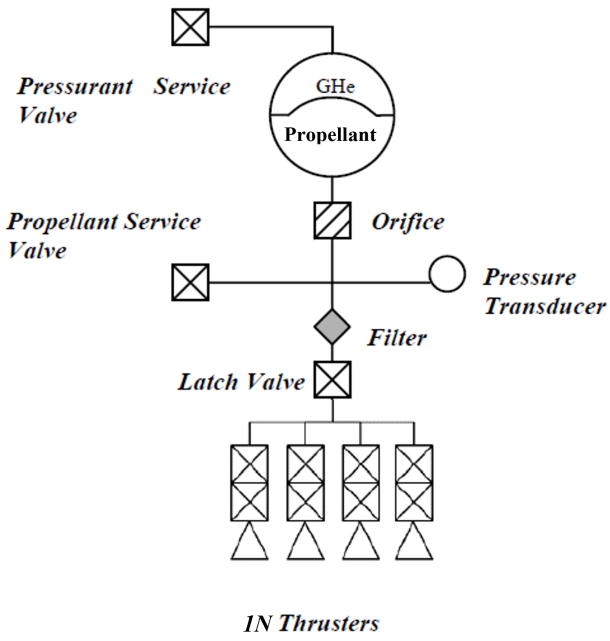

Figure 6.1: Common propulsion system architecture, collage using [62], [141]

The common system architecture also specifies two other important design constraints, namely that the system is pressurised using gaseous helium, and that four 1 N thrusters are used. As an alternative to using helium as the pressurant gas, gaseous nitrogen (N_2) could also be used, as was done in the GPIM propulsion system [67]. However, as other sources identified helium to be a more common option, in hydrazine propulsion systems such as the Myriade PS, or in the LMP-103S systems of PRISMA or SkySat, it was decided to select this option [62], [132], [141]. Using four thrusters is seen as the most straightforward way of complying with REQ-PS-PERF-15, including a level of redundancy if one of the thrusters fails. Furthermore, the use of 1 N thrusters is a typical choice for propulsion systems similar to the defined case study, as such also deemed to be sufficient to meet the stated performance requirements.

Another design constraint is imposed by REQ-PS-GEN-03, stating that all components except for the tank and thrusters must be commercially available, such that a clear component selection can take

place. While this does not imply that only flight-proven hardware can be selected for each of the considered propellants, adequate material compatibility must be in place when choosing components originally developed for use with a different propellant. This design constraint is made in light of the required data availability to set up reliable LCIs for each of the design propulsion systems. It will also feed into the trade-off, where data availability is one of the criteria as discussed in Subsection 6.2.4. Additionally, this design constraint is deemed necessary to ensure that the LCSA deals with systems that are representative of current monopropellant technologies. Furthermore, this constraint justifies a key assumption in the life cycle inventory analysis, namely that all components have a technology readiness level (TRL) of 9, such that no additional costs or activities are required to qualify the components before flight.

6.2.3. Assumptions

In the propulsion system sizing method, various assumptions are made to simplify the overall design process. An overview of the most important assumptions in this regard is shown in Table 6.5. Other smaller assumptions will always be clearly mentioned in the methodology description presented in Subsection 6.2.5.

Table 6.5: Overview of key assumptions used in propulsion system sizing method

Label	Description	Justification
A-PS-01	Detumbling is not included in the ΔV budget of the system.	This velocity increment is difficult to estimate, may be provided by other attitude control systems, and is most likely minor compared to other budget contributions.
A-PS-02	The propellant tank can be exactly sized with respect to the required propellant load.	This assumption is quite unrealistic as propellant tanks are usually not tailored to size. However, the assumption is made to reflect the performance difference between the various monopropellants as best as possible.
A-PS-03	The HTP propellant tank can be vented once a week.	This assumption allows for built-up oxygen to exit the tank. The assumption is deemed valid due to the existence of oxidizer vent valves in other systems [167].
A-PS-04	The HTP propellant tank diaphragm does not accelerate HTP decomposition.	Teflon or Viton have very low AOL values. The AOL for tank shell is overestimated, such that it may also cover the negligible portion of decomposition caused by the tank diaphragm [168].
A-PS-05	All thrusters include an integrated catalyst bed heater and flow control valve.	Commercially available hydrazine and EIL thrusters justify this assumption [125], [169].
A-PS-06	Each thruster has an I_{sp} quality factor (η_{Isp}) of 0.85.	This value is informed by Zandbergen [117, p.60].
A-PS-07	Each propellant tank has an expulsion efficiency (η_{exp}) of 0.98.	This value is informed by Sutton and Biblarz [84, p.196].
A-PS-08	The safety factor used for yield stress (SF_y) is 1.25.	This value is informed by Zandbergen [117, p.298].
A-PS-09	The tank shell mass correction factor (K_{shell}) is 1.85.	This value is informed by Zandbergen [117, p.347].
A-PS-10	The minimum tank shell thickness ($t_{shell,min}$) is 0.85 mm.	This lower limit for manufacturability is informed by commercial titanium tanks [170].

6.2.4. Propellant trade-off method

To select a set of monopropellants for which propulsion systems will be designed and compared, a graphical trade-off will be performed. As argued in Section 4.3, this qualitative type of trade-off is seen to be the most appropriate at this level of conceptual design. Not only will the evaluation of various criteria be less ambiguous or convoluted than would potentially be the case with a fully numerical trade-off, the graphical trade-off method also provides more flexibility when making a final decision. This level of flexibility is desirable for the propellant trade-off, as practical matters, such as the limited thesis timeline and feasibility of gathering sufficient data for the LCI definition, must also be taken into account.

A number of relevant trade-off criteria will be selected and a clear evaluation scheme for each will be outlined in the following subsections. Section 6.3 will present the trade-off itself with a table featuring colour-coded scores for each criterion and scaled column widths according to the criteria weights. To prove the robustness of the trade-off result and method, a sensitivity analysis will be performed. Finally, considering the practical concerns mentioned before, Subsection 6.3.4 will discuss the results and present the final selection of propellants.

Trade-off criteria

The propellant trade-off is supposed to reflect both the likelihood of each propellant being chosen in an actual conceptual PS design process, and the feasibility of performing an accurate LCSA of a propulsion system using each propellant. As such, the criteria judge the propellants on these two levels as well. Table 6.6 presents the six criteria that will be used in the trade-off. Along with their respective weights, which range from 1 to 4, a short description of what is evaluated in this criterion and a rationale for including the criterion is also presented.

Table 6.6: Overview of propellant trade-off criteria

Criterion	Weight	Description	Rationale
Specific impulse (I_{sp})	4	Main performance parameter, directly dependent on propellant.	Defines the spacecraft wet mass or inversely the possible mission lifetime.
Availability	3	Availability of public data, COTS components and propellant itself.	Indication of LCSA accuracy and likelihood of inclusion in actual missions.
System complexity	3	Considers necessity of new technologies, ignition system, design complexity.	Indication of system reliability and robustness and development cost.
Density (ρ)	2	Physical parameter of propellant.	Strongly influences system volume.
Safety	2	Propellant hazards, handling costs and risk of leakage.	Indication of pre-launch costs and suitability as non-toxic substance.
Storability	1	Material compatibility, temperature range and passive decomposition.	Indication of suitability for longer missions, ease of use within hydrazine system architectures.

The first criterion is the propellant's specific impulse, which is weighted as the most important criterion due to its direct influence on the required propellant and tank mass. The second most important criterion is Availability, referring both to the physical availability of the propellant and required propulsion system components, and the availability of data to inform an accurate LCI, thus addressing both trade-off

goals specified at the start of this subsection. System complexity is also included in the trade-off, as it provides a proxy for total system cost and reliability, which are certainly important elements for a PS for a commercial constellation mission. The same can be said for Safety, which reflects the potential handling costs and infrastructure costs to facilitate the use of toxic propellants. Because the considered PS is to be used in a minisatellite, it is also likely that the volume will be constrained, making propellant Density another criterion to consider in the overall trade-off.

Finally, Storability is considered as the least important criterion, with a weight of 1. While this aspect is often an important factor in the development of novel monopropellants and compatible systems, the criterion is given the lowest weight as the propulsion system for any propellant that is selected would have to be designed to meet all PS requirements either way. As such, the storage difficulties for some propellants are considered to be more easily dealt with than other factors such as System complexity or Safety.

Criteria evaluation method

To reduce the level of ambiguity of the graphical trade-off, a transparent evaluation scheme is set up in Table 6.7. As the table shows, the graphical trade-off will give one of four scores, with the performance for the criterion being ”Excellent”, ”Good”, ”Acceptable” or ”Poor”, each related to a colour and a colour code, respectively blue [bl], green [gr], yellow [ye] and red [re]. The colours shown in Table 6.7 will also be used for clarity in the trade-off results table. The evaluation of any trade-off criterion will be solely based on information that is found in public literature. A rationale will now be provided for each of the six criteria evaluation methods.

Starting with the specific impulse criterion (I_{sp}), the provided scale is based on the current state of the art of monopropellants. As found in Subsection 2.2.1, some experimental monopropellants provide I_{sp} values above 300 s [12], [76]. For the best performance, 260 s is therefore taken as a lower bound, as this constitutes the maximal performance for the flight-proven EIL monopropellants, with the Japanese SHP163 attaining the highest flight-proven theoretical I_{sp} of 276 s [12]. The next best category, providing a Good score, reaches until the lower bound of hydrazine’s theoretical I_{sp}, at 220 s [21]. Next, an Acceptable I_{sp} is accorded to the performance of less energetic monopropellants, such as HTP at high concentrations and nitrous oxide, providing a range between 220 and 180 s. Any monopropellant with an I_{sp} below 180 s is considered to have Poor performance.

The assessment of a propellant option’s Availability is conducted more qualitatively, considering three elements. The existence of previous flight-proven systems in literature, the material availability of the propellant itself and the availability of commercial components with transparent data are considered to be a sufficient indication of how realistic it would be to actually design a propulsion system for this propellant option, and how feasible it will be to perform a valuable LCSA of that PS design. By having a good availability for all three elements, a propellant option will be awarded an Excellent score for Availability, with the other scores being accorded as shown in Table 6.7.

Thirdly, System complexity is evaluated based on the complexity of changing the design of a baseline hydrazine system to accommodate a novel monopropellant. This includes the implicit assumption that a hydrazine PS has a low complexity, which is a reasonable assumption due to its 60 year heritage in the space industry. The development of arguments for the subsequent Good and Acceptable scores contain some ambiguity, as it may be difficult to gauge whether a propellant option requires ”some” or ”several” components to be replaced. Furthermore, the assessment will also take into account whether new components feature a greater level of complexity than those used in a hydrazine system. If a propulsion system has not yet been fully designed for the considered propellant, a Poor score is given for system complexity, as this typically indicates that specific design challenges have not yet been solved.

Moving to the propellant density (ρ), a quantitative evaluation method is used, once again based on the observed performance of conventional and novel monopropellants. Here, uniform intervals are formed starting at the round value of 1050 kg/m^3, as this presents the improvement that several monopropellants feature with respect to hydrazine’s density of 1010 kg/m^3 [22]. The other scores for density move uniformly towards the lower bound of 850 kg/m^3 as this is more or less the highest density of

Table 6.7: Evaluation scheme used for criteria in propellant trade-off

Score:	Excellent [bl]	Good [gr]	Acceptable [ye]	Poor [re]
I_{sp} **[s]**	$\geq$ 260	220-260	180-220	$\leq$ 180
Availability	Multiple flight-proven systems, COTS components AND propellant are easily available.	Some flight-proven systems, COTS components limited OR propellant limited.	Some flight-proven systems, COTS components limited AND propellant limited.	Operational flight model thruster still in development.
System complexity	Fully compatible with hydrazine system.	Some key components require adaptation.	Several key components require adaptation w.r.t. hydrazine OR different system architecture.	System is not yet fully developed.
ρ **at 20** $^{\circ}C$ **[**kg/m^3**]**	$\geq$ 1050	950-1050	850-950	$\leq$ 850
Safety	No hazards.	Careful handling is required, fatality very unlikely.	Severe safety hazards, extreme caution required.	Exposure may be fatal or lead to long-lasting harm. SCAPE or similar is required.
Storability	Proven mission lifetime of 10+ years.	No storage issues with material compatibility similar to hydrazine.	No storage issues with material compatibility more restrictive than hydrazine.	Stable storage is difficult to achieve, very limited material compatibility.

the nitrous oxide-based monopropellants.

Next, the Safety of the propellant is based on the health hazards typically reported on safety data sheets or in the data of the ECHA. The safety hazards related to hydrazine are considered as the worst case, as this has been deemed to be no longer sustainable in various use cases and stated as a key motivation for developing novel monopropellants [10]. For the final criterion, Storability, hydrazine's storability is deemed to be Excellent, as the extensive heritage has resulted in a good understanding of how to preserve the propellant for very long missions [19]. The other scores are defined in comparison to this baseline, with a Poor Storability for propellants with a very restrictive material compatibility, for which it is unlikely that flight-ready propellant tanks have been constructed.

6.2.5. Propulsion system design method

For each of the propellant options selected in the trade-off, a conceptual design will be defined meeting the requirements set in Subsection 6.2.1. As this design exercise will be repeated at least three times or more, depending on how many propellants are selected, a simple and repeatable design method is required. As the design constraints have already defined the overall PS architecture and feed system, the only remaining tasks within the PS design are to size the propellant tanks according to the specific propellant selected and ΔV, and to select COTS components that are compatible with each of the propellant options. The selection of components will be done through literature research, with the relevant sources stated for each case in Section 6.4. The method used for tank sizing will be the subject of this subsection.

Starting very broadly, Table 6.8 gives the main design constants, inputs and outputs that will be used in the sizing calculations. The constants are determined by the choice of sizing method and by the assumptions listed in Subsection 6.2.3 relevant to the design factors. The fixed inputs have been set by the definition of mission and PS requirements, and by the design constraint choosing a helium blow-down system with a BDR of 4:1. The propellant mainly influences the system's specific impulse and the materials used in the tank, as these have to be compatible with the chosen propellant. In the output, all parameters except the spacecraft total wet mass are direct inputs for the LCI later on.

Table 6.8: Overview of propulsion system design inputs and outputs

Constants	Fixed input	Propellant-dependent input	Output
g_0	ΔV	I_{sp}	m_{prop}, m_{press}, m_{tank}, m_{shell} m_{dia}, $m_{sc,wet}$
R	$m_{sc,dry}$, $p_{tank,in}$, BDR	ρ_{prop}	V_{tank}
Design factors: η_{Isp}, η_{exp}, K_{shell}, SF_y, $t_{shell,min.}$	ρ_{press}, M_{press}	Tank shell and diaphragm material	r_{tank}, t_{shell}

The sizing calculations are performed in a Python script, which is shown in full in Appendix A. As this code was written after the propellant trade-off, it only allows for PS sizing with the selected propellants. This also means that specific design considerations for some of the propellant options not selected may not be taken into account. The first step in the process is to select a propellant, thereby defining the system I_{sp} and propellant density, as well as the material properties of the tank shell and diaphragm. In the current version of the code, two tank versions are implemented, with either a titanium alloy Ti-6Al-4V shell and SIFA-35 diaphragm, a combination that has been proven to be compatible with hydrazine and LMP-103S [80], or a aluminium alloy Al5254 shell and fluorinated ethylene polymer (FEP) diaphragm, which is suitable for HTP-based propellants [168], [171]. The relevant properties for each of these propellant tank options are shown in Table 6.9.

Table 6.9: Overview of propellant tank parameters

Parameter	Ti tank	Al tank	Unit
Shell material	Ti-6Al-4V [172]	Al5254 [168]	-
Shell density (ρ_{shell})	4430 [173]	2660 [174]	kg/m^3
Shell yield stress ($\sigma_{y,shell}$)	880 [173]	117 [174]	MPa
Diaphragm material	SIFA-35 [80]	FEP [171]	-
Diaphragm density (ρ_{dia})	1120 [172]	2150 [171]	kg/m^3
Diaphragm thickness (t_{dia})	1.78 [175]	0.25 [171]	mm

Calculation of baseline required propellant mass

The sizing calculation starts by correcting the theoretical specific impulse reported for propellants by using an I_{sp} quality factor, η_{Isp}. This quality factor is assumed to equal 0.85, taking a midpoint of the typical range set up by Sutton and Biblarz, as reported by Zandbergen [117, p.60]. The ”real” I_{sp} is calculated using Equation 6.1.

$$I_{sp,real} = \eta_{Isp} \cdot I_{sp,th.} \tag{6.1}$$

Next, an adapted version of the Tsiolkovsky equation is used to calculate the propellant mass required to deliver the desired ΔV, as shown in Equation 6.2 [117, p.5]. In this equation, the initial spacecraft mass (m_0) is taken as the sum of the dry mass and the propellant mass. At the end of all manoeuvres, the final spacecraft mass will be the dry mass plus what is left of the propellant in the propellant tank. This residual propellant mass can be calculated with the tank expulsion efficiency, η_{exp}, as: $(1 - \eta_{exp})m_{prop}$. Once again taking the midpoint of the estimate provided by Sutton and Biblarz, the expulsion efficiency is assumed to equal 0.98 [84, p.196].

$$\Delta V = g_0 I_{sp,real} \ln\left(\frac{m_{sc,dry} + m_{prop}}{m_{sc,dry} + (1-\eta_{exp}) m_{prop}}\right) \tag{6.2}$$

Rearranging Equation 6.2 for m_{prop} leads to Equation 6.3. For most propellants, this equation is enough to determine the required propellant mass and the rest of the sizing can go on, determining pressurant mass and tank mass. However, HTP-based monopropellants suffer from the passive decomposition of HTP over time, requiring additional calculation steps to ensure that sufficient propellant will be on-board at EOL to perform the required manoeuvres.

$$m_{prop} = \left(\frac{e^{\frac{\Delta V}{g_0 I_{sp,real}}} - 1}{1 - (1-\eta_{exp}) e^{\frac{\Delta V}{g_0 I_{sp,real}}}}\right) m_{sc,dry} \tag{6.3}$$

Estimation of HTP decomposition

The key equation in calculating how much HTP undergoes decomposition, and how this affects the remaining HTP's concentration, is given by Equation 6.4, as defined in [168, p.176]. This equation gives the mass of oxygen generated (m_{O_2}) for a specific value of Active Oxygen Loss (AOL) with an initial concentration (c_{in}) and mass of hydrogen peroxide solution ($m_{sol,in}$) over the span of d days. Note that $m_{sol,in}$ denotes the mass of the total H_2O_2 solution and not the mass of pure H_2O_2 contained in this solution. Using the hydrogen peroxide decomposition reaction as shown in Equation 6.5 and knowing the molar mass of each of the reaction elements, the mass of reacted oxygen can be related to the mass of hydrogen peroxide that is decomposed. The new mass of the HTP solution, $m_{sol,fin}$ is found by subtracting the mass of generated oxygen from the initial solution mass, as shown in Equation 6.6. The new concentration of the HTP solution, c_{fin}, can be calculated with Equation 6.7, knowing the decomposed mass of hydrogen peroxide ($m_{H_2O_2}$) from Equation 6.5. Finally, the I_{sp} of the remaining HTP monopropellant solution can be calculated by using linear interpolation with known I_{sp} values for HTP concentrations of 98% and 85%, respectively from [31] and [12]. This is done in Equation 6.8.

$$m_{O_2} = 0.47 AOL \cdot c_{in} \cdot m_{sol,in} \cdot d \tag{6.4}$$

$$2H_2O_2 \rightarrow 2H_2O + O_2 \tag{6.5}$$

$$m_{sol,fin} = m_{sol,in} - m_{O_2} \tag{6.6}$$

$$c_{fin} = \frac{c_{in} \cdot m_{sol,in} - m_{H_2O_2}}{m_{sol,fin}} \tag{6.7}$$

$$I_{sp} = 190 - \frac{190 - 150.47}{0.98 - 0.85} \cdot (0.98 - c_{fin}) \tag{6.8}$$

An additional complication is the fact that AOL depends a variety of factors. In this methodology, it will be assumed that AOL only depends on the surface (in contact with the tank shell) to volume ratio of the propellant (S/V). For an HTP concentration of 90% and a metallic tank made of Al5052 aluminium alloy, the relation shown in Equation 6.9, adapted from an empirical relation given in [168, p.364], relates the AOL to the S/V expressed in $1/inch$. The fact that the included HTP propellant is of a 98% concentration, and that the tank material is Al5254 instead of Al5052, makes the use of Equation 6.9 conservative, as both the increased HTP concentration and usage of Al5254 instead of Al5052 would lead to lower values for AOL in reality [168, p.277].

$$AOL = \frac{0.175 \cdot S/V[\text{1/inch}] + 0.0075}{10000} \tag{6.9}$$

At each point during the mission, it is trivial to calculate the propellant volume V, but determining the wetted surface area S where passive HTP decomposition is promoted is more difficult, as it requires assumptions on the dynamics of the tank diaphragm inversion during the mission lifetime. A first assumption herein is that the FEP diaphragm is completely inert w.r.t. HTP decomposition, which is confirmed by the very low AOL values for the patented FEP material Teflon [168, p.296]. The estimation of the shell area that is in contact with the propellant as the tank empties, is based on the approximate operating conditions as shown in Figure 6.2. The image shows that as the pressurant (in green) takes up more than half the tank volume, the diaphragm starts to cover the shell in the upper half of the tank, where the HTP monopropellant is stored. Note that this illustration shows the propellant to be in the tank upper half, whereas the system diagram in Figure 6.1 follows a more conventional approach of showing the propellant in the lower half.

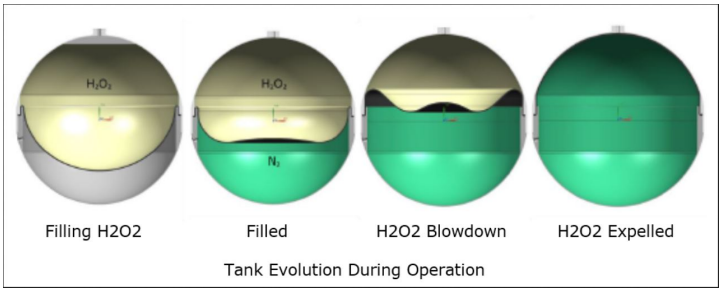

Figure 6.2: Diagram of blow-down elastomeric diaphragm tank operation, from [176]

As long as the propellant volume takes up more than half of the tank volume, it is assumed that the entire bottom half of the tank is in contact with propellant, leading to a surface area as shown in Equation 6.10.

$$S = 2\pi r_{tank}^2 \tag{6.10}$$

Once the propellant volume is less than half the tank volume, it is assumed that the elastomeric diaphragm starts folding over, as in the frame titled ”H2O2 Blowdown” in Figure 6.2. In this regime, the radius of the semi-spherical surface that is in contact with the propellant is considered to decrease by dr. This dr is assumed to be proportional to the increasing fraction of tank volume that is taken up by the pressurant. The volume of pressurant may be found with Equation 6.11. With Equation 6.12, the radius of a theoretical sphere containing V_{press} is calculated. As the pressurant volume will be larger than half the tank volume, r_{press} will also be larger than the theoretical radius of the full sphere containing half the tank volume, as calculated in Equation 6.13. The reduction in surface area radius dr is calculated with Equation 6.14, which is then used in Equation 6.15 to calculate the approximate wetted surface area left. While this approach of calculating the wetted aluminium surface for each value of V_{prop} is very approximate, it is deemed to be a good enough estimation considering the complexity of the actual dynamics of an elastomeric diaphragm in a weightless environment.

$$V_{press} = V_{tank} - V_{prop} \tag{6.11}$$

$$r_{press} = \sqrt[3]{\frac{3V_{press}}{4\pi}} \tag{6.12}$$

$$r_{S,in} = \sqrt[3]{\frac{1}{2}} r_{tank} \tag{6.13}$$

$$dr = r_{press} - r_{S,in} \tag{6.14}$$

$$S = 2\pi(r_{tank} - dr)^2 \tag{6.15}$$

With the calculations above, the rate of passive HTP decomposition can be estimated at each point during the PS lifetime, depending on the propellant mass left. The method of estimating whether a certain HTP propellant load is sufficient to achieve the PS requirements then consists of iteratively calculating the mass of HTP propellant left in the propellant tank each week, taking into account the passive decomposition and required manoeuvres. The initial guess for the total propellant mass is taken from the baseline method shown above, such that an estimated spacecraft wet mass is calculated as shown in Equation 6.16. Note that this leaves out the mass of the pressurant, which is neglected in these iterations due to its low mass. Furthermore, an estimated propellant tank volume is calculated with Equation 6.17, as this will be used in the calculation of S/V.

$$m_{sc,wet} = m_{sc,dry} + m_{prop,i} \tag{6.16}$$

$$V_{tank} = \frac{BDR \cdot m_{prop,i}}{(BDR - 1)\rho_{prop}} \tag{6.17}$$

For each manoeuvre, the required propellant to burn is calculated once again with the Tsiolkovsky equation from [117, p.5], reorganised to Equation 6.18. With the ΔV budget determined in Table 6.1 and applying a 15% margin separately for each contribution, Table 6.10 provides an overview of the ΔV values used within the iterative HTP propellant reduction calculation.

$$m_{burn} = m_{sc,wet} \cdot \left(1 - e^{\frac{-\Delta V}{g_0 I_{sp,real}}}\right) \tag{6.18}$$

Table 6.10: Overview of ΔV contributions in HTP PS sizing

Manoeuvre	ΔV **[**m/s**]**
Initial phasing	11.5
Weekly maintenance, phasing, collision avoidance	0.118
De-orbiting	80.7

Before the iterative process, the propellant mass required for initial phasing is subtracted from the initial total propellant mass estimate, using the original HTP monopropellant I_{sp} and Equation 6.18. Then, at the start of each ”calculation week” in the script, the mass, concentration and I_{sp} of propellant is corrected for the passive decomposition that has taken place in the seven days before, using the equations at the start of this subsection. A key assumption here is that the spacecraft PS is able to vent the generated oxygen once a week. To that end, the HTP PS design will include a vent valve. With the reduced propellant mass, the spacecraft wet mass is also adjusted, using Equation 6.16. Next, the required ΔV for one week of operations, as reported in Table 6.10, is related to the required mass of propellant to be burned using Equation 6.18. At the end of the ”calculation week”, this propellant amount is subtracted from the current propellant mass, providing the input for the HTP decomposition calculation of the next week. After the the program has run through the mission lifetime of 520 weeks, the final manoeuvre of de-orbiting is also implemented, providing the final reduction in propellant mass.

If the propellant mass is larger than zero at this point, this means that the initial guess for propellant mass was sufficiently large to deal with the passive HTP decomposition and the delivery of ΔV throughout the mission. However, if the remaining propellant mass at EOL is negative, this indicates that additional

propellant needs to be included to complete the mission with the HTP PS. As such, the script adds 0.1 kg to the initial guess and runs through the entire calculation process to check if this new propellant mass estimate is sufficient. Once an initial propellant mass is found for which the EOL propellant margin is positive, this is taken as an adequate propellant load, after correcting this value for the expulsion efficiency η_{exp}.

Calculation of pressurant and tank parameters

With the required propellant mass calculated, the sizing method continues by estimating the required pressurant volume at the initial PS conditions, using Equation 6.19. Then, the initial pressurant density may be found with Equation 6.20 using the ideal gas law and assuming a tank temperature (T_{tank}) of 20 $^{\circ}C$, with $p_{tank,in}$ being the initial tank pressure of 25 bar, M_{press} the pressurant molar mass (0.004 kg/mol for helium), and R the molar gas constant of 8.3145 $J/mol/K$. Using the initial pressurant volume and density, the pressurant mass is simply calculated in Equation 6.21.

$$V_{press,in} = \frac{m_{prop}}{(BDR-1)\rho_{prop}} \tag{6.19}$$

$$\rho_{press,in} = \frac{p_{tank,in} M_{press} T_{tank}}{R} \tag{6.20}$$

$$m_{press} = \rho_{press,in} V_{press,in} \tag{6.21}$$

The initial propellant and pressurant volumes are added to find the required tank volume in Equation 6.22. As the propellant tank is spherical, Equation 6.23 may be used to determine the tank radius. Next, the required tank shell thickness to withstand the internal tank pressure without yielding is calculated with Equation 6.24, with a thin-walled assumption [117, p.299]. The safety factor for yield is assumed to be 1.25 [117, p.298], whereas the yield stress of the shell is dependent on the tank material, as reported in Table 6.9.

$$V_{tank} = V_{prop} + V_{press,in} \tag{6.22}$$

$$r_{tank} = \sqrt[3]{\frac{3V_{tank}}{4\pi}} \tag{6.23}$$

$$t_{shell} = SF_y \frac{p_{tank,in} r_{tank}}{2\sigma_{y,shell}} \tag{6.24}$$

For materials with high yield strength, Equation 6.24 may lead to a thickness that is lower than what can be possibly manufactured. Based on a comparison with titanium diaphragm tanks produced by Northrop Grumman, a minimum thickness of 0.85 mm was assumed [170]. The same minimum thickness is used for aluminium tanks in the script. Next, with the tank shell thickness being 0.85 mm or more, the tank shell mass is calculated with Equation 6.25. The diaphragm mass is calculated with Equation 6.26 using the fixed diaphragm parameters given in Table 6.9 and the assumption that the nominal shape of the diaphragm is achieved when the tank is entirely filled by the pressurant, as shown in the fourth frame of Figure 6.2 [117, p.346]. Combining the shell and diaphragm mass, the total tank mass is calculated with Equation 6.27, where K_{shell} is the shell mass correction factor, assumed to equal 1.85 as a midpoint of the range provided by Zandbergen [117, p.347]. This correction factor is meant to account for additional attachments to the tank, such as mounting tabs or inlet and outlet ports.

$$m_{shell} = 4\pi \left(r_{tank} + \frac{1}{2} t_{shell} \right)^2 t_{shell} \rho_{shell} \tag{6.25}$$

$$m_{dia} = 2\pi r_{tank}^2 t_{dia} \rho_{dia} \tag{6.26}$$

$$m_{tank} = K_{shell} m_{shell} + m_{dia} \tag{6.27}$$

This concludes the PS sizing calculations, with the component selection and total dry and wet mass estimations being reported in the respective sections for each of the selected propellants in Section 6.4.

6.3. Propellant trade-off

Following the methodology provided in Subsection 6.2.4, this section will perform the propellant trade-off. After a brief discussion on the propellants considered in the trade-off in Subsection 6.3.1, the main graphical trade-off results are shown in Subsection 6.3.2. To reduce the ambiguity of the final propellant selection, a sensitivity analysis in Subsection 6.3.3 will consider different evaluations for a selection of criteria scores and weights and consider how this changes the results. Finally, Subsection 6.3.4 will summarise all the results found in the section and conclude with a final selection of propellants.

6.3.1. Propellant options

Before performing a trade-off selecting which propellants are included in the LCSA comparison, it is also a non-trivial task to choose which propellants are considered in the trade-off in the first place, where it is desirable to provide a representative sample of the state of the art in monopropellant systems, as this is valuable information for future research. Based on the findings of the literature review in Subsection 2.2.1, primarily considering [12] and [7], 12 monopropellants are selected, which feature promising performance and for which adequate information could be found to evaluate the trade-off criteria. This selection is shown in Table 6.11, along with a short rationale for including each of the options. As indicated in Subsection 6.2.3, it is assumed that the PS technology for any selected propellant is fully developed, which may not be the case in reality for some of the propellants included in Table 6.11. To that end, the Availability and System complexity criteria will penalise options for which that assumption is stretched too far.

The inclusion of water electrolysis propulsion goes against the design constraints set up in Subsection 6.2.2, as this propulsion technology cannot be facilitated with a typical monopropellant blow-down feed system. As described in Subsection 2.2.1, water electrolysis propulsion indeed has its own architecture all together. Furthermore, a water electrolysis propulsion system meeting the requirements for the present PS case study is still in development, such that it is uncertain if the same system architecture could be used at the minisatellite scale [74]. As such, the trade-off will not genuinely consider it as one of the options to select and perform the LCSA for. Nonetheless, the option is included in the trade-off to compare its overall performance with other novel monopropellant options.

6.3.2. Trade-off results

Using the evaluation method presented before, the different propellant options are scored on the basis of the different criteria, as shown in Figure 6.3. In the trade-off table, the width of the column for each of the criteria is scaled according the respective weight as defined in Table 6.6. The sources that were used in the trade-off scoring have mostly been previously discussed in the literature review, and they are presented separately in Table 6.12. Note that the column width in this table does not relate to the criteria weights.

Evaluating the results in the trade-off in Figure 6.3, there are several interesting observations to be made before moving to the selection of a set of propellants. Firstly, I_{sp} and Density are two criteria where most novel monopropellants match or exceed hydrazine's performance, indicating that the replacement of hydrazine would lead to lighter and smaller propellant tanks in most cases, if the same ΔV budget is delivered by the PS. Secondly, it is somewhat alarming to note that the Availability cri-

Table 6.11: Overview of propellants included in trade-off

Propellant group	Propellant	Rationale
Hydrazine	Hydrazine	Baseline
HTP-based	98% HTP	Simple monopropellant with possible dual use
HTP-based	90% HTP/ethanol blend	Experimental improvement for HTP
ADN-based	LMP-103S	Novel monopropellant with heritage
ADN-based	FLP-106	Safer version of LMP-103S
HAN-based	ASCENT	Novel monopropellant with heritage
HAN-based	SHP163	Novel monopropellant with heritage
HAN-based	GEM	Novel monopropellant with very high performance
NO-based	Nitrous oxide	Simple monopropellant with possible dual use
NO-based	HyNOx	Novel monopropellant with very high performance
NO-based	NOFBX	Novel monopropellant with very high performance
Water	Water electrolysis	Novel monopropellant with heritage

terion is subject to the worst scores across the board, as most novel monopropellants have not been flight-proven or only in a limited capacity. While a modern HTP system has not been demonstrated in space either, HTP still receives a Good score for Availability due to the large amount of research literature available. The Good Availability for LMP-103S, on the other hand, is thanks to the in-space demonstration of HPGP systems in the SkySat constellation, which was documented in a variety of journal and conference publications.

In terms of Safety, all considered novel monopropellants score better than hydrazine, and it is mostly the explosivity of some options that is penalised. Lastly, the Storability of all propellant options contains some ambiguity, as the limited data availability for some options, such as SHP163 and GEM, make it difficult to judge their material compatibility. The decision to award an Acceptable performance to the 98% HTP option may seem generous, as HTP has often been disregarded in the past due to its limited stability and supposedly restrictive material compatibility [29]. However, this claim has repeatedly been refuted in literature, by experimental results and by arguing that highly concentrated HTP made in current times is much more stable than the samples that were used in the 1960s, when HTP was replaced by hydrazine [27], [42]. In practice, HTP's stability does not seem to be an overly inhibiting issue either, as there are ongoing projects developing propulsion systems for various use cases, using materials compatible with HTP [34], [138].

In the selection of propellants, it is decided to exclude any options with Poor performance for any of the criteria, with exception to hydrazine. This is done as the trade-off indicates that there are enough propellants left to for the intended goal of performing an LCSA for 3-5 systems in total. Among the remaining propellants, ASCENT seems the most promising, with an Excellent I_{sp} and only one Acceptable score, for Availability. With a Good or Excellent score for each of the criteria, LMP-103S is a very good option as well. Next, SHP163 is mainly held back by its limited data availability, especially related to the design of the thruster used in the JAXA RAPIS-1 mission. As such, it is also unknown

Table 6.12: Sources used in propellant trade-off evaluation

Criteria:	I_{sp} [s]	Availability	System complexity	ρ [kg/m^3]	Safety	Storability
Hydrazine	[21]	[13], [177]	[20], [23]	[22]	[11]	[177]
98% HTP	[31]	[12], [32], [34], [41], [178]	[34], [41]	[22]	[43]	[42], [168]
90% HTP/ ethanol blend	[35]	[36]	[35]	[22], [36]	[35]	[35], [42]
LMP-103S	[52]	[51], [141]	[62]	[21]	[57], [62]	[56], [62]
FLP-106	[52]	[179]	[179]	[52]	[52], [59]	[52]
ASCENT	[12]	[12], [64], [67]	[67]	[12]	[67], [72]	[56], [67]
SHP163	[12]	[70], [71], [166]	[71]	[12]	[70]	Unknown
GEM	[12]	[12]	[12]	[12]	Unknown	Unknown
Nitrous oxide	[12]	[12], [44]	[44]	[12]	[44], [49], [50]	[12]
HyNOx	[12]	[45]	[45]	[12]	[45], [49]	[12]
NOFBX	[12]	[12]	[47]	[12]	[12], [45]	[12]
Water electrolysis	[76]	[74]–[77]	[75]	[78]	[78]	[78]

how the high combustion temperature has been dealt with in the flight model and how this would affect the overall PS design complexity.

Despite its relatively low I_{sp}, 98% HTP does not fall far behind the other options, by virtue of its Good data availability and functional simplicity, leading to a Good System complexity as well. While its toxicity may be somewhat more severe than that of the EIL monopropellants, HTP's low vapour pressure results in a lower risk of inadvertent ingestion [22]. Lastly, while water electrolysis propulsion is not considered here as one of the options for the LCSA, its performance in the trade-off is quite promising: it is the only option next to hydrazine that has an Excellent score for three criteria. If this technology is further developed in the coming years, it could score Good or Excellent for the Availability criterion as well, making it a clear favourite compared to other novel monopropellants. However, it is important to note that water electrolysis propulsion would also lead to additional requirements for the power subsystem (to operate the electrolyser), and require a different PS usage philosophy due to its unique operating principles [74]. These aspects have not been included in any of the criteria of this trade-off.

While the graphical trade-off has indicated that four novel monopropellants, being ASCENT, LMP-103S, SHP163 and 98% HTP, are the most suitable to compare with respect to hydrazine, a sensitivity analysis in the next subsection will verify how robust this result is. Furthermore, the relative ranking between these options will also be investigated. Thereafter, Subsection 6.3.4 will present the final selection of propellants to continue with in the research.

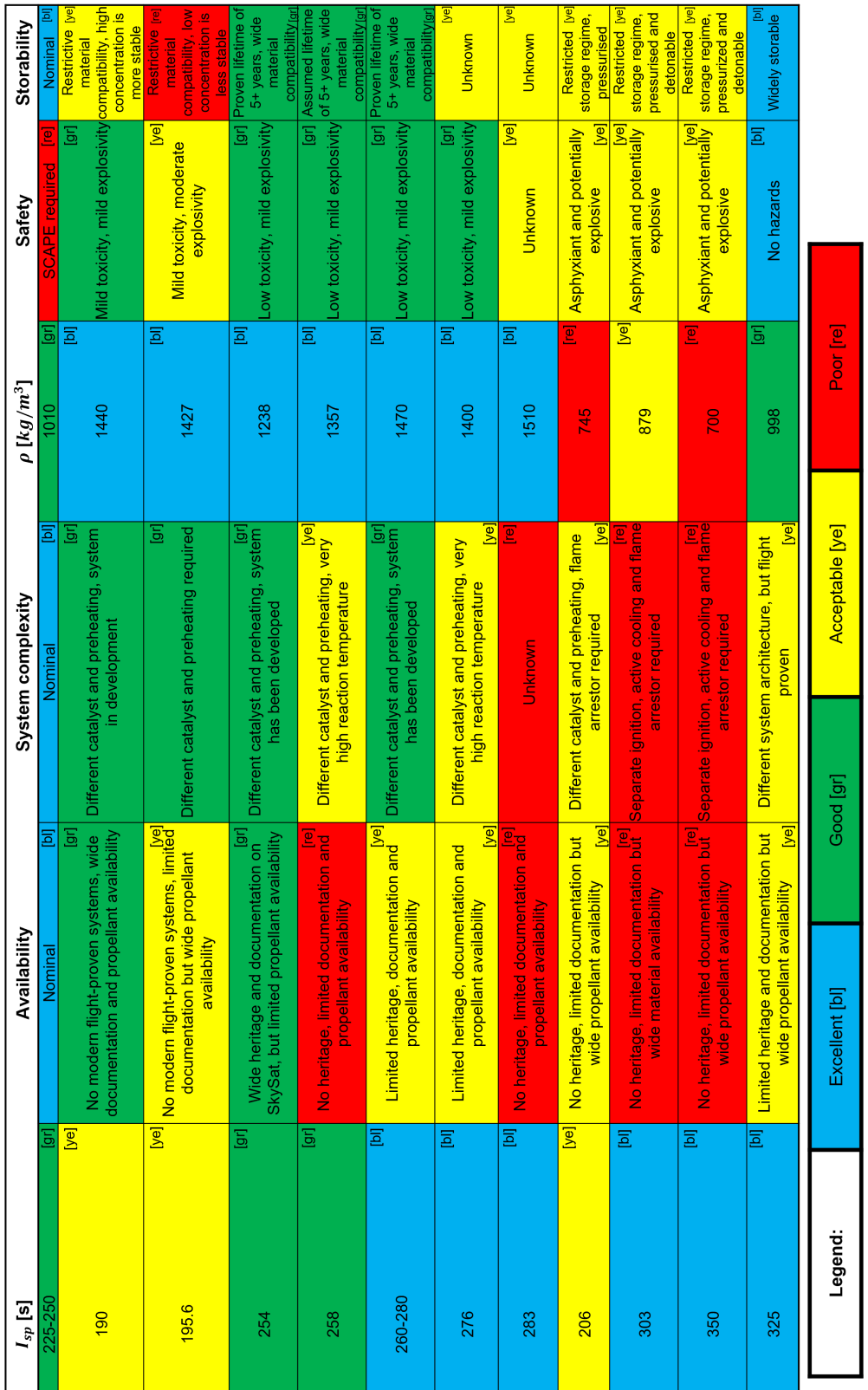

Figure 6.3: Graphical trade-off of the propellant options

6.3.3. Sensitivity analysis

While the graphical trade-off shown in Figure 6.3 is performed based on a transparent and justified evaluation scheme that was outlined in Table 6.7, it is deemed valuable to further investigate those findings in a sensitivity analysis. In this section, a few criteria weights and scores will be adapted based on well-founded doubts within the original trade-off evaluation. As such, this will not be a comprehensive sensitivity analysis where the robustness of the entire methodology is evaluated.

To facilitate an easier comparison of the results in this sensitivity analysis, the trade-off table is first converted into a numerical trade-off, by replacing each of the score categories by a number. As such, an Excellent score results in a score of 4, Good is equivalent to 3, Acceptable to 2 and Poor to 1. Then, a weighted sum of all criterion scores can be made for each propellant option, taking into account the criteria weights. The total achievable score is then equal to 60. The resulting numerical trade-off is shown in Table 6.13, where the columns are not scaled according to criterion weight. The results reveal that the 6 best performing propellants based on the graphical, qualitative assessment in the subsection above also come out on top in the numerical trade-off. Furthermore, the selected propellants may be defined as having a score of 70% or more.

Table 6.13: Numerical trade-off of the propellant options

Criteria:	I_{sp} **[s]**	**Availability**	**System complexity**	ρ **[kg/m^3]**	**Safety**	**Storability**	**Total Score**	
Criterion weight:	4	3	3	2	2	1	/ 60	**%**
Hydrazine	3	4	4	3	1	4	48	80
98% HTP	2	3	3	4	3	2	42	70
90% HTP/ ethanol blend	2	2	3	4	2	1	36	60
LMP-103S	3	3	3	4	3	3	47	78
FLP-106	3	1	3	4	3	3	41	68
ASCENT	4	2	3	4	3	3	48	80
SHP163	4	2	2	4	3	2	44	73
GEM	4	1	1	4	3	2	38	63
Nitrous oxide	2	2	2	1	2	2	28	47
HyNOx	4	2	1	2	2	2	35	58
NOFBX	4	1	1	1	2	2	30	50
Water electrolysis	4	2	2	3	4	4	46	77

The first trade-off change considered in this sensitivity analysis is to swap the weights of the I_{sp} and Availability criteria, making Availability the most important criterion of the trade-off, increasing the relative importance of the estimated feasibility of performing an accurate LCSA later on. For brevity, only the top 6 propellants of the new trade-off will be shown for each method change performed in this sensitivity analysis. For the case where Availability is weighted at 4 and I_{sp} at 3, Table 6.14 shows these results. As can be appreciated, ASCENT and SHP163 are penalised somewhat due to their Acceptable Availability. Nonetheless, each of the previously considered options still achieve a percentage score of at least 70%. Note that water electrolysis is included in brackets as it is not regarded as a legitimate choice for the following PS design and LCSA.

Alternatively, I_{sp} and Availability could also be weighted equally with a weight of 4, as this would reflect the equal importance of performing the LCSA for propellant options that are realistic options and for which sufficient data is available to construct accurate LCIs. With this distribution of criteria weights, Table 6.15 presents the results. Once again, the same 6 propellants are selected and all of them have a score above 70%.

Another debatable criterion weighting choice is that System complexity is considered as a more important propellant feature than its Safety. One may argue that, as propellant toxicity and handling cost are driving factors in the development of propellants to replace hydrazine, a higher weight should be given to Safety. To investigate the potential trade-off changes due to this consideration, the numerical

Table 6.14: Propellant trade-off results with the I_{sp} criterion weighted at 3 and the Availability criterion weighted at 4

Nr.	Propellant	Score / 60	Score %
1	**Hydrazine**	49	**82**
2	**LMP-103S**	47	**78**
3	**ASCENT**	46	**77**
4	**(Water electrolysis)**	44	**73**
5	**98% HTP**	43	**72**
6	**SHP163**	42	**70**

Table 6.15: Propellant trade-off results with the I_{sp} and Availability criteria weighted equally at 4

Nr.	Propellant	Score / 64	Score %
1	**Hydrazine**	52	**81**
2	**LMP-103S**	50	**78**
3	**ASCENT**	50	**78**
4	**(Water electrolysis)**	48	**75**
5	**SHP163**	46	**72**
6	**98% HTP**	45	**70**

trade-off was also performed for a System complexity weight of 2, with Safety weighted at 3. The resulting top 6 of propellants is shown in Table 6.16. This trade-off methodology change represents the first to result in hydrazine not being the optimal choice, as should be expected due to its large safety concerns. As in the previous results, this trade-off approach selects the same six propellants as the original graphical trade-off, and all six score at least 70%. The order of the novel monopropellants is also approximately the same, with ASCENT and LMP-103S populating the top half, while SHP163 or 98% HTP are either the fifth or sixth choice.

Table 6.16: Propellant trade-off results with the System complexity criterion weighted at 2 and the Safety criterion weighted at 3

Nr.	Propellant	Score / 60	Score %
1	**ASCENT**	48	**80**
2	**(Water electrolysis)**	48	**80**
3	**LMP-103S**	47	**78**
4	**Hydrazine**	45	**75**
5	**SHP163**	45	**75**
6	**98% HTP**	42	**70**

The last considered variation in criteria weights is an exchange of the Density and Storability weights. This is motivated by the fact that all considered monopropellants in the top 6 have a similar Density, whereas there is a greater variety in the Storability criterion. Additionally, while a dense propellant may be nice design feature leading to a smaller propellant tank, REQ-PS-BUD-02 is also in place to enforce a limit to the tank size. On the other hand, a propellant's stability may be a less predictable parameter, such that an assurance of propellant stability could lead to a reduced mission risk. The resulting top 6 is reported in Table 6.17. Again, the same propellants are featured, yet in this trade-off, 98% HTP scores worse than 70%. Additionally, the ADN-based propellant FLP-106 matches its score, making the top 6 less clearly separated from the other options.

Next to a variation in criteria weights, specific trade-off scores can also be changed. The first change in this manner is to reduce 98% HTP's score for Safety to Acceptable, as the risk of rapid HTP decomposition indeed holds dangers, especially when large amounts of HTP are being handled. Table 6.18 shows the resulting impact on the top 6, where obviously only 98% HTP's score has been affected. FLP-106 now achieves a slightly better score than HTP, which scores 40 out of 60, equivalent to 67%. This result shows that 98% HTP's place as one of the top 6 novel monopropellants is not entirely uncontested.

Table 6.17: Propellant trade-off results with the Density criterion weighted at 1 and the Storability criterion weighted at 2

Nr.	Propellant	Score / 60	Score %
1	**Hydrazine**	49	**82**
2	**ASCENT**	47	**78**
3	**(Water electrolysis)**	47	**78**
4	**LMP-103S**	46	**77**
5	**SHP163**	42	**70**
6	**98% HTP**	40	**67**

Table 6.18: Propellant trade-off results with an Acceptable Safety score for 98% HTP

Nr.	Propellant	Score / 60	Score %
1	**Hydrazine**	48	80
2	**ASCENT**	48	80
3	**LMP-103S**	47	78
4	**(Water electrolysis)**	46	77
5	**SHP163**	44	73
6	**FLP-106**	41	68

A second adaptation to the propellants' trade-off scores arises from the limited data availability for SHP163. In the original graphical trade-off, SHP163 received an Acceptable score for Availability, thanks to the more extensive literature available for ASCENT and LMP-103S and the assumption that these technologies may also be applicable for SHP163. Upon further investigation however, it is apparent that little information can be found related to the thruster design that may be used to accommodate SHP163's high combustion temperature of above 2100 $^{\circ}C$. Furthermore, it is not very clear whether SHP163 technologies are being further developed, as the most recent publications related to this development are from 2019 [70]. These factors may serve as sufficient motivation to attribute a Poor Availability score to the option. With this change, SHP163 moves to the bottom of the top 6, with the same score as FLP-106, as shown in Table 6.19.

Table 6.19: Propellant trade-off results with a Poor Availability score for SHP163

Nr.	Propellant	Score / 60	Score %
1	**Hydrazine**	48	80
2	**ASCENT**	48	80
3	**LMP-103S**	47	78
4	**(Water electrolysis)**	46	77
5	**98% HTP**	42	70
6	**SHP163**	41	68

With the six variations considered in this sensitivity analysis, there are a few clear conclusions to be made. Firstly, the four best propellant options are consistently hydrazine, ASCENT, LMP-103S and water electrolysis, in slightly different orders. A second conclusion is that 98% HTP and SHP163 have a quite similar score in most cases and are grouped at the bottom of the top 6 in all variations. Apart from FLP-106 however, there are no other novel monopropellants which approach their performance closely. Thirdly, the sensitivity analysis has proven that the graphical trade-off result is fairly robust, as the methodological changes that were investigated never resulted in completely different choices for the top 6 propellants.

6.3.4. Discussion and final propellant options

Considering the findings of the graphical trade-off in Subsection 6.3.2 and of its sensitivity analysis in Subsection 6.3.3, it is clear that five propellants stand out as the best choice to include in the further re-

search. Next to hydrazine, which is automatically included as the baseline option, ASCENT, LMP-103S, SHP163 and 98% HTP are part of this selection. As explained in Subsection 6.3.1, water electrolysis propulsion cannot be considered in the following LCSA comparison, as its system architecture is too different from the other options, such that the setup of a reliable LCI would not fit in the scope of this research.

While it would probably be feasible to include all five propellant options in the comparative LCSA, given the design similarities for the EIL options, the decision is made to exclude SHP163 from the selection, for two main reasons. Firstly, as a further investigation in the sensitivity analysis and the beginning stages of the LCI data collection process has shown, it is deemed that the data availability for this monopropellant is too scarce to be able to construct a reliable LCI. Additionally, due to the fact that SHP163 is not yet used in European or American markets, it is also unlikely that primary data collection would be a realistic solution. One way to resolve this issue would be to use data for ASCENT systems as a proxy for the SHP163 system. However, this would also lead to an undesirable convergence between the two options' LCI and final LCSA results, with the question remaining whether an SHP163 PS design is indeed similar to an ASCENT PS.

The second reason for leaving SHP163 out of the final selection is that this will allow for a more thorough LCI analysis for the remaining options, thus prioritising the quality of the LCSA over the quantity of options considered. The choice to exclude SHP163 in this regard, instead of 98% HTP which has a lower trade-off performance, is informed by a goal to have a varied selection of novel monopropellants. With ASCENT, LMP-103S and 98% HTP, LCSA results will be presented that are relevant for the HAN-, ADN- and HTP-based monopropellant families. Additionally, as has been stated before, the great amount of research conducted on HTP-based systems indicates that sufficient data will be available to set up a reliable LCI for this option. In the following section, propulsion system designs will therefore be developed for hydrazine, ASCENT, LMP-103S and 98% HTP.

6.4. Conceptual system designs

This section will present the parameters for the conceptual PS designs using hydrazine, ASCENT, LMP-103S and 98% HTP. As the system architecture for each of these systems is more or less identical, the only differentiation will be the sizing, tank materials and component selection. Before presenting these results, Subsection 6.4.1 will discuss the verification and validation efforts that were undertaken for the script performing the sizing calculations.

6.4.1. Code verification and validation

To ensure that the PS sizing script properly implements the sizing calculations, the code will be verified using a manually worked out example case. Then, validation of the entire propulsion system sizing method will be performed using four reference cases of minisatellite propulsion systems.

Verification

As the calculations implemented in the code are rather straightforward, the verification approach is also very simple. Firstly, the code was checked for any typing errors, to ensure that each of the equations was implemented as they should be. Then, only for the hydrazine PS design, all calculations were implemented in Microsoft Excel and a comparison was made between the code results and the Excel results. Table 6.20 gives an overview of the main input data for this verification case. Any other design factors, such as the various PS efficiencies, were taken equal to the values implemented in the code.

After the code was checked for errors, the output of the Excel calculations was exactly the same as the script output, as shown in Table 6.21.

Table 6.20: Overview of propulsion system sizing code verification input data

Input parameter	Value	Unit
ΔV	153.53	m/s
Propellant	Hydrazine	-
$I_{sp,th}$	239	s
Tank material	Ti-6Al-4V	-

Table 6.21: Overview of propulsion system sizing code verification output data

Output parameter	Code Value	Excel Value	Unit
m_{prop}	12.28	12.28	kg
m_{press}	0.017	0.017	kg
V_{tank}	0.0162	0.0162	m^3
$m_{tank,dry}$	2.48	2.48	kg

Validation

Whereas code verification proves that the code implements the calculations that were set up in the sizing methodology, validation serves to prove that the sizing methodology and the made assumptions result in realistic PS parameters. In this process, four reference propulsion systems are selected for which the propellant mass, tank volume and PS system dry and wet mass can be found. The selected propulsion systems are the hydrazine propulsion systems of the Myriade satellite platform used for the PARASOL mission and of the P200 platform developed by Qinetiq, and the LMP-103S propulsion systems used in the PRISMA mission and the SkySat satellites. The main input parameters relevant for the PS sizing of each of these missions are listed in Table 6.22. For each of these missions, the input data in Table 6.22 is fed to the script and PS sizing and component selection are performed. The components selected for the hydrazine and LMP-103S systems will be listed in Subsection 6.4.2 and Subsection 6.4.4 respectively.

Table 6.22: Overview of propulsion system input data for validation

Input parameter	PARASOL (Myriade) [132], [180]	Altius (P200) [80]	PRISMA HPGP [26], [62]	SkySat [133], [141]
$m_{sc,dry}$ [kg]	100	200	120	110 (approx.)
ΔV [m/s]	80	120	90	180
Propellant	Hydrazine	Hydrazine	LMP-103S	LMP-103S
$p_{tank,in}$ [bar]	22	25 (assumed)	18.5	18.5
Blow-down ratio	4	4 (assumed)	3.8	3.7
# thrusters	4	4	2	4

Starting with the results for the Myriade PS in Table 6.23, the code approaches the actual results quite closely. The largest error is an underestimation of the dry mass of about -9%. In the calculation of the total PS mass, some of the code error may also be attributed to the fact that the Myriade PS architecture is somewhat different from the standard architecture used in the PS sizing code. Furthermore, different components may be used than those selected in this study for the hydrazine PS.

Considering the bottom three output parameters that are compared in Table 6.23, it is important to realise that these are all quite dependent on propellant mass. As such, it is also to the credit of the sizing code that the error stays more or less constant across the various parameters, showing that the dependence of the other outputs on the propellant mass is similar for the actual and calculated values.

The validation case of the Altius propulsion system in Table 6.24 shows slightly larger differences between the calculated and actual values found in literature. However, as also indicated by the fact that the actual dry and wet mass of the PS could not be found, there was less information available on the

Table 6.23: Validation of propulsion system sizing code with Myriade propulsion system data from [132], [180]

Output parameter	Actual value	Code output	Code error [%]
m_{prop} [kg]	4.545	4.18	-8.0
V_{tank} [L]	6.00	5.5	-8.3
$m_{PS,dry}$	4.83	4.39	-9.1
$m_{PS,wet}$	9.38	8.61	-8.2

propulsion system used in the Altius mission, which is built on the Qinetiq P200 platform. As such, an initial tank pressure and BDR of 25 bar and 4 were assumed, as shown in Table 6.22.

Table 6.24: Validation of propulsion system sizing code with Altius propulsion system data from [80]

Output parameter	Actual value	Code output	Code error [%]
m_{prop} [kg]	15	12.69	-15.4
V_{tank} [L]	18.31	16.7	-8.8
$m_{PS,dry}$	N/A	5.98	N/A
$m_{PS,wet}$	N/A	15.24	N/A

Validating the code with the HPGP propulsion system onboard the PRISMA technology demonstration mission also provides good results, as both the calculated propellant mass and tank volume are very close to the actual values, as presented in Table 6.25. Regarding the propulsion system dry mass, the code underestimates by about 0.7 kg, which may again be due to a different selection of components. The difference in PS wet mass can be mostly attributed to the difference in dry mass and propellant mass.

Table 6.25: Validation of propulsion system sizing code with PRISMA HPGP propulsion system data from [26], [62]

Output parameter	Actual value	Code output	Code error [%]
m_{prop} [kg]	5.5	5.3	-3.6
V_{tank} [L]	5.7	5.8	+2.0
$m_{PS,dry}$	4.3	3.57	-17.0
$m_{PS,wet}$	9.9	8.87	-10.4

Lastly, the SkySat validation case shown in Table 6.26 presents the first situation where the code overestimates the required propellant mass. Still, the estimate is fairly accurate. The large error in system dry mass is attributed to the fact that the SkySat propulsion system is made up of three cylindrical tanks using metallic PMDs to trap the propellant at the bottom, whereas the PS sizing code assumes a single spherical diaphragm tank [141]. These PMD tanks result in a much heavier PS, leading to the deviations in both PS dry and wet mass.

Overall, the validation cases have shown that the PS sizing code is very accurate in estimating the required propellant mass, which provides the basis for an accurate estimation of the tank mass as well. The good estimates for PS dry mass, within 0.8 kg for the Myriade and PRISMA systems, also proves that the tank sizing method, with the assumed minimal shell thickness of 0.85 mm and shell mass correction factor of 1.85, is valid. Wherever there are large discrepancies for the different validation cases considered, there is a presumed reason for why these may be present, for example due to the lack of data for the Altius system and the different system architecture and feed system in the SkySat PS. The results of this validation effort have therefore adequately proven that the code will provide reasonable estimates for the parameters of each of the designed propulsion systems.

Table 6.26: Validation of propulsion system sizing code with SkySat propulsion system data from [141]

Output parameter	Actual value	Code output	Code error [%]
m_{prop} [kg]	10.5	10.84	+3.2
V_{tank} [L]	11.4	12	+5.3
$m_{PS,dry}$	10.9	5.42	-50.3
$m_{PS,wet}$	21.4	16.27	-24.0

6.4.2. Hydrazine system

For each of the propellants selected in the propellant trade-off, a conceptual propulsion system will now be sized using the input parameters informed by the design requirements and constraints. As the hydrazine system will be discussed first, the fixed input parameters for the PS sizing will be reported only here, but these parameters are identical for each of the other propellants and informed by other factors of the case study design presented before.

Table 6.27: Overview of fixed input parameters for each of the conceptual propulsion system designs

Input parameter	Value	Unit	Source
$m_{sc,dry}$	150	kg	Table 5.13
ΔV	153.53	m/s	Table 6.1
$p_{tank,in}$	25	bar	Subsection 6.2.2
Blow-down ratio	4	-	Subsection 6.2.2
# thrusters	4	-	Subsection 6.2.2

For hydrazine specifically, the propellant-dependent input parameters are reported in Table 6.28. Together with the fixed input parameters and the PS sizing method described in Subsection 6.2.5, this input data informs the required propellant and pressurant mass, and the necessary tank size, as reported in Table 6.29. This table also indicates that the titanium diaphragm tank has a shell wall thickness of 0.85 mm, which is considered as the lower limit for manufacturing concerns.

Table 6.28: Overview of propellant-dependent input parameters for the hydrazine propulsion system

Input parameter	Value	Unit	Source
Propellant	Hydrazine	-	-
$I_{sp,th}$	239	s	[21]
ρ_{prop}	1010	kg/m^3	[22]
Tank materials	Ti-6A-4V/ SIFA-35	-	[80]

For the selection of other components, a literature study is performed considering heritage propulsion systems and other compatible COTS components. During the component selection, components are favoured if they have heritage with both hydrazine and the two EIL propellant options considered in the comparison, as this would increase the design simplicity of changing propellants. Furthermore, this will also lead to a more straightforward approach during the construction of the LCI for each PS design. The resulting selection is shown in Table 6.30, where each of the components is indeed compatible with all four propellants that will be considered in the PS design. While some components datasheets specifically indicate compatibility with the novel EIL monopropellants, the choice to select only stainless steel components also ensures material compatibility with 98% HTP.

For each of the selected components, TRL9 COTS components have been selected from the specified suppliers shown in Table 6.30. There are some additional comments warranted however, as a few of these components have not yet been discussed in the definition of the system architecture in Subsection 6.2.2. Firstly, four patch heaters were included in the budget, as these are deemed necessary to offer double redundancy in heating the propellant tank and isolation valve. For thermal management,

Table 6.29: Overview of main propulsion system sizing results for the hydrazine propulsion system

Component	Parameter	Value	Unit
Propellant (hydrazine)	Mass	12.28	kg
	Initial Volume	12.2	L
Pressurant (helium)	Mass	0.017	kg
	Initial Volume	4.1	L
Tank	Mass	2.48	kg
	Volume	16.2	L
	Shell thickness	0.85	mm

multi-layer insulation is typically included as well, but this is not considered in the conceptual design and LCSA. Additionally, it is important to note that each of the Aerojet MR-103J 1 N thrusters includes its own double redundant flow control valve and catalyst bed heater [125].

Secondly, the amount of piping in the system was estimated to weigh 15% of the rest of the dry mass [117, p.394]. Thirdly, the orifice shown just downstream of the propellant tank in Figure 6.1 is assumed to be part of the propellant tank assembly, as such included in the propellant tank mass. These assumptions are made in the design for each of the propellant options. Lastly, a mass margin was included to consider the required electronics for control and monitoring of the system. Based on the mass breakdown of a CubeSat propulsion system, this margin was taken at 5% of the total dry mass including the piping [181]. While this assumption may not be entirely valid, it is not deemed to have a very large impact for the results of the LCSA, which is the main point of interest in this research. With a dry mass of less than 6 kg and a total tank volume of about 16 L, it is clear that this hydrazine propulsion system design meets the size and mass budget requirements set in Table 6.2.

Table 6.30: Component selection and detailed mass breakdown for hydrazine propulsion system

Component	Quantity	Total mass [kg]	Supplier
Filter	1	0.06	Mott small propellant filter [182]
Latch valve	1	0.32	Moog 1/4 inch single line stainless steel torque motor valve [183]
Patch heater	4	0.02	Minco polyimide thermofoil heater [184]
Piping	-	0.741	Stainless steel seamless tubing [185], assumed at 15% of dry mass, excluding wiring [117]
Pressure transducer	1	0.125	Bradford Space stainless steel mini pressure transducer [186]
Service valve	2	0.418	Moog low pressure stainless steel service valve [187]
Tank	1	2.479	Sizing calculations
Thruster	4	1.48	Aerojet Rocketdyne MR-103J [125]
Wiring	-	0.282	5% of dry mass, including piping [181]
Total dry mass		5.92	
Total wet mass		18.22	

6.4.3. ASCENT system

The main input parameters for the ASCENT PS sizing are shown in Table 6.31, using the data gathered in the literature study. While it has not been reported that ASCENT is compatible with the SIFA-35 diaphragm material, its compatibility is assumed due to the similarities in material compatibility between ASCENT and LMP-103S [56].

Table 6.31: Overview of propellant-dependent input parameters for the ASCENT propulsion system

Input parameter	Value	Unit	Source
Propellant	ASCENT	-	-
$I_{sp,th}$	266	s	[12]
ρ_{prop}	1470	kg/m^3	[12]
Tank materials	Ti-6A-4V/ SIFA-35	-	[56], [67]

The PS sizing script is used to determine the necessary propellant load and tank size when using ASCENT, resulting in a propellant mass of about 11 kg and a tank volume of 10 L, as shown in Table 6.32. This already indicates the novel monopropellant's superior performance compared to hydrazine, both due to its increased I_{sp} and density.

With regards to component selection, the same components are used as listed in Table 6.30, with the exception of the thrusters. For ASCENT propulsion systems, Aerojet Rocketdyne has developed the 1 N GR-1 thruster, which was flight-proven onboard the GPIM mission [67]. However, no information is available on the thruster's mass, which is why it is assumed to weigh 0.39 kg, in similarity to the ECAPS 1 N HPGP thruster using LMP-103S [169]. This proxy is used as Spores et al. mention that the GR-1 thruster uses refractory metals in the combustion chamber, similar to the ECAPS thruster [67]. A difference between the thruster designs is however that the GR-1 thruster uses a single seat flow control valve. This not only makes the ASCENT system non-compliant with PS requirements REQ-PS-FEED-03 and REQ-PS-STOR-03, but it also means that the GR-1 thruster is most likely lighter than the ECAPS HPGP thruster. While this difference is not accounted for in the ASCENT PS mass budget, it will be taken into account in the definition of the LCI in Section 7.4.

Table 6.32: Overview of main propulsion system sizing results for the ASCENT propulsion system

Component	Parameter	Value	Unit
Propellant (ASCENT)	Mass	10.99	kg
	Initial Volume	7.5	L
Pressurant (helium)	Mass	0.01	kg
	Initial Volume	2.5	L
Tank	Mass	1.79	kg
	Volume	10.0	L
	Shell thickness	0.85	mm
Total dry mass		5.19	kg
Total wet mass		16.19	kg

6.4.4. LMP-103S system

Once again, the propellant-dependent input parameters for LMP-103S are adapted from the literature review in Table 6.33 and shown in Table 6.33. This design input results in the sizing parameters and total PS masses shown in Table 6.34, using the same components as shown in Table 6.30, apart from the thrusters. In this case, ECAPS HPGP 1 N thrusters are used, which have a unit mass of 0.39 kg, including a double seat flow control valve and catalyst bed heater [169]. For each of the other components, compatibility with LMP-103S has been tested in either the PRISMA, SkySat or Altius missions.

Table 6.33: Overview of propellant-dependent input parameters for the LMP-103S propulsion system

Input parameter	Value	Unit	Source
Propellant	LMP-103S	-	-
$I_{sp,th}$	254	s	[52]
ρ_{prop}	1238	kg/m^3	[21]
Tank materials	Ti-6A-4V/ SIFA-35	-	[80]

Table 6.34: Overview of main propulsion system sizing results for the LMP-103S propulsion system

Component	Parameter	Value	Unit
Propellant (LMP-103S)	Mass	11.53	kg
	Initial Volume	9.3	L
Pressurant (helium)	Mass	0.013	kg
	Initial Volume	3.1	L
Tank	Mass	2.07	kg
	Volume	12.4	L
	Shell thickness	0.85	mm
Total dry mass		5.53	kg
Total wet mass		17.07	kg

6.4.5. 98% HTP system

For the design of the 98% HTP PS, the sizing script is once again run with the adaptation of using aluminium and FEP for the tank shell and diaphragm materials respectively, and including the iterative process determining the required propellant margin to accommodate passive HTP decomposition as presented in Subsection 6.2.5. The resulting design parameters are shown in Table 6.36.

Table 6.35: Overview of propellant-dependent input parameters for the 98% HTP propulsion system

Input parameter	Value	Unit	Source
Propellant	98% HTP	-	-
$I_{sp,th}$	190	s	[31]
ρ_{prop}	1440	kg/m^3	[22]
Tank materials	Al5254/ FEP	-	[168], [171]

In the component selection leading to the dry mass shown in Table 6.36, there are a few special considerations to mention. Firstly, following the assumption that the HTP tank can be vented every week to release the generated oxygen, an additional valve is added to the system architecture. The vent valve selected is an ArianeGroup oxidiser vent valve that is compatible with nitrogen tetroxide, weighing 0.09 kg [167]. While it is not entirely clear whether this valve will be compatible with 98% HTP, it is assumed that a similar valve could be produced or procured in a compatible material. Another assumption is made with regard to the selected thruster mass for 98% HTP, where the mass of 0.37 kg of the MR-103J thruster is used [125]. Once again, this rough assumption is due to a lack of existing flight-ready hardware for 98% HTP, and reflects that the assumption of using only TRL9 components is the least accurate for the HTP PS. Nonetheless, the differences in the required catalyst bed material and size for HTP will be taken into account in the LCI analysis in Section 7.4.

Table 6.36: Overview of main propulsion system sizing results for the 98% HTP propulsion system

Component	Parameter	Value	Unit
Propellant (98% HTP)	Mass	16.14	kg
	Initial Volume	11.2	L
Pressurant (helium)	Mass	0.015	kg
	Initial Volume	3.7	L
Tank	Mass	3.06	kg
	Volume	14.9	L
	Shell thickness	2.04	mm
Total dry mass		6.73	kg
Total wet mass		22.89	kg

6.4.6. Overview and comparison

With a conceptual propulsion system designed for each of the propellants considered, Table 6.37 presents a comparison of the different end results. As could be expected the ASCENT and LMP-103S systems provide savings of around 10% in the system wet and dry mass, due to their superior specific impulse and density compared to hydrazine. Despite the 98% HTP's propellant tank being smaller than that of the hydrazine system, the tank mass is still higher. This is because the Al5254 has a lower yield stress than Ti-6Al-4V, leading to a larger wall thickness, as reported in Table 6.36. While the comparison presented in Table 6.37 is informative for the purposes of mission design or propulsion system insights, it should be clear that this presents only very top-level design considerations. A more thorough comparison of the various propulsion system production processes will be presented in the LCI analysis later in this research.

Table 6.37: Comparison of the different conceptual propulsion system designs

Parameter	Hydrazine	ASCENT	LMP-103S	98% HTP
Propellant $I_{sp,th}$ $[s]$	239	266	254	190
Propellant mass $[kg]$	12.28	10.99	11.53	16.14
Tank mass $[kg]$	2.48	1.79	2.08	3.06
Tank volume $[L]$	16.2	10.0	12.4	14.9
System dry mass $[kg]$	**5.92**	**5.19**	**5.53**	**6.73**
Difference w.r.t baseline [%]	0	-12.33	-6.59	+13.68
System wet mass $[kg]$	**18.22**	**16.19**	**17.07**	**22.89**
Difference w.r.t baseline [%]	0	-11.14	-6.31	+25.63

6.5. Conclusion

This chapter has further developed the case study for which the LCSA will compare several monopropellants on the basis of their system-level sustainability. First, key propulsion system requirements related to the selected mission use case were specified by means of a conceptual ΔV budget and general propulsion system design considerations from heritage missions. These requirements and constraints then informed the definition of six criteria, being Specific impulse, Availability, System complexity, Density, Safety and Storability, which were used to graphically trade-off a number of monopropellant options for the considered use case. In the end, the three novel monopropellants ASCENT, LMP-103S and 98% HTP were selected alongside the baseline option hydrazine, for further propulsion system design.

For each of the propellants, conceptual propulsion systems were sized based on a shared system

architecture, using a Python script to perform the main calculations. For the propulsion system using 98% HTP, additional calculations were performed to simulate the effects of passive HTP decomposition. Next to system sizing, a number of essential propulsion system components were selected, which are compatible with all propellants due to their fabrication in stainless steel. 1 N thrusters were also selected for each of the propellants, using flight-proven hardware or suitable proxies where necessary. The final design results of this section will be used in the following chapter when modelling accurate life cycle inventories for each propulsion system in Section 7.4.

7

Life Cycle Sustainability Assessment

7.1. Introduction

With a clearly defined and well-motivated case study and a relevant selection of propellants to compare, this chapter will perform a life cycle sustainability assessment for each of the propulsion systems designed in Chapter 6. This chapter will follow the chronology of the LCSA method, first defining the assessment's goal and scope in Section 7.2, presenting the assessment's main assumptions in Section 7.3, then analysing and modelling the various system's life cycle inventories in Section 7.4, before performing the life cycle impact assessment in Section 7.5. As mentioned in the main methodology chapter in Chapter 4, this LCSA will be performed following the guidelines of the SSSD LCSA framework [14] and the ESA LCA handbook [99], and both related LCI databases will also be used to support the data collection in Section 7.4. The modelling of the LCIs and execution of the LCIA will be performed in the open-source LCA program openLCA. While the results will be discussed and interpreted in Section 7.5, considering the design features driving specific differences between the different propellant options, a more in-depth validation of these interpretations and results will be presented in Chapter 8.

7.2. Goal and scope definition

The goal and scope of any LCSA are not only important for the purpose of justifying assumptions or other methodological choices further along the LCSA, they are also key for any interpretation of the LCIA results. For this comparative LCSA, the goal is informed by the overall research question and reads as follows:

Goal: *To make a comparison between the environmental, social and economic impact of the production, assembly and testing of a conventional and three novel monopropellant systems in a 150-kg class satellite, considering hydrazine, ASCENT, LMP-103S and 98% HTP as the possible propellants.*

To make a fair comparison, it is also necessary to formulate a consistent functional unit for which the LCSA of each propulsion system option will be conducted. By creating conceptual designs for the four propellant options in accordance with the PS requirements in Section 6.4, this level of consistency has already been ensured at the level of the input data for the LCSA. The functional unit is therefore:

Functional Unit: *One fuelled monopropellant system in fulfilment of the propulsion system requirements set for a case study of a 150 kg Earth Observation satellite.*

Next to defining the LCSA's functional unit, the scope definition of the LCSA also entails the demarcation of the system boundaries, indicating which life cycle phases are included in the assessment. Furthermore, boundaries also need to be set with regards to the various components that the system is made of. As a first simplification, only the components that make up more than 5% of the propulsion

system's dry mass will be included in the LCI [99, p.98]. Considering the mass breakdown shown in Table 6.30, this means that only the isolation latch valve, piping, service valves, propellant tank and thrusters will be included in the LCSA, next to the respective propellant and pressurant.

For the production of each of the components, the system boundaries recommended by the ESA LCA handbook for equipment production are used [99, p.93]. These are shown in a schematised form in Figure 7.1. Note that for each of the activities shown in this figure, energy consumption will also be included. In the LCI of the components, a 5% mass cut-off is not used, and the construction and life cycle of the component will be modelled as accurately as possible. The infrastructure during the production of these components is excluded from the system boundaries.

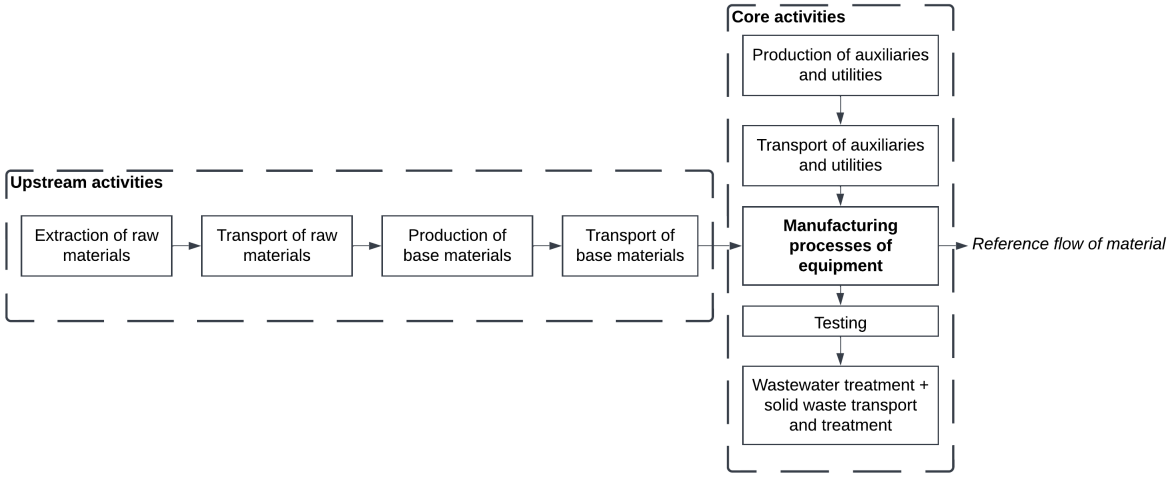

Figure 7.1: Diagram of system boundaries considered for the production of components in propulsion system LCSA, from [99, p.93]

Next to the production of each of the propulsion system components, the LCSA system boundaries will also include the assembly, testing, transport and fuelling of the propulsion system. The LCSA will thus assess the propulsion systems from cradle to gate, where their operational life starts. For these life cycle steps, it is assumed that the system is assembled in The Netherlands and fuelled at the European space port in Kourou, French Guyana. The final definition of the system boundaries is thus:

System boundaries: *Production of each propulsion system component making up more than 5% of total dry mass, from raw material extraction to final manufacturing and waste treatment, including energy consumption and transport; production of propellant and pressurant; assembly, testing and transport of the assembled propulsion system, pressurant and propellant to launch site; fuelling of the propulsion system at launch site.*

The LCIA indicators that will be used in the LCSA have been presented in Table 4.1, and are directly adapted from the SSSD Sustainability LCIA method with midpoint indicators [14]. With the goal and scope properly defined, more key assumptions for the LCSA will be presented in the following section.

7.3. Key assumptions

There are several assumptions with a significant impact for the entire LCSA method and the final results. These are listed in Table 7.1 and Table 7.2, together with a justification for their validity. Note that other assumptions made in specific LCI definitions will be indicated in the respective sections, for reading clarity.

Table 7.1: Overview of key assumptions in the life cycle sustainability assessment of the various propulsion systems, part 1

Label	Description	Justification
A-LCA-01	It is assumed that the design changes in other subsystems do not feed back into the propulsion subsystem design.	This assumption is necessary to limit the scope of the study, but is most likely unrealistic due to the iterative nature of spacecraft design.
A-LCA-02	All components in the LCI are assumed to be TRL 9.	This assumption is made to justify the fact that system design and development is not included in the system boundaries. For all propellant options except 98% HTP, this assumption is fully valid.
A-LCA-03	All components are fully qualified to be integrated with the system without further modification.	This relates to the fact that all components are considered to be readily manufactured, without requiring any design changes and qualification testing. This is most relevant for the propellant tank.
A-LCA-04	The impact allocation of processes with multiple outputs is modelled at point of substitution (APOS).	This assumption is made to be in line with the rest of the SSSD [111].
A-LCA-05	For material or component transport, packaging weighs 50% of mass to be transported.	This assumption is recommended by the ESA LCA Handbook [99].
A-LCA-06	The life cycle of transportation containers or packaging is not considered within the scope of the LCSA.	This assumption is recommended by the ESA LCA Handbook [99].
A-LCA-07	One labour hour in the space industry is assumed to create $ 237.16 of value (2021).	This assumption is recommended by Wilson as a way of linking economic and social flows in LCI definitions in the SSSD [111].
A-LCA-08	The propulsion system is assembled in The Netherlands.	This assumption is arbitrarily based on the location of the research.
A-LCA-09	The case study satellite is launched from the Kourou Space Port.	The preferred launch site for European satellites is in Kourou, French Guyana.
A-LCA-10	The social conditions in French Guyana are identical to those in France.	This assumption is made in view of the social impact assessment. French Guyana is a French territory and this assumption is mostly valid for all stakeholder subcategories related to business relations in French Guyana.

Table 7.2: Overview of key assumptions in the life cycle sustainability assessment of the various propulsion systems, part 2

Label	Description	Justification
A-LCA-11	The EIL propulsion systems use a Ir/Al_2O_3 catalyst.	The composition of proprietary catalysts for ASCENT and LMP-103S is not known, therefore the propellants are deemed to be compatible with hydrazine catalysts.
A-LCA-12	The 98% HTP propulsion system uses a Pt/Al_2O_3 catalyst.	While various options are being researched currently, platinum alumina catalyst has shown good performance in the past with HTP [41].
A-LCA-13	The fuelling procedure for all novel monopropellants is similar with respect to resource savings compared to hydrazine.	This assumption is made so that data for LMP-103S fuelling from Mulkey et al. 2016 can be also be applied for the other monopropellant options. Considering the similar level of toxicity of ASCENT, LMP-103S and 98% HTP, this assumption is sufficiently valid.
A-LCA-14	The raw material procurement for a titanium tank makes up 36% of the total cost.	Cost breakdown provided by Benedic et al [188].
A-LCA-15	The machining for a titanium tank makes up 48% of the total cost.	Cost breakdown provided by Benedic et al [188].
A-LCA-16	The material cost of aluminium alloy is 63% less than the material cost of titanium alloy.	Trading data from January 2023 [189], [190].
A-LCA-17	The machining cost of aluminium is 26% less than the machining cost of titanium alloy.	Trading data from January 2023, assuming that machining cost benefits from half the material cost reduction [189], [190].

7.4. Life cycle inventories

This section will give an overview of the newly created processes that were implemented in openLCA to facilitate an accurate LCSA of the designed propulsion systems of Chapter 6. The sources given in Table 6.30 serve as an initial indication of what each component is made up of and how it is produced, but a further literature study is performed to fully model and quantify the flows involved in each component's life cycle. The LCI for the production of the components will be included in Subsection 7.4.2, whereas new upstream processes are discussed in Subsection 7.4.1. The construction of the four Product Systems for which the LCSA is performed in openLCA, along with other processes that are specific to each of the four propellants, are presented in Subsection 7.4.3. Whenever the full tabulated definition of the process is not deemed to add a clear value for the reader, especially with respect to the results that will be shown in Section 7.5, process definitions are included in Appendix B.

As discussed in Section 4.5, in setting up the various new processes, use will be made of existing datasets and processes from the SSSD and ecoinvent 3.8 databases [101], [111]. For each process, a table will be presented with the input and output flows characterising the process. The quantification of key flows will be briefly discussed and motivated and a short rationale will be included for any flow in the process, including the relevant sources. Do note that each flow is assigned a specific provider process, determining the impact related to providing this flow. For example, if transport by lorry is used in any process, a specification must be made of the lorry's emission norm and where this transport takes place, as this affects the overall environmental footprint of that service. This information is contained within the openLCA datasets that were created for this research.

7.4.1. New upstream processes

Production of iridium

The first upstream process that is created models the production of iridium, which is a platinum group metal (PGM) commonly extracted alongside other platinum group metals and copper and nickel in South-Africa and Russia [25], [191]. The extraction and further processing of the PGM concentrate leading to pure iridium is included in the LCSA because the high-temperature resistant thrusters used in the ASCENT and LMP-103s systems use a rhenium/iridium alloy combustion chamber, and as the common S-405 catalyst also contains iridium. However, the production of iridium is not yet contained within any of the LCI databases considered in this research, resulting in the need to create a new upstream process.

Iridium and platinum are both products of the same PGM extraction and refining process, meaning that the impact related to the production of each of these metals can be considered as a fraction of the total PGM extraction and refining impact allocated among all coproducts. This is also how the existing processes of platinum, rhodium and palladium production are modelled within ecoinvent [192]. In a synthesis of LCAs for all metals in the periodic table, Nuss and Eckelman use updated data related to the production of PGMs in South Africa and Russia to reallocate the impact of PGM extraction and refining among all PGMs and the coproducts nickel and copper, based on the generated revenue of each of these coproducts [191]. Assuming that the production of iridium and platinum have the same LCI (as they are two coproducts of a larger parent process), the new dataset for iridium is set up using an appropriate combination of the platinum production processes that do exist in ecoinvent 3.8.

In a document supporting their article, Nuss and Eckelmann report the global warming potential (IPCC 2007, GWP100a) for their reallocated datasets of platinum and iridium production [191]. Reworking these results, it is found that the production of 1 kg of iridium leads to the same global warming effect as 0.527 kg of platinum in South Africa, and as 0.668 kg of platinum in Russia. Using world supply data from 2008, it is assumed that about 60% of the world supply of iridium is sourced from South Africa, whereas 40% is produced in Russia, such that the average impact of 1 kg of iridium delivered in Europe (RER) is equivalent to the combined impact of producing of 0.32147 kg of platinum in South Africa, 0.2672 kg in Russia, and the transport to Europe of 0.6 kg of South African iridium and 0.4 kg of Russian iridium. The resulting process added to the SSSD is shown in Table 7.3, where the amount of transport is expressed in the transportation of 1 $tonne$ for 1 $kilometre$ ($t * km$), which is a standard unit in LCA practices.

Table 7.3: Process definition for iridium production

Flow	Amount	Unit	Description
		INPUT	
platinum, RU	0.267	kg	Russian import. Mass determined by reallocation of PGM processing impacts [191].
platinum, ZA	0.322	kg	South African import. Mass determined by reallocation of PGM processing impacts [191].
transport, freight, aircraft, unspecified	15.225	$t * km$	Material transport to RER. 50% packaging mass assumption.
		OUTPUT	
iridium, at regional storage, RER	1	kg	-

Production of rhenium

The addition of rhenium production to the SSSD is completed in a similar manner as for iridium. Once again, the need to add this process arises from the use of rhenium in the combustion chambers for the EIL thrusters. Rhenium is also a coproduct of the production of another metal, molybdenum, which is included in ecoinvent 3.8. As such, the reallocation of impacts as proposed by Nuss and Eckelmann

is used here as well to express the impact of rhenium production in terms of impact of molybdenum production [191]. In the case of rhenium and molybdenum, the article indicates that in the production of 1 kg of molybdenum, 0.00147 kg of rhenium is also produced. Allocating the impacts based on the price of rhenium and molybdenum, Nuss and Eckelmann propose that 13.5% of this process impact should be allocated to the 0.00147 kg of rhenium produced. As such, the impact of producing 1 kg of rhenium is equivalent to the impact of 91.84 kg (=0.135/0.00147) of molybdenum using the ecoinvent dataset where 100% of the molybdenite ore roasting process is allocated to molybdenum production. Because the molybdenum dataset already contains transport to RER, no additional transport is needed in the rhenium production process, as shown in Table 7.4.

Table 7.4: Process definition for rhenium production

Flow	Amount	Unit	Description
	INPUT		
molybdenum	91.84	kg	Mass determined by reallocation of molybdenum production impacts.
	OUTPUT		
rhenium, at plant, RER	1	kg	-

7.4.2. New core processes

The new core processes are created to model the production and acceptance testing of the propulsion system components included in the LCSA. Use is made of various proxies or other secondary data to inform the definition of these production processes, meaning that the data quality for some processes is questionable. This will be further discussed in Section 8.3.

The thruster is arguably the most complex component considered in the PS LCSA model, and also features design differences between the various propellants. As such, it is treated in more detail and subdivided in four separate subcomponents, being the catalyst bed, catalyst bed heater, flow control valve and combustion chamber/nozzle assembly. The assembly and testing of the full 1 N thruster will be discussed in the next subsection where the inventories specific to each propellant are presented.

For each of the core processes, the economic and social flows will also be added, which are used in the assessment of the economic and social impact of the entire PS. The economic impact assessment method simply requires that an estimation is made of the production and transport costs for each process, whereas the required social data is an approximation of the number of labour hours involved in the process, and where this labour takes place. As this data is difficult to find for many specific processes, a standard approximation method is used to link the economic and social flows whenever one or the other cannot be found in literature. Based on the total value created in the US aerospace and defence sector in 2021 (892 billion $), and the total number of annual working hours in this sector, it is estimated that every labour hour leads to the creation of 237.16 $ [111]. Thus, if the cost of a component is known, an approximation can be made of the number of labour hours involved in its production, and vice versa. Most costing information will be expressed in 2017 $ (USD), as many of the SSSD also use this currency. In the economic impact assessment, however, the impact will be expressed in € for financial conditions in the year 2000, and openLCA automatically adjusts the currencies according to exchange and inflation rates. Any other costing data found in literature will be adjusted to account for exchange and inflation rates.

Another standard assumption is used whenever information on the material transport within a process is lacking. Following ESA guidelines, a standard assumption is used of 500 km by fleet average lorry transport, with packaging mass adding 50% to the mass being transported [99]. Lastly, pre-existing processes in the SSSD were used to provide the testing flows in each of the new core processes. These testing processes mostly add to the overall electricity consumption and creation of waste.

Alumina/iridium granular catalyst

This catalyst will be used in the hydrazine, ASCENT and LMP-103S thrusters, and is based on the S-405 catalyst produced by Aerojet Rocketdyne [193]. This granular catalyst is assumed to consist of a 30 wt% deposition of iridium on alumina granules. The production consists of the extraction and refinement of alumina and iridium, the transformation of alumina into granules (not included in the life cycle due to lacking data), the impregnation of iridium onto the alumina granules in a solution (not included due to lacking data), the drying and calcination of the impregnated granules, and final testing for structural integrity. Other process information is shown in Table 7.5.

Table 7.5: Process definition for alumina/iridium granular catalyst production and testing

Flow	Amount	Unit	Description
	INPUT		
aluminium oxide	0.7	kg	70% of total mass [193].
electricity, low voltage	12	kWh	Proxy for catalyst drying and calcination [40].
iridium, at regional storage - RER	0.3	kg	30% of total mass [193].
Organisational Time Contribution (Nat) - EU	70	work-hours	No information available, linked to cost [111].
Total Design Loads Inspection	6.33E-4	m^3	Bulk density of 1550 kg/m^3 [194].
transport, freight, lorry 16-32 metric ton, EURO4	0.75	$t*km$	Material transport, standard assumptions.
	OUTPUT		
Alumina/Iridium Granular Catalyst	1	kg	-
SPACE SEGMENT: Goods Transport via Lorry Costs	3.75	USD 2017	Average cost to move goods via road transport [111].
SPACE SEGMENT: Spacecraft Material, Component & Resource Costs	15414	USD 2017	Cost from 1981, adjusted for inflation [195].

Alumina/platinum granular catalyst

As it has been found that stabilisers included in HTP solutions tend to poison and deactivate the standard alumina/iridium catalyst, it was deemed necessary to include a different catalyst in the 98% HTP thruster. In a research article producing and testing a flight-model 1 N thruster for 87.5% HTP, Ryan et al. find that a granular catalyst of platinum deposited on alumina remained active and structurally intact during hot firing [41]. As such, the LCSA model will include this catalyst in the HTP thruster's catalytic bed, assuming a same weight fraction of 30 wt% Pt deposited on 70 wt% Al_2O_3. The other processing steps are assumed to be the same as for the alumina/iridium catalyst in Table 7.5.

As no cost estimate could be found for the alumina/platinum catalyst, its price is based on the alumina/iridium catalyst, adjusting for the lower price of platinum, as this is assumed to make up the bulk of the catalyst price. Using average data from 2021, it is found that platinum is priced on at 1094.31 $ per troy ounce, and iridium at 5158.40 $ [25]. Using this ratio of 4.174, the alumina/platinum catalyst price is adjusted accordingly. The resulting LCI definition is presented in Table B.1.

Catalyst bed heater

Each of the thrusters is assumed to use the same type of catalyst bed heater, being a coiled heater produced by the French company Thermocoax [196]. This heater is used in the ECAPS 1 N HPGP thruster, and is also deemed to be compatible with more advanced hydrazine thrusters, using coiled catalyst bed heaters instead of the heritage cartridge heater design [197]. Based on correspondence with an engineer at a Thermocoax, it is found that the heater is composed of a junction box connected to a coiled mineral insulated cable, with a outer sheath of inconel, a mineral core of magnesium oxide (MgO) and four nickel/chromium heating wires, resulting in a fault-tolerant system. The total mass of

the component is 50 g, the approximate cost is 2200 € in 2023, and the production of one heater takes up 11 labour hours, including post-production testing.

The exact dimensions and mass of the various materials used in the heater have been approximated based Figure C.6 and Figure C.3 [196], [198]. The specifications reported there are relevant for the 50 g heater used in the 1 N thrusters, but as this catalyst bed heater may be scaled up to be used in larger thrusters, it was decided to normalise the entire process to the output of a 1 kg heater, resulting in the process shown in Table 7.6. This will be scaled down when used in the thruster production LCI.

Table 7.6: Process definition for inconel coiled catalyst bed heater production and testing

Flow	Amount	Unit	Description
	INPUT		
Cable Harness	80	m	Proxy for lead wires [198].
iron-nickel-chromium alloy	0.0296	kg	Proxy for Inconel 625 outer sheath. Approximated from cross section [196].
iron-nickel-chromium alloy	1.6E-4	kg	Proxy for Nickel-Chromium (80/20) resistive wire, approximated from cross section [196].
Leak Test	1.02E-05	m^3	Total volume based on outer dimensions [198].
magnesium oxide	0.0395	kg	Approximated from cross section [196].
Organisational Time Contribution (Nat) - FR	220	work-hours	Time required for production and testing.
Thermostat	0.931	kg	Proxy for junction box [111], [196].
Total Design Loads Inspection	1.02E-05	m^3	Total volume based on outer dimensions [198].
transport, freight, lorry 16-32 metric ton, EURO4	2.489	$t * km$	Material transport from RER to FR.
welding, arc, steel	0.145	m	Proxy for brazing, approximated from technical drawings [198].
wire drawing, steel	1.6E-4	kg	Proxy for Nickel-Chromium (80/20) resistive wire, approximated from technical drawings [198].
X-Ray/Radiographic Inspection	0.0398	m^2	Approximated from cross section [196].
	OUTPUT		
Catalyst Bed Heater - Coiled - Inconel Sheath	1	kg	-
SPACE SEGMENT: Goods Transport via Lorry Costs	12.443	USD 2017	Average cost to move goods via road transport [111].
SPACE SEGMENT: Spacecraft Material, Component & Resource Costs	37940	USD 2017	Estimate from manufacturer.
SPACE SEGMENT: Spacecraft Material, Component & Resource Costs	-2171.730	EURO 2017	Compensation for thermostat cost [111].
SPACE SEGMENT: Spacecraft Material, Component & Resource Costs	-275.037	USD 2008	Compensation for cable harness cost [111].

Diaphragm propellant tank, aluminium

Next in the alphabetic listing of new core processes is the aluminium diaphragm tank used in the 98% HTP PS design. For the production of this tank, data was sourced from the aluminium propellant tank in development at Nammo Raufoss, the FEP diaphragm production of Holscot, and the existing titanium propellant tank dataset in the SSSD [111], [171], [176]. Once again, to allow for later LCAs to reuse the dataset, the process was scaled to a 1 kg tank, adjusting the values found for the propellant tank sized in Subsection 6.4.5.

Regarding the price of the tank, the price of the titanium propellant tank was used as a reference, and adjusted based on the price difference between aluminium and titanium. Based on a cost breakdown of high pressure helium tanks, used in the Ariane 5 launch vehicle, it is assumed that 36% of the total tank cost is due to material procurement, and 48% due to material machining [188]. Then, comparing current cost data for titanium and aluminium (pure, not alloyed), it is found that 1 kg of aluminium is worth 37% of the cost of 1 kg of titanium [189], [190]. The fraction of material cost for the aluminium tank therefore taken at 37% of that fraction for the titanium tank. However, it is assumed that machining does not entirely scale with material cost, such that aluminium machining is assumed to cost 74% of titanium machining, thus doubling the fractional price that a comparison of material cost results in. This assumption is yet to be validated however. The total aluminium tank price is then calculated by first taking the price for a 1 kg titanium propellant tank, and then removing 63% of the material cost and 26% of the machining cost, leaving 16% of the total cost untouched. The resulting process information is shown in Table 7.7.

Table 7.7: Process definition for aluminium/FEP diaphragm propellant tank production and testing

Flow	Amount	Unit	Description
	INPUT		
aluminium alloy, AlMg3	0.975	kg	Proxy for Al5254, mass scaled from PS sizing.
aluminium removed by milling, large parts	7.41	kg	Based on Ti tank [111].
aluminium removed by turning, average, computer numerical controlled	11.115	kg	Based on Ti tank [111].
anodising, aluminium sheet	0.356	m^2	Total surface area scaled from PS sizing.
Automated Eddy Current Inspection	0.748	m	Tank periphery scaled from PS sizing.
Dye Penetrant Inspection	0.178	m^2	Outer surface area scaled from PS sizing.
Expulsion Efficiency Inspection	0.00705	m^3	Volume scaled from PS sizing.
extrusion, plastic film	0.0256	kg	Proxy for FEP diaphragm production [171]. Mass scaled from PS sizing.
Leak Test	0.00705	m^3	Volume scaled from PS sizing.
Metal Heat Treatment	0.975	kg	Shell mass scaled from PS sizing
Metal Heat Treatment	19.5	kg	Shell mass scaled from PS sizing
Negative Pressure Inspection	0.00705	m^3	Volume scaled from PS sizing.
Organisational Time Contribution (Nat) - EU	92	work-hours	No information available, linked to cost [111].
Pressure Cycle Inspection	2x 0.00705	m^3	Volume scaled from PS sizing.
tetrafluoroethylene	0.025	kg	Proxy for FEP [171]. Mass scaled from PS sizing.
Total Design Loads Inspection	0.00705	m^3	Volume scaled from PS sizing.
transport, freight, lorry 16-32 metric ton, EURO4	0.75	$t * km$	Material transport. Standard assumptions.
Ultrasonic Inspection	0.00705	m^3	Volume scaled from PS sizing.
Vibration Test	0.00705	m^3	Volume scaled from PS sizing.
Volumetric Capacity Examination	0.00705	m^3	Volume scaled from PS sizing.
welding, arc, aluminium	0.748	m	Tank periphery scaled from PS sizing.
X-Ray/Radiographic Inspection	0.178	m^2	Outer surface area scaled from PS sizing.
	OUTPUT		
Diaphragm Propellant Tank - Spherical - Al5254	1	kg	-
SPACE SEGMENT: Goods Transport via Lorry Costs	3.75	USD 2017	Average cost to move goods via road transport [111].
SPACE SEGMENT: Spacecraft Material, Component & Resource Costs	20275.470	USD 2017	Adjusted based on Ti tank cost [188]–[190].

Diaphragm propellant tank, titanium

The definition of the production and testing process of the titanium propellant tank is mostly based on information sourced from an existing SSSD dataset for a titanium blow-down tank, and scaled to 1 kg based on the sizing method used in Subsection 6.2.5. The price of the titanium tank is based on a quote for the Rafael PEPT-230 tank using the same shell and diaphragm materials as selected in the PS design [199]. As the design of the propellant tank was based on the propellant tank to be used in the Altius mission, Northrop Grumman was taken as a supplier reference, such that the labour hours in the process are provided in the USA [80], [170]. As the process is very similar to the aluminium tank production, an overview is provided in Appendix B in Table B.2.

Fill/drain valve

The next component is the low pressure service valve of which two are included in each PS design to fill or drain the propellant tank with propellant and pressurant. The general production process and material makeup of the valve was based on the information available for the selected Moog low pressure stainless steel service valve [187]. Dimensions were estimated from the technical drawing shown in Figure C.5. The pricing of the valve was estimated based on correspondence with a product manager at a space propulsion systems manufacturer. The process description in Table B.3 shows a straightforward forging and machining process by which the valve is assumed to be produced. Note that the process outputs a single Item of ”Fill/Drain Valve”, as opposed to scaling the dataset up with mass. This is done as it is deemed too inaccurate to use this dataset as a proxy for larger fill/drain valves.

Flow control valve

A separate LCI is constructed for the flow control valve (FCV), which is a crucial part of each thruster. For all propellants except ASCENT, a double seat solenoid valve is used. Information for the working principles, production process and internal dimensions of such a valve was sourced from models produced by Moog [200], used in the Aerojet Rocketdyne MR-103J [125] and ECAPS 1N HPGP thrusters [62], and Valvetech [201], used in a 1 N hydrazine thruster built by ArianeGroup [202]. A patent document for the latter valve informed the estimated dimensions, using Figure C.7. The price of the FCV was based on information obtained through correspondence with a product manager at a space propulsion systems manufacturer.

The output flow for this process is expressed in Item(s), as shown in Table 7.8, such that the ASCENT thruster, which employs a single seat FCV, will use 0.5 Items of the created flow. Additionally, as very little data could be found on the isolation latch valve produced by Moog [183], using a torque motor instead of a solenoid, 0.5 Items of the FCV will also be used as a proxy for the production of that component. While this simplification may not be very accurate from an LCI perspective, single seat solenoid valves are also often used as isolation valves in PS architectures [67], [141].

Table 7.8: Process definition for flow control valve production and testing

Flow	Amount	Unit	Description
	INPUT		
chromium steel removed by milling, small parts	0.0242	kg	Mass based on ecoinvent recommendation.
copper	0.0731	kg	Approximated from technical drawings and datasheet [200], [201].
degreasing, metal part in alkaline bath	0.00527	m^2	Approximated from technical drawings [201].
EPDM Product	0.0225	kg	Approximated from technical drawings and datasheet [200], [201].
forging, steel	0.105	kg	Approximated from technical drawings and datasheet [200], [201].
impact extrusion of steel, hot, 3 strokes	0.105	kg	Approximated from technical drawings and datasheet [200], [201].
Leak Test	1.72E-4	m^3	Approximated from technical drawings [201].
Negative Pressure Inspection	1.72E-4	m^3	Proxy for thermal vacuum cycle, approximated from technical drawings [201].
Organisational Time Contribution (Nat) - US	98	work-hours	No exact information, linked to cost [111].
Samarium Cobalt Magnet	0.0217	kg	Approximated from technical drawings and datasheet [200], [201].
steel, chromium steel 18/8	0.105	kg	Approximated from technical drawings and datasheet [200], [201].
transport, freight, lorry 16-32 metric ton, EURO4	0.15	$t * km$	Material transport, standard assumptions.
welding, arc, steel	0.137	m	Approximated from technical drawings [201].
wire drawing, copper	0.0731	kg	Approximated from technical drawings and datasheet [200], [201].
	OUTPUT		
Flow Control Valve - Double Seat - Stainless Steel	1	Item(s)	-
SPACE SEGMENT: Goods Transport via Lorry Costs	0.75	USD 2017	Average cost to move goods via road transport [111].
SPACE SEGMENT: Spacecraft Material, Component & Resource Costs	21554	USD 2017	Estimate from correspondence with product manager.
SPACE SEGMENT: Spacecraft Material, Component & Resource Costs	-108.4	EURO 2017	Compensation for magnet cost [111].

Seamless tubing

It is assumed that each of the propulsion systems uses 1/4 inch seamless steel tubing to connect the various components in the architecture. As no dataset for this piping exists in the SSSD or ESA LCA database, a new process is created, based on the space-grade tubing produced by the British company Fine Tubes [185]. The closest possible option to 1/4 inch tubing produced by Fine Tubes is a

304 stainless steel seamless tube with an outer diameter of 6.35 mm and a wall thickness of 0.7 mm, which was used as the basis for the definition of flows in Table B.4, included in the appendix for brevity. The price of tubing was based on a commercial supplier website and may not be fully representative of the quality standards required for space-grade seamless tubing [203].

Thruster combustion chamber, inconel

For the monopropellants with a relatively low combustion temperature, being hydrazine and 98% HTP, it will be assumed that the combustion chamber and nozzle assembly is constructed out of inconel alloy 625 [84]. The exact mass of this component of the thruster could not be found separately, but is calculated by knowing the total thruster mass and the mass of the other thruster components (catalyst bed, catalyst bed heater, FCV). The main reference for this process was the Aerojet Rocketdyne MR-103J 1 N thruster, of which a technical drawing, shown in Figure C.1, and mass specifications from [125] are used.

As this component will only be used in the thruster, for which the total cost is known with relatively high accuracy, a separate cost estimation is not entirely necessary for the thruster combustion chamber. However, the labour hours involved in the process, sourced from the USA due to the reference case of the MR-103J thruster, do need to be approximated for the precise assessment of social impact. The method followed is to subtract the other thruster components' cost from the total thruster cost, to achieve an approximation of the fraction of cost that the combustion chamber constitutes. With this price estimate, the number of labour hours is approximated, using the standard assumption of $ 237.16 per hour in 2021 currency. The process' LCI is rather straightforward, and presented in Table B.5.

Thruster combustion chamber, rhenium/iridium

As indicated in the literature study, the EIL monopropellants have much higher combustion temperatures, meaning that their thrusters make use of refractory metals to withstand the high temperatures and maintain structural integrity. Both the ECAPS 1 N HPGP thruster and the Aerojet Rocketdyne GR-1 thruster feature a combustion chamber and nozzle made of an rhenium/iridium alloy, where a thin layer of iridium is deposited on the inside of a rhenium shell providing most of the structural strength [67], [141], [204]. These combustion chambers are produced by an American company, Plasma Processes, through a patented electrodeposition process named EL-Form [54], [205].

While the combustion chamber and nozzle are fully constructed out of this exotic material combination, it is assumed that other parts of the thrust chamber assembly of the ASCENT and LMP-103S thrusters are made of an inconel alloy. An estimation of the combustion chamber total mass was based on correspondence with a lead engineer at a company developing monopropellant thrusters, such that the mass of inconel used was approximated by calculating the mass of iridium and rhenium in the nozzle and subtracting this from the total mass. To approximate the mass of iridium and rhenium, technical drawings of the ECAPS 1 N HPGP thruster are used, shown in Figure C.3 and Figure C.4, together with the assumption that a layer of 0.06096 mm of iridium is coated by a layer of 1.016 mm of rhenium, resulting in a total (uniform) combustion chamber and nozzle wall thickness of about 1.08 mm [205], [206]. For the number of labour hours involved in the production process, the same approach is used as for the inconel combustion chamber. As the EL-Form process is patented by Plasma Processes, the production of these combustion chambers also takes place in the USA.

Table 7.9: Process definition for rhenium/iridium thruster combustion chamber production and testing

Flow	Amount	Unit	Description
	INPUT		
chromium steel removed by milling, small parts	0.0286	kg	Proxy for inconel milling, mass from ecoinvent recommendations.
degreasing, metal part in alkaline bath	0.00251	m^2	Approximated from technical drawings [206].
Dye Penetrant Inspection	2x 0.00126	m^2	Approximated from technical drawings [206].
forging, steel	0.124	kg	Proxy for inconel forging.
hard chromium coat, electroplating, steel substrate, 0.14 mm thickness	0.00968	m^2	Proxy for EL-Form, amount adapted for a thickness of 1.08mm [205].
iridium, at regional storage - RER	0.0120	kg	Thickness of 0.0610 mm, surface approximated from technical drawings [205], [206].
iron-nickel-chromium alloy	0.124	kg	Proxy for inconel production, mass from expert estimate and drawings [206].
Organisational Time Contribution (Nat) - US	184	work-hours	No data available, linked to cost [111].
Rhenium, at plant	0.0214	kg	Thickness of 1.016 mm, surface approximated from technical drawings [206].
transport, freight, aircraft, unspecified	2.644	$t * km$	Material transport of iridium and rhenium from RER to US.
transport, freight, lorry 16-32 metric ton, EURO4	0.0930	$t * km$	Material transport of inconel in the US, standard assumptions.
Ultrasonic Inspection	1.36E-06	m^3	Volume approximated with thin walled assumption [206].
X-Ray/Radiographic Inspection	2x 0.00126	m^2	Approximated from technical drawings [206].
	OUTPUT		
Thruster Combustion Chamber - 1N - Iridium/Rhenium Alloy	1	Item(s)	-
SPACE SEGMENT: Goods Transport via Air Costs	1.844	USD 2017	Average cost to move air freight [111].
SPACE SEGMENT: Goods Transport via Lorry Costs	0.465	USD 2017	Average cost to move goods via road transport [111].

7.4.3. Propulsion system inventories

Whereas the core processes discussed in Subsection 7.4.2 are (or could be) used in the LCI of various propulsion systems, there are also processes specific to each of the propulsion systems, for which the definition is based on the specific case study dealt with in this research. Four unique processes are linked to each PS design, being the production of propellant, the assembly and testing of the thruster, the assembly and testing of the entire propulsion system, and the transport to and fuelling of the system in French Guyana.

For the estimation of the duration and cost of fuelling, the significant assumption is made that all novel monopropellants require similar safety precautions, such that data for LMP-103S fuelling, from the

PRISMA mission [26] and a dedicated fuelling test at NASA Wallops [61], is also used for ASCENT and 98% HTP fuelling. This assumption may be least accurate for 98% HTP, due to its slightly more corrosive nature, but the reduced vapour pressure of hydrogen peroxide is deemed to reduce this hazard [22]. Furthermore, data from the PRISMA launch campaign will also be used to inform the estimation of hydrazine fuelling cost and duration [26], [197].

Hydrazine

Starting with the production of hydrazine itself, a dataset from the ESA LCA database is used, modelling the production of ultra high purity hydrazine in Europe using 99% anhydrous hydrazine sourced from China [15]. As the ESA LCA datasets do not include any social or economic flows, an older hydrazine dataset contained in the SSSD is used to fill these gaps [111]. The resulting process is shown in Table 7.10.

Table 7.10: Process definition for ultra high purity hydrazine production

Flow	Amount	Unit	Description
	INPUT		
chemical factory, organics	4E-10	Item(s)	From ESA LCA DB [15].
electricity, low voltage	0.154	kWh	From ESA LCA DB [15].
electricity, low voltage	14.7	kWh	From ESA LCA DB [15].
electricity, low voltage	0.001	kWh	From ESA LCA DB [15].
Hydrazine anhydrous 99%	1.072	kg	From ESA LCA DB [15].
Organisational Time Contribution (Nat) - DE	1.926	work-hours	From SSSD, linked to cost [111].
transport, freight, lorry 16-32 metric ton, EURO4	0.5	$t*km$	From ESA LCA DB [15].
transport, freight, sea, container ship	28	$t*km$	From ESA LCA DB [15].
	OUTPUT		
Propellant - Hydrazine ultra high purity	1	kg	-
hazardous waste, for incineration	0.072	kg	From ESA LCA DB [15].
Hydrazine - emission to air	0.002	kg	From ESA LCA DB [15].
SPACE SEGMENT: Goods Transport via Lorry Costs	15	USD 2017	Average cost to move goods via road transport [111].
SPACE SEGMENT: Spacecraft Propellant Acquisition/Production Costs	132.59	USD 2001	Aquisition cost of Hydrazine [111].

Next, the process definition for the assembly and testing of the 1 N hydrazine thruster is somewhat more complicated, as it entails an estimation of the required catalyst bed size. A sizing method for alumina/iridium catalyst beds for hydrazine thrusters is used, which takes the catalytic bed loading (G), chamber pressure (P_c) and specific area of the catalyst (A_s) as input to calculate the required catalyst bed length L_B, following the empirical correlation expressed in Equation 7.1 [207, p.133]. In the shown equation, G, P_c and A_s are expressed respectively in $lbm/in^2/s$, psi and m^2/g, to give a catalyst bed length in in.

$$L_B = 0.2 + 145\frac{G^{0.554}}{{P_c}^{0.306}{A_s}^{0.3}} \tag{7.1}$$

Calculating the catalytic bed loading (G) is done through Equation 7.2, filling in the the maximum mass flow with the required thrust of 1 N and the real I_{sp} for each of the propellants, using Equation 7.3. The chamber cross-sectional area, A_c is calculated with the standard assumption for all thrusters of a 10 mm chamber diameter, based on measurements taken from the Aerojet Rocketdyne MR-103J and ECAPS 1 N HPGP thrusters in Figure C.1 and Figure C.3 [125], [206].

$$G = \frac{\dot{m}_p}{A_c} \tag{7.2}$$

$$\dot{m}_p = \frac{F_t}{g_0 I_{sp,real}} \tag{7.3}$$

The final unknown in Equation 7.1 is the catalyst specific area A_s. To estimate this parameter, data for the Shell-405 alumina/iridium catalyst is used, for which a specific area of 130 m^2/g is reported [194]. This estimation will also be used for the alumina/platinum catalyst. Calculating the catalyst bed length with Equation 7.1 and assuming the chamber cross section A_c, the required catalyst mass is found, with a known bulk density of alumina/iridium catalyst of 1580 kg/m^3, a value which will also be assumed for the alumina/platinum catalyst [194]. While the empirical coefficients used in Equation 7.1 were based on experimental results with hydrazine, this sizing method is also used for the ASCENT, LMP-103S and 98% HTP thrusters, due to the lack of a more accurate method.

With an adequate catalyst sizing method chosen, the process definition of the thruster production consists of combining the processes to produce the other thruster subcomponents as presented before, and adding the appropriate assembly time and testing procedures. The assembly time and total thruster cost are based on correspondence with an engineer with expert knowledge of space propulsion, and a cost comparison between hydrazine and HPGP thrusters [197], whereas the testing sequence is based on that of the ECAPS 1 N HPGP thruster [62]. While the cost estimation of the thruster is deemed to be fairly accurate at the time of writing, it is important to note that this metric is subject to some variation within the industry. The process definition for the thruster assembly is shown in Table 7.11.

Table 7.11: Process definition for 1 N hydrazine thruster assembly and testing

Flow	Amount	Unit	Description
	INPUT		
Alumina/Iridium Granular Catalyst	0.00261	kg	Catalyst bed length with propellant I_{sp} [207].
Catalyst Bed Heater - Coiled - Inconel Sheath	0.05	kg	Thruster design [125].
Flow Control Valve - Double Seat - Stainless Steel	1	Item(s)	Thruster design [125].
Leak Test	3x 1.75E-4	m^3	Total internal volume of all components.
Organisational Time Contribution (Nat) - US	12	work-hours	Based on correspondence with expert.
Proof Pressure Inspection	1.75E-4	m^3	Total internal volume of all components.
Thruster Combustion Chamber- 1N - Inconel	1	Item(s)	Thruster design [84].
transport, freight, aircraft, unspecified	0.574	$t*km$	Transport of catalyst bed heater from FR to US.
transport, freight, lorry 16-32 metric ton, EURO4	0.152	$t*km$	Transport of catalyst and valve within US.
Vibration Test	1.75E-4	m^3	Total internal volume of all components.
welding, arc, steel	0.191	m	Proxy for brazing, based on technical drawings [125].
X-Ray/Radiographic Inspection	0.00622	m^2	Total outer surface area of all components.
	OUTPUT		
Thruster - 1N - Hydrazine	1	Item(s)	-
SPACE SEGMENT: Goods Transport via Air Costs	0.400	USD 2017	Average cost to move air freight [111].
SPACE SEGMENT: Goods Transport via Lorry Costs	0.760	USD 2017	Average cost to move goods via road transport [111].
SPACE SEGMENT: Spacecraft Material, Component & Resource Costs	42927	USD 2017	Estimated cost for hydrazine thruster [197].
SPACE SEGMENT: Spacecraft Material, Component & Resource Costs	-40.231	USD 2017	Compensation for catalyst bed cost.
SPACE SEGMENT: Spacecraft Material, Component & Resource Costs	-21554	USD 2017	Compensation for FCV cost.
SPACE SEGMENT: Spacecraft Material, Component & Resource Costs	-1896.75	USD 2017	Compensation for catalyst bed heater cost.

In the assembly process of the entire propulsion system, the transport of various components to the assembly site in The Netherlands is considered, as well as the acceptance testing, based on the sequence performed for the SkySat PS [141]. The labour hours related to the assembly and testing procedure of the propulsion are estimated based on correspondence with a lead systems engineer of a propulsion subsystem supplier. The cost of this process could not be estimated directly and is as such linked to the labour hours with the method proposed by Wilson as presented before [111]. The entire process definition is provided in Table 7.12. Note that the total cost of the PS is reflected by the fact that the cost contributions of all input flows are considered in the economic impact assessment.

Table 7.12: Process definition for hydrazine propulsion system assembly and testing

Flow	Amount	Unit	Description
	INPUT		
Diaphragm Propellant Tank - Spherical - Ti6Al4V	2.479	kg	Based on PS sizing.
Fill/Drain Valve - Low Pressure - Stainless Steel	2	Item(s)	Service valves, based on PS architecture
Flow Control Valve - Double Seat - Stainless Steel	0.5	Item(s)	Proxy for isolation latch valve, based on PS architecture.
Leak Test	2x 0.0169	m^3	Tank volume and thruster internal volumes.
Organisational Time Contribution (Nat) - NL	1000	work-hours	Based on correspondence with expert.
Proof Pressure Inspection	0.0169	m^3	Tank volume and thruster internal volumes.
Seamless Tubing - Stainless Steel	0.741	kg	Based on PS sizing.
Thruster - 1N - Hydrazine	4	Item(s)	Based on PS architecture.
transport, freight, aircraft, unspecified	27.740	$t * km$	Transport of propellant tank, from US to NL.
transport, freight, aircraft, unspecified	5.796	$t * km$	Transport of valves, from US to NL.
transport, freight, aircraft, unspecified	16.561	$t * km$	Transport of thrusters from US to NL.
Vibration Test	0.0169	m^3	Tank volume and thruster internal volumes.
	OUTPUT		
Minisatellite Propulsion System - 4x1N - Monopropellant Hydrazine	1	Item(s)	-
SPACE SEGMENT: Goods Transport via Air Costs	11.551	USD 2017	Average cost to move air freight [111].
SPACE SEGMENT: Goods Transport via Air Costs	4.043	USD 2017	Average cost to move air freight [111].
SPACE SEGMENT: Goods Transport via Air Costs	19.349	USD 2017	Average cost to move air freight [111].
SPACE SEGMENT: Spacecraft Assembly & Integration Costs	219593	USD 2017	No exact information, linked to labour hours [111].

The final step considered in the life cycle of the propulsion system is the transport to the launch site and on-site propellant handling and fuelling procedures. As mentioned before, the duration of this campaign is based on the PRISMA loading campaign, which included both hydrazine and LMP-103S, facilitating a fair comparison. It is reported that clean room fuelling of the hydrazine PS took two full working days (assumed at 8 hours per day), and that the entire hydrazine loading campaign took two working weeks, occupying a 5-person crew full-time [26]. In the dataset definition, this time is adjusted for the slightly increased amount of hydrazine included in the case study PS (12.28 kg), as compared to the PRISMA hydrazine PS (11 kg).

The cost of the fuelling campaign is estimated by combining the results of two publications on hydrazine and LMP-103S fuelling. In a cost comparison between small satellite hydrazine and LMP-103S propulsion systems, Dinardi and Persson report an estimated cost reduction of $ 480000 for the fuelling

operations, if hydrazine is replaced by LMP-103S [197]. Separately, Mulkey et al. report an overall resource reduction, assumed to roughly reflect cost, of 40% for the fuelling and safety procedures when comparing LMP-103S fuelling to hydrazine fuelling [61]. Equating these two cost reductions, it is found that fuelling a small satellite hydrazine propulsion system approximately costs $ 1200000 in 2012, such that the fuelling campaign for the novel monopropellants is assumed to cost $ 720000 in 2012 currency. The resulting process definition is presented in Table 7.10. This process is the final element of the propulsion system's LCI and will be used as the Product System for which the LCIA is performed in openLCA for each propellant.

Table 7.13: Process definition for hydrazine propulsion system fuelling at launch site

Flow	Amount	Unit	Description
	INPUT		
Clean Room Fuelling	17.862	h	Scaled from PRISMA launch campaign [26].
General Handling of Propellant/Pressurant	125.033	h	Scaled from PRISMA launch campaign [26].
Minisatellite Propulsion System - 4x1N - Monopropellant Hydrazine	1	Item(s)	-
Organisational Time Contribution (Nat) - FR	625.164	work-hours	Scaled from PRISMA launch campaign [26].
Pressurant - Helium	0.017	kg	Based on PS sizing.
Propellant - Hydrazine	12.28	kg	Based on PS sizing.
Storage of Propellant/Pressurant	16.2	L	Based on PS sizing.
transport, freight, aircraft, unspecified	62.173	$t * km$	Transport of dry PS from NL to GF.
transport, freight, sea, container ship	143.952	$t * km$	Transport of hydrazine from DE to GF.
	OUTPUT		
Loaded Minisatellite Propulsion System - Hydrazine	1	Item(s)	-
SPACE SEGMENT: Goods Transport via Air Costs	43.366	USD 2017	Average cost to move air freight [111].
SPACE SEGMENT: Goods Transport via Ship Costs	314.896	EURO 2017	Average cost to move freight via transoceanic ship [111].
SPACE SEGMENT: Spacecraft Assembly & Integration Costs	1584000	USD 2017	Based on fuelling comparisons between hydrazine and LMP-103S [61], [197].

ASCENT

Similarly as for hydrazine, new processes are created in the SSSD to update the ASCENT production process, to model thruster assembly and propulsion system assembly and fuelling. The propellant production process shown in Table 7.14 is adapted from an existing validated dataset in the ESA LSA database [15]. Once again, the economic and social data is adapted from an SSSD dataset modelling ASCENT production.

Table 7.14: Process definition for ASCENT production

Flow	Amount	Unit	Description
	INPUT		
chemical factory, organics	4E-10	Item(s)	From ESA LCA DB [15].
Hydroxyl ethyl hydrazinium nitrate (HEHN) 99%	0.445	kg	From ESA LCA DB [15].
Hydroxylammonium nitrate (HAN)	0.445	kg	From ESA LCA DB [15].
Organisational Time Contribution (Nat) - US	1.321	work-hours	From SSSD, linked to cost [111].
water, deionised, from tap water, at user	0.11	kg	From ESA LCA DB [15].
	OUTPUT		
Propellant - ASCENT	1	kg	-
SPACE SEGMENT: Goods Transport via Lorry Costs	5	USD 2017	Average cost to move goods via road transport [111].
SPACE SEGMENT: Spacecraft Propellant Acquisition/Production Costs	118.6	USD 2017	Acquisition cost of ASCENT [111].

In the assembly process for the ASCENT thruster, two features are notable. Firstly, the required amount of catalyst is based on the hydrazine catalyst sizing method described above. Secondly, as the Aerojet Rocketdyne GR-1 thruster is taken as the main reference for the ASCENT thruster, a single seat FCV is used, together with a high-temperature resistant combustion chamber made of rhenium and iridium [67]. The resulting LCI is shown in Table 7.15. The price of the thruster is assumed to equal that of the ECAPS 1 N HPGP thruster, which is higher than the hydrazine thruster cost due to the use of the rhenium/iridium combustion chamber. Note that this may constitute an overestimation of the ASCENT thruster cost, given that the use of a single seat FCV will most likely lead to a cost reduction with respect to the ECAPS 1 N HPGP thruster.

Table 7.15: Process definition for 1 N ASCENT thruster assembly and testing

Flow	Amount	Unit	Description
	INPUT		
Alumina/Iridium Granular Catalyst	0.00250	kg	Catalyst bed length with propellant I_{sp} [207].
Catalyst Bed Heater - Coiled - Inconel Sheath	0.05	kg	Thruster design [67].
Flow Control Valve - Double Seat - Stainless Steel	0.5	Item(s)	Thruster design [67].
Leak Test	3x 8.95E-05	m^3	Total internal volume of all components.
Organisational Time Contribution (Nat) - US	12	work-hours	Based on correspondence with expert.
Proof Pressure Inspection	8.95E-05	m^3	Total internal volume of all components.
Thruster Combustion Chamber - 1N - Iridium/Rhenium Alloy	1	Item(s)	Thruster design [67].
transport, freight, aircraft, unspecified	0.574	$t*km$	Transport of catalyst bed heater from FR to US.
transport, freight, lorry 16-32 metric ton, EURO4	0.0769	$t*km$	Transport of components within US.
Vibration Test	8.95E-05	m^3	Total internal volume of all components.
welding, arc, steel	0.427	m	Proxy for brazing, based on technical drawings [198].
X-Ray/Radiographic Inspection	0.00515	m^2	Total outer surface area of all components [206].
	OUTPUT		
Thruster - 1N - ASCENT	1	Item(s)	-
SPACE SEGMENT: Goods Transport via Air Costs	0.400	USD 2017	Average cost to move air freight [111].
SPACE SEGMENT: Goods Transport via Lorry Costs	0.384	USD 2017	Average cost to move goods via road transport [111].
SPACE SEGMENT: Spacecraft Material, Component & Resource Costs	64390	USD 2017	Estimated cost for HPGP thruster [197].
SPACE SEGMENT: Spacecraft Material, Component & Resource Costs	-38.381	USD 2017	Compensation for catalyst bed cost.
SPACE SEGMENT: Spacecraft Material, Component & Resource Costs	-10777	USD 2017	Compensation for FCV cost.
SPACE SEGMENT: Spacecraft Material, Component & Resource Costs	-1896.75	USD 2017	Compensation for catalyst bed heater cost.

The process definition for the assembly and testing of the ASCENT PS in The Netherlands follows the same approach and assumptions as for the hydrazine PS. As such, the process is shown in the appendix in Table B.6. In the process definition of the transport and fuelling of the propulsion system, the assumption is made that ASCENT can be handled and fuelled with the same safety precautions that were in place for LMP-103S during NASA Wallops green propellant loading demonstration [61]. As such, an overall 72% reduction is applied to the time required for clean room fuelling and general handling of the propellant in the hydrazine system LCI. To estimate the organisational time contribution, data from the PRISMA launch campaign is used, where the LMP-103S loading campaign occupied a crew of three people for one working week [26]. For the fuelling LCI of each novel monopropellant system, that time is adjusted for the increased LMP-103S load required in this use case (11.48 kg) as compared to the load included in PRISMA (5.6 kg).

Table 7.16: Process definition for ASCENT propulsion system fuelling at launch site

Flow	Amount	Unit	Description
	INPUT		
Clean Room Fuelling	5.001	h	Scaled from PRISMA launch campaign [26], [61].
General Handling of Propellant/Pressurant	35.009	h	Scaled from PRISMA launch campaign [26], [61].
Minisatellite Propulsion System - 4x1N - Monopropellant ASCENT	1	Item(s)	-
Organisational Time Contribution (Nat) - FR	344.4	work-hours	Scaled from PRISMA launch campaign [26].
Pressurant - Helium	0.01	kg	Based on PS sizing.
Propellant - ASCENT	10.99	kg	Based on PS sizing.
Storage of Propellant/Pressurant	10	L	Based on PS sizing.
transport, freight, aircraft, unspecified	53.685	$t * km$	Transport of dry PS from NL to GF.
transport, freight, aircraft, unspecified	99.471	$t * km$	Transport of ASCENT from US to GF.
	OUTPUT		
Loaded Minisatellite Propulsion System - ASCENT	1	Item(s)	-
SPACE SEGMENT: Goods Transport via Air Costs	37.445	USD 2017	Average cost to move air freight [111].
SPACE SEGMENT: Goods Transport via Air Costs	69.381	USD 2017	Average cost to move air freight [111].
SPACE SEGMENT: Spacecraft Assembly & Integration Costs	950400	USD 2017	Based on fuelling comparisons between hydrazine and LMP-103S [61], [197].

LMP-103S

As for the previous two propellants, an existing dataset in the SSSD modelling the LCI of propellant production is updated using data from the ESA LCA database [15], [111]. The cost of propellant included in the SSSD dataset is based on an early estimate reported by Dinardi and Persson [197], and has been verified to still be accurate through correspondence with a lead engineer at a space propulsion company, stating a price of $ 1200 in 2023. Other process information is shown in Table 7.17.

Table 7.17: Process definition for LMP-103S production

Flow	Amount	Unit	Description
	INPUT		
ammonia, liquid	0.0465	kg	From ESA LCSA DB [15].
Ammonium Dinitramide	0.63	kg	From ESA LCSA DB [15].
chemical factory, organics	4E-10	Item(s)	From ESA LCSA DB [15].
electricity, medium voltage	6.3	kWh	From ESA LCSA DB [15].
methanol	0.184	kg	From ESA LCSA DB [15].
Organisational Time Contribution (Nat) - SE	12.129	work-hours	From SSSD, linked to cost [111].
transport, freight, lorry 16-32 metric ton, EURO4	0.5	$t * km$	From ESA LCSA DB [15].
water, deionised, from tap water, at user	0.140	kg	From ESA LCSA DB [15].
	OUTPUT		
Propellant - LMP-103S	1	kg	-
SPACE SEGMENT: Goods Transport via Lorry Costs	5	USD 2017	Average cost to move goods via road transport [111].
SPACE SEGMENT: Spacecraft Propellant Acquisition/Production Costs	976	USD 2017	Aquisition cost of LMP-103S [197].

As the LCI definitions for the LMP-103S thruster and propulsion system assembly are both constructed using the same method and assumptions as for ASCENT, they are included in the appendix, respectively in Table B.7 and Table B.8. The Product System for which the LCSA is performed for LMP-103S is shown in Table 7.18, which combines all previously described components and processes.

Table 7.18: Process definition for LMP-103S propulsion system fuelling at launch site

Flow	Amount	Unit	Description
	INPUT		
Clean Room Fuelling	5.00131	h	Scaled from PRISMA launch campaign [26], [61].
General Handling of Propellant/Pressurant	35.00916	h	Scaled from PRISMA launch campaign [26], [61].
Minisatellite Propulsion System - 4x1N - Monopropellant LMP-103S	1	Item(s)	-
Organisational Time Contribution (Nat) - FR	344.4	work-hours	Scaled from PRISMA launch campaign [26].
Pressurant - Helium	0.013	kg	Based on PS sizing.
Propellant - LMP-103S	11.53	kg	Based on PS sizing.
Storage of Propellant/Pressurant	12.4	L	Based on PS sizing.
transport, freight, aircraft, unspecified	57.600	$t * km$	Transport of dry PS from NL to GF.
transport, freight, aircraft, unspecified	147.198	$t * km$	Transport of LMP-103S from SE to GF.
	OUTPUT		
Loaded Minisatellite Propulsion System - LMP-103S	1	Item(s)	-
SPACE SEGMENT: Goods Transport via Air Costs	40.176	USD 2017	Average cost to move air freight [111].
SPACE SEGMENT: Goods Transport via Air Costs	102.670	USD 2017	Average cost to move air freight [111].
SPACE SEGMENT: Spacecraft Assembly & Integration Costs	950400	USD 2017	Based on fuelling comparisons between hydrazine and LMP-103S [61], [197].

98% HTP

A new process is created for the production of 98% HTP, as this was not yet included in the SSSD and access to the ESA LCA database, which does contain a dataset for 98% HTP, was only granted late in the LCI definition process. In Section 8.2, a comparison will be made between this new dataset for 98% HTP production and that contained in the ESA LCA database, to validate the LCI presented here.

There are three main assumptions reducing the accuracy of this dataset with respect to the actual production of rocket grade 98% HTP. Firstly, the process has been modelled based on data from a large hydrogen peroxide plant, the Solvay Voikaa Plant in Finland, which produces hydrogen peroxide at a maximum concentration of 60% through a continuous vacuum distillation process [208]. In reality, it is more likely that HTP used for propulsion purposes would be produced in a batch process, which has a few differences in the operating principles.

Secondly, actual data from the Solvay Voikaa plant related to the consumption of steam, dimineralised and cooling water, heat and electricity, for the distillation of 50% and 60% concentrated hydrogen peroxide starting with an input feed of 40% concentrated hydrogen peroxide, was linearly extrapolated for a concentration of 98% HTP. In reality, it is very unlikely that the required resources to reach a 98% concentration vary linearly with the concentration, as it becomes much more difficult to extract the little water that is left in the solution as the concentration increases.

Finally, while even rocket grade hydrogen peroxide contains some stabilisers, typically sodium stannate trihydrate [208], no stabilisers are included in the modelled life cycle analysis, due to a lack of exact data specifying the amount of stabilisers in monopropellant HTP. In the process definition in Table 7.19, it is also assumed that the production can take place in various places in the EU. Cost information was based on correspondence with a hydrogen peroxide sector expert.

Table 7.19: Process definition for 98% HTP production

Flow	Amount	Unit	Description
	INPUT		
electricity, medium voltage	17.314	Wh	Scaled from Solvay Voikaa [208].
heat, from steam, in chemical industry	3.143	kWh	Scaled from Solvay Voikaa [208].
hydrogen peroxide, without water, in 50% solution state	1.089	kg	Assuming 90% efficiency for feed HP [15].
Organisational Time Contribution (Nat) - EU	0.39	work-hours	No exact information available, linked to cost [111].
steam, in chemical industry	3.625	kg	Scaled from Solvay Voikaa [208].
water, deionised, from tap water, at user	0.568	kg	Proxy for demineralised water. Scaled from Solvay Voikaa [208].
Water, cooling, unspecified natural origin, Europe without Switzerland	90.187	L	Cooling water. Scaled from Solvay Voikaa [208].
	OUTPUT		
Hydrogen Peroxide - 98% Concentrated	1	kg	-
SPACE SEGMENT: Spacecraft Propellant Acquisition/Production Costs	86	USD 2017	Estimate from supplier.
Water, IAI Area, EU27 & EFTA - Emission to water	90.187	L	Cooling water returned to river [208].

The assembly of the 98% HTP thruster and full propulsion system are presented in Table B.9 and Table B.10, included in the appendix due to the general similarity in assumptions with the hydrazine system LCI data. The LCI definition for the fuelled 98% HTP PS is shown in Table 7.20, which, in similarity to the other propellant options, is the process for which the LCIA will be performed.

Table 7.20: Process definition for 98% HTP propulsion system fuelling at launch site

Flow	Amount	Unit	Description
	INPUT		
Clean Room Fuelling	5.00131	h	Scaled from PRISMA launch campaign [26], [61].
General Handling of Propellant/Pressurant	35.00916	h	Scaled from PRISMA launch campaign [26], [61].
Hydrogen Peroxide - 98% Concentrated	16.136	kg	Based on PS sizing.
Minisatellite Propulsion System - 4x1N - Monopropellant 98% HTP	1	Item(s)	-
Organisational Time Contribution (Nat) - FR	344.4	work-hours	Scaled from PRISMA launch campaign [26].
Pressurant - Helium	0.015	kg	Based on PS sizing.
Storage of Propellant/Pressurant	14.9	L	Based on PS sizing.
transport, freight, aircraft, unspecified	70.286	$t * km$	Transport of dry PS from NL to GF.
transport, freight, sea, container ship	200.409	$t * km$	Transport of 98% HTP from RER to GF.
	OUTPUT		
Loaded Minisatellite Propulsion System - 98% HTP	1	Item(s)	-
SPACE SEGMENT: Goods Transport via Air Costs	49.0248	USD 2017	Average cost to move air freight [111].
SPACE SEGMENT: Goods Transport via Ship Costs	438.395	EURO 2017	Average cost to move freight via transoceanic ship [111].
SPACE SEGMENT: Spacecraft Assembly & Integration Costs	950400	USD 2017	Based on fuelling comparisons between hydrazine and LMP-103S [61], [197].

7.5. Life cycle impact assessment: results and discussion

With an accurate representation of the life cycle for each of the designed propulsion systems, from raw material extraction to fuelling, the next step in the LCSA is to perform the life cycle impact assessment (LCIA). As discussed in Subsection 4.4.1, the LCIA method in this research is the SSSD Sustainability LCIA method, using 23 midpoint impact categories. Through a normalisation and weighting approach, estimating the relative impact with respect to the multi-criteria impact of an average EU citizen each year, single scores can be calculated for the environmental, economic and social dimensions of the LCSA, and these scores can be combined to calculate a total sustainability score based a weighting approach connected to the UN SDGs [14]. This section will first discuss the results for each of the sustainability dimensions in the LCIA, before combining the normalised single scores for the environmental, economic and social impacts into a single sustainability score.

For each of the discussed impact categories, the main processes driving the differences between the design options and general respective results will be identified and discussed. These results are direct outputs from the LCIA calculation performed in openLCA. Note that in the following discussion, each of the systems may be referred to by the shorthand of the used propellant, such that the impact of the LMP-103S system is sometimes referred to as the LMP-103S impact. It should be stressed that the entire system is being addressed in this case. Whenever a reference is made to the propellant itself, this will be explicitly stated. In Chapter 8, these findings will be further interpreted and validated with respect to previous research and the methodological framework of this research.

7.5.1. Environmental sustainability

Given that the environmental impact assessed in the LCSA contains the highest degree of detail, with 21 categories in total, and most likely also the highest accuracy of assessment, with the environmental flows included in the processes of Section 7.4 being the most validated, these results will be discussed first and with the most depth. As a comparison of the four systems could be the subject of lengthy discussions for each impact category, priority will be given to the impact categories with the largest contribution to the single score calculation. Presenting the top five contributing impact categories places a focus on the areas where the environmental life cycle impact of the propulsion systems is relatively the worst, compared to the average annual environmental impact of an EU citizen. This will accurately represent which environmental hotspots exist within each propulsion system option.

Starting comprehensively, Table 7.21 shows the environmental LCIA scores for every system design and impact category. These results are expressed in the correct units for each impact category, without being normalised or weighted yet. For each category, the average and relative standard deviation (SD) is also included, showing the general spread in the results and indicating for which impact categories the differences between the propellants are the greatest. Out of the 21 impact categories, the LMP-103S system achieves the worst score for 16, usually closely followed by the ASCENT system, whereas the hydrazine system has the worst performance for four impact categories and the 98% HTP system for one, being *Resource use, minerals and metals, reserve base*. Looking into the contributions for the latter result, it is presumed that the extraction of titanium is improperly characterised for this impact category, such that the HTP system's use of an aluminium tank is incorrectly considered as resulting in a larger usage of metals and minerals than the use of a titanium propellant tank.

The single score results clearly indicate that the LMP-103S and ASCENT propulsion systems have a much higher environmental impact than the hydrazine and 98% HTP system designs, as shown in Figure 7.2. Expressing the environmental single scores in a percentage relative to the hydrazine results, the LMP-103S system scores 448%, the ASCENT system 427% and the 98% HTP system only 35%. The calculation of the single score, using the normalised and weighted contributions of the impact categories included in the EF framework, is shown in Appendix D. Inspecting Table D.1, it is clear that the five impact categories contributing the most to the large environmental impact of the EIL systems are, in order: *Ecotoxicity, freshwater*, *Resource use, minerals and metals, ultimate reserve*, *Acidification*, *Eutrophication, freshwater* and *Climate change*. Each of these categories will now be discussed in more detail.

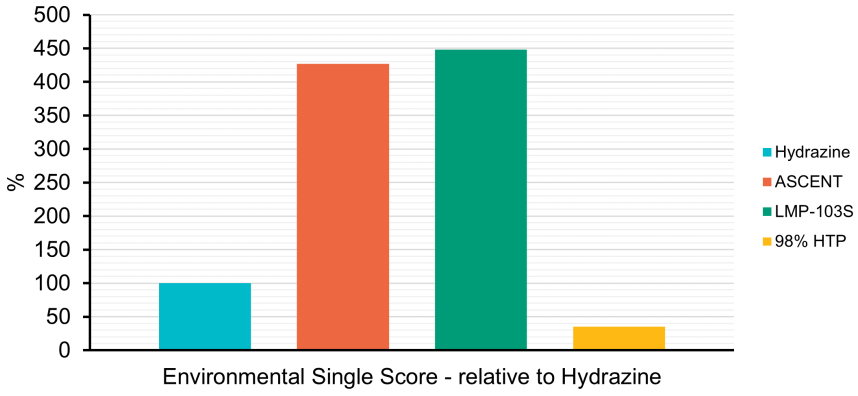

Figure 7.2: Environmental single score results, relative to hydrazine

Table 7.21: Comparative overview of environmental LCIA results for the various propulsion systems.* indicates that the impact category is included in the EF3.0 framework and single score calculation. **Bold** indicates the highest score for the respective category.

Impact category	Unit	Hydrazine	ASCENT	LMP-103S	98% HTP	Average	Relative SD
Acidification*	mol H+ eq	6.13E+01	2.91E+02	**2.98E+02**	2.67E+01	1.69E+02	0.74
Air acidification	kg SO2 eq	5.03E+01	2.23E+02	**2.29E+02**	2.19E+01	1.31E+02	0.73
Climate change*	kg CO2 eq	4.13E+03	4.12E+03	**5.33E+03**	1.87E+03	3.86E+03	0.32
Critical raw materials	kg mass	**3.79E+00**	2.87E+00	3.59E+00	1.38E+00	2.90E+00	0.33
Ecotoxicity, freshwater*	CTUe	2.48E+05	1.45E+06	**1.51E+06**	4.27E+04	8.14E+05	0.83
Ecotoxicity, marine	kg 1,4-dichlorobenzene eq	1.40E+07	2.56E+07	**2.75E+07**	1.21E+07	1.98E+07	0.34
Eutrophication, freshwater*	kg P eq	2.03E+00	4.18E+00	**4.50E+00**	9.80E-01	2.92E+00	0.50
Eutrophication, marine*	kg N eq	1.26E+01	1.39E+01	**1.48E+01**	4.03E+00	1.13E+01	0.38
Eutrophication, terrestrial*	mol N eq	1.59E+02	1.91E+02	**2.04E+02**	4.95E+01	1.51E+02	0.40
Human toxicity, cancer*	CTUh	5.51E-06	5.10E-06	**5.80E-06**	1.67E-06	4.52E-06	0.37
Human toxicity, non-cancer*	CTUh	8.40E-05	1.18E-04	**1.29E-04**	3.83E-05	9.24E-05	0.38
Ionising radiation*	kBq U-235 eq	**5.58E+02**	4.21E+02	5.26E+02	2.29E+02	4.33E+02	0.30
Land use*	Pt	5.64E+03	6.71E+03	**7.56E+03**	9.08E+02	5.21E+03	0.49
Ozone depletion*	kg CFC11 eq	**9.39E-04**	7.31E-04	8.58E-04	6.87E-04	8.04E-04	0.12
Particulate matter*	disease inc.	3.51E-04	6.11E-04	**6.66E-04**	1.24E-04	4.38E-04	0.50
Photochemical ozone formation*	kg NMVOC eq	3.51E+01	5.61E+01	**6.05E+01**	1.14E+01	4.08E+01	0.48
Resource use, fossils*	MJ	5.41E+04	5.62E+04	**8.26E+04**	2.23E+04	5.38E+04	0.40
Resource use, minerals and metals, reserve base	kg Sb eq	5.09E-01	4.66E-01	5.42E-01	**9.01E-01**	6.04E-01	0.29
Resource use, minerals and metals, ultimate reserve*	kg Sb eq	3.90E-02	7.19E-01	**7.23E-01**	3.42E-02	3.79E-01	0.90
Total cumulative energy demand	MJ	6.28E+04	6.35E+04	**9.27E+04**	2.63E+04	6.13E+04	0.38
Water use*	m^3 depriv.	**5.03E+03**	4.11E+03	4.94E+03	4.54E+03	4.66E+03	0.08
Single Score, EF categories*	-	0.97	4.14	**4.35**	0.34	2.45	0.74
Single Score, EF categories*, relative to hydrazine	%	100.00	426.91	**448.22**	35.27	252.60	0.74

#1: Ecotoxicity, freshwater

The greatest contribution to the single score environmental impact, as such indicating that it is the impact category where the propulsion system life cycles have the highest impact on the natural environment when compared to other products, is *Ecotoxicity, freshwater*. This impact category is expressed in terms of Comparative Toxicity Units (CTUe), as defined by the USEtox standard [14]. In the case of the LMP-103S system, it makes up about 57% of the total environmental impact score, after being normalised and weighted with respect to the other environmental impact categories. A comparison of the impact scores is shown in Figure 7.3, showing that the performance of the ASCENT and LMP-103S systems is quite similar and about an order of magnitude worse than the hydrazine score. The large difference between the results of the EIL systems and the other two options is also reflected in the high relative standard deviation of 0.83, shown in Table 7.22. Considering the share that *Ecotoxicity, freshwater* takes up of the environmental single score, the results are somewhat more similar.

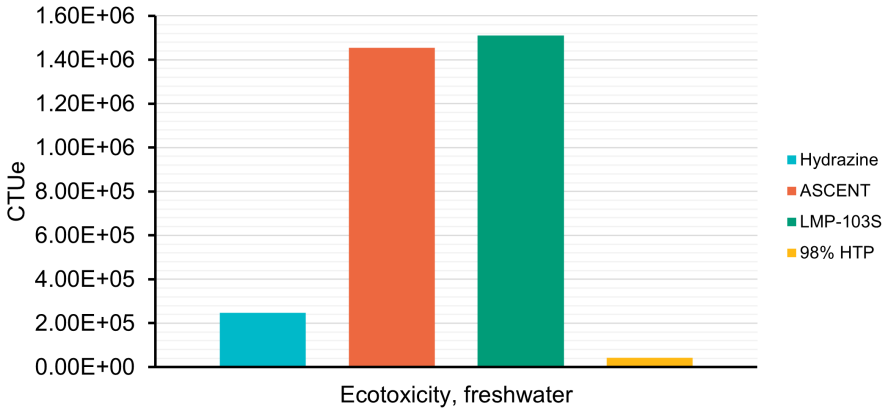

Figure 7.3: Ecotoxicity, freshwater impact results

Looking into the contributions to this impact category provided by the various processes in the PS LCIs in Table 7.22, it is found that the production of iridium, used in the catalyst for the hydrazine, ASCENT and LMP-103S thrusters, as well as in the combustion chamber of the ASCENT and LMP-103S thrusters, and platinum, used in the HTP catalytic bed, make up the largest portion of the impact for most of the PS options. Furthermore, it is found that especially the proxy of platinum mined in South Africa results in a very high impact. This dataset was updated in 2019 in ecoinvent 3.6 [101]. An in-depth LCA of PGM production indicates that this large environmental impact is due to the large amount of electricity required for PGM mining, which is mostly sourced from coal-fired plants in South Africa [209]. For the hydrazine case study, the production of hydrazine results in the largest single contribution to the *Ecotoxicity, freshwater* impact category. The contributions of the titanium and aluminium tank in the case of the hydrazine and 98% HTP system respectively arise from the large amount of material that is turned and milled away during the production of the half-spherical tank domes.

Table 7.22: Comparative overview of *Ecotoxicity, freshwater* impact results. CB=Catalyst bed, CC=Combustion chamber, FCV=Flow control valve.

	Hydrazine	ASCENT	LMP-103S	98% HTP	Average	Rel. SD
Impact score [CTUe]	2.48E+05	1.45E+06	**1.51E+06**	4.27E+04	8.14E+05	0.83
Single score contribution [%]	41.58	57.14	56.52	20.30	43.88	0.34
#1 Contribution	41 %: Hydrazine	83 %: Iridium (CC)	80 %: Iridium (CC)	47 %: Platinum (CB)		
#2 Contribution	31 %: Iridium (CB)	8 %: Rhenium (CC)	8 %: Rhenium (CC)	39 %: Al tank		
#3 Contribution	23 %: Ti tank	5 %: Iridium (CB)	5 %: Iridium (CB)	3 %: FCV		

#2: Resource use, metals and minerals, ultimate reserve

The second most important environmental impact category is that of *Resource use, metals and minerals, ultimate reserve*, where the usage of rhenium in the combustion chamber leads to the relatively high impact scores for the ASCENT and LMP-103S propulsion systems. As presented in Figure 7.4, the impact of the EIL PS options once again exceeds that of the other two options by an order of magnitude. The impact category is characterised in terms of kg Sb eq, as this is the unit preferred in the European EF methodology [111].

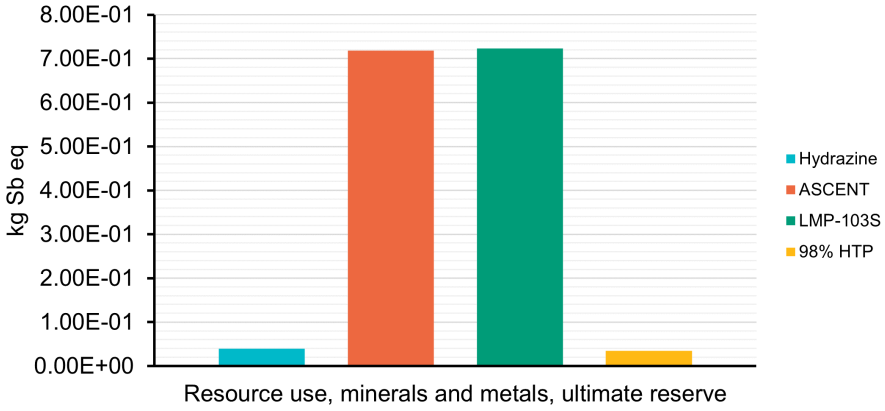

Figure 7.4: Resource use, metals and minerals ultimate reserve impact results

Next to the use of rhenium and iridium, which are both relatively rare metals, the use of silver in the wires and junction box of the catalyst bed heater is also a contributor for each of the PS options as indicated in Table 7.23. The table also shows that the aluminium tank makes up a larger contribution to the HTP system's impact than the titanium tank does for the hydrazine system. This is partly due to the fact that a larger tank, thus more aluminium, is required for the HTP system. However, as indicated before, the fact that titanium production results in a smaller impact for resource use than aluminium production seems to indicate an error in the characterisation of the titanium production dataset included in the SSSD.

Table 7.23: Comparative overview of *Resource use, minerals and metals, ultimate reserve* impact results. CB=Catalyst bed, CC=Combustion chamber.

	Hydrazine	ASCENT	LMP-103S	98% HTP	Average	Rel. SD
Impact score [kg Sb eq]	3.90E-02	7.19E-01	**7.23E-01**	3.42E-02	3.79E-01	0.90
Single score contribution [%]	4.78	20.60	19.75	11.86	14.25	0.45
#1 Contribution	28 %: CB heater	83 %: Rhenium (CC)	82 %: Rhenium (CC)	37 %: Al tank		
#2 Contribution	16 %: Iridium (CB)	14 %: Iridium (CC)	13 %: Iridium (CC)	32 %: CB heater		
#3 Contribution	25 %: Ti tank	2 %: CB heater	2 %: CB heater	23 %: Platinum (CB)		

#3: Acidification

The bar chart representation for the *Acidification* impact category in Figure 7.5 continues the trend of the previous two categories, where ASCENT and LMP-103S score much worse than the other two options due to their use of iridium in the thruster combustion chamber. *Acidification* describes the deposition of acidifying substances in sensitive terrestrial and freshwater ecosystems in terms of mol of hydrogen ions.

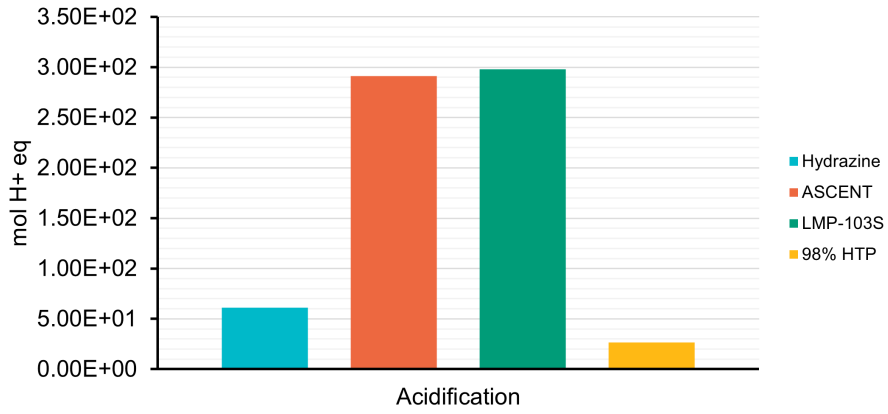

Figure 7.5: Acidification impact results

As for the *Ecotoxicity, freshwater* category, the environmental burden of iridium and platinum production for *Acidification* is explained by its use of electricity sourced from coal in South Africa. This impact category is the first where the environmental impact of clean room fuelling makes a significant contribution to the hydrazine system's score. The main contribution of this process to *Acidification* is the release of ammonia and nitrogen oxides to the air [111]. Once again, the material- and energy-intensive process of tank production also contributes significantly for the hydrazine and HTP systems.

Table 7.24: Comparative overview of *Acidification* impact results. CB=Catalyst bed, CC=Combustion chamber.

	Hydrazine	ASCENT	LMP-103S	98% HTP	Average	Rel. SD
Impact score [mol H+ eq]	6.01E+01	2.91E+02	**2.98E+02**	2.67E+01	1.69E+02	0.74
Single score contribution [%]	7.06	7.86	7.66	8.73	7.83	0.08
#1 Contribution	36 %: Fuelling	87 %: Iridium (CC)	86 %: Iridium (CC)	36 %: Platinum (CB)		
#2 Contribution	27 %: Iridium (CB)	5 %: Iridium (CB)	5 %: Iridium (CB)	32 %: Al tank		
#3 Contribution	26 %: Ti tank	4 %: Ti tank	4 %: Ti tank	23 %: Fuelling		

#4: Eutrophication, freshwater

In the impact category of *Eutrophication, freshwater*, the scores of the EIL propulsion systems lie somewhat closer to that of hydrazine, as shown in Figure 7.6. *Eutrophication, freshwater* expresses the degree to which nutrients are deposited in aquatic ecosystems, in terms of kg of phosphorus (P), which is included as phosphate in many fertilisers. As indicated by the tabulated top 3 of processes contributing to this impact category in Table 7.25, the extraction and processing of iridium and rhenium again explain the poor results of the ASCENT and LMP-103S systems. In the other contributing processes, it is mostly the usage of fossil energy that leads to eutrophication.

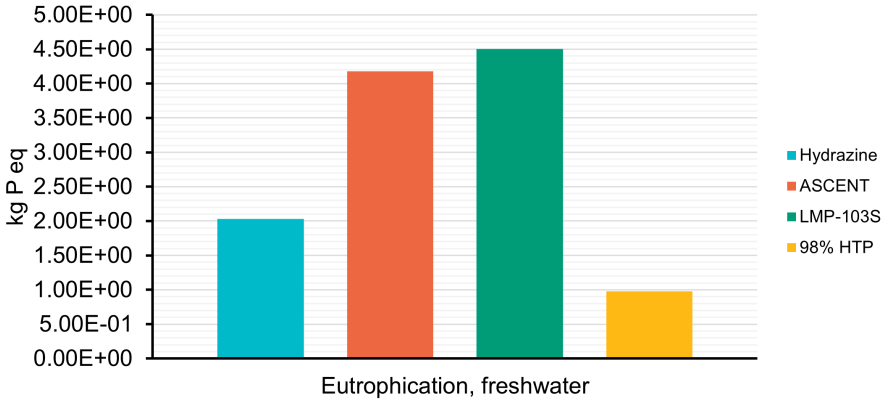

Figure 7.6: Eutrophication impact results

In all the impact categories presented so far, it is remarkable that the impact of ASCENT and LMP-103S is quite similar, with LMP-103S always performing slightly worse. This is explained by the fact that the impact assessment results are dominated by the use of iridium and rhenium in the combustion chambers of the ASCENT and LMP-103S thrusters, with the extraction of iridium or rhenium being the largest two contributors by far in each of the impact categories. As the ASCENT thruster LCI is entirely based on the ECAPS 1 N HPGP thruster, the amount of rhenium and iridium used for the combustion chambers of both EIL propellants is the same. Nonetheless, as a closer inspection of Tables 7.22, 7.23, 7.24 and 7.25 reveals, this impact consistently represents a smaller portion for the LMP-103S system, because of two main reasons. Firstly, due to LMP-103S' lower I_{sp} with respect to ASCENT, the LMP-103S PS requires a larger propellant tank to meet the case study PS requirements, leading to a larger contribution of the titanium tank. Secondly, although this is not shown in the tables so far, the LCIA data reveals that the production process of LMP-103S, and more specifically of ADN, is more environmentally damaging than that of ASCENT. As such, these differences between the ASCENT and

LMP-103S systems mean that using LMP-103S leads to a larger system environmental impact.

Table 7.25: Comparative overview of *Eutrophication, freshwater* impact results. CB=Catalyst bed, CC=Combustion chamber.

	Hydrazine	ASCENT	LMP-103S	98% HTP	Average	Rel. SD
Impact score [kg P eq]	2.03E+00	4.18E+00	**4.50E+00**	9.80E-01	2.92E+00	0.50
Single score contribution [%]	7.99	3.85	3.95	10.93	6.68	0.44
#1 Contribution	66 %: Ti tank	44 %: Iridium (CC)	40 %: Iridium (CC)	56 %: Al tank		
#2 Contribution	13 %: Fuelling	26 %: Rhenium (CC)	25 %: Ti tank	29 %: Platinum (CB)		
#3 Contribution	10 %: Hydrazine	23 %: Ti tank	24 %: Rhenium (CC)	8 %: Fuelling		

#5: Climate change

The fifth most important environmental impact category in this LCSA is *Climate change*, estimating the release of greenhouse gases in $kg\ CO_2$ eq. The scores of the various PS options are closer to each other here, as shown graphically in Figure 7.7, and quantitatively by the relative standard deviation of only 0.32 shown in Table 7.26.

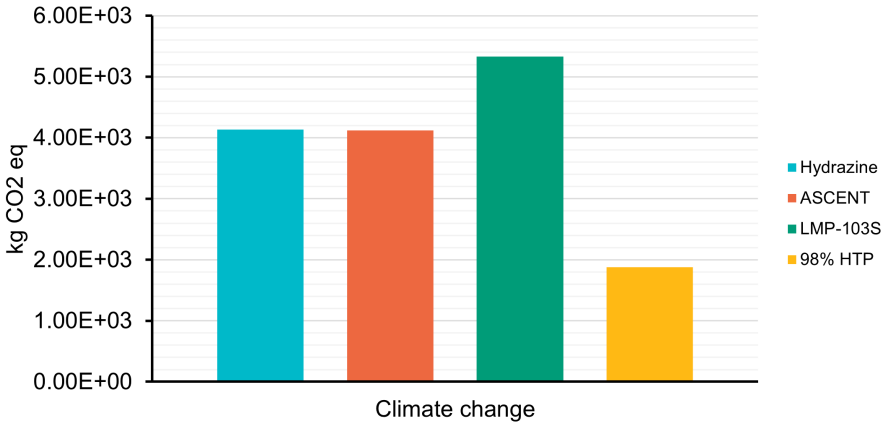

Figure 7.7: Climate change impact results

A main contribution to the *Climate change* impact of each of the systems is electricity consumption in propellant tank production. This impact is partly due to the significant material production of either Ti-6Al-4V or Al5254, removed during tank manufacturing. As an illustration: to produce the 2.48 kg titanium tank in the hydrazine system, about 41 kg of titanium is removed by milling and turning. While the material waste can be reused, the milling and turning processes are also energy-intensive. Next to the production of the propellant tanks, the extraction of iridium once again is one of the top contributors for the ASCENT and LMP-103S systems. In the end, the LMP-103S system scores the worst because of the *Climate change* impact of its propellant production.

Table 7.26: Comparative overview of *Climate change* impact results. CB=Catalyst bed, CC=Combustion chamber.

	Hydrazine	ASCENT	LMP-103S	98% HTP	Average	Rel. SD
Impact score [kg CO2 eq]	4.13E+03	4.12E+03	**5.33E+03**	1.87E+03	3.86E+03	0.32
Single score contribution [%]	10.68	2.49	3.07	13.74	7.50	0.65
#1 Contribution	58 %: Ti tank	42 %: Ti tank	38 %: Ti tank	70 %: Al tank		
#2 Contribution	17 %: Prop. handling	37 %: Iridium (CC)	29 %: Iridium (CC)	10 %: Prop. handling		
#3 Contribution	13 %: Hydrazine	5 %: Prop. handling	19 %: LMP-103S	6 %: Platinum (CB)		

7.5.2. Economic sustainability

Turning to the economic dimension, the dominant impact of hydrazine fuelling becomes quite noticeable, indicating that for the size of PS considered here, the fuelling cost represents a large portion of the total cost. The cost of the novel monopropellant systems including fuelling are all similar, as shown in Figure 7.8 and Table 7.27, primarily due to the assumption that the system assembly and fuelling cost for these propellants are the same. The finding that using hydrazine results in a more costly PS life cycle also seems to align well with literature indicating that using novel monopropellants would results in significant cost savings [9], [197].

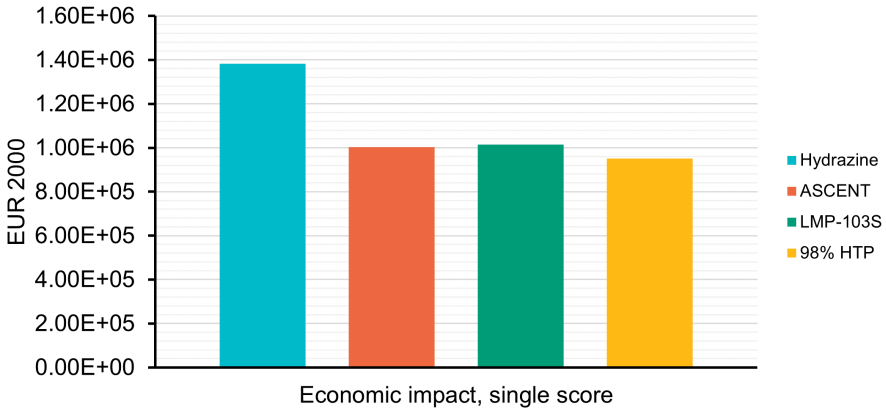

Figure 7.8: Economic impact single score results

Ranking the different processes contributing to the overall cost of each PS life cycle, the same top 3 appears for each of the propellant options, with fuelling contributing much more than the system assembly and thruster production costs. The cost of PS assembly was based on the estimation that 1000 labour hours are involved in this process, irrespective of the propellant type. This constant contribution to each system cost has partly led to a convergence of all the results, indicated by the small relative standard deviation of 0.16. In the fiscal conditions of 2023, it is estimated that the hydrazine PS plus fuelling would cost 2.40 million €, whereas the other propulsion system options would cost less than 1.77 million €. The increased thruster cost for the EIL PS options makes them more expensive than the 98% HTP option, but relative to the estimated novel monopropellant fuelling cost of around 1.1 million €, this difference is rather minor.

Table 7.27: Comparative overview of the *Economic impact, single score* results

	Hydrazine	ASCENT	LMP-103S	98% HTP	Average	Rel. SD
Impact score [EUR 2000]	**1.38E+06**	1.00E+05	1.02E+05	9.51E+05	1.89E+05	0.16
Impact score [EUR 2023]	**2.40E+06**	1.75E+06	1.77E+06	1.65E+06	1.89E+06	0.16
Score relative to hydrazine [%]	100	73	74	69	78.22	0.16
#1 Contribution	76 %: Fuelling	63 %: Fuelling	62 %: Fuelling	66 %: Fuelling		
#2 Contribution	11 %: PS Assembly	15 %: PS Assembly	14 %: PS Assembly	15 %: PS Assembly		
#3 Contribution	8 %: Thrusters	17 %: Thrusters	17 %: Thrusters	12 %: Thrusters		

While it is likely that fuelling cost would account for a large share of the total life cycle cost of a small monopropellant propulsion system, it is also true that this cost has only been estimated very approximately, using secondary data. As such, it is also interesting to make a comparison of the PS options without including this estimated cost of fuelling. In Figure 7.9, the life cycle cost of the different PS options is shown with the (much lower) clean room fuelling cost estimation included in the SSSD dataset [111]. This indicates that the two EIL options are the most expensive, due to the increased thruster cost and, for LMP-103S, the relatively high propellant cost at 1200$ per kg in 2023 currency. This finding is once again not entirely unambiguous, as the estimation of thruster cost has been based on secondary data in a single source. Nevertheless, the finding that the EIL monopropellant systems cost more to produce is also somewhat intuitive, due to the novelty of these systems.

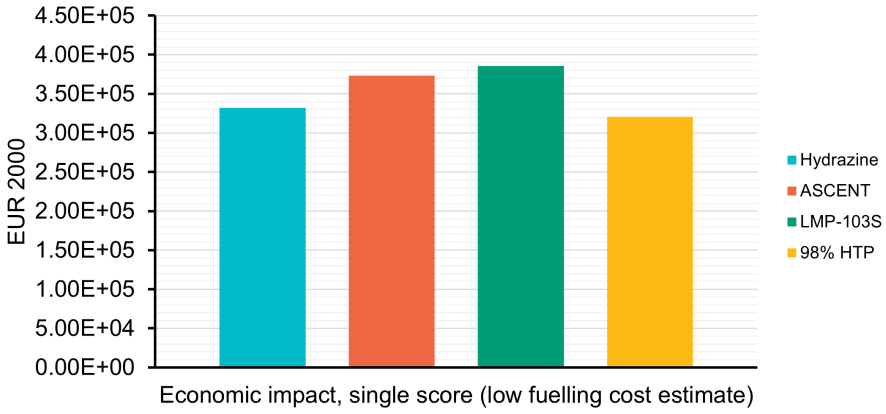

Figure 7.9: Economic impact single score results, without including fuelling cost

7.5.3. Social sustainability

As discussed in Subsection 4.4.2, the social score in the SSSD Sustainability LCIA methodology is based on an assessment of the various impact categories in the Worker and Value Chain Actors stakeholder groups, at the level of the countries where labour is performed during the life cycle phases within the system boundaries of the LCSA. As a first disclaimer, it should be stated that social flows are only included for core processes, such that the social impact of upstream processes, for example related to raw material extraction, are not included in the assessment. The impact of this omission will be further investigated in Section 8.4.

Secondly, due to the relative lack of data regarding the number of labour hours involved in certain processes, much of the social data was approximated using the cost of the respective process. This simplifying assumption reduces the accuracy of the social impact assessment. Still, the specification of where the process takes place, which also influences the social score, was based on the choice of components in Section 6.4 and implemented in the LCIs shown in Section 7.4.

The social single score results are shown in Figure 7.10, expressed relative to the hydrazine system's impact in percentage, as the absolute values in the social score do not have a significant meaning. As the bar chart indicates, the LMP-103S system scores slightly worse than hydrazine, while the 98% HTP once again has the lowest impact.

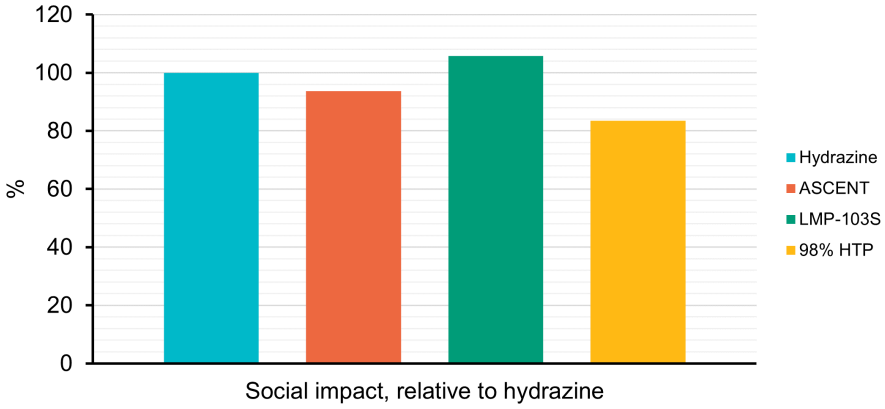

Figure 7.10: Social impact single score results, relative to hydrazine

The uniformly assumed PS assembly time of 1000 labour hours constitutes the largest social impact for each of the propellant options. The fact that the same amount of labour hours is assumed here for each option has the consequence that the results lie very close to each other, with a relative SD of only 0.09 shown in Table 7.28. A more detailed look into the social impact of the various processes indicates that the most expensive components, such as the thruster FCV or combustion chamber, are main contributors to the overall social impact, showing the effect of the assumption linking cost to social score. In that regard, the fact that the ASCENT thruster uses a single seat FCV, which is assumed to be produced twice as fast as a double seat FCV, results in its lower social score compared to LMP-103S. It is also notable that many of the production processes shown in Table 7.28 take place in the US, which has a worse social score per labour hour than the general EU dataset (13.9 for US and 9.8 for EU). As such, it might be possible to reduce the social impact of labour-intensive processes by performing them in Europe.

Clean room fuelling is also included as one of the main contributors to the social impact, and it is important to note that this inclusion is solely due to the number and location of working hours in this process. As such, the potential social harm that exposure to hydrazine may cause to human health or overall working conditions, is not reflected by these results. This is deemed to be a general limitation of the social LCIA method used in this research, and will be further discussed in Section 8.4.

7.5.4. Single score sustainability

Combining the three sustainability dimensions in a single score is done by normalising each of the impact scores, using the normalisation factors shown in Table 4.1, and then weighting each of the sustainability dimensions according to the number of UN SDGs that are related to each of them [14]. This leads to the weighting as shown in Equation 4.1, where the environmental, economic and social scores respectively account for 18%, 29% and 53% of the total sustainability score. Before applying this weighting, it is important to note that the social score is first multiplied by 3, as the current version of the SSSD only contains social flows for two out of a total of six stakeholder categories [14]. Because the method of the SSSD combining the various sustainability concerns is quite subjective to the selected weighting and normalisation factors, only a minor importance is given to the sustainability single score

Table 7.28: Comparative overview of *Social impact, single score* results. CC=Combustion chamber, FCV=Flow control valve.

	Hydrazine	**ASCENT**	**LMP-103S**	**98% HTP**	**Average**	**Rel. SD**
Impact score [-]	3.73E+04	3.49E+04	**3.94E+04**	3.11E+04	3.57E+04	0.09
Score relative to hydrazine [%]	100	94	**106**	83	95.71	0.09
#1 Contribution	29 %: PS Assembly	30 %: PS Assembly	27 %: PS Assembly	34 %: PS Assembly		
#2 Contribution	22 %: Fuelling	29 %: Re/Ir CC	26 %: Re/Ir CC	18 %: FCV		
#3 Contribution	15 %: FCV	13 %: Fuelling	14 %: FCV	15 %: Inconel CC		

results, while it does provide a way of answering the question as to which monopropellant system is ”the most sustainable overall”.

The overall sustainability single scores are shown in Table 7.29. The contributions from the environmental, economic and social impacts in the table are already normalised and weighted, showing the dominance of the economic dimension. With the overall sustainability being almost entirely defined by the economic sustainability, the hydrazine option is identified as the least sustainable option, due to its high fuelling cost. The fact that the economic dimension dominates the overall sustainability is interesting for a few reasons. Firstly, it seems to indicate that the largest sustainability issues of the various monopropellant system life cycles are not related to their social or environmental impact, but to the use of funds that could alternatively be used for other purposes. Secondly, this normalisation and weighting method has resulted in the economic dimension being deemed more important than the environmental and social, which is consistent with the economic motivation present in novel monopropellant research to avoid hydrazine fuelling costs.

The large dependence of the total sustainability results on the economic impact also has the effect of reducing the relative difference between the sustainability of each of the monopropellant options, as indicated by the low relative standard deviation of 0.16 in Table 7.29. In a scenario where the environmental impact would result in the dominant contribution to overall sustainability, this difference would be much larger, with the ASCENT and LMP-103S systems scoring much worse than the other two. This also shows why it may be misleading to use the single score sustainability as a metric to compare the ”overall” sustainability of the various propulsion systems. While it does allow for a more straightforward comparison between the different options and a potential inclusion in quantitative trade-off procedures, a single sustainability score may obscure important differences between the options, and result in misleading conclusions. As an alternative, one may consider which option scores the worst in each of the sustainability dimensions, as indicated in bold in Table 7.29. With this approach, it is clear that the LMP-103S system is the least sustainable ”overall”, as it has the largest environmental and social impact, and the second largest economic impact.

Table 7.29: Comparative overview of *Sustainability impact, single score* results. Reported environmental, economic and social impact scores are normalised and weighted.

	Hydrazine	ASCENT	LMP-103S	98% HTP	Average	Rel. SD
Environmental impact score	0.17	0.75	**0.78**	0.06	0.44	0.74
Economic impact score	**55883.97**	40568.89	41072.29	38445.78	43992.73	0.16
Social impact score	1.80	1.69	**1.90**	1.50	1.72	0.09
Sustainability impact score [-]	**55885.94**	40571.32	41074.98	38447.34	43994.90	0.16
Relative to hydrazine [%]	100	72.60	73.50	68.80	78.72	0.16

7.6. Conclusion

This chapter has discussed the execution and results of the LCSA comparing the life cycle sustainability of the various propulsion systems, designed in Section 6.4. In accordance with the standard LCSA procedure, the goal and scope of the LCSA was first clearly defined, using the guidelines of the ESA LCA handbook [15]. Herein, it was specified that the LCSA would consider the production and testing of each separate component in the PS designs making up more than 5% of the dry mass, including upstream processes, the assembly and testing of the propulsion systems, the transport of the systems to the launch site, assumed to be Kourou in French Guyana, and their fuelling before launch.

To accurately model the production of these components, new processes were added to the SSSD using the LCA software openLCA, the life cycle inventories of which were based on publicly available data. In total, two new upstream processes were created, modelling the extraction of iridium and rhenium, and 24 new core processes were created, modelling the production of various components, the assembly and fuelling of the various propulsion systems and the production of 98% concentrated HTP. For life cycle inventories deemed to have a large influence on the final results, further validation will be performed in Section 8.2 where sufficient data is available to do this.

With an accurate representation of the life cycle inventory for each of the propulsion systems, a life cycle impact assessment was carried out using the SSSD Sustainability LCIA method, which includes 21 environmental impact categories and single score assessments for the economic and social dimensions. In the environmental realm, the ASCENT and LMP-103S systems have a much greater impact than the hydrazine and 98% HTP options. This was found to be due to their use of iridium and rhenium in the thruster combustion chamber, with both refractory metals having a very environmentally straining production process. Normalising the environmental impact categories, the *Ecotoxicity, freshwater* category was deemed to be the most relevant for this case study. Across the different impact categories, the LMP-103S system has the largest environmental impact, performing worse than ASCENT due to its larger propellant tank size and more polluting propellant production process. The 98% HTP system leads to the lowest environmental impact, with an overall environmental score around a third as large as that of the hydrazine propulsion system.

In the assessment of the economic life cycle impact of each of the systems, the estimated cost of fuelling dominates the score for each of the propellant options. This is probably realistic, as the reduced cost of fuelling novel monopropellants has been discussed as having the most potential for small satellite propulsion systems [7]. It is therefore somewhat problematic that the fuelling cost of the hydrazine and novel monopropellant systems could only be approximated using secondary data sources. Acknowledging the lack of accuracy in this part of the results, an overview has also been presented of the economic impact of each PS without considering the fuelling cost. This comparison reveals that the EIL options once again perform the worst, due to their increased thruster cost, with the LMP-103S system resulting in the highest cost, due to the relatively high cost of the LMP-103S propellant.

The LMP-103S system also has the highest social score, followed by the hydrazine system. As the social LCIA methodology uses the number and location of labour hours included in each process, this reflects the estimation that the LMP-103S system has the most labour-intensive life cycle, due to the exotic manufacturing process for its rhenium/iridium combustion chamber and its use of double seat FCVs, whereas the ASCENT thrusters also feature the rhenium/iridium combustion chamber but only include single seat FCVs. For the hydrazine system, the lengthy fuelling procedure is a main contributor to the social impact. The PS assembly procedure is the number 1 contributor for the social impact of each propellant option, and the required labour hours in this process are estimated with relatively high accuracy.

In comparing the overall sustainability of the four monopropellant systems, one may calculate a total sustainability score, which normalises and weights the single impact scores for each of the sustainability dimensions. In doing this, it is found that the economic impact of the systems outweighs the environmental and social impact by four orders of magnitude, leading to the finding that the hydrazine system is the least sustainable. However, this approach is deemed to only be of minor use, as the assignment of normalisation and weighting factors to compare environmental, economic and social sustainability is rather subjective. Instead, it is considered more relevant to consider the ranking of each of the PS options in each of the sustainability dimensions, to produce a more detailed representation of the overall sustainability profile of each option. Using this method, it is concluded that the LMP-103S system is the least sustainable option, as it has the highest environmental and social impact, and the second highest economic impact. A further validation and evaluation of the LCSA results is presented in Chapter 8.

8

Evaluation and Interpretation of Results

8.1. Introduction

In the previous chapter, the results from the LCSA of the four monopropellant systems have been presented and discussed, indicating that the EIL propulsion systems using ASCENT and LMP-103S score the worst environmentally, whereas the hydrazine system has the largest life cycle economic impact and the LMP-103S system is the least socially sustainable option. These outcomes were respectively attributed to the use of rhenium and iridium in the EIL thruster, the high cost of fuelling hydrazine and the labour-intensive and American production of complex components of the LMP-103S thruster. While this interpretation of the results has been justified somewhat within Section 7.5, this chapter will delve deeper into this reasoning and validate whether these proposed explanations are accurate.

First, Section 8.2 will consider key results from the LCI analysis and LCIA and validate these with literature. This section will focus on the processes that have been identified in Section 7.5 as being main contributors to the various impact categories. As such, it is acknowledged that this does not constitute a full validation of the LCSA, which would include a validation of each LCI dataset, but this is considered outside the scope of the current research.

While also being discussed as part of Section 8.2, Section 8.3 will concentrate on the data quality of the newly added processes. In this discussion the data quality pedigree matrix, introduced in Subsection 4.4.2, of each process is considered, to estimate which areas of the LCSA hold the most and least uncertainty. After this, Section 8.4 will evaluate the used research methodology more broadly, to consider what can and cannot be inferred from its results. This will include a discussion on the pre-existing LCIA methodology that was used, and consider how this might be adjusted to facilitate a more thorough assessment of the sustainability of propulsion systems in particular.

Finally, Section 8.5 will further build onto the results of the LCSA to provide specific design recommendations which would improve the sustainability of each of the systems. This will be done based on the identification of environmental, economic and social hotspots within the LCSA results of each monopropellant system.

8.2. Validation of LCSA results

As this research has been set up to specifically fill the gap that exists regarding the life cycle sustainability of monopropellant systems using either hydrazine or novel monopropellants, it is generally difficult to validate the overall results or findings with results from other LCA or LCSA studies. In a previous application of the SSSD LCSA methodology, Wilson et al. have found that producing hydrazine propellant

has a lower environmental impact than the production of LMP-103S, while the increased performance of LMP-103S does lead to mass savings, in turn resulting in a lower environmental impact when the entire spacecraft is considered [14]. However, as the datasets leading to this conclusion are already included in the SSSD, while not containing the level of detail added in this research, for example differentiating the thruster materials for hydrazine and LMP-103S, it is somewhat redundant to perform validation using this data. What this does indicate however, is that the scope of this research being limited to the propulsion system most likely has a significant impact on the overall conclusions that are drawn. This will be further discussed in Section 8.4.

In this section, a brief validation will first be performed of the LCI definition of some important components and processes, keeping in mind the impact on the final LCSA results in Subsection 8.2.1. This is mainly done by critically evaluating the setup of the life cycles and comparing this with literature, due to the lack of comparable datasets. Due to a greater data availability, the validation of the LCIA process will be somewhat more extensive, mostly looking into the validity of the estimated environmental impact of key processes in Subsection 8.2.2.

8.2.1. Validation of LCI definitions

As a first note on the validity of the used datasets in the LCSA, it is worth indicating that most of the secondary data used in defining the new core processes is sourced from either ecoinvent or the SSSD, the former being frequently updated and validated with reliable international data, and the latter having been formally validated with the ESA LCA database in 2018 and since then being updated in line with new findings in the further development of the ESA LCA database [101], [110]. Almost all of the upstream processes in this LCSA are therefore deemed to be previously validated, which already adds a degree of reliability to the results. For the two new upstream processes modelling the production of iridium and rhenium, validation of their environmental impact will be performed in the following section.

For almost all of the newly added core processes, no comparable datasets can be found in the SSSD, ESA LCA database or ecoinvent, making it infeasible to perform a detailed validation of each process' LCI. This is only deemed possible for the newly created process of 98% HTP production, for which a process also exists in the ESA LCA database. Validating the LCI of other processes with literature outside of LCA databases is also somewhat complicated, as much of what could be found in public sources has been used to inform the construction of the LCIs. Nonetheless, the implementation of certain assumptions in the LCI definitions is not entirely unambiguous and can be interrogated through further literature research. Additionally, the definition of system boundaries for each of the core processes could not be performed entirely consistently, making it another subject for validation.

LCI of valves

In the LCI definition of each of the valves included in the propulsion systems, substantial assumptions had to be made regarding the production process of these complex components. Firstly, due to a lack of data, the Moog 1/4 inch single line stainless steel torque motor valve [183], which had been selected in Section 6.4 as the isolation valve in the PS architecture inspired by the component selection of the PRISMA HPGP PS [62], was modelled as a single seat solenoid latch valve [200]. This should not be considered as a very accurate proxy, given the fact that torque motor valves operate with working principles that are somewhat different from solenoid valves, likely resulting in different materials or proportions of materials being used in the two valve types [210].

Additionally, the LCI of both the fill/drain valve and solenoid double seat flow control valve were based on cutaway technical drawings showing the approximate dimensions of internal components, as shown in Appendix C. While this is deemed to give a relatively accurate estimate of the required volume and mass of specific materials (e.g. copper used in the solenoid coil, rubber used in the valve seat), these drawings and the documents from which they are adapted do not provide an adequate description of how the internal components are fabricated. Instead, the valve LCIs only consider a generic metalworking procedure for the external housing, with steel being forged, extruded and machined. As indicated by prior LCAs of complex space-specific components, the simplification of the LCI can have a large and unpredictable impact on the final results, with some impact categories improving and other deteriorating

with an increase in LCI accuracy [211].

Comparing the top-level parameters of the selected Moog fill/drain valve with other possible options, produced by Nammo or ArianeGroup, it is found that the Moog model is around four times heavier (200 g compared to around 50 g) [167], [187], [212]. The exact reason for this difference has not yet been identified, but as the overall LCIA impact of the fill/drain valve is minor, this is acceptable. For the selected Moog flow control valve used in each of the thrusters, a comparable model produced by Nammo does have a similar total mass of 200 g, and similar outer dimensions are also found for the Nammo and Valvetech FCVs [200], [202], [213].

LCI of propellant tanks

To validate the LCI of the titanium and aluminium diaphragm tanks included in the different PS options, reference is made to the ESA LCA DB entry for *Spherical tank, TiAl6V4, average*, on which the definition of the tank LCIs in the SSSD are based. This dataset was set up and validated under an ESA contract, and concerns a PMD tank, as such only containing metallic components and not an elastomeric diaphragm [15], [98]. In the LCI definition for the diaphragm tanks in this study, the general production chronology was adapted from the ESA LCA dataset, consisting of material production, forging of large alloyed blocks, roughly machining these forgings to create two semi-spherical domes, strengthening these parts through solution heat treatment and quenching, and then further machining the domes to their final shape. A deviation from the ESA LCA dataset is obviously made with regards to the inclusion of a metallic PMD, and based on the tank sizing in Section 6.4, an estimation is made of the proportion of shell mass to diaphragm mass for a 1 kg tank, considering the titanium and aluminium model separately. The elastomeric diaphragm is then considered to be clamped between the two semi-spherical shell halves that are welded together by tungsten inert gas (TIG) welding. The validated ESA LCA dataset is again adhered to for the acceptance testing procedure, where use can be made of pre-existing testing processes in the SSSD.

Although the propellant tank LCI in the ESA LCA DB models a PMD tank while the new LCI datasets model diaphragm tanks, it is still useful to make a direct comparison between the two, to consider whether the observed differences reflect the physical differences between the tank types. This comparison is shown in Table 8.1, where it is immediately clear that the general process definition has been based on the existing ESA LCA dataset. The most obvious difference is firstly that the diaphragm tank LCI contains a few additional processes, including the production of the elastomeric diaphragm, and transport and social flows. There is also a difference in the amount of titanium produced with the *Titanium, TiAl6V4* flow, due to a difference in process definition for the milling and turning processes, where the SSSD versions include the production of the titanium that is removed.

There are also noticeable discrepancies related to the tank dimensions, where the ESA LCA DB tank predicts a shorter welded seam and smaller outer surface area, but a larger internal volume. This is deemed to be an inconsistency in the ESA LCA dataset, due to the fact that the dataset for the 1 kg propellant tank has been constructed based on a uniform downscaling of the 1 m^3 tank dataset for which primary data was obtained [15]. This adaptation did not take into account the fact that tank parameters such as the internal volume or total surface area do not scale linearly with tank mass. In any case, it is somewhat intuitive that the diaphragm tank would feature a larger internal volume for the same mass, given the fact that the absence of a titanium PMD allows for more mass to be allocated to a larger tank shell. In the newly created process, it was also chosen to replace the *Degreasing, metal part in alkaline bath* process with an anodising process deemed to more relevant for the surface treatment procedure of the diaphragm tank. Both the inner and outer surface area of the shell are assumed to be anodised.

Overall, the validation of the propellant tank LCI is not conclusive, as it is unclear whether the observed differences are due to deliberate modelling assumptions or due to the limitations of scaling up or down processes to result in output flows in different units. The majority of the life cycle steps included in the new dataset have been sourced directly from the SSSD, which has incorporated the custom ESA LCA datasets that were created to model the PMD propellant tank considered in this comparison. The possible errors included in the new LCI are not deemed to be very dramatic however, as the quantity of most included flows is estimated at a similar order of magnitude as the ESA LCA dataset.

Table 8.1: Validation of titanium propellant tank life cycle inventory with respect to ESA LCA dataset [15]

ESA LCA DB: Spherical Tank, TiAl6V4, average (1 kg) [15]		**New: Diaphragm propellant tank-spherical-Ti6Al4V (1 kg)**		
Flow	Amount	Flow	Amount	Unit
Automated Eddy Current inspection	0.0170	same	0.855	m
Degreasing, metal part in alkaline bath	0.187	anodising, aluminium sheet	0.464	m^2
Dye penetrant inspection	0.0934	same	0.232	m^2
Expulsion Efficiency inspection	0.0193	same	0.0105	m^3
External Leak inspection	0.0193	same	0.0105	m^3
Heat Treatment, Solution Treatment and Aging, Titanium alloys	15.962	same	17.5	kg
Heat Treatment, Stress Relieving, Titanium alloys	0.788	same	0.875	kg
Negative Pressure inspection	0.0193	same	0.0105	m^3
Pressure Cycle inspection	0.0193	same	0.0105	m^3
Proof Pressure inspection	0.0193	same	0.0105	m^3
TIG welding, TiAl6V4	0.0170	same	0.855	m
Titanium Alloys removed by milling, CNC	8.977	same	6.65	kg
Titanium Alloys removed by turning, CNC	5.985	same	9.975	kg
Titanium, TiAl6V4	15.962	same	0.875	kg
Total Design Loads inspection	0.0193	same	0.0105	m^3
Ultrasonic inspection	0.0193	same	0.0105	m^3
Vibration test	0.0193	same	0.0105	m^3
Volumetric Capacity examination	0.0193	same	0.0105	m^3
X-ray/radiographic inspection	0.0934	same	0.232	m^2
		Additional flows		
		EPDM Product	0.125	kg
		Org. Time Contribution (Nat) - US	132	work-hours
		transport, freight, lorry	0.75	$t * km$

LCI of thrusters

Similar to the LCI definition of the valves in the propulsion system, the production and assembly of thruster components was also based mostly on secondary data. There is also a dataset in the SSSD modelling the production of a 1 N hydrazine monopropellant thruster, but as the LCI definition contained a limited level of detail, roughly considering a 1 kg thruster to be made up of 0.98 kg of aluminium and 0.02 kg of polyurethane foam, it is considered to be of little use for the present research.

There are several parts of the thruster life cycles where the accuracy of the current LCI are limited. Firstly, in the modelling of the catalyst bed production, the main focus was on the extraction and production of the catalyst materials, whereas other crucial production steps, for example related to the creation of alumina pellets, or the impregnation of these pellets with a catalytic top layer, were neglected, due to the limited description of the exact steps in catalyst production reported in open literature. Furthermore, as the use of granulated alumina/iridium catalyst is rather specific to its use in monopropellant thrusters, no LCI data could be found to validate the created dataset. The LCI of the catalyst bed heater may be considered to be more accurate, as it was constructed based on correspondence with an engineer at Thermocoax. Still, there is a very large simplification in the usage of the SSSD *Thermostat* dataset to model the production of the catalyst bed heater's junction box. While it is probable that similar materials and electronics are included in both components, limited information could be obtained related to the internal configuration of the junction box.

The production of the thruster combustion chambers was based on the available data for flight-proven 1 N monopropellant thrusters, using technical drawings or renderings of the Aerojet Rocketdyne MR-103J, ArianeGroup 1 N thruster and ECAPS 1 N HPGP thruster [125], [202], [206], which are included in Appendix B. This modelling is therefore mostly based on outer dimensions, with the exact configuration or materials of internal combustion chamber components not being known. Furthermore, while the SSSD dataset of the 1 N thruster seems to assume combustion chamber and nozzle are formed through casting, the new datasets have considered the production to be composed of forging and milling. In the case of the rhenium/iridium combustion chamber, the patented electroforming process used to deposit the layers of iridium and rhenium on a mandrel with a very precise thickness was proxied using an electroplating process with chromium steel in ecoinvent. While both processes use the same electrochemical principles, the production of a mandrel on which the material deposition occurs is not included in the ecoivent process. Furthermore, the processes use different solutions for the plating process and the effect of this modelling difference has not yet been assessed. Additionally, no additional processes have been included to transform the iridium and rhenium source material into conditions suitable for the electroforming process.

LCI of 98% HTP production

The last LCI that will be considered for validation is that of 98% HTP production, which also represents the only dataset for which a completely equivalent dataset in the ESA LCA database exists. As mentioned in Subsection 7.4.3, the SSSD datasets for hydrazine, ASCENT and LMP-103S production were updated with the data in the ESA LCA database, while an entirely new process was created for 98% HTP production, based on hydrogen peroxide distillation data from the Solvay Voikaa plant [208]. The assumptions made in that process will be validated now.

Table 8.2 compares the new and existing datasets for the production of 98% HTP. There are a few differences in the dataset due to a difference in system boundaries: firstly, the ESA LCA dataset includes a portion of the impact for the infrastructure of the HTP distillation plant, while this is not included in the new process. Secondly, the new process includes the social flow of organisational time contribution. Evaluating the quantification of the environmental flows, it is positive that the new LCI definition includes almost all of the same flows as the ESA LCA dataset. In the new dataset, the energy use is split up in a portion provided by medium voltage electricity, and a portion of heat provided by steam. Taken together, this amount of energy exceeds the 1.3 kWh provided by low voltage energy in the ESA LCA dataset, which may be due to the differences between continuous and batch distillation processes of hydrogen peroxide. Additionally, the ESA LCA dataset includes the amount of water included in the initial 50% HTP solution as an input flow, whereas the new process considers this water to be fully resused in the continuous distillation.

In the new dataset, it is also assumed that cooling water is provided directly from a natural source, as is the case in the Solvay Voikaa plant [208]. A separate flow is also added to account for the production of steam that rises up through the distillation column to remove water molecules from the HTP solution and create a vacuum in the process. Overall, the LCI of the new dataset and the ESA LCA dataset are quite similar, also with regards to the quantification of flows, indicating that the assumptions used in the new process definition are sufficiently accurate.

Table 8.2: Validation of 98% HTP production life cycle inventory with respect to ESA LCA dataset [15]

ESA LCA DB: Hydrogen peroxide (HTP), type 98 (1 kg) [15]		**New: Hydrogen Peroxide - 98% concentrated (1 kg)**		
Flow	Amount	Flow	Amount	Unit
Chemical factory, organics	4.00E-10	not included	0	Item(s)
Electricity, low voltage	1.293	electricity, medium voltage	0.0173	kWh
Hydrogen peroxide, without water, in 50% solution state	1.09	same	1.09	kg
Tap water	96.1	Water, cooling, unspecified natural origin	90.186	kg
Water, deionised	1.09	same	0.5684	kg
		Additional flows		
		heat, from steam	3.142	kWh
		steam	3.625	kg
		Org.Time Contribution (Nat) - EU	0.36	work-hours

8.2.2. Validation of LCIA results

Next to critically evaluating the definition of various LCIs in the performed LCSA, it is also necessary to consider whether the resulting impacts of these process definitions are realistic. To that end, LCIA results related to functional units of single processes included in the LCSA will be validated now. This is arguably less difficult than the validation of LCIs, as the environmental impacts of a process are discussed more often within public literature than the exact composition of a process' life cycle. As the social and economic impact assessments of processes are very direct transformations of the social and economic LCIs, validating their accuracy is again more difficult. As in the validation of LCI definitions, only a selection of important LCIA results will be considered here, meaning that the validation should not be considered as a full or formal validation.

LCIA of iridium production

The first process considered for LCIA validation may also be the most important, as the extraction and refining of iridium has been identified as an environmental hotspot in Subsection 7.5.1, where this process almost entirely dominates the worse environmental performance of the ASCENT and LMP-103S systems with respect to the hydrazine and 98% HTP propulsion systems. Its LCI was defined based on a reallocation of the platinum extraction and refining processes in South Africa and Russia, using the approach proposed by Nuss and Eckelman [191]. There is one major difference between the iridium production process modelled here and that of Nuss and Eckelman: in this research, a dataset from ecoinvent 3.8 is used for platinum production in South Africa, and an ecoinvent 3.3 dataset for platinum production in Russia, whereas Nuss and Eckelman base their LCI definition entirely on ecoinvent 2.2 data. While the ecoinvent 3.8 and 3.3 documentation indicate that the platinum datasets are entirely equivalent to the datasets included in ecoinvent 2.2, this difference in proxy data leads to discrepancies in the LCIA results, as shown in Table 8.3.

Table 8.3 shows the LCIA results for the five environmental impact categories that were assessed in Nuss and Eckelman's paper using the assessment methods reported. In brackets, the percentual difference between the reference and new process data are shown. It is immediately apparent that the new process using ecoinvent (ei) 3.3 and 3.8 data leads to a substantial increase in the estimated environmental impact of iridium production. As an additional verification to check that the reallocation method of Nuss and Eckelman has been implemented properly in openLCA, Table 8.3 also reports values for a new iridium production process that was set up in openLCA using ecoinvent 2.2 data. The

differences between the LCIA results of this process and that reported by Nuss and Eckelman are minor and as such may be attributed to the fact that the specified impact assessment methods may not be entirely equivalent to those included in openLCA.

As indicated already in Section 7.5, it is primarily the portion of South African platinum production in the iridium LCI that leads to the high LCIA scores, which is the input flow using the most recent data, having been updated in ecoinvent 3.6, released in 2019 [101]. A dedicated LCA study on the production and usage of the platinum group metals platinum, palladium and rhodium indicates the the main environmental impact in their life cycle is due to power consumption during mining, with South Africa's electricity mainly being sourced from coal-fired plants. It is therefore presumable that the increased environmental impact of this extraction process in ecoinvent 3.6 reflects the reality of more challenging extraction conditions, a better characterisation of South Africa's electricity mix and a more accurate modelling of the environmental impact of coal-based electricity generation. Comparing the *Ecotoxicity, freshwater* impact of the South African platinum production processes included in the ecoinvent 3.3 and ecoinvent 3.6 processes, it is found that the latter leads to an order of magnitude increase in the impact (7.74E4 versus 7.10E3 CTUe), which also has a large consequence for the overall LCSA results, where it has been indicated that this impact category is the most important contributor to the environmental single score impact.

Table 8.3: Validation of environmental impact assessment results for iridium production (FU=1 kg) with respect to data from Nuss and Eckelman [191]

Impact category	Assessment method	Unit	Reference data (ei 2.2 data) [191]	New process (ei 3.3/3.8 data)	New process (ei 2.2 data)
Acidification, terrestrial	ReCiPe H Midpoint v1.08	kg SO2 eq	3.10E+03	3.95E+03 (+27 %)	3.48E+03 (+12 %)
Cumulative energy demand	CED v1.08	MJ eq	1.69E+05	5.11E+05 (+203 %)	1.71E+05 (+1 %)
Eutrophication, freshwater	ReCiPe H Midpoint v1.08	kg P eq	2.80E+01	3.79E+01 (+35 %)	2.88E+01 (+3 %)
Global warming potential	IPCC 2007 (100a)	kg CO2 eq	8.86E+03	3.12E+04 (+253 %)	8.98E+03 (+1 %)
Human toxicity	USETox v1.02	CTUh	5.00E-02	1.78E-01 (+256 %)	4.26E-02 (-15 %)

As will be shown in the subsection below, a similar observation can be made for the LCIA of the new rhenium production dataset, with it exceeding the impact scores as presented by Nuss and Eckelman [191]. To evaluate the consequence of potentially overestimating the environmental harm related to iridium and rhenium production with the ecoinvent 3.3/3.8 data, the entire PS LCSA can be performed once again, replacing the iridium and rhenium datasets with those based on proxy data from ecoinvent 2.2. The main results are shown in Table 8.4, with the environmental single score presented in reference to hydrazine, and the top 5 contributing impact categories from Subsection 7.5.1 also included in the table. Comparing these results with the original LCIA results discussed in Subsection 7.5.1, it is firstly important to note that the relative ranking of impact categories remains largely the same, albeit that the *Resource use, metals and minerals, reserve base* impact category becomes the highest contributor to the environmental single score by a small margin over *Ecotoxicity, freshwater*. The overall ranking of the PS options in terms of environmental impact also remains the same, with ASCENT and LMP-103S scoring decidedly higher than hydrazine, with 98% HTP's score being much lower.

Looking into the processes contributing the most to the ASCENT and LMP-103S systems' environmental impact, it is found that the use of iridium and rhenium in the combustion chamber are still the main contributors, as was found in Subsection 7.5.1. As the main research question of this thesis is to determine how a monopropellant system's life cycle sustainability depends on the choice of propellant, it is deemed that both the results using ecoinvent 2.2 and ecoinvent 3.3/3.8 to model iridium and rhenium production indicate the same trend: that the use of EIL propellants leads to the necessity of using re-

fractory metals and as such a much higher environmental impact during raw material extraction. While it is recommended that the environmental impact of iridium production is further evaluated with recent primary data, the LCIA results presented before are considered valid.

Table 8.4: Comparative overview of environmental single score and top 5 contributing impact categories results, using ecoinvent 2.2 data in iridium and rhenium life cycle inventories. **Bold** indicates the highest score for each impact category.

Impact category	Unit	Hydrazine	ASCENT	LMP-103S	98% HTP
Single score, environmental	%	100.00	207.41	**232.17**	38.55
Ecotoxicity, freshwater	CTUe	1.76E+05	2.41E+05	**2.95E+05**	4.27E+04
Resource use, metals and minerals, ultimate reserve	kg Sb eq	3.73E-02	4.06E-01	**4.10E-01**	3.42E-02
Acidification	mol H+ eq	5.92E+01	2.56E+02	**2.62E+02**	2.67E+01
Eutrophication, freshwater	kg P eq	2.00E+00	6.55E+00	**6.87E+00**	9.80E-01
Climate change	kg CO2 eq	4.06E+03	2.91E+03	**4.12E+03**	1.87E+03

LCIA of rhenium production

Similar to the life cycle inventory of iridium production, the environmental characterisation of rhenium production was fully based on a reallocation of the impact of an existing ecoinvent dataset, following the findings of Nuss and Eckelman [191]. In the case of rhenium, the molybdenum production dataset was used, as rhenium is primarily produced as a coproduct of this process. A comparison between the LCIA results of the reference article and the new process with ecoinvent 3.8 data or ecoinvent 2.2 data is shown in Table 8.5. For the process implemented in openLCA with both the more recent and older ecoinvent data, the LCIA results diverge from the reference results. Looking into the ecoinvent documentation, it is notable to add that the molybdenum production LCI has not been updated since ecoinvent version 2, with subsequent ecoinvent versions only including more accurate and recent estimates related to the electricity mix or other background data [101].

Table 8.5: Validation of environmental impact assessment results for rhenium production (FU=1 kg) with respect to data from Nuss and Eckelman [191]

Impact category	Assessment method	Unit	Reference data (ei 2.2 data)	New process (ei 3.8 data)	New process (ei 2.2 data)
Acidification, terrestrial	ReCiPe H Midpoint v1.08	kg SO2 eq	1.10E+01	1.10E+01 (+101 %)	2.21E+01 (+ 45%)
Cumulative energy demand	CED v1.08	MJ eq	9.04E+03	2.11E+04 (+134 %)	1.38E+04 (+53 %)
Eutrophication, freshwater	ReCiPe H Midpoint v1.08	kg P eq	3.50E+01	1.27E+01 (-64 %)	4.57E+01 (+31 %)
Global warming potential	IPCC 2007 (100a)	kg CO2 eq	4.50E+02	1.40E+03 (+210 %)	7.05E+02 (+57 %)
Human toxicity	USETox v1.02	CTUh	5.90E-2	1.07E-02 (-82 %)	4.28E-02 (-27 %)

The large discrepancies with respect to the reference data might be due to an incorrect implementation of the impact reallocation or due to the fact that some of the impact assessment methods used by Nuss

and Eckelman have been replaced by more recent versions in openLCA (e.g. the ReCiPe and CED impact assessment methods). It is difficult to compare the LCIA results for rhenium or molybdenum production with other literature besides the data included in ecoinvent, as the availability of LCA studies on this production process is rather limited [214], [215]. The overall impact of implementing a rhenium extraction dataset based on ecoinvent 2.2 data instead of ecoinvent 3.8 data in the PS LCSA has already been evaluated in Table 8.4. As this change does not dramatically alter the overall conclusions of the research, it is deemed that the environmental impact of rhenium production is accurate enough for the purposes of the LCIA performed in Section 7.5.

LCIA of clean room fuelling

Clean room fuelling is another process with a noticeable influence on the overall LCSA results. The process that was used in this LCSA was already included in the SSSD and is in line with the ESA LCA dataset, which has been set up using primary data from the Kourou Launch site [15]. As such, the environmental LCI and LCIA of this process are deemed to be valid. Secondly, this research used the assumption that novel monopropellant fuelling is performed using the same general materials and procedure as hydrazine fuelling, but over a shorter period of time due to the reduced safety precautions. This same assumption is used in the ESA LCA database, such that it is considered valid and justified.

While the creation and disposal of waste in the hydrazine fuelling process have not been directly discussed in the LCI definition in Section 7.4, Anflo and Crowe describe that the fuelling of LMP-103S also presents a major reduction of resources in this regard [26]. For the PRISMA launch campaign, where the spacecraft was fuelled with 11 kg of hydrazine and 5.6 kg of LMP-103S, hydrazine fuelling resulted in 29 L of hydrazine, 400 L of contaminated deionised water and 70 L of iso-propanol alcohol to be disposed of. In contrast, the LMP-103S loading only resulted in 1 L of waste propellant and 3 L of a contaminated mix of deionised water and IPA to be disposed of. Per kg of propellant, this constitutes a resource reduction of around 93% for the wasted propellant, and 99% for the contaminated IPA and water. The fact that these resources are included in the clean room fuelling process that is scaled based on the number of hours required, and that the novel monopropellant fuelling procedures are assumed to require 28% of the time required for hydrazine fuelling, is deemed to be justified and rather conservative.

While clean room fuelling has a very important impact on the system's life cycle social and economic sustainability, there is little information available to validate the scores estimated in Subsection 7.5.2 and Subsection 7.5.3. This is also apparent in the limited accuracy of these estimates themselves, mostly being based on two sources in literature comparing hydrazine fuelling and LMP-103S fuelling [61], [197]. It is important to note that one of these two sources, namely the conference paper by Dinardi and Persson [197] was written with the goal of promoting LMP-103S as a high-performance alternative to hydrazine. As such, the reported life cycle cost savings may be somewhat overestimated. Additionally, Lange et al. indicate that the hydrazine fuelling campaign for the PRISMA mission was somewhat lengthy, with some Myriade propulsion system loading campaigns requiring less time in the clean room [216]. Considering the sensitivity of the economic and social sustainability scores on the estimated time of clean room fuelling, it is clear that this element of the research requires further validation.

LCIA of 98% HTP production

As mentioned before, the new process created to model the production of 98% HTP presents the only opportunity to perform a true validation of the environmental LCIA results with respect to the ESA LCA database's estimate. As already presented in Subsection 8.2.1, the process definition of this new process differs only slightly from the ESA LCA database dataset, such that it is expected that the LCIA results will also be quite similar. A comparison of the results for all impact categories included in the ESA LCIA - EF 3.0 method, which is equivalent to the SSSD environmental LCIA method, is shown in Table 8.6. The comparison shows that the results are somewhat similar (within 50 %) for about half of the impact categories, while the other half shows much larger discrepancies.

The factors contributing to the differences in the results are various, as indicated by the lack of a

uniform trend in the discrepancies, with some impact scores being over- and others underestimated in the results of the new process. A first factor contributing to the differences is the difference in life cycle inventories: the added flows of *heat from steam*, and *steam* itself contribute significantly to the impact categories of *Ecotoxicity, freshwater* and *Ozone depletion*, resulting in the greater impact of the new process there. Furthermore, the allocation method for upstream ecoinvent flows in the ESA LCA database follows a cut-off approach, whereas the SSSD uses ecoinvent processes allocated at point of substitution (APOS), also resulting in significant LCIA differences. For the impact category of *Water use*, where the ESA LCA dataset estimates a net production of water, it is presumed that the ESA LCA database contains a mistake in the characterisation, or that the impact assessment of the 98% HTP production with a cut-off allocation approach leads to a result that is not reflective of the physical realities of the process. Considering the small impact that 98% HTP production has for the overall LCSA results, it is not likely that increasing the validity of this dataset would greatly impact the conclusions of this research.

Table 8.6: Validation of environmental impact assessment results for 98% HTP production (FU=1 kg) with respect to data from ESA LCA database [15]

Impact category	Unit	Reference data (ESA LCA DB)	New process	Difference [%]
Acidification	mol H+ eq	7.96E-03	1.19E-02	+ 49
Air acidification	kg SO2 eq	6.71E-03	9.75E-03	+ 45
Climate change	kg CO2 eq	1.83E+00	3.18E+00	+ 73
Ecotoxicity, freshwater	CTUe	5.60E+00	2.55E+01	+ 354
Ecotoxicity, marine	kg 1,4-DB eq	1.42E+04	2.30E+04	+ 62
Eutrophication, freshwater	kg P eq	9.11E-04	6.59E-04	- 28
Eutrophication, marine	kg N eq	1.42E-03	1.63E-03	+ 15
Eutrophication, terrestrial	mol N eq	1.29E-02	1.60E-02	+ 24
Human toxicity, cancer	CTUh	1.56E-09	3.37E-09	+ 116
Human toxicity, non-cancer	CTUh	3.41E-08	2.04E-08	- 40
Ionising radiation	kBq U-235 eq	5.07E-01	2.85E-01	- 44
Land use	Pt	6.39E+00	1.84E+00	- 71
Ozone depletion	kg CFC11 eq	6.57E-08	4.55E-07	+ 593
Particulate matter	disease inc.	5.52E-08	8.50E-08	+ 54
Photochemical ozone formation	kg NMVOC eq	5.43E-03	5.90E-03	+ 9
Resource use, fossils	MJ	3.34E+01	5.01E+01	+ 50
Resource use, minerals and metals, reserve base	kg Sb eq	7.28E-05	6.74E-05	- 7
Resource use, minerals and metals, ultimate reserve	kg Sb eq	2.40E-05	6.49E-06	- 73
Total cumulative energy demand	MJ	3.99E+01	5.64E+01	+ 41
Water use	m^3 depriv.	-1.73E-01	3.71E+00	- 2249

8.3. LCSA data quality

The importance of assessing the quality of the data used in this research has already been highlighted at different points throughout this report and will be discussed once again, in a more comprehensive manner, in this section. As the final outcome of an LCSA, in terms of the impact scores resulting from the

LCIA, is very closely linked to the definition of the analysed system's LCI, the reliability and quality of this definition is always highly important. In the specific case of space LCA and LCSAs, there is an additional difficulty posed within this step of the research, due to the fact that most specific system information is somewhat confidential [98]. To overcome this scarcity of public information, it is recommended to use as much primary data as possible, developing LCIs using data from companies. This is also the approach followed in the construction of the ESA LCA database [15]. In this research, primary data collection was pursued where possible, by contacting company employees by email whenever specific product or process information could not be found in literature. This was especially necessary in the quantification of economic and social flows.

Sourcing information directly from commercial actors also holds uncertainties however, as companies have an interest in minimising the estimated environmental, economic or social impact of their practices. This concern also holds for the results presented in conference publications, where findings are not peer-reviewed and therefore may be embellished. In the case of this research specifically, this may be most problematic with respect to the estimation of the fuelling process for hydrazine and LMP-103S, where two out three sources used in the approximation are conference papers from ECAPS employees [26], [197]. Still, the possible cost reduction in novel monopropellant fuelling has also been indicated in other publications, albeit qualitatively [10], [13], [61].

Another source of uncertainty within the LCI definition in this research is related to the fact that some materials or processes contained within multiple PS component LCIs were not yet included in the SSSD and were not modelled with new upstream processes due to the limited research scope. In that case, consistent proxies were used to model the actual products or processes as accurately as possible. In the LCI of all thrusters, inconel alloy production was proxied by the *iron-nickel-chromium alloy* dataset included in ecoinvent 3.8, while inconel milling was proxied by *chromium steel removed by milling*. Secondly, the brazing included in the production or assembly of various components was modelled with the *welding, arc, steel* dataset from ecoinvent 3.8. Other proxy processes have been indicated in the various LCI definition tables in Section 7.4 and Appendix B. Next to this, some ecoinvent processes are themselves proxies based on other processes for which primary data was available.

One way of quantifying the overall data quality of a created LCI definition is to fill in the data quality pedigree matrix as shown in Figure 4.5. In this research, the ESA data quality matrix was used, which assesses the data quality based on six criteria (Technological (TeR), Geographical (GR) and Temporal representativeness (TiR), Completeness (C), Precision/uncertainty (P), and Methodological appropriateness and consistency (M)), each with a highest possible score of 5. The profile of a dataset in the data quality matrix is thus able to give an intuitive understanding of how accurate the LCI definition is in approximating the actual process. In a recent publication, Wilson et al. have also proposed a method of combining these six criteria scores into a single score, being the data quality rating (DQR), as calculated in Equation 8.1, where each of the data quality criteria scores are added with the abbreviations stated above, with X_w being the weakest (highest) data quality score, and I being the number of data quality indicators used, 6 in this case [217]. The single DQR allows for an assessment of an LCI's overall data quality, with the authors of the paper indicating that any score below 1.6 represents high quality data, with scores between 1.6 and 3 exhibiting basic quality, and scores between 3 and 4 representing a data estimate.

$$DQR = \frac{TeR + GR + TiR + C + P + M + 4 \cdot X_w}{I + 6} \tag{8.1}$$

An overview of the data quality assessment for each of the new upstream and component-level core processes is given in Table 8.7. The table shows that none of the modelled processes can be considered to be high quality, which is somewhat unsurprising given the general reliance on public secondary data in the definition of the LCIs. What is more disconcerting regarding the overall reliability of the results is the low data quality for the alumina/iridium catalyst, the flow control valve and the rhenium/iridium alloy combustion chamber, as these three production processes are all key contributors to the PS designs' overall sustainability impact. For each of these processes, the poor data quality is mostly related to the fact that outdated documents had to be used in the LCI definition. If more recent data were available, data quality would noticeably increase. For the production process of the Re/Ir combustion chamber,

an additional factor reducing the data quality is the fact that the exact production process is not precisely known, such that the scores for Completeness and Precision are themselves uncertain and therefore conservatively assumed. While the assumed values of rhenium and iridium usage in this process are deemed to be justified estimates, increasing the accuracy of this important LCI definition should be a point of focus in further research.

Table 8.7: Data quality assessment for new upstream and core processes. TeR=Technological representativeness, GR=Geographical representativeness, TiR=Temporal representativeness, C=Completeness, P=Precision/uncertainty, M=Methodological appropriateness and consistency, DQR=Data quality rating as calculated following [217].

Process	TeR	GR	TiR	C	P	M	DQR
Iridium	1	1	3	1	2	1	**1.75**
Rhenium	1	1	3	1	2	1	**1.75**
Alumina/iridium granular catalyst	1	1	5	3	4	4	**3.17**
Alumina/platinum granular catalyst	2	2	1	2	4	4	**2.58**
Catalyst bed heater	1	1	1	3	2	3	**1.92**
Diaphragm propellant tank - Al4254	4	1	1	2	3	2	**2.42**
Diaphragm propellant tank -Ti-6Al4V	2	1	1	2	3	2	**1.92**
Fill/ drain valve	1	1	3	3	3	3	**2.17**
Flow control valve	2	1	5	5	4	3	**3.33**
Seamless tubing	1	1	1	3	3	4	**2.42**
Thruster combustion chamber - inconel	2	3	2	3	4	4	**2.83**
Thruster combustion chamber - $Re/\ Ir$ alloy	4	2	4	4	5	4	**3.58**

The data quality assessments for the dry and wet propulsion systems are shown in Table 8.8. Note that the data quality scores here only concern the definition of the assembly and fuelling processes, and do not consider the data quality of the flows used in each LCI definition. The manner by which upstream data quality ratings are included in the data quality of a process of interest is an area in space LCA research that is still under investigation, therefore not included in this research [218]. As these LCI definitions could be based on rather accurate estimates from literature, each of the processes has a basic quality. The data quality for other propellant specific processes, concerning propellant and thruster production are shown in Appendix E.

Table 8.8: Data quality assessment for propulsion system production processes. TeR=Technological representativeness, GR=Geographical representativeness, TiR=Temporal representativeness, C=Completeness, P=Precision/uncertainty, M=Methodological appropriateness and consistency, DQR=Data quality rating as calculated following [217].

Process	TeR	GR	TiR	C	P	M	DQR
Hydrazine propulsion system	1	1	2	2	3	3	**2.00**
Loaded hydrazine propulsion system	1	1	3	1	3	3	**2.00**
ASCENT propulsion system	1	1	3	2	3	3	**2.08**
Loaded ASCENT propulsion system	1	1	3	1	4	3	**2.42**
LMP-103S propulsion system	1	1	2	2	3	3	**2.00**
Loaded LMP-103S propulsion system	1	1	2	1	3	3	**1.92**
98% HTP propulsion system	3	1	3	2	4	3	**2.67**
Loaded 98% HTP propulsion system	1	1	3	1	3	3	**2.00**

Overall, it may be concluded that the LCI definition in this research has mostly achieved a basic quality, with some key processes, such as the production of the Re/Ir combustion chamber, only being modelled with a basic estimate. The main reason for this poor data quality is the lack of accurate and recent data on the commercial and patented production processes. In future research, this could be solved by performing LCAs in collaboration with the companies involved in these production processes. This would also aid in avoiding the usage of inaccurate data that is publicly available. With a basic data quality, it may be assumed that the conclusions drawn in this research are legitimate.

8.4. Methodological limitations

Even if the conclusions drawn in this research are sufficiently accurate, it is important to understand what these conclusions exactly implicate on a broader and more practical level. This is especially necessary due to the nature of LCSAs, wherein the multi-criteria LCIA may make the final results difficult to interpret. In the discussion presented in Section 7.5, an effort has been made to relate each of the LCSA results to the physical components and processes which lie at the cause of these outcomes. However, it is equally crucial to indicate what cannot be concluded based on the results. This section will present a number of methodological features of this research that simplify or otherwise limit the significance of the overall conclusions.

Firstly, by limiting the LCSA to the propulsion system, the changes in other subsystems due to the use of a different propellant are not considered. There are various subsystems of which the design depends on the propulsion subsystem. A first example is the power subsystem, which may have to be sized differently as the novel monopropellants considered in this study generally require more catalyst bed preheating for proper thruster operation than hydrazine. Secondly, the spacecraft structure may be designed for a lower spacecraft mass in the case of the EIL monopropellants, as the propellant load and tank mass will be lower compared to the hydrazine option. Lastly, the different thermal constraints of the various propellants could lead to differences in the thermal subsystem. Each of these changes might result in significant discrepancies in the sustainability impact of the spacecraft taken as a whole. It is thus vital to keep in mind that the sustainability of each of the propellant options at the level of the propulsion subsystem may not reflect the sustainability at the level of the entire spacecraft.

A second limitation of this research, more at the level of implementation than pure methodology, is

that the potential reductions in material usage and production cost due to the fact that the propulsion systems are manufactured for a spacecraft constellation have not been accounted for. Additionally, the existence of previous propulsion system designs similar to the use case investigated here has not been given any importance with respect to cost or required labour hours in production. Instead, it was assumed that the propulsion systems for each of the propellant options would be manufactured in a more or less identical manner, using fully developed and flight-proven hardware. While neglecting the impact of the spacecraft constellation most likely does not change the comparison between the different propellant options, the latter assumption is significant, as it may take away some sustainability advantages of well-established technologies and production lines.

The choice to consider a single use case means that the conclusions found here may not be valid for other monopropellant use cases. For example, in use cases where fuelling cost takes up a smaller portion of the propulsion system's life cycle cost, it may be that using hydrazine is not the most expensive option. Furthermore, the use of a different propulsion system size or architecture may also lead to a different identification of hotspots in each of the sustainability dimensions.

Beyond evaluating how the chosen LCSA methodology has been implemented, the limitations of this methodology itself must also be evaluated. Due to the necessity of using quantitative impact categories, other facets influencing the sustainability or overall suitability of using a certain propellant over another option are not reflected in this comparison. A first element herein is the increasing importance of strategic autonomy in the European context [219]. With this concept, the European Union wishes to reduce its reliance on other countries, either allies or rivals, in critical areas, such as the defence and space industries. As such, the usage of hydrazine, which is now sourced from China [15], may become untenable in the future, not due to environmental or economic reasons, but due to political motivations. Additionally, European institutions such as ESA may want to strengthen the European space industry and therefore prefer a European novel monopropellant such as LMP-103S over an American alternative such as ASCENT. Additionally, the European Commission has made it a policy priority to gain a greater autonomy in the supply chain of a list of critical raw materials that are expected to play an important role in the transition to a more renewable and sustainable economy [220]. The platinum group metals included in the PS designs in this research (iridium, platinum) and titanium are included in this list. The worldwide supply of each of these metals is dominated by a select number of countries, with 92% of the iridium supply and 71% of the platinum supply being South African and 45% of titanium supply coming from China. Being overly reliant on single suppliers for critical materials or components makes any company developing propulsion systems more vulnerable to geopolitical or other global instabilities. As such, it is a very important facet to be taken into account in the move away from hydrazine propulsion systems, which has not been included in this research.

Another key limitation connected to the chosen LCSA framework is related to the evaluation of social sustainability. Because of the scarcity of appropriate data and impact assessment methods, social sustainability was assessed at a national level, as such not being closely connected to the specificities of the activities included in the LCIs themselves. This might be most problematic for the social sustainability impact of hydrazine fuelling, where workers face serious health risks. Furthermore, while the LCSA framework does allow for it, this research did not consider the social sustainability of upstream processes, related to raw material extraction, waste treatment, electricity production or other auxiliary activities. This is expected to be a significant omission, as the social impact related to the dangerous and straining working conditions in these processes, or to the disruption within communities living near sites of raw material extraction can be a serious cause of concern. Assessing these nuanced and complex impacts may not be very feasible within an LCA framework, where impact quantification is required.

8.5. Design recommendations

The final step in the interpretation of the LCSA results of each PS design is to translate the findings into concrete recommendations to improve the sustainability of monopropellant propulsion systems in the future. When considering environmental sustainability, this translation serves the purposes of ecodesign. This section will investigate which measures would be most effective in improving the systems'

overall sustainability. Due to the multitude of environmental impact categories and the specificity by which the environmental flows could be defined, most of the design recommendations mentioned here are meant to reduce the environmental impact of the PS designs.

The clearest environmental hotspot is related to the use of refractory metals in the combustion chambers of the EIL thrusters. By reducing the amount used or by replacing these metals, especially iridium, by other elements with lower environmental footprints, the life cycle environmental impact of the ASCENT and LMP-103S systems could be reduced. To make this material replacement more feasible, the EIL monopropellants' combustion chamber temperature could be lowered, for example by increasing the percentage of water in the propellant compositions. While this might decrease the performance improvement w.r.t. hydrazine facilitated by these novel monopropellants, the LCSA results have certainly shown that the reduced propellant load and tank mass do not compensate for the increased environmental impact of the required use of iridium and rhenium.

For the hydrazine PS design, the environmental impact is mostly driven by the production of iridium used in the thruster catalyst bed, the production and fuelling of the propellant, and the production of the titanium propellant tank. As such, the main recommendations in this regard are to find a different catalytic material than iridium, and to somehow reduce the toxicity of the propellant. Once again, an option could be to dilute the propellant somewhat, reducing the severity of exposure to hydrazine, which would result in a reduction of I_{sp}, however. As propellant fuelling is also a dominant factor in the economic and social sustainability of the hydrazine system, it is understandable that the development of novel monopropellants has targeted this aspect of hydrazine use as being the most problematic. The 98% HTP PS has a relatively low environmental impact, and if further improvements would be desired, this could be achieved by finding less environmentally straining materials than platinum in the catalyst and by improving the performance of the propellant, reducing the propellant tank size, potentially by blending a fuel into the monopropellant.

While it may seem more difficult to achieve from the perspective of a space propulsion engineer, the systems' environmental sustainability could also be improved by ensuring that environmentally straining materials such as iridium, rhenium or titanium are sourced from suppliers with a reduced environmental footprint, for example by proving that the production is performed using fully renewable energy sources. In the case of platinum or iridium, the fact that South African mines provide the very large majority of the supply may make this goal difficult to achieve. Instead, one could also aim to source as many metals as possible from recycled sources, for example from recycled automotive catalysts in the case of platinum.

Regarding the economic sustainability of the systems, the key activity which may facilitate cost reductions is the fuelling process. As hydrazine may be used less in the near future, it would be interesting to reconsider the overall chronology and requirements in the fuelling process, to fully make use of the reduced toxicity of the novel monopropellants. By potentially combining fuelling with other clean room activities, or by shipping propellant tanks pre-fuelled, further cost reductions could be achieved. Additionally, the cost of EIL thrusters is also an area where costs would preferably be reduced. If production volumes increase, the benefits of series production could enable cost reductions. Additionally, if less exotic metals were used in the combustion chamber, the production process could also be completed using more conventional production processes.

Lastly, it is also recommended to reduce the use of platinum group metals from the perspective of social sustainability, as PGM mining in South Africa has been identified in the past as an industry with poor safety standards for workers, which also causes significant hindrance and harm to the social fabric of surrounding communities [221]. While these concerns have not been addressed in the social impact assessment of this research, they have been highlighted and investigated in previous research. Clean room fuelling is also a driver of the social impact for each of the PS options, such that reducing the required fuelling time would lead to significant improvements. More specifically, it is also recommended to improve the working conditions during clean room fuelling, potentially making use of automation or remote control, as to reduce the human exposure to toxic propellants as much as possible. Regarding general working conditions, it is advised to perform as much work as possible in the EU, where the social conditions are better than in the USA or other foreign territories, as informed by the evaluation of the SSSD's social criteria.

8.6. Conclusion

This chapter has aimed to evaluate the reliability and validity of the LCSA results presented in Chapter 7, to further interpret the results and to indicate where further work may be required. Firstly, the LCI analysis and LCIA results for key processes within the propulsion system life cycles have been validated, with comparable data wherever possible. This validation effort has shown that the accuracy of LCIA results for the important processes of iridium and rhenium production may be somewhat questionable, with the judgement of overall validity also being difficult due to the scarcity of recent and adequate data. However, it is not expected that the inaccuracies contained within this research have the potential to entirely overturn the conclusions of the comparative LCSA.

An assessment of the data quality of the LCIs of newly created processes is also in line with this judgement, where key processes unfortunately feature the poorest data quality, due to the fact that these processes are also the most specific to the case study considered in this research. Despite these inaccuracies, the overall conclusions are still deemed to be valid, as the presumed drivers behind the poor environmental performance of the ASCENT and LMP-103S designs are confirmed in other literature as being polluting processes [191], [209], [214], [221], and the dominant processes in economic and social sustainability also being identified in novel monopropellant literature as areas of concern [7], [9].

Still, the conclusions of this research only reach as far as the chosen methodology allows for, which is why it is important to be conscious of these limitations. The most important limitations in this respect are that the scope of the LCSA is constrained to the propulsion system, thereby neglecting any follow-on changes in the overall spacecraft sustainability, and that the social impact of the PS life cycles is only assessed at the national level of core processes, neglecting the potentially significant social harm caused in upstream processes. The latter limitation is especially relevant regarding the extraction of PGMs in South Africa, where worker conditions and relations towards local communities are problematic [221].

Translating the LCSA findings into design cues to improve the sustainability of future propulsion systems is done by identifying the hotspots in each of the sustainability dimensions and then proposing potential alternatives with a lower impact. It should be stressed however that no LCIA has been performed to verify whether these design recommendations would actually lead to improvements in the different dimensions of sustainability. The first area to target would be the usage of rare metals in the catalysts of all PS designs and in the combustion chambers of the EIL systems. By reducing the use of these metals, or by replacing them with alternative materials, the environmental impact of all, and the economic and social impact of the EIL systems could be improved. To make this replacement more feasible, it is proposed that the combustion chamber temperature of the considered EIL monopropellants could be lowered, at the cost of reducing the propellants' performance. Wherever the use of these rare metals is unavoidable, the elements should be sourced from suppliers that are undertaking action to reduce the environmental and social harm of their extractive processes.

Clean room fuelling is another process that could be adapted to result in a lower impact in all three sustainability dimensions. For the novel monopropellants, it is recommended to consider how the safety improvements can be leveraged to integrate fuelling better within the overall spacecraft assembly process. For hydrazine, reducing the exposure of humans to the toxicity of the propellant, potentially by increasing the usage of automated systems, may lead to cost and social impact reductions. As stated before, this should be verified by future LCSA studies.

9

Conclusion and recommendations

In the field of monopropellant research, there is an ongoing effort to find replacements for hydrazine, which is a simple and effective, yet highly toxic, monopropellant that has been widely used for in-space propulsion since the 1960s. The usage of hydrazine requires very strict procedures during fuelling leading to high on-ground operational costs. As such, the propellants identified to replace hydrazine, termed novel monopropellants, should lead to a reduction in handling costs while not compromising on hydrazine's robust performance. Simultaneously however, this research trend also targets the environmental sustainability of hydrazine propulsion systems, envisioning novel monopropellants with reduced harm to humans and ecosystems. This has led to a diffuse definition of "green" monopropellants, where the actual environmental impact of these systems has not yet been investigated.

This thesis therefore identified that the growing application of life cycle assessment (LCA) methodologies within the space industry could be used to develop a more thorough comparison of the life cycle sustainability of monopropellant systems. The main research objective was therefore:

To gain a better understanding of the three-pillar, system-level sustainability of novel and conventional monopropellant systems, using the analytical tools afforded by life cycle assessment methodologies.

As the social and economic dimensions of sustainability are also relevant in the context of monopropellants, illustrated by the issues identified with hydrazine fuelling, the life cycle sustainability assessment (LCSA) framework previously developed with the Strathclyde Space Systems Database (SSSD) was used in this research. This LCSA framework, constructed specifically for LCSA research of space systems, entails an assessment of environmental, social and economic criteria, facilitating an adequate answer to the following main research question:

How does the choice of propellant impact the environmental, social and economic life cycle sustainability of a representative monopropellant system?

Comparing a variety of use cases for monopropellant systems, it was decided that the comparative LCSA would be most feasible and valuable for the case study of the main propulsion system for an Earth Observation (EO) minisatellite with a dry mass of maximally 150 kg, to be used in a Low Earth Orbit (LEO) satellite constellation. This answered subquestion SQ-1.1, which is listed along with all other subquestions of the research in Table 9.1. Following a conceptual definition of this use case, preliminary propulsion system requirements were set up to inform the propulsion system design process, addressing SQ-1.2. The requirements also guided the definition of the trade-off criteria used to select hydrazine, ASCENT, LMP-103S and 98% HTP as the four monopropellants which were included in the comparative LCSA, which answers SQ-1.3.

Table 9.1: Overview of research subquestions

Label	Question	Answered in
SQ-1.1	For which use case of monopropellant systems is a better understanding of life cycle sustainability most valuable?	Section 5.2
SQ-1.2	What are the propulsion system requirements for the use case found in SQ-1.1?	Section 6.2
SQ-1.3	Which novel monopropellants are best suited for the use case found in SQ-1.1?	Section 6.3
SQ-1.4	Which sustainability issues are currently considered to be the most problematic for the use case found in SQ-1.1?	Section 5.2, Section 2.2
SQ-1.5	What is the design of a propulsion subsystem fulfilling each of the system requirements found in SQ-1.2, for each of the monopropellants selected in SQ-1.3?	Section 6.4
SQ-2.1	Which monopropellant system scores the best in each of the sustainability dimensions?	Section 7.5
SQ-2.2	Which monopropellant system is the most sustainable overall?	Section 7.5
SQ-2.3	Which impact categories feature the largest and smallest differences between the different monopropellant systems?	Section 7.5
SQ-2.4	Which life cycle phases feature the largest and smallest differences between the different monopropellant systems?	Section 7.5
SQ-3.1	Which components in the monopropellant systems have the largest impact in each of the sustainability dimensions?	Section 7.5
SQ-3.2	Which components in the monopropellant systems drive the differences between the sustainability scores of each of the options?	Section 7.5
SQ-3.3	Which activities and processes in the life cycle of the monopropellant systems have the largest impact in each of the sustainability dimensions?	Section 7.5
SQ-3.4	Which activities and processes in the life cycle of the monopropellant systems drive the differences between the sustainability scores of each of the options?	Section 7.5

Following a propulsion system sizing and component selection, answering SQ-1.5, the life cycle inventory (LCI) for each propulsion system was developed and implemented in openLCA, which is the LCA software used to navigate the SSSD and apply the SSSD Sustainability life cycle impact assessment (LCIA) methodology, quantifying the impact of each propulsion system for 23 impact categories, including single score assessments for the social and economic impacts. Analysing the results of the LCIA, it is found that the 98% HTP system has the lowest impact across environmental, economic and social sustainability, whereas the LMP-103S system results in the highest environmental score, closely followed by the ASCENT system, and the highest social score, closely followed by the hydrazine system. Regarding economic sustainability, it was found that the fuelling cost of the propulsion systems had a dominating impact, such that the hydrazine system, which features the lengthiest fuelling procedure, has the highest life cycle cost. Furthermore, by normalising and weighting the environmental, economic and social impact scores, it was determined that the economic impact of each of the systems very largely outweighed the environmental and social impact, with the result that the hydrazine system could be considered as the least sustainable. However, this method of determining ”overall” sustainability is somewhat subjective, such that it may be more meaningful to consider the three sustainability dimensions separately and conclude that the LMP-103S system performs the worst overall. These findings provide conclusive answers for SQ-2.1 and SQ-2.2.

Looking into the impact categories driving the differences between the propulsion system options in SQ-2.3, it was found that the environmental impact categories featured the largest spread in results, with the ASCENT and LMP-103S systems scoring about four times worse overall than the hydrazine system. The impact categories related to *Ecotoxicity, freshwater*, *Resource use, metals and minerals* and *Acidification* contribute the most to a normalised and weighted environmental single score and also feature the largest variation between the four options, with the ASCENT and LMP-103S scores always greatly exceeding those of the hydrazine and 98% HTP options. The propulsion systems have the lowest relative differences in their environmental impact on *Water use*, *Ozone depletion* and *Ionising radiation*, and also feature relatively small differences in the economic and social single scores.

The life cycle phase with the largest difference in environmental results is decidedly that of raw material extraction, where the extraction and refining of iridium and rhenium, two rare metals used in the combustion chamber wall of the ASCENT and LMP-103S thrusters, has a dominant impact. Next to SQ-2.4, this also answers SQ-3.2 and SQ-3.4, where the main driver for the worse environmental scores of ASCENT and LMP-103S are related to their use of iridium and rhenium. In the economic impact of the various systems, the largest difference is found in the pre-launch fuelling phase, where hydrazine fuelling is substantially more expensive than novel monopropellant fuelling. The fuelling cost is also the main driver of the system life cycle cost for each monopropellant option. In the social dimension of sustainability, the largest differences are found in the production phase, where the production of rhenium/iridium combustion chambers for the ASCENT and LMP-103S thrusters leads to some discrepancy between the different options. The social impact for each propellant option is quite similar however, being dominated by the labour impact of the dry propulsion system assembly.

A detailed answer to the subquestions from SQ-3.1 to SQ-3.4 can be found in the various tables in Section 7.5. In brief, it is clear that the thruster combustion chambers of the ASCENT and LMP-103S systems lead both to the high environmental impact of these options and to the difference in impact with respect to the hydrazine and 98% HTP options. The extraction of rhenium and iridium are almost entirely responsible for this dependence. In the economic assessment, propellant fuelling dominates the impact of all four systems, as such not being entirely related to a single component. While this activity leads to a difference in cost between the hydrazine and novel monopropellant systems, the fuelling cost of novel monopropellants was assumed to be the same. The difference among novel monopropellant system costs is thus found in the different cost of thrusters, with those in the ASCENT and LMP-103S systems being more expensive than those in the 98% HTP system. Lastly, in the social realm, the labour-intensive propulsion assembly process accounts for about 30% of each system's impact. Next to this, it is found that the most expensive thruster components, being the combustion chamber and flow control valve, where the propellant choice also leads to design differences, cause the slightly different social scores. This may be in part due to the simplifying assumption relating social to economic data, which was made out of necessity due to the limited social data available. As the social assessment was only performed for core processes, the differences in social scores are entirely related to production and testing activities.

Overall, this research has indicated that a comparison of monopropellant system sustainability is much more multifaceted than a focus on propellant toxicity and handling cost would indicate. The use of iridium and rhenium within ASCENT and LMP-103S thrusters has been indicated as a environmental and social sustainability hotspot, leading to the recommendation of replacing these metals or finding less environmentally harmful processes for their production. Clean room fuelling has been confirmed to be a dominant factor in the life cycle cost of minisatellite propulsion systems, whereas the production of high-temperature resistant thrusters results in the ASCENT and LMP-103S systems having a higher cost than the 98% HTP system. Another conclusion of this research is that there are few environmental, economic or social hotspots identified within the life cycle of the 98% HTP propulsion system, indicating that this could be considered as the most sustainable monopropellant technology in the future, with the crucial prerequisite that flight-ready hardware is developed and sufficiently qualified.

Recommendations for future research

While this research has led to several new insights allowing for a more advanced understanding of the sustainability of novel monopropellant systems, there are also various findings demanding further research. First and foremost, the environmental impact of the production of the rhenium/iridium alloy combustion chamber used in the ASCENT and LMP-103S thrusters should be further validated. As this production process is responsible for the large differences between the environmental impact of the EIL systems and of the other two monopropellant systems, the method used in this research to model iridium and rhenium extraction should be further detailed, using primary and recent data. Additionally, the life cycle definition of the thruster catalysts should be further detailed, considering that the current LCI is almost entirely limited to raw material extraction and transport.

Improving the data quality of the LCIs contained in this research is a general recommendation, given that the scope of this research did not allow for extensive primary data collection. As the processes

and materials used in the space industry are often quite specific, defining inventories with data from public sources or using proxies within existing LCA databases are both often inaccurate. By conducting more LCA and LCSA studies on novel monopropellant systems in collaboration with larger institutions such as ESA, that have industrial partners, the accuracy of the LCI definitions could be improved. This especially holds for the social and economic flows included in the new LCI definitions.

Considering the very large dependence of the economic impact on the clean room fuelling cost, this estimate should be further validated as well, as it has only been based on a very rough approximation in this research. A more thorough overview of the makeup of the economic and social impact of this process would also allow for a more precise quantification of the novel monopropellants' advantages in this regard. Again, due to the specificity and confidentiality of this process, a greater level of detail may only be feasible through research supported by industrial partners.

Even if the accuracy of the LCI definitions may be greatly increased in future research, there will always be a level of uncertainty included in the LCI analysis, or later on in the LCIA phase. This may be due to the fact that datasets approximate the reality of activities only to a certain extent, for example giving an average representation of a probabilistic process, or because primary data of specific processes remains unavailable. By performing a formal sensitivity analysis, for example through Monte Carlo simulation, the impact of this data uncertainty on the LCIA outcome should be quantified. The results of this sensitivity analysis would in turn indicate which components in the LCI should be targeted to further improve the accuracy of the LCA results.

It is also recommended to conduct similar LCSA studies for other monopropellant use cases, to consider whether the comparison between various propellants still leads to the same conclusions. In particular, it would be interesting to investigate what the key drivers in each of the sustainability dimensions are for each case study. This would clarify which design and development recommendations would be most effective to improve the sustainability of monopropellant systems across all use cases. Additionally, different case study comparisons could also consider more monopropellants, such as the promising water electrolysis technology, or other propulsion types, such as electric propulsion, to further characterise the sustainability of space propulsion systems.

A final research recommendation extends to the application of the SSSD LCSA framework in general, where it is deemed that the assessment of social impact should be further improved. At this stage, it is not possible to very directly include the features or social issues related to specific activities in the social impact assessment. This is especially problematic for the activities for which there are known social issues that cannot be captured by the current LCIA methodology. The social LCIA method could be updated by considering recent advancements within the field of social LCA studies. By enabling a more thorough assessment of monopropellant systems' social impact, the SSSD LCSA methodology would be able to better assist in the comparison of the sustainability of novel monopropellant and hydrazine propulsion systems.

References

[1] European Space Agency. “Preparing to fuel MTG-i1.” (Nov. 28, 2022), [Online]. Available: https://www.esa.int/ESA_Multimedia/Images/2022/11/Preparing_to_fuel_MTG-I1 (visited on 01/08/2024).

[2] K. Crowley, “Platinum drop fires social unrest as villagers turn on mines,” *Bloomberg.com*, Jun. 12, 2017. [Online]. Available: https://www.bloomberg.com/news/articles/2017-06-12/platinum-plunge-ignites-social-unrest-as-villagers-turn-on-mines (visited on 01/08/2024).

[3] A. R. Wilson and M. Vasile, “The space sustainability paradox,” *Journal of Cleaner Production*, vol. 423, Oct. 15, 2023, ISSN: 0959-6526. DOI: 10.1016/j.jclepro.2023.138869. [Online]. Available: https://www.sciencedirect.com/science/article/pii/S0959652623030275 (visited on 12/30/2023).

[4] T. Maury, P. Loubet, S. M. Serrano, A. Gallice, and G. Sonnemann, “Application of environmental life cycle assessment (LCA) within the space sector: A state of the art,” *Acta Astronautica*, vol. 170, pp. 122–135, May 1, 2020, ISSN: 0094-5765. DOI: 10.1016/j.actaastro.2020.01.035. [Online]. Available: https://www.sciencedirect.com/science/article/pii/S0094576520300552 (visited on 12/08/2022).

[5] L. Miraux, A. R. Wilson, and G. J. Dominguez Calabuig, “Environmental sustainability of future proposed space activities,” *Acta Astronautica*, vol. 200, pp. 329–346, Nov. 1, 2022, ISSN: 0094-5765. DOI: 10.1016/j.actaastro.2022.07.034. [Online]. Available: https://www.sciencedirect.com/science/article/pii/S0094576522003800 (visited on 03/03/2023).

[6] L. Miraux, “Environmental limits to the space sector’s growth,” *Science of The Total Environment*, vol. 806, Feb. 1, 2022, ISSN: 0048-9697. DOI: 10.1016/j.scitotenv.2021.150862. [Online]. Available: https://www.sciencedirect.com/science/article/pii/S0048969721059404 (visited on 12/30/2023).

[7] U. Gotzig, “Challenges and Economic Benefits of Green Propellants for Satellite Propulsion,” in *7th European Conference for Aeronautics and Space Sciences*, Milan, Italy, 2015. [Online]. Available: https://elib.dlr.de/119357/1/Gotzig_2017_EUCASS[1].pdf.

[8] W. M. Marshall and M. C. Deans, “Recommended Figures of Merit for Green Monopropellants,” in *49th AIAA/ASME/SAE/ASEE Joint Propulsion Conference*, San Jose, CA: American Institute of Aeronautics and Astronautics, Jul. 2013, ISBN: 978-1-62410-222-6. DOI: 10.2514/6.2013-3722. [Online]. Available: https://arc.aiaa.org/doi/10.2514/6.2013-3722 (visited on 12/19/2022).

[9] V. Bombelli, D. Simon, J.-L. Moerel, and T. Marée, “Economic benefits of the use of non-toxic mono-propellants for spacecraft applications,” in *39th AIAA/ASME/SAE/ASEE Joint Propulsion Conference and Exhibit*, Huntsville, Alabama: American Institute of Aeronautics and Astronautics, Jul. 20, 2003, ISBN: 978-1-62410-098-7. DOI: 10.2514/6.2003-4783. [Online]. Available: https://arc.aiaa.org/doi/10.2514/6.2003-4783 (visited on 01/17/2023).

[10] E. Schmidt and E. Wucherer, “Hydrazine(s) vs. Nontoxic Propellants – Where Do We Stand Now?” In *2nd Int. Conference on Green Propellants for Space Propulsion*, Cagliari, Sardinia, Italy, 2004. [Online]. Available: https://adsabs.harvard.edu/full/2004ESASP.557E...3S (visited on 01/07/2023).

[11] European Chemicals Agency, *Hydrazine Substance Information - ECHA*, 2022. [Online]. Available: https://echa.europa.eu/substance-information/-/substanceinfo/100.005.560 (visited on 01/15/2023).

[12] A. E. S. Nosseir, A. Cervone, and A. Pasini, “Review of State-of-the-Art Green Monopropellants: For Propulsion Systems Analysts and Designers,” *Aerospace*, vol. 8, no. 1, Jan. 2021, Publisher: Multidisciplinary Digital Publishing Institute, ISSN: 2226-4310. DOI: 10.3390/aerospace8010020. [Online]. Available: https://www.mdpi.com/2226-4310/8/1/20 (visited on 12/19/2022).

[13] R. L. Sackheim and R. K. Masse, “Green Propulsion Advancement: Challenging the Maturity of Monopropellant Hydrazine,” *Journal of Propulsion and Power*, vol. 30, no. 2, pp. 265–276, 2014, Publisher: American Institute of Aeronautics and Astronautics, ISSN: 0748-4658. DOI: 10.2514/1.B35086. [Online]. Available: https://doi.org/10.2514/1.B35086 (visited on 12/19/2022).

[14] A. R. Wilson, M. Vasile, C. Maddock, and K. Baker, “Implementing life cycle sustainability assessment for improved space mission design,” *Integrated Environmental Assessment and Management*, Jan. 18, 2023, ISSN: 1551-3777, 1551-3793. DOI: 10.1002/ieam.4722. [Online]. Available: https://onlinelibrary.wiley.com/doi/10.1002/ieam.4722 (visited on 02/22/2023).

[15] ESA Clean Space, *ESA LCA Database*, Oct. 2023.

[16] P. Deroo, “Sustainability analysis of liquid propulsion systems, literature study,” Mar. 16, 2023.

[17] O. Morgan and D. Meinhardt, “Monopropellant selection criteria - hydrazine and other options,” in *35th Joint Propulsion Conference and Exhibit*, Los Angeles,CA,U.S.A.: American Institute of Aeronautics and Astronautics, Jun. 20, 1999. DOI: 10.2514/6.1999-2595. [Online]. Available: https://arc.aiaa.org/doi/10.2514/6.1999-2595 (visited on 01/16/2023).

[18] Aerojet Rocketdyne, *Aerojet rocketdyne helping to propel modernization of gps satellite constellation*, Sep. 13, 2017. [Online]. Available: https://www.rocket.com/article/aerojet-rocketdyne-helping-propel-modernization-gps-satellite-constellation (visited on 01/23/2023).

[19] Aerojet Rocketdyne, *Aerojet rocketdyne propulsion guides cassini on its grand finale at saturn*, Sep. 17, 2017. [Online]. Available: https://www.rocket.com/article/aerojet-rocketdyne-propulsion-guides-cassini-its-grand-finale-saturn (visited on 01/23/2023).

[20] T. W. Price and D. D. Evans, “The status of monopropellant hydrazine technology,” Jet Propulsion Laboratory, Pasadena, California, USA, Feb. 15, 1968. [Online]. Available: https://ntrs.nasa.gov/api/citations/19680006875/downloads/19680006875.pdf (visited on 01/17/2023).

[21] A. S. Gohardani, J. Stanojev, A. Demairé, *et al.*, “Green space propulsion: Opportunities and prospects,” *Progress in Aerospace Sciences*, vol. 71, pp. 128–149, Nov. 2014, ISSN: 0376-0421. DOI: 10.1016/j.paerosci.2014.08.001. [Online]. Available: https://www.sciencedirect.com/science/article/pii/S0376042114000797 (visited on 12/19/2022).

[22] S. Carlotti and F. Maggi, “Evaluating New Liquid Storable Bipropellants: Safety and Performance Assessments,” *Aerospace*, vol. 9, no. 10, Oct. 2022, Publisher: Multidisciplinary Digital Publishing Institute, ISSN: 2226-4310. DOI: 10.3390/aerospace9100561. [Online]. Available: https://www.mdpi.com/2226-4310/9/10/561 (visited on 11/29/2022).

[23] M. Russi, “A survey of monopropellant hydrazine thruster technology,” in *9th Propulsion Conference*, Las Vegas, Nevada: American Institute of Aeronautics and Astronautics, Nov. 5, 1973. DOI: 10.2514/6.1973-1263. [Online]. Available: https://arc.aiaa.org/doi/10.2514/6.1973-1263 (visited on 01/23/2023).

[24] Heraeus Holding, *H-KC12GA*, 2023. [Online]. Available: https://www.heraeus.com/en/hpm/hmp_products_solutions/heterogeneous_catalysts/catalyst_product_selector/productdetail/89612108.html (visited on 11/18/2023).

[25] R. Schulte and C. Pisut, “Platinum group metals in november 2022,” US Geological Survey, 2022. [Online]. Available: https://www.usgs.gov/centers/national-minerals-information-center/platinum-group-metals-statistics-and-information (visited on 2023).

[26] K. Anflo and B. Crowe, “In-space demonstration of an adn-based propulsion system,” in *47th AIAA/ASME/SAE/ASEE Joint Propulsion Conference & Exhibit*, 2011. [Online]. Available: https://arc.aiaa.org/doi/abs/10.2514/6.2011-5832 (visited on 2022).

[27] E. Wernimont, M. Ventura, G. Garboden, and P. Mullens, “Past and Present Uses of Rocket Grade Hydrogen Peroxide,” 1999. [Online]. Available: https://citeseerx.ist.psu.edu/document?repid=rep1&type=pdf&doi=71eeddfe1f09fe59c1057592426c9636e85d361d (visited on 01/06/2023).

[28] S. L. Guseinov, S. G. Fedorov, V. A. Kosykh, and P. A. Storozhenko, “Hydrogen peroxide decomposition catalysts used in rocket engines,” *Russian Journal of Applied Chemistry*, vol. 93, no. 4, pp. 467–487, Apr. 1, 2020, ISSN: 1608-3296. DOI: 10.1134/S1070427220040011. [Online]. Available: https://doi.org/10.1134/S1070427220040011 (visited on 01/23/2023).

[29] M. Ventura, E. Wernimont, S. Heister, and S. Yuan, “Rocket Grade Hydrogen Peroxide (RGHP) for use in Propulsion and Power Devices - Historical Discussion of Hazards,” in *43rd AIAA/ASME/SAE/ASEE Joint Propulsion Conference & Exhibit*, Cincinnati, OH: American Institute of Aeronautics and Astronautics, Jul. 2007, ISBN: 978-1-62410-011-6. DOI: 10.2514/6.2007-5468. [Online]. Available: http://arc.aiaa.org/doi/abs/10.2514/6.2007-5468 (visited on 01/06/2023).

[30] A. Cervone, L. Torre, L. d’Agostino, *et al.*, “Development of hydrogen peroxide monopropellant rockets,” in *42nd AIAA/ASME/SAE/ASEE Joint Propulsion Conference & Exhibit*, 2006. [Online]. Available: https://arc.aiaa.org/doi/abs/10.2514/6.2006-5239 (visited on 01/24/2023).

[31] E. Wernimont, “System trade parameter comparison of monopropellants: Hydrogen peroxide vs hydrazine and others,” in *42nd AIAA/ASME/SAE/ASEE Joint Propulsion Conference & Exhibit*, Sacramento, California: American Institute of Aeronautics and Astronautics, Jul. 9, 2006, ISBN: 978-1-62410-038-3. DOI: 10.2514/6.2006-5236. [Online]. Available: http://arc.aiaa.org/doi/abs/10.2514/6.2006-5236 (visited on 01/17/2023).

[32] P. Surmacz, “Green rocket propulsion research and development at the institute of aviation : Problems and perspectives,” *Journal of KONES*, vol. Vol. 23, No. 1, pp. 337–344, 2016, ISSN: 1231-4005. DOI: 10.5604/12314005.1213534. [Online]. Available: http://yadda.icm.edu.pl/baztech/element/bwmeta1.element.baztech-452367c9-bcdc-4a01-b4d8-1da576658c6b (visited on 01/07/2023).

[33] P. Surmacz, “Influence of various types of al2o3/MnxOy catalysts on performance of a 100mm chamber for decomposition of 98%+ hydrogen peroxide,” *Prace Instytutu Lotnictwa*, vol. Nr 3 (240), 2015, ISSN: 0509-6669. DOI: 10.5604/05096669.1194986. [Online]. Available: http://yadda.icm.edu.pl/baztech/element/bwmeta1.element.baztech-ca70dfb8-99cb-44ef-b36e-a52db3d26867 (visited on 01/24/2023).

[34] J. Gramatyka, P. Paszkiewicz, D. Grabowski, *et al.*, “Development of POLON—A Green Microsatellite Propulsion Module Utilizing 98% Hydrogen Peroxide,” *Aerospace*, vol. 9, no. 6, Jun. 2022, Publisher: Multidisciplinary Digital Publishing Institute, ISSN: 2226-4310. DOI: 10.3390/aerospace9060297. [Online]. Available: https://www.mdpi.com/2226-4310/9/6/297 (visited on 01/08/2023).

[35] J. Lee, D. Jang, and S. Kwon, “Performance improvement of hydrogen peroxide monopropellant by blending ethanol,” in *48th AIAA/ASME/SAE/ASEE Joint Propulsion Conference & Exhibit*, Atlanta, Georgia: American Institute of Aeronautics and Astronautics, Jul. 30, 2012, ISBN: 978-1-60086-935-8. DOI: 10.2514/6.2012-3818. [Online]. Available: http://arc.aiaa.org/doi/abs/10.2514/6.2012-3818 (visited on 01/30/2023).

[36] J. Lee and S. Kwon, “Evaluation of ethanol-blended hydrogen peroxide monopropellant on a 10 n class thruster,” *Journal of Propulsion and Power*, vol. 29, no. 5, pp. 1164–1170, Sep. 2013, ISSN: 0748-4658, 1533-3876. DOI: 10.2514/1.B34790. [Online]. Available: https://arc.aiaa.org/doi/10.2514/1.B34790 (visited on 01/30/2023).

[37] J. Huh, J. Lee, D. Seo, S. Kang, and S. Kwon, “Fabrication of ethanol blended hydrogen peroxide 50 mN class MEMS thruster,” *Journal of Physics: Conference Series*, vol. 476, p. 012 124, Dec. 4, 2013, ISSN: 1742-6588, 1742-6596. DOI: 10.1088/1742-6596/476/1/012124. [Online]. Available: https://iopscience.iop.org/article/10.1088/1742-6596/476/1/012124 (visited on 01/30/2023).

[38] S. Baek, W. Jung, H. Kang, and S. Kwon, “Development of high-performance green-monopropellant thruster with hydrogen peroxide and ethanol,” *Journal of Propulsion and Power*, vol. 34, no. 5, pp. 1256–1261, 2018, Publisher: American Institute of Aeronautics and Astronautics, ISSN: 0748-4658. DOI: 10.2514/1.B37081. [Online]. Available: https://doi.org/10.2514/1.B37081 (visited on 12/19/2022).

[39] M. Palmer, G. Roberts, and A. Musker, “Design, build and test of a 20 n hydrogen peroxide monopropellant thruster,” in *47th AIAA/ASME/SAE/ASEE Joint Propulsion Conference & Exhibit*, San Diego, California: American Institute of Aeronautics and Astronautics, Jul. 31, 2011, ISBN: 978-1-60086-949-5. DOI: 10.2514/6.2011-5697. [Online]. Available: http://arc.aiaa.org/doi/abs/10.2514/6.2011-5697 (visited on 01/24/2023).

[40] H. Tian, T. Zhang, X. Sun, D. Liang, and L. Lin, “Performance and deactivation of ir/γ-al2o3 catalyst in the hydrogen peroxide monopropellant thruster,” *Applied Catalysis A: General*, vol. 210, no. 1, pp. 55–62, Mar. 9, 2001, ISSN: 0926-860X. DOI: 10.1016/S0926-860X(00)00829-2. [Online]. Available: https://www.sciencedirect.com/science/article/pii/S0926860X00008292 (visited on 01/30/2023).

[41] C. N. Ryan, E. Fonda-Marsland, G. T. Roberts, *et al.*, “Experimental validation of a 1-newton hydrogen peroxide thruster,” *Journal of Propulsion and Power*, vol. 36, no. 2, pp. 158–166, Mar. 2020, ISSN: 1533-3876. DOI: 10.2514/1.B37418. [Online]. Available: https://arc.aiaa.org/doi/10.2514/1.B37418 (visited on 05/30/2023).

[42] M. Ventura, “Long term storability of hydrogen peroxide,” in *41st AIAA/ASME/SAE/ASEE Joint Propulsion Conference*, Tucson, Arizona: American Institute of Aeronautics and Astronautics, Jul. 10, 2005, ISBN: 978-1-62410-063-5. DOI: 10.2514/6.2005-4551. [Online]. Available: http://arc.aiaa.org/doi/abs/10.2514/6.2005-4551 (visited on 01/30/2023).

[43] European Chemicals Agency. “Hydrogen peroxide substance information - ECHA.” (2022), [Online]. Available: https://echa.europa.eu/substance-information/-/substanceinfo/100.028.878 (visited on 01/31/2023).

[44] J. Wallbank, “Nitrous Oxide as a Green Monopropellant for Small Satellites,” in *2 nd Int. Conference on Green Propellants for Space Propulsion*, Cagliari, Sardinia, Italy, Jun. 2004.

[45] L. K. Werling, T. Hörger, K. Manassis, *et al.*, “Nitrous Oxide Fuels Blends: Research on Premixed Monopropellants at the German Aerospace Center (DLR) since 2014,” in *AIAA Propulsion and Energy 2020 Forum*, American Institute of Aeronautics and Astronautics, 2022. DOI: 10.2514/6.2020-3807. [Online]. Available: https://arc.aiaa.org/doi/abs/10.2514/6.2020-3807 (visited on 12/20/2022).

[46] A. Mayer, W. Wieling, A. Watts, M. Poucet, I. Waugh, and J. Macfarlane, “European fuel blend development for in-space propulsion,” in *Space Propulsion Conference*, Seville, Spain, May 2018. [Online]. Available: https://www.researchgate.net/profile/Alfons-Mayer/publication/326265722_EUROPEAN_FUEL_BLEND_DEVELOPMENT_FOR_IN-SPACE_PROPULSION/links/5c8f45fb299bf14e7e828044/EUROPEAN-FUEL-BLEND-DEVELOPMENT-FOR-IN-SPACE-PROPULSION.pdf (visited on 2023).

[47] R. Taylor, “Safety and Performance Advantages of Nitrous Oxide Fuel Blends (NOFBX) Propellants for Manned and Unmanned Spaceflight Applications,” in *IAASS Conference ‘A Safer Space for a Safer World’*, Versaille, France, Jan. 2012. [Online]. Available: https://ui.adsabs.harvard.edu/abs/2012ESASP.699E..67T (visited on 12/20/2022).

[48] S. La Luna, F. Maggi, and D. Zuin, “Prospective of self-pressurized technology for in space satellite mission,” in *9th European Conference for Aeronautics and Space Sciences (EUCASS)*, Lille, France, 2022. DOI: 10.13009/EUCASS2022-4904. [Online]. Available: https://www.eucass.eu/doi/EUCASS2022-4904.pdf (visited on 01/22/2023).

[49] European Chemicals Agency. “Dinitrogen oxide substance information - ECHA.” (2022), [Online]. Available: https://echa.europa.eu/substance-information/-/substanceinfo/100.030.017 (visited on 02/09/2023).

[50] L. David, *Explosion kills three at mojave air and space port*, 2007. [Online]. Available: https://www.space.com/4123-explosion-kills-mojave-air-space-port.html (visited on 02/09/2023).

[51] M. Persson, K. Anflo, and P. Friedhoff, “Flight heritage of ammonium dinitramide (ADN) based high performance green propulsion (HPGP) systems,” *Propellants, Explosives, Pyrotechnics*, vol. 44, no. 9, pp. 1073–1079, 2019, ISSN: 1521-4087. DOI: 10.1002/prep.201900248. [Online]. Available: https://onlinelibrary.wiley.com/doi/abs/10.1002/prep.201900248 (visited on 01/23/2023).

[52] M. Negri, “Replacement of hydrazine: Overview and first results of the h2020 project rheform,” in *6th European Conference for Aeronautics and Space Sciences (EUCASS)*, Kraków, Poland, 2015. [Online]. Available: https://www.dlr.de/ra/portaldata/55/resources/dokumente/rheform/replacement-of-hydrazine.pdf (visited on 12/27/2022).

[53] Bradford ECAPS, *High performance green propulsion*, 2022. [Online]. Available: https://www.ecaps.space/hpgp-characteristics.php (visited on 12/27/2022).

[54] D. Toenshoff, R. Lanam, J. Ragaini, A. Shchetkovskiy, and A. Smirnov, “Iridium coated rhenium rocket chambers produced by electroforming,” in *36th AIAA/ASME/SAE/ASEE Joint Propulsion Conference and Exhibit*, Las Vegas, Nevada: American Institute of Aeronautics and Astronautics, Jul. 24, 2000. DOI: 10.2514/6.2000-3166. [Online]. Available: https://arc.aiaa.org/doi/10.2514/6.2000-3166 (visited on 08/10/2023).

[55] Bradford ECAPS, *1n gp thruster*, 2022. [Online]. Available: https://www.ecaps.space/products-1ngp.php (visited on 12/27/2022).

[56] D. Freudenmann and H. K. Ciezki, “ADN and HAN-based monopropellants – a minireview on compatibility and chemical stability in aqueous media,” *Propellants, Explosives, Pyrotechnics*, vol. 44, no. 9, pp. 1084–1089, 2019, ISSN: 1521-4087. DOI: 10.1002/prep.201900127. [Online]. Available: https://onlinelibrary.wiley.com/doi/abs/10.1002/prep.201900127 (visited on 02/01/2023).

[57] M. Lennemar, *Propellant LMP-103s safety data sheet*, Jun. 9, 2016. [Online]. Available: https://static1.squarespace.com/static/603ed12be884730013401d7a/t/605916aae0a9e2324c7bc739/1616451243559/LMP-103S+MSDS.pdf (visited on 02/09/2023).

[58] European Chemicals Agency. “Methanol substance information - ECHA.” (2023), [Online]. Available: https://echa.europa.eu/substance-information/-/substanceinfo/100.000.599 (visited on 02/01/2023).

[59] European Chemicals Agency. “N-methylformamide substance information - ECHA.” (2022), [Online]. Available: https://echa.europa.eu/substance-information/-/substanceinfo/100.004.205 (visited on 02/01/2023).

[60] European Chemicals Agency. “Nitramide, n-nitro-, ammonium salt (1:1) substance information - ECHA.” (2021), [Online]. Available: https://echa.europa.eu/substance-information/-/substanceinfo/100.126.585 (visited on 02/01/2023).

[61] H. Mulkey, J. T. Miller, and C. Bacha, “Green Propellant Loading Demonstration at U.S. Range,” in *52nd AIAA/SAE/ASEE Joint Propulsion Conference*, Salt Lake City, Utah: American Institute of Aeronautics and Astronautics, Jul. 2016, ISBN: 978-1-62410-406-0. DOI: 10.2514/6.2016-4576. [Online]. Available: http://arc.aiaa.org/doi/10.2514/6.2016-4576 (visited on 01/13/2023).

[62] K. Anflo and R. Möllerberg, “Flight demonstration of new thruster and green propellant technology on the PRISMA satellite,” *Acta Astronautica*, vol. 65, no. 9, pp. 1238–1249, Nov. 2009, ISSN: 0094-5765. DOI: 10.1016/j.actaastro.2009.03.056. [Online]. Available: https://www.sciencedirect.com/science/article/pii/S0094576509001970 (visited on 12/27/2022).

[63] R. Jankovsky, “HAN-based monopropellant assessment for spacecraft,” in *32nd Joint Propulsion Conference and Exhibit*, Lake Buena Vista, Florida: American Institute of Aeronautics and Astronautics, Jul. 1, 1996. DOI: 10.2514/6.1996-2863. [Online]. Available: https://arc.aiaa.org/doi/10.2514/6.1996-2863 (visited on 01/17/2023).

[64] R. Masse, M. Allen, R. Spores, and E. A. Driscoll, “AF-M315E Propulsion System Advances and Improvements,” in *52nd AIAA/SAE/ASEE Joint Propulsion Conference*, Salt Lake City, Utah: American Institute of Aeronautics and Astronautics, Jul. 2016, ISBN: 978-1-62410-406-0. DOI: 10.2514/6.2016-4577. [Online]. Available: http://arc.aiaa.org/doi/10.2514/6.2016-4577 (visited on 01/05/2023).

[65] W. S. Chai, K. H. Cheah, M.-H. Wu, K. S. Koh, D. Sun, and H. Meng, “A review on hydroxylammonium nitrate (HAN) decomposition techniques for propulsion application,” *Acta Astronautica*, vol. 196, pp. 194–214, Jul. 1, 2022, ISSN: 0094-5765. DOI: 10.1016/j.actaastro.2022.04.011. [Online]. Available: https://www.sciencedirect.com/science/article/pii/S0094576522001588 (visited on 02/02/2023).

[66] M. Fokema and J. Torkelson, *Thermally stable catalyst and process for the decomposition of liquid propellants*, US Patent App. 11/457,985, 2007. [Online]. Available: https://patentimages.storage.googleapis.com/68/0a/0a/32b303f95c7b99/US20070184971A1.pdf (visited on 02/02/2023).

[67] R. A. Spores, “GPIM AF-m315e propulsion system,” in *51st AIAA/SAE/ASEE Joint Propulsion Conference*, Orlando, Florida: American Institute of Aeronautics and Astronautics, Jul. 27, 2015, ISBN: 978-1-62410-321-6. DOI: 10.2514/6.2015-3753. [Online]. Available: http://arc.aiaa.org/doi/10.2514/6.2015-3753 (visited on 01/17/2023).

[68] D. Andrews, G. Huggins, E. G. Lightsey, *et al.*, “Design of a green monopropellant propulsion system for the lunar flashlight CubeSat mission,” in *34th Annual Small Satellite Conference*, Logan, Utah, 2020. [Online]. Available: https://digitalcommons.usu.edu/smallsat/2020/all2020/155/ (visited on 01/21/2023).

[69] T. Malik, *Nasa’s tiny lunar flashlight moon probe may be in trouble in deep space*, Jan. 12, 2023. [Online]. Available: https://www.space.com/nasa-lunar-spacecraft-moon-probe-in-trouble (visited on 02/02/2023).

[70] K. Hori, T. Katsumi, S. Sawai, N. Azuma, K. Hatai, and J. Nakatsuka, “HAN-based green propellant, SHP163 – its r&d and test in space,” *Propellants, Explosives, Pyrotechnics*, vol. 44, no. 9, pp. 1080–1083, 2019, ISSN: 1521-4087. DOI: 10.1002/prep.201900237. [Online]. Available: https://onlinelibrary.wiley.com/doi/abs/10.1002/prep.201900237 (visited on 02/02/2023).

[71] R. Amrousse, T. Katsumi, N. Azuma, and K. Hori, “Hydroxylammonium nitrate (HAN)-based green propellant as alternative energy resource for potential hydrazine substitution: From lab scale to pilot plant scale-up,” *Combustion and Flame*, vol. 176, pp. 334–348, Feb. 2017, ISSN: 0010-2180. DOI: 10.1016/j.combustflame.2016.11.011. [Online]. Available: https://www.sciencedirect.com/science/article/pii/S0010218016303510 (visited on 01/05/2023).

[72] Digital Solid State Propulsion Inc, *Af-m315e safety data sheet*, 2020. [Online]. Available: https://static1.squarespace.com/static/59de9c9c18b27ddf3bac610a/t/5e3af2d0fb8df43f9b2ae377/1580921553250/AF-M315E+SDS.pdf (visited on 02/03/2023).

[73] European Chemicals Agency. “Hydroxylammonium nitrate - substance information - ECHA.” (2022), [Online]. Available: https://echa.europa.eu/substance-information/-/substanceinfo/100.033.342 (visited on 02/10/2023).

[74] U. Gotzig, M. Wurdak, and N. Harmansa, “Development and coupled thruster / electrolyser tests of a water propulsion system,” *Acta Astronautica*, vol. 202, pp. 751–759, Jan. 1, 2023, ISSN: 0094-5765. DOI: 10.1016/j.actaastro.2022.09.059. [Online]. Available: https://www.sciencedirect.com/science/article/pii/S0094576522005367 (visited on 02/10/2023).

[75] A. Porter, M. Freedman, R. Grist, C. Wesson, and M. Hanson, “Flight qualification of a water electrolysis propulsion system,” in *35th Annual Small Satellite Conference*, Logan, Utah, Jul. 9, 2021. [Online]. Available: https://digitalcommons.usu.edu/cgi/viewcontent.cgi?article=5083&context=smallsat (visited on 02/10/2023).

[76] N. Harmansa, G. Herdrich, and S. Fasoulas, “Development of a water propulsion system for small satellites,” in *68th International Astronautical Conference*, Adelaide, Australia, Sep. 29, 2017. [Online]. Available: https://www.researchgate.net/profile/Nicholas-Harmansa/publication/320407544_Development_of_a_Water_Propulsion_System_for_Small_Satellites_-_IAC_2017/links/59e304b1458515393d5b3b4f/Development-of-a-Water-Propulsion-System-for-Small-Satellites-IAC-2017.pdf (visited on 02/10/2023).

[77] M. Hwang, T.-S. Rho, and H. J. Lee, “Conceptual design and performance analysis of water electrolysis propulsion system with catalytic igniter for CubeSats,” *Acta Astronautica*, vol. 200, pp. 316–328, Nov. 1, 2022, ISSN: 0094-5765. DOI: 10.1016/j.actaastro.2022.08.022. [Online]. Available: https://www.sciencedirect.com/science/article/pii/S00945765220 0426X (visited on 02/13/2023).

[78] U.S. Secretary of Commerce, *Nist chemistry webbook | water*, 2021. [Online]. Available: https://webbook.nist.gov/cgi/cbook.cgi?Name=water&Units=SI (visited on 02/13/2023).

[79] Moog Inc., *Rolling diaphragm tanks*, 2013. [Online]. Available: https://www.moog.com/content/dam/moog/literature/sdg/space/propulsion/moog-rolling-diaphragm-tanks-datasheet.pdf (visited on 01/17/2023).

[80] W. van Meerbeeck, R. Deijs, K. Das, R. Koopmans, and P. van Put, “Design and development of the p200 propulsion system,” in *Space Propulsion 2022*, Estoril, Portugal, May 9, 2022.

[81] K. V. Mani, A. Cervone, and F. Topputo, “Combined chemical–electric propulsion for a standalone mars CubeSat,” *Journal of Spacecraft and Rockets*, vol. 56, no. 6, pp. 1816–1830, Nov. 2019, ISSN: 0022-4650, 1533-6794. DOI: 10.2514/1.A34519. [Online]. Available: https://arc.aiaa.org/doi/10.2514/1.A34519 (visited on 01/17/2023).

[82] A. Talaksi and E. G. Lightsey, “Manufacturing, Integration, and Testing of the Green Monopropellant Propulsion System for NASA’s Lunar Flashlight Mission,” M.S. thesis, The Georgia Institute of Technology, Atlanta, GA, 2020. [Online]. Available: https://ssdl.gatech.edu/sites/default/files/ssdl-files/papers/mastersProjects/AE%5C%208900%5C%20Paper_Talaksi.pdf (visited on 12/19/2022).

[83] G. M. Huggins, A. Talaksi, D. Andrews, *et al.*, “Development of a CubeSat-scale green monopropellant propulsion system for NASA’s lunar flashlight mission,” in *AIAA Scitech 2021 Forum*, VIRTUAL EVENT: American Institute of Aeronautics and Astronautics, Jan. 11, 2021, ISBN: 978-1-62410-609-5. DOI: 10.2514/6.2021-1976. [Online]. Available: https://arc.aiaa.org/doi/10.2514/6.2021-1976 (visited on 01/21/2023).

[84] G. P. Sutton and O. Biblarz, *Rocket Propulsion Elements*, 9th. Hoboken, New Jersey: John Wiley & Sons, 2017.

[85] European Space Agency, *Clean space*, 2023. [Online]. Available: https://technology.esa.int/program/clean-space (visited on 03/04/2023).

[86] B. Purvis, Y. Mao, and D. Robinson, “Three pillars of sustainability: In search of conceptual origins,” *Sustainability Science*, vol. 14, no. 3, pp. 681–695, May 1, 2019, ISSN: 1862-4057. DOI: 10.1007/s11625-018-0627-5. [Online]. Available: https://doi.org/10.1007/s11625-018-0627-5 (visited on 02/20/2023).

[87] D. H. Meadows, D. L. Meadows, J. Randers, and W. W. Behrens, *The Limits to growth: a report for the Club of Rome’s project on the predicament of mankind*. New York: Universe Books, 1972, 205 pp., ISBN: 978-0-87663-165-2.

[88] G. H. Brundtland, “Our common future—call for action,” *Environmental conservation*, vol. 14, no. 4, pp. 291–294, 1987.

[89] United Nations, *The 17 goals | sustainable development*, 2023. [Online]. Available: https://sdgs.un.org/goals (visited on 03/04/2023).

[90] P. T. Anastas and M. M. Kirchhoff, “Origins, current status, and future challenges of green chemistry,” *Accounts of Chemical Research*, vol. 35, no. 9, pp. 686–694, Sep. 1, 2002, ISSN: 0001-4842, 1520-4898. DOI: 10.1021/ar010065m. [Online]. Available: https://pubs.acs.org/doi/10.1021/ar010065m (visited on 03/09/2023).

[91] P. T. Anastas and R. L. Lankey, “Life cycle assessment and green chemistry: The yin and yang of industrial ecology,” *Green Chemistry*, vol. 2, no. 6, pp. 289–295, 2000, ISSN: 14639262, 14639270. DOI: 10.1039/b005650m. [Online]. Available: http://xlink.rsc.org/?DOI=b005650m (visited on 03/09/2023).

[92] G. J. D. Calabuig, L. Miraux, A. R. Wilson, A. Sarritzu, and A. Pasini, "Eco-design of future reusable launchers: Insight into their life cycle and atmospheric impact," in *9th European Conference for Aeronautics and Aerospace Sciences*, Lille, France, 2022. [Online]. Available: https://elib.dlr.de/187098/1/EUCASS-2022_Eco-Design_of_future_reusable_launchers_insight_into_their_life_cycle_and_atmospheric_impact.pdf (visited on 02/22/2023).

[93] ClearSpace, *Clearspace - a mission to make space sustainable*, 2023. [Online]. Available: https://clearspace.today/ (visited on 11/17/2023).

[94] MaiaSpace, *Maiaspace - homepage*, 2023. [Online]. Available: https://maia-space.com/ (visited on 11/17/2023).

[95] J. B. Guinée, R. Heijungs, G. Huppes, *et al.*, "Life cycle assessment: Past, present, and future," *Environmental Science & Technology*, vol. 45, no. 1, pp. 90–96, Jan. 1, 2011, Publisher: American Chemical Society, ISSN: 0013-936X. DOI: 10.1021/es101316v. [Online]. Available: https://doi.org/10.1021/es101316v (visited on 03/02/2023).

[96] International Standards Office, *ISO 14040:2006, environmental management - life cycle assessment - principles and framework*, Jul. 1, 2006. [Online]. Available: https://wapsustainability.com/wp-content/uploads/2020/11/ISO-14040.pdf (visited on 03/03/2023).

[97] M. Finkbeiner, E. M. Schau, A. Lehmann, and M. Traverso, "Towards life cycle sustainability assessment," *Sustainability*, vol. 2, no. 10, pp. 3309–3322, Oct. 2010, Publisher:Multidisciplinary Digital Publishing Institute, ISSN: 2071-1050. DOI: 10.3390/su2103309. [Online]. Available: https://www.mdpi.com/2071-1050/2/10/3309 (visited on 02/22/2023).

[98] J. B. Pettersen, H. Bergsdal, M. M. Bjørnbet, *et al.*, "Ecodesign for space and aerospace: What happens when we make ecodesign relevant for demanding applications?" In *Challenges in European Aerospace− 5th CEAS Air & Space Conference*, Delft, The Netherlands, 2015. [Online]. Available: https://aerospace-europe.eu/media/books/CEAS2015_062.pdf (visited on 02/26/2023).

[99] ESA LCA Working Group, *Space system Life Cycle Assessment (LCA) guidelines Prepared by*. ESA, Oct. 2016.

[100] ESA Clean Space, *Lca - space debris user portal*, 2023. [Online]. Available: https://sdup.esoc.esa.int/lca/ (visited on 11/17/2023).

[101] ecoinvent. "Ecoinvent database - ecoinvent." (Jul. 15, 2020), [Online]. Available: https://ecoinvent.org/the-ecoinvent-database/ (visited on 12/02/2023).

[102] J. A. Dallas, S. Raval, J. P. Alvarez Gaitan, S. Saydam, and A. G. Dempster, "The environmental impact of emissions from space launches: A comprehensive review," *Journal of Cleaner Production*, vol. 255, May 10, 2020, ISSN: 0959-6526. DOI: 10.1016/j.jclepro.2020.120209. [Online]. Available: https://www.sciencedirect.com/science/article/pii/S0959652620302560 (visited on 12/08/2022).

[103] S. S. Neumann, "Environmental life cycle assessment of commercial space transportation activities in the united states," Doctor of Philosophy, University of Texas at Arlington, Apr. 20, 2018. [Online]. Available: https://rc.library.uta.edu/uta-ir/handle/10106/27352 (visited on 12/07/2022).

[104] A. Chanoine, "Environmental impacts of launchers and space missions," ESA Clean Space Industrial Days 2017, Noordwijk, The Netherlands, Oct. 25, 2017. [Online]. Available: https://indico.esa.int/event/181/contributions/1443/attachments/1336/1561/2017_CSID_Chanoine_LCA_launcher_space_missions_FV.PDF (visited on 02/23/2023).

[105] A. Gallice, T. Maury, and E. del Olmo, "Environmental impact of the exploitation of the ariane 6 launch system," ESA Cleanspace Industrial Days 2018, Noordwijk, The Netherlands, Oct. 23, 2018. [Online]. Available: https://indico.esa.int/event/234/contributions/3918/attachments/3115/4259/2018CSID_AGallice_EnvironmentalLifeCycleImpactAnalysisOfA6ExploitationPhase.pdf (visited on 03/01/2023).

[106] P. E. Schabedoth, "Life cycle assessment of rocket launches and the effects of the propellant choice on their environmental performance," Master thesis, NTNU, 2020. [Online]. Available: https://ntnuopen.ntnu.no/ntnu-xmlui/handle/11250/2779647 (visited on 12/08/2022).

[107] S. Morales and A. Chanoine, “Environmental expert evaluation of ESA space system life cycle assessment guidelines,” ESA Cleanspace Industrial Days 2021, Noordwijk, The Netherlands. [Online]. Available: https://indico.esa.int/event/321/contributions/6356/attachments/4381/6605/ESA_CSID%5C%202021_Evaluation%5C%20of%5C%20LCA%5C%20guidelines_v1.pdf (visited on 12/08/2022).

[108] J. Austin, “Developing a standardised methodology for space- specific life cycle assessment,” in *Challenges in European Aerospace− 5th CEAS Air & Space Conference*, Delft, The Netherlands, 2015. [Online]. Available: https://aerospace-europe.eu/media/books/CEAS2015_237.pdf (visited on 12/08/2022).

[109] W. Kloepffer, “Life cycle sustainability assessment of products,” *The International Journal of Life Cycle Assessment*, vol. 13, no. 2, pp. 89–95, Mar. 2008, ISSN: 0948-3349, 1614-7502. DOI: 10.1065/lca2008.02.376. [Online]. Available: http://link.springer.com/10.1065/lca2008.02.376 (visited on 11/25/2023).

[110] A. R. Wilson, “Advanced methods of life cycle assessment for space systems,” Doctor of Philosophy, University of Strathclyde, Glasgow, United Kingdom, Dec. 2019. [Online]. Available: http://stax.strath.ac.uk/downloads/vh53ww116 (visited on 02/22/2023).

[111] Metasat UK, *Strathclyde space systems database v1.0.3*, Sep. 2023.

[112] A. R. Wilson, M. Vasile, C. Maddock, and K. J. Baker, “The strathclyde space systems database: A new life cycle sustainability assessment tool for the design of next generation green space systems,” in *8th International Systems & Concurrent Engineering for Space Applications Conference*, Glasgow, United Kingdom, Sep. 26, 2018. [Online]. Available: https://strathprints.strath.ac.uk/65685/1/Wilson_etal_SECESA_2018_The_Strathclyde_space_system_database.pdf (visited on 02/17/2023).

[113] J.-S. Fischer, S. Fasoulas, C. Brun-Buisson, and E. del Olmo, “Comparison of the environmental impact of production and launch emissions of different common launcher architectures,” presented at the ESA Clean Space Industry Days 2023, Noordwijk, The Netherlands, 2023. [Online]. Available: https://indico.esa.int/event/450/contributions/8861/attachments/5686/9442/2023_10_17_Presentation_CSID_Lifecyast_v1_1.pdf (visited on 11/20/2023).

[114] J. R. Wertz, D. F. Everett, and J. J. Puschell, *Space Mission Analysis and Design*, 3rd ed. Microcosm Press, 1999, ISBN: 978-1-881883-16-6.

[115] European Commission. “European platform on LCA | EPLCA.” (2023), [Online]. Available: https://eplca.jrc.ec.europa.eu/EnvironmentalFootprint.html (visited on 11/22/2023).

[116] US Department of Transport, *Systems engineering for its handbook - section 3 what is systems engineering?* Jan. 2007. [Online]. Available: https://ops.fhwa.dot.gov/publications/seitsguide/section3.htm (visited on 02/25/2023).

[117] B. Zandbergen, *Thermal Rocket Propulsion*. TU Delft, Aug. 20, 2020.

[118] E. Williams and Eikenaar. “Finding your way in multifunctional processes and recycling,” PRé Sustainability. (Jul. 14, 2022), [Online]. Available: https://pre-sustainability.com/articles/finding-your-way-in-allocation-methods-multifunctional-processes-recycling/ (visited on 11/22/2023).

[119] A. R. Wilson, *Strathclyde space systems database user guide version 1.0.0*, Dec. 2019.

[120] GreenDelta. “Openlca.org | homepage.” (2022), [Online]. Available: https://www.openlca.org/ (visited on 11/28/2023).

[121] B. Yost, S. Weston, R. Alena, R. De Rosee, and A. Dono, “State-of-the-art small spacecraft technology,” NASA Ames Research Center, Moffett Field, California, Oct. 2022. [Online]. Available: https://www.nasa.gov/sites/default/files/atoms/files/2022_soa_full_0.pdf (visited on 01/17/2023).

[122] Kepler Communications Inc., *Network - kepler communications*, 2022. [Online]. Available: https://kepler.space/network/ (visited on 06/22/2023).

[123] G. D. Krebs, *Lemur-2 (6u) - gunter’s space page*, 2023. [Online]. Available: https://space.skyrocket.de/doc_sdat/lemur-2_6u.htm (visited on 06/22/2023).

[124] Planet, *Planet | insights - our constellations*, 2022. [Online]. Available: https://www.planet.com/our-constellations/ (visited on 06/22/2023).

[125] Aerojet Rocketdyne, *In-space propulsion data sheets*, 2019. [Online]. Available: https://www.rocket.com/sites/default/files/documents/In-Space%5C%20Data%5C%20Sheets_7.19.21.pdf (visited on 02/05/2023).

[126] R. Lea, *Artemis 1 cubesats: The 10 tiny satellites hitching a nasa ride to the moon | space*, Aug. 22, 2022. [Online]. Available: https://www.space.com/nasa-artemis-1-moon-mission-cubesats (visited on 06/22/2023).

[127] A. Tabor, *Innovative propulsion system gets ready to help study moon orbit for artemis | nasa*, Mar. 23, 2021. [Online]. Available: https://www.nasa.gov/feature/ames/innovative-propulsion-system-gets-ready-to-help-study-moon-orbit-for-artemis (visited on 06/22/2023).

[128] A. Cervone, F. Topputo, S. Speretta, *et al.*, "LUMIO: A CubeSat for observing and characterizing micro-meteoroid impacts on the lunar far side," *Acta Astronautica*, vol. 195, pp. 309–317, Jun. 1, 2022, ISSN: 0094-5765. DOI: 10.1016/j.actaastro.2022.03.032. [Online]. Available: https://www.sciencedirect.com/science/article/pii/S0094576522001424 (visited on 04/06/2023).

[129] T. Gardner, B. Cheetham, J. Parker, *et al.*, "CAPSTONE: A summary of flight operations to date in the cislunar environment," in *36th Annual Small Satellite Conference*, Logan, Utah, Aug. 6, 2022. [Online]. Available: https://digitalcommons.usu.edu/cgi/viewcontent.cgi?article=5267&context=smallsat (visited on 06/23/2023).

[130] Starlink, *How starlink works*, 2023. [Online]. Available: https://www.starlink.com/technology (visited on 02/06/2023).

[131] BryceTech, "Smallsats by the numbers 2023," Feb. 6, 2023. [Online]. Available: https://brycetech.com/reports/report-documents/Bryce_Smallsats_2023.pdf (visited on 02/23/2023).

[132] R. Salome and L. Godard, "The myriade microsatellite hydrazine propulsion subsystem," in *38th AIAA/ASME/SAE/ASEE Joint Propulsion Conference & Exhibit*, Indianapolis, Indiana: American Institute of Aeronautics and Astronautics, Jul. 7, 2002, ISBN: 978-1-62410-115-1. DOI: 10.2514/6.2002-4153. [Online]. Available: http://arc.aiaa.org/doi/abs/10.2514/6.2002-4153 (visited on 06/14/2023).

[133] G. D. Krebs, *Skysat 3, ..., 21 (skysat c1, ..., 19) - gunter's space page*, Jan. 14, 2023. [Online]. Available: https://space.skyrocket.de/doc_sdat/skysat-3.htm (visited on 06/23/2023).

[134] G. D. Krebs, *Galileo 5, ..., 34 (galileo-foc fm1, ..., fm30) - gunter's space page*, Jan. 14, 2023. [Online]. Available: https://space.skyrocket.de/doc_sdat/galileo-foc.htm (visited on 02/24/2023).

[135] G. D. Krebs, *Gps-3 (navstar-3) - gunter's space page*, Jan. 22, 2023. [Online]. Available: https://space.skyrocket.de/doc_sdat/navstar-3.htm (visited on 02/24/2023).

[136] National Coordination Office for Space-Based Positioning, Navigation, and Timing, *Gps.gov: Space segment*, Jun. 28, 2022. [Online]. Available: https://www.gps.gov/systems/gps/space/ (visited on 02/24/2023).

[137] M. Persson, K. Anflo, A. Dinardi, and J. Bahu, "A family of thrusters for ADN-based monopropellant LMP-103s," in *48th AIAA/ASME/SAE/ASEE Joint Propulsion Conference & Exhibit*, Atlanta, Georgia: American Institute of Aeronautics and Astronautics, Jul. 30, 2012, ISBN: 978-1-60086-935-8. DOI: 10.2514/6.2012-3815. [Online]. Available: http://arc.aiaa.org/doi/abs/10.2514/6.2012-3815 (visited on 01/17/2023).

[138] B. Haemmerli, D. Digre, T. Jøraholmen, *et al.*, "Overview of the development of a h2o2 based chemical attitude control system for vega-c," in *7th Space Propulsion Conference*, Estoril, Portugal, Mar. 17, 2021. [Online]. Available: https://www.ecosimpro.com/wp-content/uploads/2021/05/SP2020_363_Haemmerli.pdf (visited on 01/17/2023).

[139] SpaceX, *Falcon user's guide*, Sep. 2021. [Online]. Available: https://www.spacex.com/media/falcon-users-guide-2021-09.pdf (visited on 01/03/2024).

[140] United Nations Development Program (UNDP), *Environment and development nexus in kazakhstan*, 2004. [Online]. Available: https://www.thegef.org/sites/default/files/ncsa-documents/2147-22347.pdf (visited on 2023).

[141] A. Dinardi, K. Anflo, and P. Friedhoff, "On-orbit commissioning of high performance green propulsion (HPGP) in the SkySat constellation," presented at the 31st Annual AIAA/USU Conference on Small Satellites, Salt Lake City, Utah, Aug. 2017. [Online]. Available: https://digitalcommons.usu.edu/cgi/viewcontent.cgi?article=3670&context=smallsat (visited on 04/06/2023).

[142] European Space Agency, *Esa - vega-c*, 2023. [Online]. Available: https://www.esa.int/Enabling_Support/Space_Transportation/Launch_vehicles/Vega-C (visited on 02/24/2023).

[143] G. D. Krebs, *Flock-1, -1b, -1c, -1d, -1d', -1e, -1f, -2b, -2e, -2e', -2k, -2p, -3m, -3p, -3p', -3r, -3s, -4a, -4e, -4e', -4p, -4s, -4v, -4x, -4y - gunter's space page*, Jan. 20, 2023. [Online]. Available: https://space.skyrocket.de/doc_sdat/flock-1.htm (visited on 02/24/2023).

[144] S. R. Tsitas and J. Kingston, "6u CubeSat commercial applications," *The Aeronautical Journal*, vol. 116, no. 1176, pp. 189–198, Feb. 2012, ISSN: 0001-9240, 2059-6464. DOI: 10.1017/S0001924000006692. [Online]. Available: https://www.cambridge.org/core/product/identifier/S0001924000006692/type/journal_article (visited on 04/16/2023).

[145] G. D. Krebs, *Orbital launches of 2022 - gunter's space page*, Jun. 14, 2023. [Online]. Available: https://space.skyrocket.de/doc_chr/lau2022.htm (visited on 02/25/2023).

[146] R. Sandau, "Status and trends of small satellite missions for earth observation," *Acta Astronautica*, vol. 66, no. 1, pp. 1–12, Jan. 1, 2010, ISSN: 0094-5765. DOI: 10.1016/j.actaastro.2009.06.008. [Online]. Available: https://www.sciencedirect.com/science/article/pii/S0094576509003488 (visited on 04/19/2023).

[147] J. C. McDowell, "The low earth orbit satellite population and impacts of the spacex starlink constellation," *The Astrophysical Journal Letters*, vol. 892, no. 2, 2020. [Online]. Available: https://iopscience.iop.org/article/10.3847/2041-8213/ab8016 (visited on 06/25/2023).

[148] R. J. Boain, "A-b-cs of sun-synchronous orbit mission design," in *14th AAS/AIAA Space Flight Mechanics Conference*, Maui, Hawaii, Feb. 8, 2004. [Online]. Available: https://dataverse.jpl.nasa.gov/dataset.xhtml?persistentId=hdl:2014/37900 (visited on 05/03/2023).

[149] K. Murthy, M. Shearn, B. D. Smiley, A. H. Chau, J. Levine, and M. D. Robinson, "Skysat-1: Very high-resolution imagery from a small satellite," in *Sensors, systems, and next-generation Satellites XVIII*, SPIE, vol. 9241, 2014, pp. 367–378. [Online]. Available: https://ui.adsabs.harvard.edu/abs/2014SPIE.9241E..1EM/abstract (visited on 04/24/2023).

[150] B. Randolph, W. Hreha, and A. Q. Rogers, "Key technology, programmatic drivers, and lessons learned for production of proliferated small satellite constellations," presented at the 33rd Annual Small Satellite Conference, Logan, Utah, Jul. 16, 2019. [Online]. Available: https://digitalcommons.usu.edu/cgi/viewcontent.cgi?article=4562&context=smallsat (visited on 04/24/2023).

[151] European Space Agency, *SkySat - earth online*, 2023. [Online]. Available: https://earth.esa.int/eogateway/missions/skysat (visited on 04/24/2023).

[152] J. Dyer, A. Dinardi, and K. Anflo, "First implementation of high performance green propulsion in a constellation of small satellites," in *27th Annual AIAA/USU Conference on Small Satellites*, Boulder, Colorado, Aug. 14, 2013. [Online]. Available: https://digitalcommons.usu.edu/smallsat/2013/all2013/92 (visited on 05/13/2023).

[153] G. Tyc, J. Tulip, D. Schulten, M. Krischke, and M. Oxfort, "The RapidEye mission design," *Acta Astronautica*, 4th IAA International Symposium on Small Satellites for Earth Observation, vol. 56, no. 1, pp. 213–219, Jan. 1, 2005, ISSN: 0094-5765. DOI: 10.1016/j.actaastro.2004.09.029. [Online]. Available: https://www.sciencedirect.com/science/article/pii/S0094576504003170 (visited on 04/21/2023).

[154] D. Schulten, G. Tyc, Y. Brown, J. Steyn, N. Hannaford, and W. Larson, "Rapideye system commissioning and on-orbit performance," in *23rd Annual AIAA/USU Conference on Small Satellites*, 2009. [Online]. Available: https://digitalcommons.usu.edu/cgi/viewcontent.cgi?referer=&httpsredir=1&article=1287&context=smallsat (visited on 04/21/2023).

[155] National Aeronautics and Space Administration, *The benefits of constellation flying*, 2023. [Online]. Available: https://atrain.nasa.gov/constellation_flying.php (visited on 06/27/2023).

[156] National Aeronautics and Space Administration, *The afternoon constellation - a-train*, Jun. 28, 2023. [Online]. Available: https://atrain.nasa.gov/index.php (visited on 06/28/2023).

[157] Centre National D'Études Spatiales, *Myriade platform*, Mar. 17, 2015. [Online]. Available: https://parasol.cnes.fr/en/PARASOL/plateforme.htm (visited on 06/28/2023).

[158] National Aeronautics and Space Administration, *CloudSat-CALIPSO launch press kit*, Apr. 18, 2006. [Online]. Available: https://www.jpl.nasa.gov/news/press_kits/cloudsat-calipso-launch.pdf (visited on 06/28/2023).

[159] Centre National D'Études Spatiales, *Spacecraft bus*, Mar. 20, 2017. [Online]. Available: https://proteus.cnes.fr/en/PROTEUS/platform.htm (visited on 06/28/2023).

[160] J. Harbaugh, *Nasa's green propellant infusion mission nears completion | nasa*, Oct. 20, 2020. [Online]. Available: https://www.nasa.gov/mission_pages/tdm/green/gpim-nears-completion.html (visited on 06/28/2023).

[161] National Research & Development Agency, Japan Aerospace Exploration Agency, *Rapid innovative payload demonstration satellite 1 (rapis-1) ends its operation*, Jun. 25, 2020. [Online]. Available: https://global.jaxa.jp/press/2020/06/20200625-1_e.html (visited on 06/28/2023).

[162] Planet, *Pelican | planet*, 2020. [Online]. Available: https://www.planet.com/products/pelican/ (visited on 06/28/2023).

[163] G. D. Krebs, *Pelican 1, ..., x - gunter's space page*, Jan. 14, 2023. [Online]. Available: https://space.skyrocket.de/doc_sdat/pelican.htm (visited on 06/28/2023).

[164] A. Hawkins, J. Carrico, S. Motiwala, and C. MacLachlan, "Flight dynamics operations and collision avoidance for the skysat imaging constellation," in *9th International Workshop on Satellite Constellations and Formation Flying*, Boulder, Colorado, Jul. 2017. [Online]. Available: https://www.researchgate.net/publication/327050155_Flight_Dynamics_Operations_And_Collision_Avoidance_For_The_Skysat_Imaging_Constellation (visited on 06/29/2023).

[165] Airbus Defence and Space, *Pléiades neo | the best of very-high resolution imagery*, 2023. [Online]. Available: https://www.intelligence-airbusds.com/imagery/constellation/pleiades-neo/ (visited on 06/29/2023).

[166] N. Tanaka, T. Matsuo, K. Furukawa, M. Nishida, S. Suemori, and A. Yasutake, "The "greening" of spacecraft reaction control systems," *Mitsubishi Heavy Industries Technical Review*, vol. 48, no. 4, Dec. 2011. [Online]. Available: https://www.mhi.co.jp/technology/review/pdf/e484/e484044.pdf (visited on 05/19/2023).

[167] ArianeGroup. "Orbital propulsion fluidic equipment." (2023), [Online]. Available: https://www.space-propulsion.com/brochures/valves/space-propulsion-valves.pdf (visited on 05/30/2023).

[168] Chemical and Material Sciences Department Research Division Rocketdyne, "Hydrogen peroxide handbook," Air Force Rocket Propulsion Laboratory Research and Technology Division, Edwards, California, Jul. 1967.

[169] ECAPS. "Rocket engines," ECAPS. (2023), [Online]. Available: https://www.ecaps.se/rocket-engines (visited on 12/02/2023).

[170] Northrop Grumman. "Diaphragm tanks data sheets – sorted by volume," Northrop Grumman. (2023), [Online]. Available: https://www.northropgrumman.com/space/diaphragm-tanks-data-sheets-sorted-by-volume (visited on 05/31/2023).

[171] Holscot. "Bladders and diaphragms for containment of space propellants," Holscot Fluoropolymers. (2023), [Online]. Available: https://holscot.com/products/fluoroplastic-containment-tanks/satellite-propulsion-tank-containment/ (visited on 06/15/2023).

[172] I. Ballinger and D. Sims, "Development of an EPDM elastomeric material for use in hydrazine propulsion systems," in *39th AIAA Propulsion Conference*, Huntsville, Alabama, Jul. 21, 2003. [Online]. Available: https://docplayer.net/64997961-Development-of-an-epdm-elastomeric-material-for-use-in-hydrazine-propulsion-systems.html (visited on 05/31/2023).

[173] Aerospace Specification Metals Inc. “ASM material data sheet: Titanium ti-6al-4v (grade 5), annealed.” (2023), [Online]. Available: https://asm.matweb.com/search/SpecificMaterial.asp?bassnum=mtp641 (visited on 05/23/2023).

[174] Matweb. “Aluminum 5254-h112.” (2023), [Online]. Available: https://www.matweb.com/search/datasheet.aspx?matguid=8326e8e1fda74b41ba0375e3010b463e (visited on 05/23/2023).

[175] W. Tam, G. Kawahara, K. Wlodarczyk, H. Gutierrez, and D. Kirk, “Review of ATK diaphragm tanks-an update,” Jun. 1, 2018. [Online]. Available: https://www.researchgate.net/publication/325499162_Review_of_ATK_Diaphragm_Tanks-An_Update (visited on 05/22/2023).

[176] Nammo Raufoss, *Aluminium propellant tank*, 2021. [Online]. Available: https://www.nammo.com/wp-content/uploads/2021/04/2021-Nammo-Raufoss-Aluminium-Propellant-Tank.pdf (visited on 06/20/2023).

[177] Aerojet Rocketdyne, *Monopropellant rocket engines*, 2019. [Online]. Available: https://www.rocket.com/space/space-power-propulsion/monopropellant-rocket-engines (visited on 01/23/2023).

[178] G. Rarata, W. Florczuk, and J. Smetek, “Research on preparation and propulsive applications of highly concentrated hydrogen peroxide,” *Jour. of Aerospace Science and Technology*, vol. 2, no. 1, Jan. 28, 2016, ISSN: 23328258, 23328258. DOI: 10.17265/2332-8258/2016.01.006. [Online]. Available: http://www.davidpublisher.org/index.php/Home/Article/index?id=26756.html (visited on 08/17/2023).

[179] M. Negri, M. Wilhelm, C. Hendrich, *et al.*, “New technologies for ammonium dinitramide based monopropellant thrusters – the project RHEFORM,” *Acta Astronautica*, vol. 143, pp. 105–117, Feb. 1, 2018, ISSN: 0094-5765. DOI: 10.1016/j.actaastro.2017.11.016. [Online]. Available: https://www.sciencedirect.com/science/article/pii/S0094576517309402 (visited on 02/01/2023).

[180] P. Lier and M. Bach, “PARASOL a microsatellite in the a-train for earth atmospheric observations,” *Acta Astronautica*, vol. 62, no. 2, pp. 257–263, Jan. 1, 2008, ISSN: 0094-5765. DOI: 10.1016/j.actaastro.2006.12.052. [Online]. Available: https://www.sciencedirect.com/science/article/pii/S0094576507001804 (visited on 06/21/2023).

[181] A. E. S. Nosseir, A. Cervone, and A. Pasini, “Modular impulsive green monopropellant propulsion system (MIMPS-g): For CubeSats in LEO and to the moon,” *Aerospace*, vol. 8, no. 6, Jun. 2021, Publisher: Multidisciplinary Digital Publishing Institute, ISSN: 2226-4310. DOI: 10.3390/aerospace8060169. [Online]. Available: https://www.mdpi.com/2226-4310/8/6/169 (visited on 06/13/2023).

[182] Mott Corporation. “Propellant/actuator filters for space.” (Jan. 2022), [Online]. Available: https://mottcorp.com/wp-content/uploads/2022/01/Mott-Propellant-Filters-Rev-0122.pdf (visited on 12/02/2023).

[183] Moog. “Single line isolation latch valves.” (2022), [Online]. Available: https://www.moog.com/content/dam/moog/literature/sdg/space/propulsion/moog-single-line-isolation-latch-valves-datasheet.pdf (visited on 08/10/2023).

[184] Minco. “Minco thermal solutions design guide.” (2023), [Online]. Available: https://www.minco.com/wp-content/uploads/Minco-Thermal-Solutions-Design-Guide.pdf (visited on 12/02/2023).

[185] Fine Tubes. “Seamless tubes: Stainless steel, nickel, titanium.” (2023), [Online]. Available: https://www.finetubes.co.uk/products/www.finetubes.co.uk/products/seamless-tubes (visited on 08/09/2023).

[186] Bradford Space. “Mini pressure transducer.” (Apr. 2018), [Online]. Available: https://static1.squarespace.com/static/603ed12be884730013401d7a/t/6054f4c51001e742aa4111b0/1616180422980/be_datasheet_minipt_2018apr.pdf (visited on 12/02/2023).

[187] Moog. “Fill and drain service valves.” (2022), [Online]. Available: https://www.moog.com/content/dam/moog/literature/sdg/space/propulsion/moog-manual-fill-and-drain-valves-datasheet.pdf (visited on 05/30/2023).

[188] F. Benedic, J.-P. Leard, and C. Lefloch, “Helium high pressure tanks at EADS space transportation new technology with thermoplastic liner,” EADS ST, Jul. 13, 2005. [Online]. Available: https://apps.dtic.mil/sti/citations/ADA445482 (visited on 10/31/2023).

[189] Tradingeconomics. “Aluminum - price - chart - historical data - news.” (Nov. 2023), [Online]. Available: https://tradingeconomics.com/commodity/aluminum (visited on 11/02/2023).

[190] Tradingeconomics. “Titanium - price - chart - historical data - news.” (Nov. 2023), [Online]. Available: https://tradingeconomics.com/commodity/titanium (visited on 11/02/2023).

[191] P. Nuss and M. J. Eckelman, “Life cycle assessment of metals: A scientific synthesis,” *PLOS ONE*, vol. 9, no. 7, Jul. 7, 2014, Publisher: Public Library of Science, ISSN: 1932-6203. DOI: 10.1371/journal.pone.0101298. [Online]. Available: https://journals.plos.org/plosone/article?id=10.1371/journal.pone.0101298 (visited on 08/21/2023).

[192] M. Classen, H.-J. Althaus, S. Blaser, and W. Scharnhorst, “Life cycle inventories of metals,” Swiss Centre for Life Cycle Inventories, Dübendorf, Germany, Mar. 2009. [Online]. Available: https://db.ecoinvent.org/reports/10_Metals_v2.1.pdf?area=463ee7e58cbf8 (visited on 08/21/2023).

[193] E. J. Wucherer, T. Cook, M. Stiefel, R. Humphries, and J. Parker, “Hydrazine catalyst production - sustaining s-405 technology,” in *39th AIAA/ASME/SAE/ASEE Joint Propulsion Conference and Exhibit*, Huntsville, Alabama: American Institute of Aeronautics and Astronautics, Jul. 20, 2003, ISBN: 978-1-62410-098-7. DOI: 10.2514/6.2003-5079. [Online]. Available: https://arc.aiaa.org/doi/10.2514/6.2003-5079 (visited on 01/23/2023).

[194] W. L. Petty, “Variation in shell 405 catalyst physical characteristics, test catalyst preparation:” Defense Technical Information Center, Fort Belvoir, VA, Jul. 1, 1973. DOI: 10.21236/AD0769888. [Online]. Available: http://www.dtic.mil/docs/citations/AD0769888 (visited on 09/07/2023).

[195] P. J. Birbara, “Catalyst for hydrazine decomposition,” U.S. Patent 4348303A, Sep. 7, 1982. [Online]. Available: https://patents.google.com/patent/US4348303A/en (visited on 10/25/2023).

[196] Thermocoax Space. “Catalyst bed heaters - our solutions for space mission thrusters.” (2023), [Online]. Available: https://www.thermocoax-space.com/catalyst-bed-heater/ (visited on 08/15/2023).

[197] A. Dinardi and M. Persson, “High performance green propulsion (HPGP): A flight-proven capability and cost game-changer for small and secondary satellites,” in *26th Annual AIAA/USU Conference on Small Satellites*, Logan, Utah, Aug. 14, 2012. [Online]. Available: https://digitalcommons.usu.edu/cgi/viewcontent.cgi?article=1033&context=smallsat (visited on 09/29/2023).

[198] N. Pokrupa, K. Anflo, and O. Svensson, “Spacecraft system level design with regards to incorporation of a new green propulsion system,” in *47th AIAA/ASME/SAE/ASEE Joint Propulsion Conference & Exhibit*, San Diego, California: American Institute of Aeronautics and Astronautics, Jul. 31, 2011. DOI: 10.2514/6.2011-6129. [Online]. Available: https://arc.aiaa.org/doi/abs/10.2514/6.2011-6129 (visited on 05/02/2023).

[199] satsearch. “PEPT-230 | satsearch.” (May 2023), [Online]. Available: https://satsearch.co/products/rafael-pept-230 (visited on 12/03/2023).

[200] Moog. “Monopropellant thruster valves.” (2018), [Online]. Available: https://www.moog.com/content/dam/moog/literature/sdg/space/propulsion/moog-monopropellant-thruster-valves-datasheet.pdf (visited on 08/11/2023).

[201] M. J. Mullally, “Thruster Valve,” U.S. Patent 5,150,879, Sep. 29, 1992. [Online]. Available: https://patents.google.com/patent/US5150879A/en?oq=US5%2c150%2c879 (visited on 09/05/2023).

[202] ArianeGroup. “1 n monopropellant hydrazine thruster.” (2023), [Online]. Available: https://www.space-propulsion.com/spacecraft-propulsion/hydrazine-thrusters/1n-hydrazine-thruster.html (visited on 12/03/2023).

[203] Stainless Europe. “Stainless steel acid-resistant seamless tube OD 6,35 mm x 0,71 mm steel grade 1.4301 / 1.4307 / 304 / 304l 300cm,” Stainless Europe online shop. (Nov. 2023), [Online]. Available: https://en.stainlesseurope.com/en_US/p/Stainless-steel-acid-resistant-seamless-tube-OD-6%2C35-mm-x-0%2C71-mm-steel-grade-1.4301-1.4307-304-304L-300cm/24248 (visited on 11/01/2023).

[204] T. McKechnie and A. Shchetkovskiy, “High temperature combustion chambers produced by electroforming,” in *Space Propulsion Conference*, Cologne, Germany, May 2014. [Online]. Available: https://www.researchgate.net/publication/301221541_High_Temperature_Combustion_Chambers_Produced_by_Electroforming (visited on 08/10/2023).

[205] R. H. Tuffias, J. Harding, and R. Kaplan, “High temperature corrosion resistant composite structure,” U.S. Patent 4917968A, Apr. 17, 1990. [Online]. Available: https://patents.google.com/patent/US4917968A/en?oq=patent+4%2c917%2c968 (visited on 09/25/2023).

[206] J. Stachowicz, “Optimization and additive manufacturing for HPGP rocket engines,” Master of Science, KTH Royal Institute of Technology, Stockholm, Sweden, 2022. [Online]. Available: http://kth.diva-portal.org/smash/get/diva2:1721906/FULLTEXT01.pdf (visited on 09/25/2023).

[207] Rocket Research Corporation, *Development of design and scaling criteria for monopropellant hydrazine reactors employing shell 405 spontaneous catalyst*, Jan. 19, 1967.

[208] I. Pekkanen, “Concentration of hydrogen peroxide and improving its energy efficiency,” Master thesis, Lappeenranta University of Technology, 2014. [Online]. Available: https://lutpub.lut.fi/bitstream/handle/10024/101947/Concentration%20of%20hydrogen%20peroxide%20and%20improving%20its%20energy%20efficiency.pdf?sequence=2&isAllowed=y (visited on 08/16/2023).

[209] T. Bossi and J. Gediga, “The environmental profile of platinum group metals,” *Johnson Matthey Technology Review*, vol. 61, no. 2, pp. 111–121, Apr. 1, 2017, ISSN: 2056-5135. DOI: 10.1595/205651317X694713. [Online]. Available: http://www.ingentaconnect.com/content/10.1595/205651317X694713 (visited on 11/09/2023).

[210] G. Changbin, Chenjun, and J. Zongxia, “Dynamic characteristic analysis of monostable torque motor valve of bipropellant thrusters,” in *2015 International Conference on Fluid Power and Mechatronics (FPM)*, Harbin, China: IEEE, Aug. 2015, pp. 332–336, ISBN: 978-1-4799-8770-2. DOI: 10.1109/FPM.2015.7337135. [Online]. Available: http://ieeexplore.ieee.org/document/7337135/ (visited on 12/08/2023).

[211] J. B. Pettersen and M. A. Salgado Delgado, “Harmonized space LCA data for efficient ecodesign,” ESA Cleanspace Industrial Days 2018, Noordwijk, The Netherlands, Oct. 23, 2018. [Online]. Available: https://indico.esa.int/event/234/contributions/3745/attachments/3029/3678/Harmonized_space_LCA_Pettersen_2018.pdf (visited on 03/03/2023).

[212] Nammo. “Fill and drain valve - nammo.” (2021), [Online]. Available: https://www.nammo.com/product/fdv-fvv/ (visited on 12/03/2023).

[213] Nammo. “Dual in-line thruster valve - nammo.” (2021), [Online]. Available: https://www.nammo.com/product/dual-inline-thruster-valve/ (visited on 12/03/2023).

[214] W. Wei, P. B. Samuelsson, A. Tilliander, R. Gyllenram, and P. G. Jönsson, “Energy consumption and greenhouse gas emissions during ferromolybdenum production,” *Journal of Sustainable Metallurgy*, vol. 6, no. 1, pp. 103–112, Mar. 1, 2020, ISSN: 2199-3831. DOI: 10.1007/s40831-019-00260-8. [Online]. Available: https://doi.org/10.1007/s40831-019-00260-8 (visited on 12/12/2023).

[215] A. L. Greig and S. Carey, “International molybdenum association (IMOA) life cycle assessment program and perspectives on the LCA harmonization effort,” *The International Journal of Life Cycle Assessment*, vol. 21, no. 11, pp. 1554–1558, Nov. 1, 2016, ISSN: 1614-7502. DOI: 10.1007/s11367-015-0990-8. [Online]. Available: https://doi.org/10.1007/s11367-015-0990-8 (visited on 12/12/2023).

[216] M. Lange, A. Lein, U. Gotzig, *et al.*, “Introduction of a high-performance ADN based monopropellant thruster on the myriade propulsion subsystem,” in *2013 6th International Conference on Recent Advances in Space Technologies (RAST)*, Jun. 2013, pp. 549–553. DOI: 10.1109/RAST.2013.6581271. [Online]. Available: https://ieeexplore.ieee.org/document/6581271/ (visited on 01/17/2023).

[217] A. Wilson, M. Vasile, and H. Oqab, “Life cycle assessment of the UK space energy initiative technology roadmap,” *Journal of the British Interplanetary Society*, vol. 76, no. 1, pp. 18–28, Apr. 7, 2023, ISSN: 0007084X. DOI: 10.59332/jbis-076-01-0018. [Online]. Available: https://bis-space.com/shop/product/jbis-076-01-0018 (visited on 12/13/2023).

[218] F. Bagchus, “A data quality assessment method for life cycle inventories in LCA,” ESA Clean Space Industry Days 2023, Noordwijk, The Netherlands, Oct. 17, 2023. [Online]. Available: https://indico.esa.int/event/450/contributions/8874/attachments/5673/9429/V2_Presentation_DQA_CSID_17-10-2023.pdf (visited on 12/19/2023).

[219] M. Damen, “EU strategic autonomy 2013-2023,” European Parliamentary Research Service, Jul. 2022. [Online]. Available: https://www.europarl.europa.eu/RegData/etudes/BRIE/2022/733589/EPRS_BRI(2022)733589_EN.pdf (visited on 12/18/2023).

[220] European Commission, “Critical raw materials resilience: Charting a path towards greater security and sustainability,” European Commission, Brussels, 52020DC0474, 2020. [Online]. Available: https://eur-lex.europa.eu/legal-content/EN/TXT/?uri=CELEX:52020DC0474 (visited on 08/09/2023).

[221] T. Jaekel, “Problematic platinum: The responsibility of swedish companies in south africa,” Swedwatch, 64, Oct. 2013. [Online]. Available: https://swedwatch.org/wp-content/uploads/2017/12/Problematic-Platinum-web.pdf (visited on 12/18/2023).

A

Propulsion system sizing code

This appendix presents the code used in the propulsion system sizing for the various propellant options, the method for which was discussed in Subsection 6.2.5.

```
# Import packages
import numpy as np
from matplotlib import pyplot as plt


# Create Propulsion System class
class Propsystem():
    def __init__(self):
        # Initialize with default settings
        # Propellant properties (default = Hydrazine, MR-103J)
        self.prop = {'type': "Hyd", 'rho': 1010, 'Isp': 239, 'm_thruster': 0.37}
        # Pressurant properties (default = Helium)
        self.press = {'type': "He", 'M': 0.004}
        # Tank material properties (default = Ti-6Al-4V, SIFA 35 diaphragm: Matweb and
            Ballinger and Sims)
        self.tank = {'type': "Ti", 'rho': 4430, 'yield': 880*10**6, 'rho_dia': 1120, 't_dia':
             0.00178}

        self.systemmass = 0         # Total propulsion system mass [kg]
        self.nthrusters = 4         # Number of thrusters (default = 4)
        self.T_thruster = 1         # Thrust per thruster [N] (default = 1N)
        self.m_dry = 150            # Satellite dry mass [kg]

        # Delta-V contributions (all with 15% margin)
        self.dV_deorbit = 80.70             # De-orbit from 567 km orbit [m/s]
        self.dV_positioning = 11.5          # Initial phasing into constellation [m/s]
        self.dV_maintenance_1year = 3.45    # Orbit maintenance per year [m/s]
        self.dV_phasing_1year = 1.15        # Phasing per year [m/s]
        self.dV_avoidance_1year = 1.33333*1.15   # Collision avoidance budget per year [m/s]

        # Constants
        self.g_0 = 9.80665          # Gravitational acceleration [m/s^2]
        self.R = 8.3145             # Gas constant [J/mol/K]

    def choosepropandpress(self, prop='Hyd', press='He'):
        # LMP-103S properties (Isp: Negri et al. 2015, thruster: Bradford ECAPS 1N HPGP)
        LMP_props = {'type': "LMP", 'rho': 1238, 'Isp': 254, 'm_thruster': 0.39}

        # ASCENT properties (Isp: Uramachi et al. 2019, thruster: Aerojet GR-1 (mass from
            ECAPS 1N HPGP))
        ASC_props = {'type': "ASC", 'rho': 1470, 'Isp': 266, 'm_thruster': 0.39}

        # SHP163 properties (Isp: Uramachi et al. 2019)
        SHP_props = {'type': "SHP", 'rho': 1400, 'Isp': 276, 'm_thruster': 0.37}

```

```
        # 98% HTP properties (Isp: Wernimont 2006)
        HTP_props = {'type': "HTP", 'rho': 1440, 'Isp': 190, 'm_thruster': 0.37}

        # Tank material properties for Al 5254 and FEP (Teflon) diaphragm (Matweb (entries 2-3), NASA (4)  Holscot(5-6))
        Al_props = {'type': "Al", 'rho': 2660, 'yield': 117*10**6, 'AOL': 0.00205, 'rho_dia': 2150, 't_dia': 0.00025}
        N2_props = {'type': 'N2', 'M': 0.028}                       # Nitrogen properties

        if prop not in ('Hyd', 'LMP', 'ASC', 'SHP', 'HTP'):
            print("Propellant not included in model")
        if press not in ('He', 'N2'):
            print("Pressurant not included in model")

        # Set propellant and pressurant properties according to input
        if prop == 'LMP':
            self.prop = LMP_props
            print("Propellant set to LMP-103S")
        elif prop == 'ASC':
            self.prop = ASC_props
            print("Propellant set to ASCENT")
        elif prop == 'SHP':
            self.prop = SHP_props
            print("Propellant set to SHP163")
        elif prop == 'HTP':
            self.prop = HTP_props
            self.tank = Al_props
            print("Propellant set to 98% HTP")
            print("Tank material set to AL 5254")
        if press == 'N2':
            self.press = N2_props
            print("Pressurant set to N2")

    # Function to determine
    @staticmethod
    def AOLcalculator(m1, c1, V_tank, V, days):
        # Chemical constants
        M_O2 = 0.032                                    # Oxygen molar mass [kg/mol]
        M_H2O = 0.018                                   # Water molar mass [kg/mol]
        M_H2O2 = 0.034                                  # Hydrogen peroxide molar mass [kg/mol]

        # Tank properties
        r_tank = (V_tank / np.pi * 3 / 4) ** (1 / 3)    # Tank radius (assumed spherical) [m]

        # AOL determination in function of S/V
        if V > V_tank/2:                                # Lower hemisphere is fully covered with propellant
            S = 2 * np.pi * r_tank ** 2                 # Wetted tank surface [m^2]

        else:
            V_press = V_tank - V                            # Pressurant volume [m^3]
            r_press = (V_press / np.pi * 3 / 4) ** (1 / 3)  # Radius of spherical pressurant volume [m]
            r_tank2 = r_tank * (1 / 2) ** (1 / 3)           # Radius of half-tank sphere [m]
            r_diff = r_press - r_tank2                      # Radial difference [m]
            S = 2 * np.pi * (r_tank - r_diff) ** 2          # Surface of tank exposed (not covered by diaphragm) [m^2]

        surfvolratio_inch = S / V / 39.3701                 # Surface to volume ratio [1/inch]
        AOL = (0.175 * surfvolratio_inch + 0.0075) / 100 ** 2       # AOL for Al 5052, 90% HTP (conservative)

        # Determination of reacted mass and moles
        m_O2 = AOL * 0.47 * c1 * m1 * days                          # Mass of generated oxygen [kg]
        n_O2 = m_O2 / M_O2                                          # Moles of generated oxygen [mol]
        m_H2O2 = 2 * n_O2 * M_H2O2                                  # Mass of decomposed HTP [kg]
```

```
103         m_H2O = 2 * n_O2 * M_H2O                                    # Mass of generated water
                [kg]
104
105         # New HTP values
106         m2 = m1 - m_O2                                              # New total mass [kg]
107         c2 = (m1 * c1 - m_H2O2)/m2                                  # New HTP concentration
                [%/100]
108         Isp = 190 - (190-150.47)/(0.98-0.85) * (0.98-c2)            # New Isp, source Nosseir
                et al. 2021 [s]
109
110         return m2, c2, Isp, surfvolratio_inch
111
112     def sizetank(self, years_lifetime, p0=25*10**5, bdr=4, dV=0):
113
114         # Setting up dV budget if mission lifetime is given
115         if dV ==0:
116             dV = years_lifetime*(self.dV_avoidance_1year+self.dV_phasing_1year+self.
                    dV_maintenance_1year)\
117                  + self.dV_deorbit + self.dV_positioning
118             print(dV)
119
120         # Design constants
121         expulsion_ratio = 0.98      # Percentage of propellant effectively expelled
122         n_Isp = 0.85                # Isp quality
123         sf_tank = 1.25              # Tank yield strength safety factor (TRP Reader)
124         mountf_tank = 1.85          # Sizing factor for tank mounting and interfaces (TRP
                Reader)
125         t_min = 0.00085             # Minimum tank thickness (TRP reader) [m]
126
127         Isp = self.prop['Isp']      # Specific impulse [s]
128         p1 = p0 / bdr               # Final tank pressure [Pa]
129         T_tank = 273.15 + 20        # Tank temperature [K]
130         m_dry = self.m_dry          # System dry mass [kg]
131         g_0 = self.g_0              # Gravitational constant [m/s^2]
132
133         # Required propellant mass [kg]
134         m_prop_req = (np.exp(dV/g_0/Isp/n_Isp)-1)*m_dry/(1-(1-expulsion_ratio)*np.exp(dV/g_0/
                Isp/n_Isp))
135
136         # Iterative procedure to ensure acceptable HTP loss
137         if self.prop['type'] == 'HTP':
138             print("Required usable propellant mass:", np.round(m_prop_req, 2), "kg")
139             done = False                                            # Initial mass not
                    yet found
140             m_prop_i = m_prop_req                                   # Initial guess
141
142             # Average delta-V per week [m/s]
143             dV_week = (self.dV_maintenance_1year + self.dV_phasing_1year + self.
                    dV_avoidance_1year) / 52
144
145             while not done:
146                 m_prop = m_prop_i                                   # Initial propellant
                        mass [kg]
147                 c = 0.98                                            # Initial HTP
                        concentration
148                 m_sc = self.m_dry + m_prop_i                        # Initial spacecraft
                        wet mass [kg]
149
150                 V_prop_i = m_prop_i / self.prop['rho']              # Initial propellant
                        volume [m^3]
151                 V_press_i = V_prop_i / (bdr - 1)                    # Initial pressurant
                        volume [m^3]
152                 V_tank_i = V_press_i + V_prop_i                     # Tank volume for
                        this iteration [m^3]
153
154                 # Propellant burned for initial phasing [kg]
155                 m_burn_positioning = m_sc * (1-np.exp(-self.dV_positioning/g_0/Isp/n_Isp))
156                 m_prop -= m_burn_positioning                        # Update total
                        propellant mass
157                 m_sc -= m_burn_positioning                          # Update total
                        spacecraft wet mass
```

```
158
159                 for i in range(years_lifetime*52):                      # Decrease mass per
                        week
160                     # Passive HTP decomp. per week
161                     V_prop_i = m_prop / self.prop['rho']
162                     m_prop, c, Isp, _ = self.AOLcalculator(m_prop, c, V_tank_i, V_prop_i, 7)
163                     m_sc = self.m_dry + m_prop
164
165                     # Propellant burned per week [kg]
166                     m_burn_week = m_sc * (1-np.exp(-dV_week/g_0/Isp/n_Isp))
167                     # Update propellant and spacecraft wet mass
168                     m_prop -= m_burn_week
169                     m_sc -= m_burn_week
170
171                 # Propellant burned for final de-orbit maneuver [kg]
172                 m_burn_deorbit = m_sc * (1-np.exp(-self.dV_deorbit/g_0/Isp/n_Isp))
173                 # Update propellant and spacecraft wet mass
174                 m_prop -= m_burn_deorbit
175                 m_sc -= m_burn_deorbit
176
177                 if m_prop >= 0:         # If there is propellant left after mission maneuvers
                        , design is good
178                     print("Propellant margin:", np.round(m_prop, 2), "kg")
179                     m_prop = m_prop_i/expulsion_ratio   # Required initial propellant mass
                            with HTP loss
180                     done = True
181                 else:                   # Increase initial propellant mass for next iteration
182                     m_prop_i = m_prop_i + 0.1
183         else:
184             m_prop = m_prop_req         # If another propellant than HTP is used, no
                    additional propellant is required
185
186         V_prop = m_prop/self.prop['rho']                                # Propellant volume [
                m^3]
187         self.prop['Mass'] = m_prop                                      # Save mass to class
                variable
188         self.prop['Vol'] = V_prop                                       # Save volume to
                class variable
189
190         # Pressurant load
191         V_press0 = V_prop / (bdr-1)                                     # Initial pressurant
                volume [m^3]
192         rho_press0 = p0 / (self.R/self.press['M']*T_tank)               # Initial pressurant
                density [kg/m^3]
193         m_press = V_press0 * rho_press0                                 # Pressurant mass [kg
                ]
194         V_press1 = m_press / (p1/(self.R/self.press['M']*T_tank))       # Final pressurant
                volume [m^3]
195         self.press['Mass'] = m_press                                    # Save mass to class
                variable
196         self.press['Vol'] = V_press0                                    # Save volume to
                class variable
197
198         # Tank parameters
199         V_tank = V_prop + V_press0                                      # Tank inner volume [
                m^3]
200         r_tank = (V_tank / np.pi * 3/4)**(1/3)                          # Tank radius (
                assumed spherical) [m]
201
202         t_tank_press = sf_tank * p0 * r_tank / 2 / self.tank['yield']   # Tank wall thickness
                 for pressure load [m]
203         t_tank = np.max((t_tank_press, t_min))                          # Minimum tank wall
                thickness [m]
204         V_tank_mat = 4 * np.pi * (r_tank+t_tank/2)**2 * t_tank          # Tank material
                volume [m^3]
205         m_tank_shell = V_tank_mat * self.tank['rho']                    # Tank shell mass [kg
                ]
206         m_dia = 2 * np.pi * r_tank**2 * self.tank['t_dia'] * self.tank['rho_dia']   # Tank
                diaphragm mass [kg]
207
```

```
208         m_tank_dry = m_tank_shell * mountf_tank + m_dia                 # Total tank dry mass
                [kg]
209
210         self.tank['m_dry'] = m_tank_dry                                 # Save dry mass to
                class variable
211         self.tank['m_wet'] = m_tank_dry + m_prop + m_press              # Save wet mass to
                class variable
212         self.tank['Vol'] = V_tank                                       # Save volume to
                class variable
213
214         # Print results
215         print("Total propellant mass:", np.round(m_prop, 3), "kg")
216         print("Propellant volume:", np.round(V_prop, 4), "m^3")
217         print("Pressurant mass:", np.round(m_press, 3), "kg")
218         print("BOL pressurant volume:", np.round(V_press0, 4), "m^3")
219         print("Tank inner diameter:", np.round(r_tank*2, 2), "m")
220         print("Tank volume:", np.round(V_tank, 4), "m^3")
221         print("Tank dry mass:", np.round(self.tank['m_dry'], 3), "kg")
222         print("Tank wall thickness", np.round(t_tank*10**3, 2), "mm")
223         print("Tank wet mass:", np.round(self.tank['m_wet'], 2), "kg\n")
224
225     def sizesystem(self, years_lifetime, p0=25*10**5, bdr=4, n_thrusters=4, dV=0,
            massbreakdown=False):
226         # Design constants
227         if n_thrusters != 4:
228             self.nthrusters = n_thrusters
229
230         # Set component masses
231         if self.tank['type'] == 'Ti':
232             m_latch = 0.320             # Latch valve mass (Moog SS single line isolation
                    valve)[kg]
233             m_service = 0.209           # Fill-drain valve mass (Moog SS low pressure)[kg]
234             m_PT = 0.125                # Pressure transducer mass (Bradford SS Mini PT)[kg]
235             m_orifice = 0               # Flow restrictor mass [kg]
236             m_filter = 0.06             # Filter mass (Mott small filter for mass flow of
                    0.45 g/s)[kg]
237             m_heater = 0.005            # Heater mass [kg] (Polyimide+Acrylic heater, mass
                    assumed from Minco Thermofoil)
238
239         if self.tank['type'] == 'Al':
240             m_latch = 0.320             # Latch valve mass (Moog SS single line isolation
                    valve)[kg]
241             m_service = 0.209           # Fill-drain valve mass (Moog SS low pressure)[kg]
242             m_vent = 0.09               # HTP vent valve (ArianeGroup Oxidiser vent valve) [
                    kg]
243             m_PT = 0.125                # Pressure transducer mass (Bradford SS Mini PT)[kg]
244             m_orifice = 0               # Flow restrictor mass [kg]
245             m_filter = 0.06             # Filter mass (Mott small filter for mass flow of
                    0.45 g/s)[kg]
246             m_heater = 0.005            # Heater mass [kg](Polyimide+Acrylic heater, mass
                    assumed from Minco Thermofoil)
247
248         # Size tank
249         self.sizetank(years_lifetime, p0, bdr, dV)
250
251         # Add components to total system mass
252         self.systemmass = self.tank['m_dry']                            # Start with tank dry
                mass
253         self.systemmass += n_thrusters * self.prop['m_thruster']        # Add thrusters to the
                system
254         self.systemmass += 2 * m_service                                # Add service valves to
                the system
255         self.systemmass += m_latch                                      # Add latch valve to the
                system
256         if self.prop['type'] == 'HTP':                                  # Add relief valve if HTP
                 is used
257             self.systemmass += m_vent
258         self.systemmass += m_PT                                         # Add PT to the system
259         self.systemmass += m_filter                                     # Add propellant filter
                to the system
```

```
260         self.systemmass += 4 * m_heater                                 # Add heaters to the
                system (2 + 2)
261
262         m_piping = self.systemmass * 0.15                               # Take 15% for piping (
                assumed from TRP reader)
263         self.systemmass += m_piping
264         m_wiring = self.systemmass * 0.05                               # Add 5% margin for
                wiring and control (assumed from
265                                                                         # Nosseir et al. MIMPS-G
                                                                                )
266         self.systemmass += m_wiring
267
268         print("Total system dry mass:", np.round(self.systemmass, 2), "kg")
269         print("Total system wet mass:", np.round(self.systemmass + self.prop['Mass'] + self.
                press['Mass'], 2), "kg\n")
270
271         if massbreakdown:
272             print("Mass Breakdown (kg):")
273             print("Propellant filter:", np.round(m_filter, 3))
274             print("Latch valve:", np.round(m_latch, 3))
275             print("Patch heater:", np.round(4*m_heater, 3))
276             print("Piping:", np.round(m_piping, 3))
277             print("Pressure transducer", np.round(m_PT, 3))
278             if self.prop['type'] == 'HTP':
279                 print("Relief valve:", np.round(m_vent, 3))
280             print("Fill/drain valves", np.round(m_service*2, 3))
281             print("Tank", np.round(self.tank['m_dry'], 3))
282             print("Thrusters", np.round(4*self.prop['m_thruster'], 3))
283             print("Wiring", np.round(m_wiring, 3),"\n")
284
285
286 if __name__ == "__main__":
287
288     # Hydrazine
289     hydsystem = Propsystem()
290     hydsystem.sizesystem(10, p0=25*10**5, massbreakdown=True)
291
292     # ASCENT
293     ASCsystem = Propsystem()
294     ASCsystem.choosepropandpress('ASC')
295     ASCsystem.sizesystem(10, massbreakdown=True)
296
297     # LMP-103S
298     LMPsystem = Propsystem()
299     LMPsystem.choosepropandpress('LMP')
300     LMPsystem.sizesystem(10, massbreakdown=True)
301
302
303
304     # HTP
305     HTPsystem = Propsystem()
306     HTPsystem.choosepropandpress('HTP')
307     HTPsystem.sizesystem(10, massbreakdown=True)
308
309
310     # Validation
311     print("SkySat Validation")
312     SkySat = Propsystem()
313     SkySat.m_dry = 120
314     SkySat.choosepropandpress('LMP')
315     SkySat.dV_deorbit = 0
316     SkySat.sizesystem(1, p0=18.5*10**5, bdr=3.7, dV=180)
317
318     print("Altius Validation")
319     Altius = Propsystem()
320     Altius.m_dry = 200
321     Altius.dV_deorbit = 0
322     Altius.sizesystem(1, dV=120)
323
324     print("PRISMA VAlidation")
325     PRISMA = Propsystem()
```

```
    PRISMA.m_dry = 120
    PRISMA.choosepropandpress('LMP')
    PRISMA.dV_deorbit = 0
    PRISMA.sizesystem(1, p0=18.5*10**5, bdr=3.8, n_thrusters=2, dV=90)

    print("Myriade Validation")
    Myriade = Propsystem()
    Myriade.choosepropandpress(press='N2')
    Myriade.m_dry = 100
    Myriade.dV_deorbit = 0
    Myriade.sizesystem(1, p0=22*10**5, bdr=4, dV=80, massbreakdown=True)
```

B

Remaining life cycle inventory definitions

This appendix will provide process definition tables which were omitted from the report due to brevity. Each process included here has been discussed and justified in Section 7.4.

B.1. New core processes

B.1.1. Alumina/platinum granular catalyst

Table B.1: Process definition for alumina/platinum granular catalyst production and testing

Flow	Amount	Unit	Description
	INPUT		
aluminium oxide	0.7	kg	70% of total mass [193].
electricity, low voltage	12	kWh	Proxy for catalyst drying and calcination [40].
Organisational Time Contribution (Nat) - EU	15	work-hours	No information available, linked to cost [111].
platinum	0.3	kg	30% of total mass [193].
Total Design Loads Inspection	6.33E-04	m^3	Same bulk density as Al_2O_3/Ir catalyst [194].
transport, freight, lorry 16-32 metric ton, EURO4	0.75	$t*km$	Material transport, standard assumptions.
	OUTPUT		
Alumina/Platinum Granular Catalyst	1	kg	-
SPACE SEGMENT: Goods Transport via Lorry Costs	3.75	USD 2017	Average cost to move goods via road transport [111].
SPACE SEGMENT: Spacecraft Material, Component & Resource Costs	3269.398	USD 2017	Adjusted from Al_2O_3/Ir catalyst [25], [195].

B.1.2. Diaphragm propellant tank, titanium

Table B.2: Process definition for titanium/SIFA-35 diaphragm propellant tank production and testing

Flow	Amount	Unit	Description
	INPUT		
anodising, aluminium sheet	0.464	m^2	Total surface area scaled from PS sizing.
Automated Eddy Current Inspection	0.855	m	Tank periphery scaled from PS sizing.
Dye Penetrant Inspection	0.232	m^2	Outer surface area scaled from PS sizing.
EPDM Product	0.125	kg	Proxy for SIFA-35 diaphragm production. Mass scaled from PS sizing.
Expulsion Efficiency Inspection	0.0105	m^3	Volume scaled from PS sizing.
Leak Test	0.0105	m^3	Volume scaled from PS sizing.
Metal Heat Treatment	0.875	kg	Shell mass scaled from PS sizing
Metal Heat Treatment	17.5	kg	Shell mass scaled from PS sizing
Negative Pressure Inspection	0.0105	m^3	Volume scaled from PS sizing.
Organisational Time Contribution (Nat) - US	142	work-hours	No information available, linked to cost [111].
Pressure Cycle Inspection	0.0105	m^3	Volume scaled from PS sizing.
Proof Pressure Inspection	0.0105	m^3	Volume scaled from PS sizing.
TIG Welding, TiAl6V4	0.855	m	Tank periphery scaled from PS sizing.
Titanium, Milling	6.65	kg	Adapted from existing SSSD dataset [111].
Titanium, TiAl6V4	0.875	kg	Mass scaled from PS sizing.
Titanium, Turning	9.975	kg	Adapted from existing SSSD dataset [111].
Total Design Loads Inspection	0.0105	m^3	Volume scaled from PS sizing.
transport, freight, lorry 16-32 metric ton, EURO4	0.75	$t * km$	Material transport, standard assumptions.
Ultrasonic Inspection	0.0105	m^3	Volume scaled from PS sizing.
Vibration Test	0.0105	m^3	Volume scaled from PS sizing.
Volumetric Capacity Examination	0.0105	m^3	Volume scaled from PS sizing.
X-Ray/Radiographic Inspection	0.232	m^2	Outer surface area scaled from PS sizing.
	OUTPUT		
Diaphragm Propellant Tank - Spherical - Ti6Al4V	1	kg	-
SPACE SEGMENT: Goods Transport via Lorry Costs	3.75	USD 2017	Average cost to move goods via road transport [111].
SPACE SEGMENT: Spacecraft Material, Component & Resource Costs	31270	USD 2017	Scaled from Rafael PEPT-230 data [199].

B.1.3. Fill/drain valve

Table B.3: Process definition for fill/drain valve production and testing

Flow	Amount	Unit	Description
	INPUT		
chromium steel removed by milling, small parts	0.0479	kg	Mass based on ecoinvent recommendation.
degreasing, metal part in alkaline bath	0.00976	m^2	Approximated from technical drawings [187].
EPDM Product	6E-4	kg	Approximated from technical drawings [187].
forging, steel	0.208	kg	Mass from datasheet [187].
impact extrusion of steel, hot, 3 strokes	0.208	kg	Mass from datasheet [187].
Leak Test	1.45E-06	m^3	Approximated from technical drawings [187].
Negative Pressure Inspection	1.45E-06	m^3	Approximated from technical drawings [187].
Organisational Time Contribution (Nat) - US	39	work-hours	No exact information, linked to cost [111].
steel, chromium steel 18/8	0.208	kg	Mass from datasheet [187].
transport, freight, lorry 16-32 metric ton, EURO4	0.157	$t * km$	Material transport, standard assumptions.
welding, arc, steel	0.232	m	Approximated from technical drawings [187].
	OUTPUT		
Fill/Drain Valve - Low Pressure - Stainless Steel	1	Item(s)	-
SPACE SEGMENT: Goods Transport via Lorry Costs	0.784	USD 2017	Average cost to move goods via road transport [111].
SPACE SEGMENT: Spacecraft Material, Component & Resource Costs	8622	USD 2017	Estimate from correspondence with product manager.

B.1.4. Seamless tubing

Table B.4: Process definition for seamless tubing production and testing

Flow	Amount	Unit	Description
	INPUT		
Automated Eddy Current Inspection	11.11	m	Calculated based on 1 kg mass [185].
degreasing, metal part in alkaline bath	0.443	m^2	Calculated based on 1 kg mass [185].
drawing of pipe, steel	1	kg	Seamless tube forming.
Metal Heat Treatment	2x 1	kg	Seamless tube forming [185].
Organisational Time Contribution (Nat) - UK	0.72	work-hours	No exact information, linked to cost [111].
steel, chromium steel 18/8	1	kg	Proxy for 304 alloy [185].
transport, freight, lorry 16-32 metric ton, EURO4	0.75	$t * km$	Material transport, standard assumptions.
Ultrasonic Inspection	0.00016	m^3	Calculated based on 1 kg mass [185].
	OUTPUT		
Seamless Tubing - Stainless Steel	1	kg	-
SPACE SEGMENT: Goods Transport via Lorry Costs	3.75	USD 2017	Average cost to move goods via road transport [111].
SPACE SEGMENT: Spacecraft Material, Component & Resource Costs	158	USD 2017	Estimate from supplier, adjusted for inflation [203].

B.1.5. Thruster combustion chamber, inconel

Table B.5: Process definition for inconel thruster combustion chamber production and testing

Flow	Amount	Unit	Description
	INPUT		
chromium steel removed by milling, small parts	0.0247	kg	Proxy for inconel milling, mass from ecoinvent recommendation.
degreasing, metal part in alkaline bath	9.51E-4	m^2	Approximated from technical drawings [125].
Dye Penetrant Inspection	9.51E-4	m^2	Approximated from technical drawings [125].
forging, steel	0.107	kg	Proxy for inconel forging [125].
iron-nickel-chromium alloy	0.107	kg	Proxy for inconel production [125].
Metal Heat Treatment	0.107	kg	-
Organisational Time Contribution (Nat) - US	86	work-hours	No data available, linked to cost [111].
transport, freight, lorry 16-32 metric ton, EURO4	0.0805	$t * km$	Material transport, standard assumptions.
X-Ray/Radiographic Inspection	9.51E-4	m^2	Approximated from technical drawings [125].
	OUTPUT		
Seamless Tubing - Stainless Steel	1	Item(s)	-
SPACE SEGMENT: Goods Transport via Lorry Costs	0.402	USD 2017	Average cost to move goods via road transport [111].

B.2. Propulsion system inventories

B.2.1. ASCENT

Table B.6: Process definition for ASCENT propulsion system assembly and testing

Flow	Amount	Unit	Description
INPUT			
Diaphragm Propellant Tank - Spherical - Ti6Al4V	1.79	kg	Based on PS sizing.
Fill/Drain Valve - Low Pressure - Stainless Steel	2	Item(s)	Service valves, based on PS architecture.
Flow Control Valve - Double Seat - Stainless Steel	0.5	Item(s)	Proxy for isolation latch valve, based on PS architecture.
Leak Test	2x 0.0104	m^3	Tank volume and thruster internal volumes.
Organisational Time Contribution (Nat) - NL	1000	work-hours	Based on correspondence with expert.
Proof Pressure Inspection	0.0104	m^3	Tank volume and thruster internal volumes.
Seamless Tubing - Stainless Steel	0.638	kg	Based on PS sizing.
Thruster - 1N - ASCENT	4	Item(s)	Based on PS architecture.
transport, freight, aircraft, unspecified	5.796	$t*km$	Transport of valves, from US to NL.
transport, freight, aircraft, unspecified	20.030	$t*km$	Transport of propellant tank, from US to NL.
transport, freight, aircraft, unspecified	17.456	$t*km$	Transport of thrusters from US to NL.
Vibration Test	0.0104	m^3	Tank volume and thruster internal volumes.
OUTPUT			
Minisatellite Propulsion System - 4x1N - Monopropellant ASCENT	1	Item(s)	-
SPACE SEGMENT: Goods Transport via Air Costs	4.043	USD 2017	Average cost to move air freight [111].
SPACE SEGMENT: Goods Transport via Air Costs	13.971	USD 2017	Average cost to move air freight [111].
SPACE SEGMENT: Goods Transport via Air Costs	12.176	USD 2017	Average cost to move air freight [111].
SPACE SEGMENT: Spacecraft Assembly & Integration Costs	219593	USD 2017	No exact information, linked to labour hours [111].

B.2.2. LMP-103S

Table B.7: Process definition for 1 N LMP-103S thruster assembly and testing

Flow	Amount	Unit	Description
	INPUT		
Alumina/Iridium Granular Catalyst	0.00254	kg	Catalyst bed length with propellant I_{sp} [207].
Catalyst Bed Heater - Coiled - Inconel Sheath	0.05	kg	Thruster design [141].
Flow Control Valve - Double Seat - Stainless Steel	1	Item(s)	Thruster design [141].
Leak Test	3x 1.76E-4	m^3	Total internal volume of all components.
Organisational Time Contribution (Nat) - SE	12	work-hours	Based on correspondence with expert.
Proof Pressure Inspection	1.76E-4	m^3	Total internal volume of all components.
Thruster Combustion Chamber - 1N - Iridium/Rhenium Alloy	1	Item(s)	Thruster design [141].
transport, freight, aircraft, unspecified	1.716	$t*km$	Transport of combustion chamber from US to SE.
transport, freight, aircraft, unspecified	2.179	$t*km$	Transport of FCV from US to SE.
transport, freight, lorry 16-32 metric ton, EURO4	0.194	$t*km$	Transport of catalyst bed heater from FR to SE.
Vibration Test	1.76E-4	m^3	Total internal volume of all components.
welding, arc, steel	0.427	m	Proxy for brazing, based on technical drawings [198].
X-Ray/Radiographic Inspection	0.00778	m^2	Total outer surface area of all components.
	OUTPUT		
Thruster - 1N - LMP-103S	1	Item(s)	-
SPACE SEGMENT: Goods Transport via Air Costs	1.197	USD 2017	Average cost to move air freight [111].
SPACE SEGMENT: Goods Transport via Air Costs	1.520	USD 2017	Average cost to move air freight [111].
SPACE SEGMENT: Goods Transport via Lorry Costs	0.968	USD 2017	Average cost to move goods via road transport [111].
SPACE SEGMENT: Spacecraft Material, Component & Resource Costs	64390	USD 2017	Estimated cost of HPGP thruster [197].
SPACE SEGMENT: Spacecraft Material, Component & Resource Costs	-39.152	USD 2017	Compensation for catalyst bed cost.
SPACE SEGMENT: Spacecraft Material, Component & Resource Costs	-1896.75	USD 2017	Compensation for catalyst bed heater cost.
SPACE SEGMENT: Spacecraft Material, Component & Resource Costs	-21554	USD 2017	Compensation for FCV cost.

Table B.8: Process definition for LMP-103S propulsion system assembly and testing

Flow	Amount	Unit	Description
	INPUT		
Diaphragm Propellant Tank - Spherical - Ti6Al4V	2.07	kg	Based on PS sizing.
Fill/Drain Valve - Low Pressure - Stainless Steel	2	Item(s)	Service valves, based on PS architecture.
Flow Control Valve - Double Seat - Stainless Steel	0.5	Item(s)	Proxy for isolation latch valve, based on PS architecture.
Leak Test	2x 0.0131	m^3	Tank volume and thruster internal volumes.
Organisational Time Contribution (Nat) - NL	1000	work-hours	Based on correspondence with expert.
Proof Pressure Inspection	0.0131	m^3	Tank volume and thruster internal volumes.
Seamless Tubing - Stainless Steel	0.686	kg	Based on PS sizing.
Thruster - 1N - LMP-103S	4	Item(s)	Based on PS architecture.
transport, freight, aircraft, unspecified	5.796	$t * km$	Transport of valves, from US to NL.
transport, freight, aircraft, unspecified	23.163	$t * km$	Transport of propellant tank, from US to NL.
transport, freight, aircraft, unspecified	4.238	$t * km$	Transport of thrusters from SE to NL.
Vibration Test	0.0131	m^3	Tank volume and thruster internal volumes.
	OUTPUT		
Minisatellite Propulsion System - 4x1N - Monopropellant LMP-103S	1	Item(s)	-
SPACE SEGMENT: Goods Transport via Air Costs	4.043	USD 2017	Average cost to move air freight [111].
SPACE SEGMENT: Goods Transport via Air Costs	16.156	USD 2017	Average cost to move air freight [111].
SPACE SEGMENT: Goods Transport via Lorry Costs	21.189	USD 2017	Average cost to move goods via road transport [111].
SPACE SEGMENT: Spacecraft Assembly & Integration Costs	219593	USD 2017	No exact information, linked to labour hours [111].

B.2.3. 98% HTP

Table B.9: Process definition for 1 N 98% HTP thruster assembly and testing

Flow	Amount	Unit	Description
	INPUT		
Alumina/Platinum Granular Catalyst	0.00288	kg	Catalyst bed length with propellant I_{sp} [207].
Catalyst Bed Heater - Coiled - Inconel Sheath	0.05	kg	Thruster design [125].
Flow Control Valve - Double Seat - Stainless Steel	1	Item(s)	Thruster design [125].
Leak Test	3x 1.75E-4	m^3	Total internal volume of all components.
Organisational Time Contribution (Nat) - EU	12	work-hours	Based on correspondence with expert.
Proof Pressure Inspection	1.75E-4	m^3	Total internal volume of all components.
Thruster Combustion Chamber - 1N - Inconel	1	Item(s)	Thruster design [34].
transport, freight, aircraft, unspecified	1.253	$t*km$	Transport of combustion chamber from US to EU.
transport, freight, aircraft, unspecified	2.336	$t*km$	Transport of FCV from US to RER.
transport, freight, lorry 16-32 metric ton, EURO4	0.124	$t*km$	Transport of catalyst bed heater from FR to RER.
Vibration Test	1.75E-4	m^3	Total internal volume of all components.
welding, arc, steel	0.191	m	Proxy for brazing, based on technical drawings [125].
X-Ray/Radiographic Inspection	0.00622	m^2	Total outer surface area of all components.
	OUTPUT		
Thruster - 1N - 98% HTP	1	Item(s)	-
SPACE SEGMENT: Goods Transport via Air Costs	1.629	USD 2017	Average cost to move air freight [111].
SPACE SEGMENT: Goods Transport via Air Costs	0.874	USD 2017	Average cost to move air freight [111].
SPACE SEGMENT: Goods Transport via Lorry Costs	0.622	USD 2017	Average cost to move goods via road transport [111].
SPACE SEGMENT: Spacecraft Material, Component & Resource Costs	42927	USD 2017	Estimated cost of hydrazine thruster [197].
SPACE SEGMENT: Spacecraft Material, Component & Resource Costs	-1896.75	USD 2017	Compensation for catalyst bed cost.
SPACE SEGMENT: Spacecraft Material, Component & Resource Costs	-9.385	USD 2017	Compensation for catalyst bed heater cost.
SPACE SEGMENT: Spacecraft Material, Component & Resource Costs	-21554	USD 2017	Compensation for FCV cost.

Table B.10: Process definition for 98% HTP propulsion system assembly and testing

Flow	Amount	Unit	Description
	INPUT		
Diaphragm Propellant Tank - Spherical - Al5254	3.064	kg	Based on PS sizing
Fill/Drain Valve - Low Pressure - Stainless Steel	2	Item(s)	Service valves, based on PS architecture.
Flow Control Valve - Double Seat - Stainless Steel	0.5	Item(s)	Proxy for isolation latch valve, based on PS architecture.
Leak Test	2x 0.0156	m^3	Tank volume and thruster internal volumes.
Organisational Time Contribution (Nat) - NL	1000	work-hours	Based on correspondence with expert.
Proof Pressure Inspection	0.0156	m^3	Tank volume and thruster internal volumes.
Seamless Tubing - Stainless Steel	0.837	kg	Based on PS sizing.
Thruster - 1N - 98% HTP	4	Item(s)	Based on PS architecture.
transport, freight, aircraft, unspecified	5.797	$t * km$	Transport of valves, from US to NL.
transport, freight, lorry 16-32 metric ton, EURO4	4.219	$t * km$	Transport of propellant tank, from RER to NL.
transport, freight, lorry 16-32 metric ton, EURO4	1.983	$t * km$	Transport of thrusters from RER to NL.
Vibration Test	0.0156	m^3	Tank volume and thruster internal volumes.
	OUTPUT		
Minisatellite Propulsion System - 4x1N - Monopropellant 98% HTP	1	Item(s)	-
SPACE SEGMENT: Goods Transport via Air Costs	4.043	USD 2017	Average cost to move air freight [111].
SPACE SEGMENT: Goods Transport via Lorry Costs	31.0094	USD 2017	Average cost to move goods via road transport [111].
SPACE SEGMENT: Spacecraft Assembly & Integration Costs	219593	USD 2017	No exact information, linked to labour hours [111].

C

Technical drawings used for life cycle inventory definitions

This appendix presents the technical diagrams, images or renders that were used in the development of the various component LCIs in Section 7.4. In each image, a red line shows the known dimension used to estimate other dimensions in the diagram. While the diagrams are grouped based on the component they depict, it should be noted that some component dimensions were estimated using diagrams of other components. For example, to estimate the diameter of the catalyst bed heater coil, a technical drawing of the ECAPS 1 N thruster was used.

C.1. Aerojet Rocketdyne MR-103J 1 N hydrazine thruster

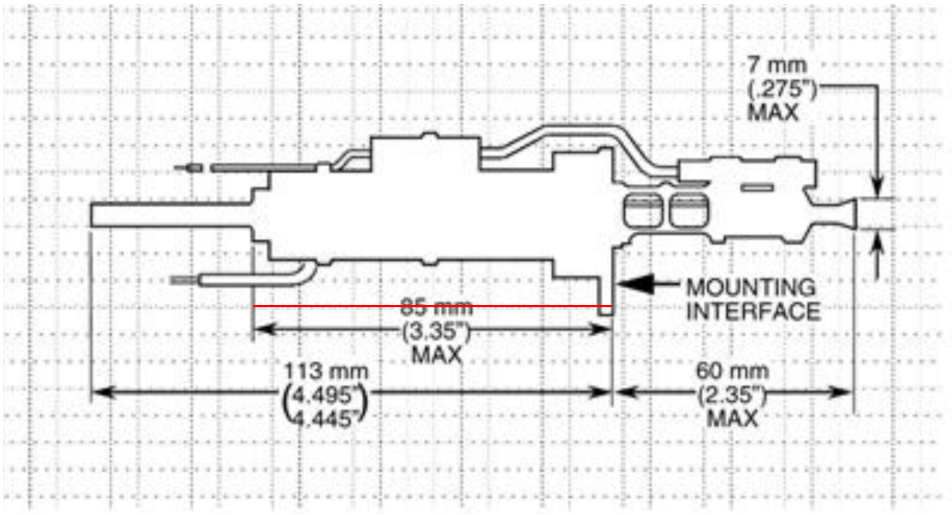

Figure C.1: Diagram of MR-103J hydrazine thruster developed by Aerojet Rocketdyne [125]. Reference dimension is flow control valve length, equal to 85 mm.

C.2. ArianeGroup 1 N hydrazine thruster

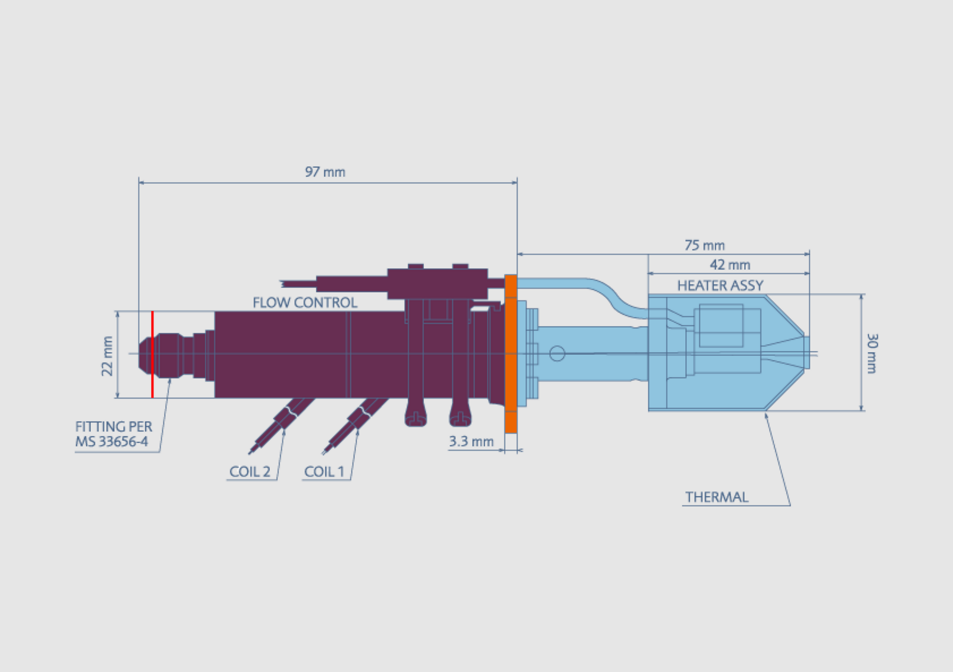

Figure C.2: Diagram of 1 N hydrazine thruster developed by ArianeGroup [202]. Reference dimension is flow control valve diameter, equal to 22 mm.

C.3. ECAPS 1 N HPGP thruster

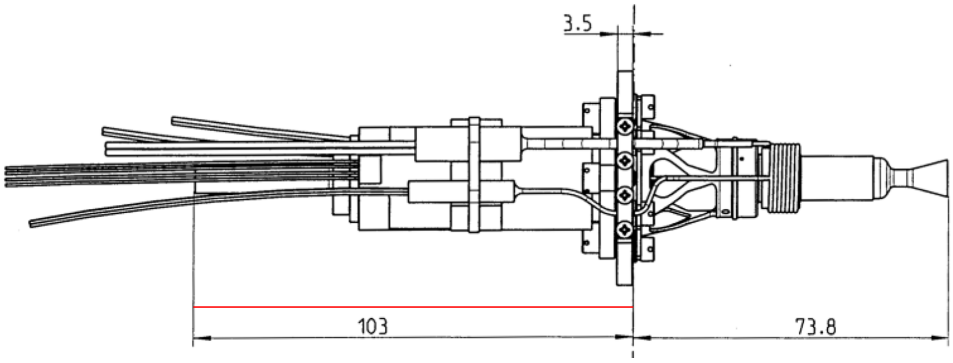

Figure C.3: Top view technical drawing of 1 N HPGP thruster developed by ECAPS [198]. Reference dimension is flow control valve length, equal to 103 mm.

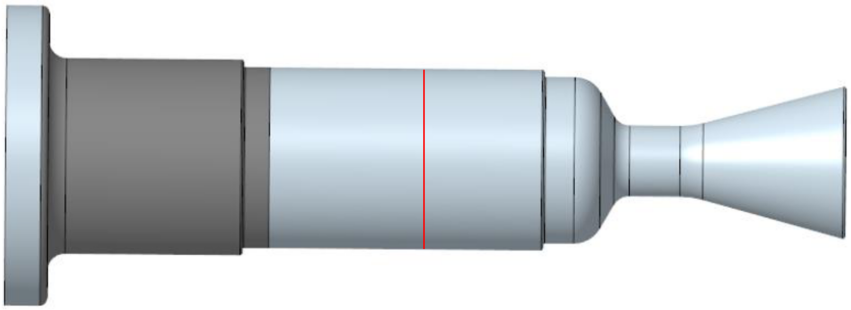

Figure C.4: Side view rendering of 1 N HPGP thruster combustion chamber [206]. Reference dimension is combustion chamber diameter, estimated at 10 mm, based on Figure C.3.

C.4. Moog fill/ drain valve

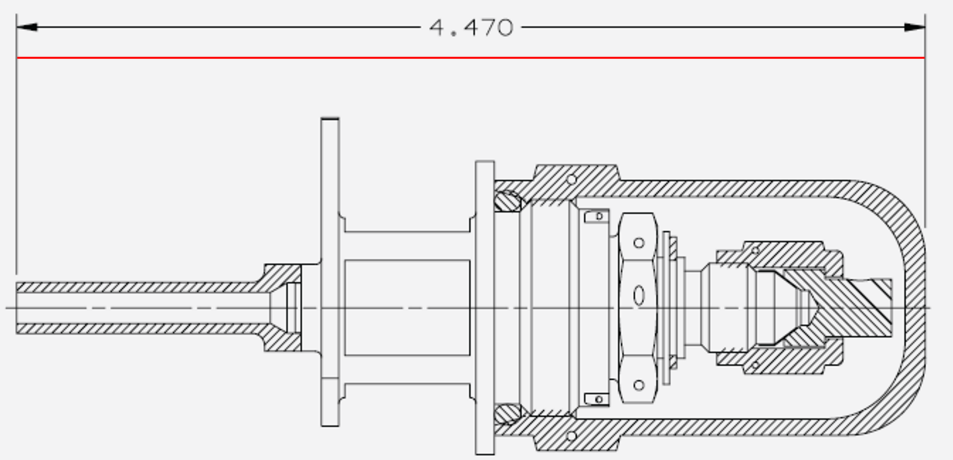

Figure C.5: Side view technical drawing of low pressure stainless steel fill/ drain valve developed by Moog [187]. Reference dimension is total valve length, equal to 113.54 mm.

C.5. Thermocoax coiled catalyst bed heater

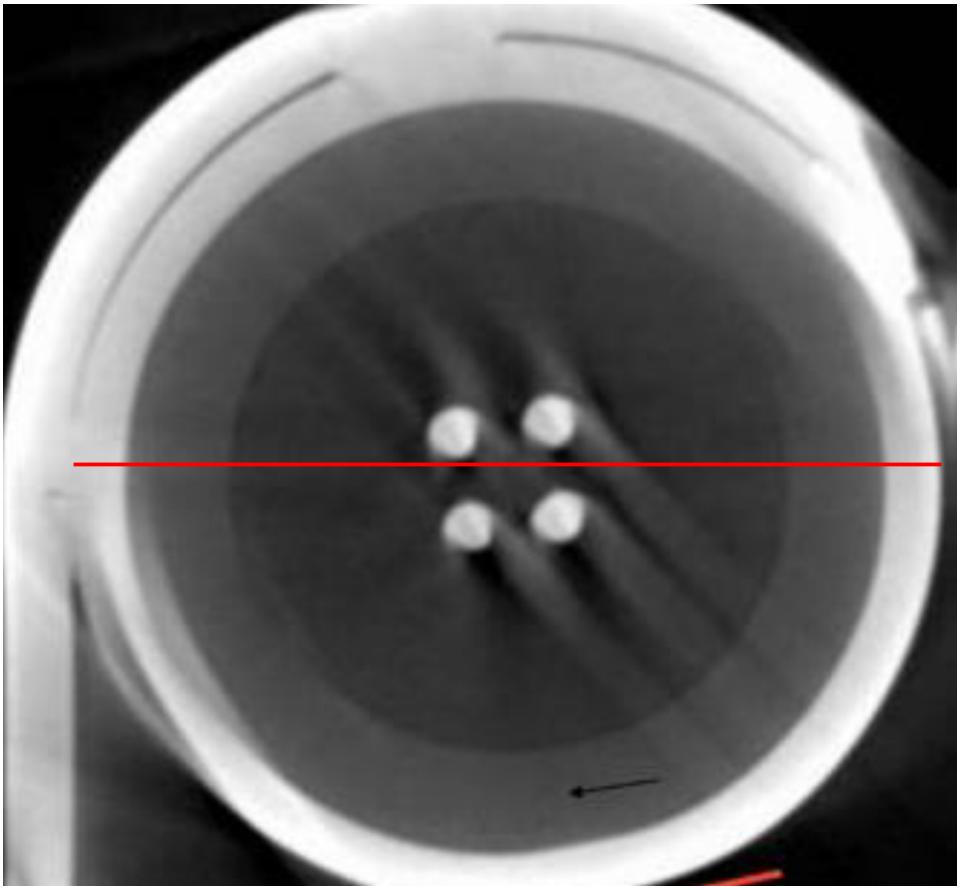

Figure C.6: Cross section image of mineral insulated cable used in coiled catalyst bed heater [196]. Reference dimension is cable diameter, equal to 1.5 mm

C.6. Valvetech flow control valve

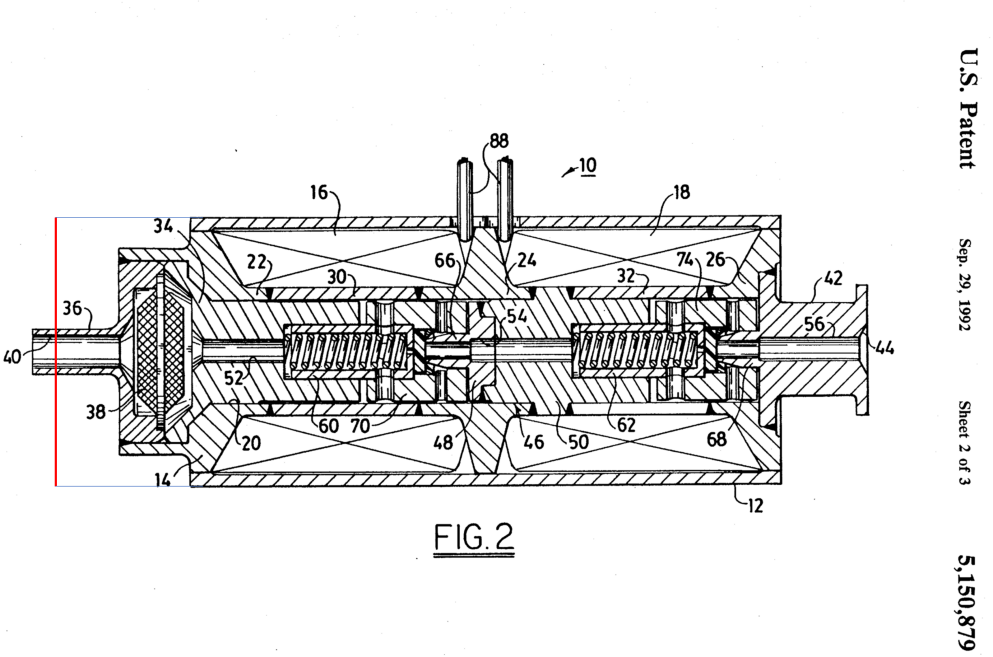

Figure C.7: Side view technical drawing of thruster flow control valve [201]. Reference dimension is valve outer diameter, estimated at 22 mm, based on Figure C.2.

D

Environmental LCIA single score calculation

Using the absolute scores for each of the environmental impact categories reported in Table 7.21 and the normalisation and weighting factors reported in Table 4.1, Table D.1 shows the calculation of the environmental single score of each of the considered propulsion systems. Note that no units are given for each impact category as the reported scores are all normalised to a comparable non-dimensional unit.

Table D.1: Environmental single score calculation for the environmental LCIA of the various propulsion systems, using the impact categories included in the Environmental Footprint framework [115].**Bold** indicates the highest score for the respective category.

Impact category	Hydrazine	ASCENT	LMP-103S	98% HTP
Acidification	6.85E-02	3.25E-01	**3.33E-01**	2.99E-02
Climate change	1.04E-01	1.03E-01	**1.34E-01**	4.70E-02
Ecotoxicity, freshwater	4.03E-01	2.37E+00	**2.46E+00**	6.94E-02
Eutrophication, freshwater	7.75E-02	1.59E-01	**1.72E-01**	3.74E-02
Eutrophication, marine	1.32E-02	1.45E-02	**1.55E-02**	4.22E-03
Eutrophication, terrestrial	5.04E-02	6.04E-02	**6.47E-02**	1.57E-02
Human toxicity, cancer	3.05E-03	2.82E-03	**3.21E-03**	9.23E-04
Human toxicity, non-cancer	3.25E-03	4.57E-03	**5.00E-03**	1.48E-03
Ionising radiation	**6.62E-03**	4.99E-03	6.24E-03	2.72E-03
Land use	3.20E-04	3.81E-04	**4.29E-04**	5.15E-05
Ozone depletion	**2.53E-03**	1.97E-03	2.31E-03	1.85E-03
Particulate matter	4.39E-02	7.62E-02	**8.31E-02**	1.54E-02
Photochemical ozone formation	4.13E-02	6.60E-02	**7.12E-02**	1.34E-02
Resource use, fossils	6.89E-02	7.16E-02	**1.05E-01**	2.84E-02
Resource use, minerals and metals, ultimate reserve	4.63E-02	8.53E-01	**8.59E-01**	4.06E-02
Water use	**3.72E-02**	3.04E-02	3.66E-02	3.36E-02
Environmental single score	0.97	4.14	**4.35**	0.34
Environmental single score, relative to hydrazine [%]	100.00	426.91	**448.22**	35.27

E

Remaining data quality assessments

In Table E.1, an overview is given of the processes relating to propellant and thruster production. As all data quality ratings are lower than 3, it is deemed that these LCI definitions obtain a basic quality [217].

Table E.1: Data quality assessment for propellant specific processes. TeR=Technological representativeness, GR=Geographical representativeness, TiR=Temporal representativeness, C=Completeness, P=Precision/uncertainty, M=Methodological appropriateness and consistency, DQR=Data quality rating as calculated following [217].

Process	TeR	GR	TiR	C	P	M	DQR
Hydrazine ultra high purity	1	2	1	2	2	2	**1.50**
1N hydrazine thruster	1	1	2	3	4	3	**2.50**
ASCENT	1	1	5	1	2	2	**2.67**
1N ASCENT thruster	3	4	3	3	4	3	**3.00**
LMP-103S	2	1	1	1	1	2	**1.33**
1N LMP-103S thruster	3	1	2	3	3	3	**2.25**
98% HTP	3	1	3	3	3	3	**2.33**
1N 98% HTP thruster	3	2	3	3	4	3	**2.83**